

*The pivotal role of sulfite species in shaping
the oxygen isotope composition of sulfate: new
insights from a stable isotope perspective*

Inigo Andreas Müller

Dissertation zur Erlangung des Doktorgrades der
Naturwissenschaften -Dr. Rer. Nat.-

Vorgelegt dem Fachbereich Geowissenschaften der
Universität Bremen

Bremen
Januar 2013

Die vorliegende Arbeit wurde in der Zeit vom Oktober 2009 bis zum Januar 2013 im Biogeochemie Department des Max-Planck-Instituts für marine Mikrobiologie, Bremen, erarbeitet und entspringt einer Zusammenarbeit zwischen dem Max-Planck-Institut und dem MARUM-Zentrum für Marine Umweltwissenschaften der Universität Bremen (GB3 Projekt "Transformation of matter and the role of microbes in subsurface sediments").

1. Gutachter Prof. Dr. Wolfgang Bach
2. Gutachter Dr. Timothy G. Ferdelman

Tag des öffentlichen Promotionskolloquiums:
19. März 2013

Table of Contents:

Preface	VII
Abstract	VIII
Zusammenfassung	XII
1. General introduction	1
1.1. The sulfur cycle.....	1
1.1.1. The global sulfur cycle: sources and sinks	2
1.1.2. Oxidation of reduced sulfur compounds.....	4
1.1.3. Dissimilatory sulfate reduction (DSR).....	7
1.1.4. Disproportionation of sulfur intermediates.....	10
1.2. Stable isotope studies on sulfate	11
1.3. Sulfite species and its role as sulfoxy intermediate	16
1.4. Motivation and outline of the dissertation	17
1.5. References.....	20
2. The oxygen isotope equilibrium fractionation between sulfite species and water 27	
2.1. Abstract	27
2.2. Introduction.....	28
2.2.1. The role of sulfite in shaping the oxygen isotope composition of sulfate.....	28
2.2.2. Species-dependent oxygen isotope exchange between sulfite and water.....	29
2.2.3. Precipitation of sulfite salts for subsequent oxygen isotope analysis and determination of isotope fractionation between sulfite and water	30
2.3. Methods.....	31
2.3.1. Experiment challenges and approaches on how to cope with them	31
2.3.2. Equilibrium experiments.....	33
2.3.3. Precipitation of sulfite salts with isotopically distinct precipitation solutions and with different cations (Ag^+ , Ba^{2+}).....	35
2.3.4. Stable isotope measurements	37
2.3.5. Isotope mass balances for the determination of the oxygen isotope equilibrium fractionation between dissolved sulfite and water	38
2.4. Results and discussion	43
2.4.1. Comparison between different precipitation agents (Ba^{2+} and Ag^+) and differences between precipitation at constant pH and with pH shift (with NaOH)	43
2.4.2. Oxygen isotope equilibrium fractionation between sulfite and water in barium sulfite precipitates BaSO_3	45
2.4.3. Determination of the oxygen isotope equilibrium fractionation between dissolved SO_2 and water from experiments at pH 1.5	48
2.4.4. Implications of the obtained oxygen isotope equilibrium fractionation values.....	50
2.5. Conclusions.....	52
2.6. Acknowledgments.....	53

2.7. References.....	53
2.8. Appendices.....	57
3. Isotopic evidence of the pivotal role of sulfite oxidation in shaping the oxygen isotope signature of sulfate.....	61
3.1. Abstract.....	61
3.2. Introduction.....	62
3.2.1. Tracing of biogeochemical sulfur cycling by oxygen isotopes of sulfate.....	62
3.2.2. The role of sulfite as intermediate in oxidative and reductive S-cycling.....	63
3.2.3. Potential pivotal role of sulfite for oxygen isotope composition of sulfate from oxidation of reduced sulfur compounds.....	63
3.2.4. Isotope effects during sulfite oxidation.....	64
3.2.5. Aim of this study.....	69
3.3. Methods.....	69
3.3.1. Experimental approaches based on isotope mass balance considerations.....	69
3.3.2. Experimental setup.....	75
3.3.3. Setup of different experiments (A-D).....	76
3.3.4. Measurements.....	78
3.3.5. Determination of Y , isotope enrichment factors and isotope offsets.....	80
3.4. Results and discussion.....	81
3.4.1. Hydrochemistry.....	81
3.4.2. Isotopes.....	83
3.4.3. Comparison to results from studies on biological oxidation of sulfur compounds.....	94
3.5. Conclusions.....	95
3.6. Acknowledgments.....	97
3.7. References.....	97
3.8. Appendix.....	103
4. The isotope signature of magmatic SO₂ disproportionation: A comparison between laboratory experiments and a hydrothermally active site in the Manus Basin, Papua New Guinea.....	105
4.1. Abstract.....	105
4.2. Introduction.....	106
4.2.1. Geochemistry of hydrothermal systems.....	106
4.2.2. SO ₂ disproportionation at the hydrothermal vent site North Su in the eastern Manus Basin.....	107
4.2.3. The oxygen isotope signature of chemical SO ₂ disproportionation and consequences for the oxygen isotope composition of seawater sulfate.....	109
4.3. Study site in the Manus Basin.....	110
4.4. Methods.....	112

4.4.1. Sampling of hydrothermal fluids in the Manus Basin	112
4.4.2. Laboratory SO ₂ disproportionation experiments	114
4.4.3. Analytical methods	116
4.4.4. Stable isotope measurements	117
4.5. Results and discussion	118
4.5.1. Disproportionation of magmatic SO ₂ in a hydrothermal fluid at North Su	118
4.5.2. Laboratory insights on the abiotic disproportionation of SO ₂	125
4.5.3. Consequences of magmatic SO ₂ disproportionation for the oxygen isotope composition of seawater sulfate	131
4.6. Conclusions	132
4.7. Acknowledgments	133
4.8. References	133
5. Synthesis and outlook	141
5.1. Synthesis	141
5.2. Outlook	144
5.3. References	145
6. Appendix: The reversibility of dissimilatory sulphate reduction and the cell-internal multi-step reduction of sulphite to sulphide: insights from the oxygen isotope composition of sulphate	148
6.1. Abstract	148
Acknowledgments	150
Curriculum vitae	153
Erklärung	155

Preface

-Sulfite, an underestimated sulfoxy intermediate?-

“*To Be or Not to Be, That is the Question*”, this famous phrase by W. Shakespeare followed me for a long time during this work. On one side I permanently struggled with the question if sulfite is at all a prominent sulfoxy intermediate during sulfur cycling and on the other side, if the abiotic processes that I was analyzing play a significant role in the sulfur system that seems to be overprinted by microbial traces. With the help of stable isotope techniques we tried to shed some light on this mystery, a quite complex task because of the instability and/or high reactivity of sulfite. Although it was originally planned to perform microbial experiments to determine the stable isotope signature of dissimilatory sulfate reduction at high temperatures I had to abandon this idea due to time shortage and due to the fact that my experimental findings guided me into other directions, because of their high relevance for the oxidative part of sulfur cycling. Suddenly, a major part of an apparently miraculous isotopic fractionation pattern observed during microbial experiments on the oxidation of reduced sulfur compounds could be reproduced by pure abiotic processes. This finding fascinated me because it shows us that even during microbial processes pure chemical reactions can co-occur and be responsible for a crucial part of the observed isotope effects. This observation should not make the reader of my dissertation believe that we can stop performing incubation experiments to determine the isotope fractionation signatures of microbial processes: these experiments remain of highest importance for using stable isotopes to understand what microbial processes occurred during the geologic past or operate in the deep biosphere. However, at the same time it becomes evident that it is necessary to include more abiotic experiments to be able to distinguish between biological and abiotic isotope effects in natural environments. Especially for the oxygen isotope composition of the most prominent sulfur compound on our planet, sulfate, the ability of sulfite to exchange its oxygen with water and the speed of the sulfite oxidation step seem to be the controlling factors – notably two properties that are governed by chemical parameters.

The final project of my thesis dealt with the isotope patterns during the chemical disproportionation of sulfur dioxide, an unprotonated sulfite species, in a temperature range common in hydrothermal fluids. Besides today’s anthropogenic gas emissions sulfur dioxide is being emitted in high amounts from volcanoes all over the world. These emissions persisted through the Earth’s history, therefore being an important sulfur source over geological time. Recent studies at the seafloor, based on remotely operating vehicles, revealed that the contribution magmatic sulfur dioxide to the global sulfur budget might be much higher than known so far. The oxygen isotope signature of sulfate produced by the disproportionation of sulfur dioxide – an isotope signature that I determined for the first time during my work – might play a significant role in shaping the stable isotopes of seawater sulfate.

Although sulfite is detectable only in minor concentrations in natural environments it cannot be ignored. I hope that with this study on the role of sulfite species during sulfur cycling I can excite the readership for this still underestimated sulfoxy intermediate.

To Be or Not to Be – Sulfite Is.

Abstract

Sulfate (SO_4^{2-}) is highly abundant on our planet and is one of the most important terminal electron acceptors during the degradation of organic matter by microorganisms in anoxic environments. During the dissimilatory sulfate reduction (DSR) SO_4^{2-} is reduced to other sulfur compounds at lower oxidation state such as hydrogen sulfide (H_2S) which is excreted from the microorganisms and in most cases is oxidized back to SO_4^{2-} . The H_2S or other reduced sulfur compounds can be oxidized via different pathways depending on the absence/presence of sulfur oxidizing microorganisms, as well as on the chemical conditions of the environment. For example, the chemical conditions in the environment can vary with respect to the presence of air O_2 or ferric iron (Fe^{3+}) as oxidizing agents. Changes in the abundance of these oxidants lead to slight differences in the oxidation pathways, but both pathways will produce in the end SO_4^{2-} . Adding to the complexity of the sulfur cycle is the fact that sulfoxy intermediates (e.g. $\text{S}_2\text{O}_3^{2-}$, SO_3^{2-}) or elemental sulfur (S^0) can be disproportionated into sulfur compounds with higher and lower oxidation state. The sulfur compound with higher oxidation state is typically SO_4^{2-} and the compound with lower oxidation state can be subsequently oxidized to SO_4^{2-} . All these different processes will leave a specific oxygen isotope imprints on the produced SO_4^{2-} . Sulfate is a very inert molecule that does not exchange its oxygen with the water (only under extreme conditions), thus the oxygen isotope composition of SO_4^{2-} can be considered an archive for the various production processes.

In my dissertation I was especially interested in the role of sulfite (SO_3^{2-}) during the oxidative part of sulfur cycling and if the presence of SO_3^{2-} as an intermediate in sulfur cycling has the potential to affect the oxygen isotope composition of SO_4^{2-} . Sulfite is a highly interesting sulfur compound because it is often considered the final intermediate during the oxidation of reduced sulfur compounds. In contrast to SO_4^{2-} , SO_3^{2-} rapidly exchanges its oxygen with water quickly approaching equilibrium isotope exchange conditions. Due to these characteristics the presence of SO_3^{2-} as final sulfoxy intermediate in oxidative sulfur cycling must be visible in the oxygen isotope composition of the produced SO_4^{2-} . Although SO_3^{2-} is often considered an important intermediate and despite its potential in affecting the oxygen isotope composition of sulfate during the oxidative part of sulfur cycling, direct studies on the isotope effects caused by the presence of SO_3^{2-} are scarce.

To unravel the role of sulfite on the oxygen isotope patterns of SO_4^{2-} we first had to determine the oxygen isotope equilibrium fractionation between SO_3^{2-} and water by performing anoxic experiments where sodium sulfite was dissolved in de-ionized water (Chapter 2: “The oxygen isotope equilibrium fractionation between sulfite species and water”). After pinpointing the oxygen isotope equilibrium fractionation between SO_3^{2-} and water we could use this value to determine the oxygen isotope effects during the abiotic oxidation of SO_3^{2-} to SO_4^{2-} (Chapter 3: “Isotopic evidence of the pivotal role of sulfite oxidation in shaping the oxygen isotope signature of sulfate”). As the final project of this dissertation we analyzed the isotope effects that take place during the disproportionation of sulfur dioxide (SO_2) to HSO_4^- and S^0 at hydrothermal temperatures. This process appears to occur more often than expected in hydrothermal systems at the seafloor at subduction zones, contributing high amounts of sulfate and sulfur to the marine environment. We hypothesize that the disproportionation of SO_2 in hydrothermal

systems might have an impact on the oxygen isotope composition of the seawater sulfate (Chapter 4: “The isotope signature of magmatic SO₂ disproportionation: A comparison between laboratory experiments and a hydrothermally active site in the Manus Basin, Papua New Guinea”).

Below, I will shortly summarize the three main projects of my thesis, highlighting the challenges, major procedural steps and outcomes of the studies.

Chapter 2 describes my efforts to determine the oxygen isotope equilibrium fractionation between sulfite species and water and the results of this study, including the implications of our findings for the interpretation of oxygen isotope signatures of SO₄²⁻. We performed abiotic SO₃²⁻-water oxygen isotope equilibration experiments in isotopically distinct solutions at different pH. Sulfite exists in solution as different species with the same oxidation state (+IV), such as sulfur dioxide (SO₂), bisulfite (HSO₃⁻), pyrosulfite (S₂O₅²⁻) and sulfite *sensu stricto* (SO₃²⁻). During these experiments we faced many challenges, such as the fact that different sulfite species have different oxygen isotope equilibrium fractionations with respect to water, that water oxygen is incorporated into sulfite salts during their precipitation, that oxygen isotope exchange continues during the precipitation of sulfite salts and that a contaminant is entrained into the sulfite precipitate. By performing the experiments in solutions with distinct isotopic compositions we were able to determine the amount of SO₃²⁻ oxygen in equilibrium with the experiment solutions and by performing the sulfite salt precipitation with isotopically distinct precipitation solutions it was possible to quantify the amount of water oxygen that gets incorporated during the precipitation procedure. By adding a barium hydroxide solution during the precipitation, the pH of the solution was shifted rapidly to values above 12, which immediately stopped the oxygen exchange between SO₃²⁻ and water. With this approach it was possible to cope with all experimental challenges and by using an isotope mass balance that takes into account all possible oxygen sources we were able to pin down a value for the oxygen isotope equilibrium fractionation between SO₃²⁻ and water of $\epsilon^{\text{EQ}}_{\text{SO}_3^{2-} \leftrightarrow \text{H}_2\text{O}} = 15.2\text{‰}$ and give a rough estimate for the oxygen isotope equilibrium fractionation between SO₂ and water of $\epsilon^{\text{EQ}}_{\text{SO}_2 \leftrightarrow \text{H}_2\text{O}} = 37.0\text{‰}$.

After the determination of the oxygen isotope equilibrium fractionation between sulfite species and water, we used this new value for the interpretation of the results of experiments where I oxidized SO₃²⁻ to SO₄²⁻. These experiments were designed to provide new insights on the mechanisms that are responsible for the observed oxygen isotope signature in SO₄²⁻ produced during oxidative processes. Chapter 3 describes the abiotic oxidation of SO₃²⁻ to SO₄²⁻ with different oxidizing agents (O₂ or/and Fe³⁺) under different pH conditions. Depending on the oxidant that is present in solution the final oxygen atom during the oxidation process will be derived from O₂ or H₂O, respectively. In the natural environment these two oxygen sources typically have very distinct oxygen isotope compositions allowing for the discrimination between the two oxidation pathways. With an isotope mass balance it is even possible to quantify in oxidation experiments the relative contribution of the different oxygen sources. In case of the oxidation of SO₃²⁻, the question arises if SO₃²⁻ fully equilibrates its oxygen with water prior to the subsequent oxidation to SO₄²⁻ or if a part of the original isotope signature of SO₃²⁻ is retained in the formed SO₄²⁻. Such an isotopic signature preserved in SO₄²⁻ would provide information on the processes that produced the SO₃²⁻ that was subsequently oxidized. We observed that the preservation of such a signature strongly depends on the interplay between the

rate of oxygen exchange between SO_3^{2-} and water and the SO_3^{2-} oxidation rate. Because of the strong pH dependence of the oxygen exchange rate and the oxidation rate we performed the experiments at different pH (1, 4.9 and 13.3), and found that, as a consequence, the oxygen isotope composition of the produced SO_4^{2-} can be very distinct. By performing the experiments in isotopically distinct solutions or isotopically distinct O_2 in the gas-phase we evaluated if the oxygen isotopes of SO_3^{2-} were in equilibrium with water before the oxidation to SO_4^{2-} and also determined the relative oxygen source contribution. With this information and by knowing the oxygen isotope equilibrium fractionation between sulfite species and water it was possible to calculate the isotope effects of the abiotic oxidation of SO_3^{2-} to SO_4^{2-} by using an isotope mass balance. The anoxic experiments with Fe^{3+} as sole oxidant showed a normal isotope effect of -5.8‰ which is composed of $\frac{3}{4}$ the kinetic fractionation of SO_3^{2-} molecules ($\epsilon_{\text{SO}_3^{2-}\text{Fe}^{3+}\text{H}_2\text{O}\rightarrow\text{SO}_4^{2-}}$) and of $\frac{1}{4}$ the kinetic fractionation of oxygen, which is incorporated from water ($\epsilon_{\text{H}_2\text{O}\text{Fe}^{3+}\text{SO}_3^{2-}\rightarrow\text{SO}_4^{2-}}$). The oxidation of SO_3^{2-} by O_2 ($\epsilon_{\text{SO}_3^{2-}\text{O}_2(\text{aq})\rightarrow\text{SO}_4^{2-}}$) is associated to a normal kinetic fractionation ranging from -5.4‰ to -9.7‰ which is in the range of observed isotope effects in experiments on the oxidation of more reduced sulfur compounds. A consequence of our findings is that the observation of an apparently inverse oxygen isotope effect in studies on the oxidation of reduced sulfur compounds by Fe^{3+} can now be explained by a combination of SO_3^{2-} equilibrium isotope effects and normal kinetic isotope effects related to SO_3^{2-} oxidation. The oxygen isotope offset between SO_4^{2-} and water ($\Delta^{18}\text{O}_{\text{SO}_4\text{-H}_2\text{O}}$) in experiments at different pH conditions and in the presence/absence of $\text{O}_2/\text{Fe}^{3+}$ as oxidant range from 5.9‰ to 17.8‰ (smallest offset observed in experiments at pH 1 and Fe^{3+} as oxidant and highest offset observed in experiments at pH 1 and O_2 as oxidant) and cover the entire range of oxygen isotope signatures of SO_4^{2-} in natural environments. These findings corroborate the importance of SO_3^{2-} in being the final sulfoxy intermediate during the oxidation of reduced sulfur compounds.

Another important process for the production of sulfate is the disproportionation of magmatic SO_2 in hydrothermal vent fluids at the seafloor or in active crater lakes in terrestrial environments (Chapter 4). During the scientific SO-216 cruise onboard of the RV SONNE in the eastern Manus Basin, Papua New Guinea we thoroughly analyzed the sulfur chemistry and isotope composition of sulfur species from a hydrothermally active vent site at North Su which is known to be driven by the disproportionation of magmatic SO_2 . At the southern flank of North Su a vigorous venting area of white smokers was discovered where liquid S^0 is extruded and where the discharged hydrothermal fluids have a pH value as low as 1.2. The fluids contained HSO_4^- concentrations of approximately 71 mmol kg^{-1} , which is double the normal seawater concentration and must have been produced along with the large amounts of S^0 by the disproportionation of SO_2 . Due to the high $\text{SO}_2(\text{aq})$ concentrations in the hydrothermal fluid, I was able to measure for the first the sulfur isotope composition of the magmatic SO_2 in the form of HSO_3^- with a $\delta^{34}\text{S}$ of 12.0‰. The oxygen and sulfur isotope composition of the large amounts of discharged HSO_4^- is close to the seawater sulfate isotope composition whereas the S^0 had a $\delta^{34}\text{S}$ of -4.5‰. The finding that the offset between the oxygen isotope composition of HSO_4^- and the hydrothermal fluid was in a similar range as the offset between the oxygen isotope composition of seawater sulfate and the seawater raises the question if this is more than a coincidence. To answer this question we

performed SO₂ disproportionation experiments in the laboratory. We transferred liquid SO₂ into a glass vial, sealed the vial and transferred it into a bigger glass vial filled with deionized water, which was subsequently sealed as well. The experiment containers were heated to the chosen temperatures (150°C to 320°C). When the designated temperature was reached, the container was shaken vigorously to start the SO₂ disproportionation reaction by breaking the inner glass vial. Similar experiments were performed before, but did not consider the oxygen isotope effects during this process. The oxygen isotope signature during our experiments showed an initial kinetic fractionation between the HSO₄⁻ and the H₂O which is in the range of the known oxygen isotope offset between seawater sulfate and the seawater. With longer duration of the experiment the oxygen isotope offsets approach the oxygen isotope equilibrium fractionation. The sulfur isotope signature was similar to previous studies and showed an initial large kinetic isotope fractionation between the HSO₄⁻ and S⁰ or H₂S approaching as well the equilibrium isotope fractionation at longer duration of the experiments. The laboratory experiments confirm that the similarity between the oxygen isotope composition of sulfate produced from the disproportionation of SO₂ at North Su and seawater sulfate is not a coincidence. Rather, it highlights that the disproportionation of magmatic SO₂ might play a significant role in shaping the oxygen isotope composition of seawater sulfate, by anchoring the oxygen isotope composition of the seawater sulfate over geological times to a narrow range of offsets to the isotope composition of the seawater.

In summary, my dissertation shows that sulfite species play a significant role in shaping the oxygen isotope composition of SO₄²⁻ produced during the oxidative part of sulfur cycling and that this role always needs to be taken into account in the interpretation of oxygen isotope signatures of SO₄²⁻. Our new findings on the oxygen isotope patterns during the disproportionation of SO₂ reveal that this process might act as an anchor for the oxygen isotope composition of seawater sulfate.

Zusammenfassung

Sulfat (SO_4^{2-}) kommt in bedeutenden Mengen auf unseren Planeten vor und ist einer der wichtigsten terminalen Elektronenakzeptoren während des mikrobiellen Abbaus von organischen Material in sauerstofffreier Umgebung. Während der dissimilatorischen Sulfatreduktion (DSR) wird das SO_4^{2-} zu Schwefelverbindungen mit geringerer Oxidationsstufe, wie Schwefelwasserstoff (H_2S), reduziert. Das H_2S wird von den Mikroorganismen wieder ausgestossen und grösstenteils wieder zu SO_4^{2-} oxidiert. Dabei können H_2S , oder andere reduzierte Schwefelverbindungen, über verschiedene Wege oxidiert werden, je nachdem welche Oxidanten in der Lösung vorhanden sind. Potentielle Oxidanten sind Sauerstoff (O_2) aus der Luft und/oder Eisen(III) (Fe^{3+}) im gelösten Zustand. Veränderungen in der relativen Häufigkeit der beiden Oxidanten, führen über unterschiedlichen Wegen zu der Herstellung von SO_4^{2-} . Während der Oxidierung können auch intermediäre Schwefelverbindungen (z.B. $\text{S}_2\text{O}_3^{2-}$, SO_3^{2-} , S^0) auftreten, die zu Schwefelverbindungen mit höherer und niedrigerer Oxidationsstufe disproportioniert werden können. Die Schwefelverbindung mit höherer Oxidationsstufe ist üblicherweise SO_4^{2-} , währenddessen die Schwefelverbindung mit geringerer Oxidationsstufe anschliessend zu SO_4^{2-} aufoxidiert wird. Jeder dieser Prozesse hinterlässt dabei eine spezifische Spur in den Sauerstoffisotopen des SO_4^{2-} und da SO_4^{2-} sehr inert ist und nur unter extremsten Bedingungen Sauerstoff mit dem Wasser austauschen kann, eignen sich die Sauerstoffisotope von SO_4^{2-} bestens, als Archiv für diese Prozesse.

In meiner Dissertation war ich besonders daran interessiert, die Rolle von Sulfit (SO_3^{2-}) im oxidativen Teil des Schwefelkreislaufs zu untersuchen und ob das Vorhandensein von SO_3^{2-} das Potential hat, die Sauerstoffisotopenzusammensetzung des SO_4^{2-} zu beeinflussen. Sulfit ist eine sehr interessante Schwefelverbindung, da es oft als das letzte Schwefelintermediat, während der Oxidierung reduzierter Schwefelverbindungen erachtet wird. Sulfit tauscht im Gegensatz zu SO_4^{2-} sehr rasch seine Sauerstoffatome mit dem Wasser aus und nähert sich zügig dem Sauerstoffisotopenaustauschgleichgewicht an. Wegen der Eigenschaften von SO_3^{2-} müsste sein Vorkommen, als intermediäres Produkt während oxidativer Prozesse im Schwefelkreislauf, in der Sauerstoffisotopenzusammensetzung des SO_4^{2-} zu erkennen sein. Obwohl SO_3^{2-} oft als wichtiges Intermediat erwähnt wird und sein potentieller Einfluss auf die Sauerstoffisotopenzusammensetzung von SO_4^{2-} nicht unsere Erfindung ist, gibt es kaum Studien die die Isotopeneffekte des SO_3^{2-} genauer erforscht haben.

Damit wir die Rolle des SO_3^{2-} in den Signalen der Sauerstoffisotope des SO_4^{2-} entwirren konnten, war es nötig, dass wir erst einmal die Sauerstoffisotopengleichgewichtsfractionierung zwischen SO_3^{2-} und Wasser, mit Hilfe von anoxischen Experimenten bestimmen, in denen wir Natriumsulfit in de-ionisiertes Wasser auflösten (Kapitel 2: "The oxygen isotope equilibrium fractionation between sulfite species and water"). Nachdem wir den Gleichgewichtswert bestimmt hatten, konnten wir den Wert dafür verwenden, um die Sauerstoffisotopeneffekte während der abiotischen Oxidierung von SO_3^{2-} zu SO_4^{2-} zu bestimmen (Kapitel 3: "Isotope evidence of the pivotal role of sulfite oxidation in shaping the oxygen isotope signature of sulfate"). Im letzten Projekt meiner Dissertation untersuchte ich die Isotopeneffekte, die während der Disproportionierung von Schwefeldioxid (SO_2) zu HSO_4^- und elementarem Schwefel (S^0), bei hydrothermalen Temperaturen auftreten. Dieser Prozess scheint öfters als erwartet, in

hydrothermalen Systemen auf dem Meeresboden an Subduktionszonen aufzutreten und dabei grosse Mengen an HSO_4^- und S^0 in das Marine Gefüge einzubringen. Wir vermuten, dass die Disproportionierung von SO_2 in hydrothermalen Systemen, einen Einfluss auf die Sauerstoffisotopenzusammensetzung des Meerwassersulfates haben könnte (Kapitel 4: "The isotope signature of magmatic SO_2 disproportionation: A comparison between laboratory experiments and a hydrothermally active site in the Manus Basin, Papua New Guinea").

Im Folgenden werde ich kurz die drei Projekte meiner Dissertation zusammenfassen und die Höhepunkte, die Prozeduren und die wichtigsten Ergebnisse der Studien erläutern.

Kapitel 2 beschreibt meine Anstrengungen um die Sauerstoffisotopengleichgewichtsfractionierung zwischen SO_3^{2-} und Wasser zu bestimmen und zeigt die Resultate dieser Studie, samt den Implikationen für die Sauerstoffisotopensignatur des SO_4^{2-} . Ich absolvierte dafür abiotische SO_3^{2-} -Wasser-Sauerstoffaustausch Experimente in isotopisch markierten Lösungen, unter verschiedenen pH Bedingungen. Sulfid kommt in Lösung in Form unterschiedlicher Speziationen vor, die die gleiche Oxidationsstufe (+IV) haben, Schwefeldioxid (SO_2), Bisulfid (HSO_3^-), Pyrosulfid ($\text{S}_2\text{O}_5^{2-}$) und das eigentliche Sulfid (SO_3^{2-}). Während der Experimente hatten wir es mit einigen Herausforderungen zu tun, wie zum Beispiel, dass die einzelnen Speziationen unterschiedliche Sauerstoffisotopengleichgewichtsfractionierungen gegenüber dem Wasser haben, dass Wassersauerstoff während der Ausfällung in die Sulfidsalze eingebaut wird, dass während der Ausfällung noch Sauerstoffaustausch mit dem Wasser stattfindet und dass ein Kontaminant in das Sulfidfällungsprodukt miteingebaut wird. Da wir die Experimente in Lösungen mit unterschiedlicher Isotopenzusammensetzung ausführten, konnten wir den Anteil des SO_3^{2-} Sauerstoffes bestimmen, der im Isotopengleichgewicht mit der Experimentallösung ist und mit Hilfe isotopisch unterschiedlicher Ausfällungslösungen, konnten wir den Anteil des Wassersauerstoffes bestimmen, der während der Ausfällung mit in das Präzipitat eingebaut wird. Durch das Zufügen einer Bariumhydroxidlösung während der Ausfällung, konnten wir den pH der Lösung rasch zu Werten über 12 schieben und damit sofort den Sauerstoffaustausch zwischen dem SO_3^{2-} und dem Wasser unterbinden. Mit dieser Vorgehensweise, die auf alle experimentellen Herausforderungen eine Antwort parat hat und mit einer Isotopenmassenbilanz die alle Sauerstoffquellen berücksichtigt, war es uns möglich, einen genauen Wert für die Sauerstoffisotopengleichgewichtsfractionierung zwischen SO_3^{2-} und Wasser, von $\epsilon^{\text{EQ}}_{\text{SO}_3^{2-} \leftrightarrow \text{H}_2\text{O}} = 15.2\%$ zu bestimmen und eine grobe Schätzung für die Sauerstoffisotopengleichgewichtsfractionierung zwischen SO_2 und Wasser, von $\epsilon^{\text{EQ}}_{\text{SO}_2 \leftrightarrow \text{H}_2\text{O}} = 37.0\%$ abzugeben.

Nach der Bestimmung des Gleichgewichtswertes der Sauerstoffisotopenfractionierung zwischen den Sulfid Speziationen und Wasser, benützten wir diesen Wert für die Interpretierung von Resultaten der Experimente, in denen wir SO_3^{2-} zu SO_4^{2-} oxidierten. Diese Experimente waren genau geplant, um neue Einsichten in den Mechanismus zu erhalten, der für die beobachtete Sauerstoffisotopensignatur in oxidativen Prozessen des Schwefelkreislauf verantwortlich ist. Kapitel 3 beschreibt die abiotische Oxidierung von SO_3^{2-} zu SO_4^{2-} mit unterschiedlichen Oxidanten (O_2 und/oder Fe^{3+}) und unterschiedlichen pH Bedingungen. Abhängig von dem Oxidant, der in der Lösung vorhanden ist, wird der letzte Sauerstoff während der Oxidation zu SO_4^{2-} , von O_2 oder H_2O kommen. In natürlichen Umgebungen haben diese beiden Sauerstoffquellen sehr unterschiedliche Sauerstoffisotopenzusammensetzungen, dank denen man die zwei

Oxidierungswege voneinander unterscheiden kann. Mit einer Isotopenmassenbilanz ist es sogar möglich die relativen Beiträge der beiden Sauerstoffquellen zu quantifizieren. Im Fall der SO_3^{2-} Oxidierung stellt sich die Frage, ob SO_3^{2-} seinen Sauerstoff komplett mit dem Wasser austauscht, bevor er zu SO_4^{2-} oxidiert wird, oder ob nur ein Teil des Sauerstoffes ausgetauscht wird und ein Teil der ursprünglichen Sauerstoffisotopenzusammensetzung des SO_3^{2-} im SO_4^{2-} erhalten bleibt. Solch eine Isotopensignatur die im SO_4^{2-} erhalten bleibt, würde Informationen über die Prozesse beinhalten, die das SO_3^{2-} produziert haben. Wir beobachteten in unseren Experimenten, dass die Erhaltung so einer Isotopensignatur, stark von dem Zusammenspiel der Rate des Sauerstoffaustausches zwischen SO_3^{2-} und Wasser und der Oxidierungsrate von SO_3^{2-} abhängig ist. Wegen der starken pH Abhängigkeit beider Raten, führten wir die Experimente bei unterschiedlichen pH Bedingungen durch (1, 4.9 und 13.3) und beobachteten, dass die Sauerstoffisotopenzusammensetzung des SO_4^{2-} stark variiert. Dadurch, dass wir die Experimente in isotopisch unterschiedlichen Lösungen oder isotopisch unterschiedlichem O_2 in der Gasphase ausführten, konnten wir evaluieren, ob sich die Sauerstoffisotope des SO_3^{2-} vor der Oxidierung im Gleichgewicht mit dem Wasser befinden und konnten die relativen Anteile beider Sauerstoffquellen, im SO_4^{2-} bestimmen. Mit dieser Information und dem Wert für die Sauerstoffisotopengleichgewichtsfractionierung zwischen SO_3^{2-} und Wasser, war es uns möglich mit Hilfe einer Isotopenmassenbilanz die Isotopeneffekte der abiotischen Oxidierung von SO_3^{2-} zu bestimmen. Die anoxischen Experimente mit Fe^{3+} als einzigen Oxidant, zeigten einen normalen Isotopeneffekt von -5.8% , der zu $\frac{3}{4}$ aus der kinetischen Fraktionierung der SO_3^{2-} Moleküle ($\epsilon_{\text{SO}_3^{2-}/\text{Fe}^{3+}/\text{H}_2\text{O} \rightarrow \text{SO}_4^{2-}}$) und zu $\frac{1}{4}$ aus der kinetischen Fraktionierung des Sauerstoffes aus dem Wasser kommend ($\epsilon_{\text{H}_2\text{O}/\text{Fe}^{3+}/\text{SO}_3^{2-} \rightarrow \text{SO}_4^{2-}}$) besteht. Die Oxidierung des SO_3^{2-} mit O_2 ist mit einer normalen kinetischen Fraktionierung verbunden ($\epsilon_{\text{SO}_3^{2-}/\text{O}_2(\text{aq}) \rightarrow \text{SO}_4^{2-}}$), die zwischen -5.4% und -9.7% liegt. Eine Folgerung unserer Ergebnisse ist, dass die Beobachtung einer scheinbar inversen Isotopenfraktionierung in Studien über die Oxidierung reduzierter Schwefelverbindungen mit Fe^{3+} , nun mit der Kombination eines SO_3^{2-} -Wasser-Sauerstoffgleichgewichtsaustauscheffekts und eines normalen kinetischen Isotopeneffektes, während der Oxidierung von SO_3^{2-} , erklärt werden kann. Die Sauerstoffisotopenunterschiede zwischen SO_4^{2-} und Wasser ($\Delta^{18}\text{O}_{\text{SO}_4\text{-H}_2\text{O}}$) in den Experimenten mit unterschiedlichen pH Bedingungen und unterschiedlichen Oxidanten (O_2 und/oder Fe^{3+}), liegen zwischen 5.9% und 17.8% (kleinste Wert beobachtet in Experimenten mit pH 1 und Fe^{3+} , höchster Wert beobachtet in Experimenten mit pH 1 und O_2) und decken den ganzen Bereich der Sauerstoffisotopensignaturen von SO_4^{2-} in natürlicher Umgebung ab. Diese Ergebnisse bekräftigen die Wichtigkeit von SO_3^{2-} als letztes Intermediat, während der Oxidierung reduzierter Schwefelverbindungen.

Ein anderer wichtiger Prozess für die Herstellung von SO_4^{2-} , ist die Disproportionierung von magmatischen SO_2 in hydrothermalen Fluiden am Meeresboden, oder in aktiven Kraterseen in terrestrischen Umfeld (Kapitel 4). Während der wissenschaftlichen Ausfahrt SO-216 an Bord der FS SONNE, im östlichen Manus Becken von Papua Neuguinea, analysierten wir die Schwefelchemie und die Isotopenzusammensetzung der Schwefelverbindungen von der hydrothermal aktiven Gegend bei North Su, von der bekannt ist, dass ihre Prozesse von der Disproportionierung magmatischen SO_2 's angetrieben werden. An der südlichen Flanke von North Su

entdeckten wir eine heftig austauschende Gegend mit Weissen Rauchern, bei der flüssiger S^0 aus dem Meeresboden austrat und die hydrothermalen Fluide einen extrem niedrigen pH Wert von nur 1.2 hatten. Die Fluide beinhalteten HSO_4^- Konzentrationen (71 mmol kg^{-1}) doppelt so hoch wie die normalen Meereswasserkonzentrationen und die, zusammen mit den grossen Mengen S^0 , aus der Disproportionierung von SO_2 entstanden sind. Wegen der hohen Konzentrationen von $SO_2(aq)$ war es uns möglich, als erste jemals die Schwefelisotopenzusammensetzung des magmatischen SO_2 von 12.0‰, aus hydrothermalen Fluiden des Meeresbodens zu bestimmen. Die Sauerstoff- und die Schwefelisotopenzusammensetzung des HSO_4^- ist ähnlich der Zusammensetzung von Meerwassersulfat, wohingegen der S^0 eine Schwefelisotopenzusammensetzung von -4.5‰ hatte. Die Beobachtung, dass der Unterschied der Sauerstoffisotopenzusammensetzung zwischen HSO_4^- und dem hydrothermalen Fluid im gleichen Bereich lag, wie der Sauerstoffisotopenunterschied zwischen Meerwassersulfat und Meerwasser, warf die Frage auf, ob das mehr als Zufall war. Um diese Frage zu beantworten, machten wir SO_2 Disproportionierungsexperimente im Labor. Dabei füllten wir flüssiges SO_2 in ein kleines Glasgefäss, schlossen es und gaben es in ein grösseres Glasgefäss mit Wasser. Dieses wurde ebenfalls verschlossen und danach auf die gewünschte Temperatur aufgeheizt (150°C bis 320°C). Nachdem die gewünschte Temperatur erreicht war, wurden die Experimentbehälter kräftig geschüttelt, damit das SO_2 Disproportionierungsexperiment durch das Brechen des inneren Glases gestartet wird. Ähnliche Experimente wurden bereits ausgeführt um die Schwefelisotopeneffekte zu untersuchen, allerdings wurde dabei den Sauerstoffisotopen keine Beachtung geschenkt. Die Sauerstoffisotopensignatur in unseren Experimenten, zeigte eine grosse initiale kinetische Fraktionierung zwischen dem HSO_4^- und dem Wasser, die im gleichen Bereich lag, wie der bekannte Sauerstoffisotopenunterschied zwischen Meerwassersulfat und Meerwasser. Mit längerer Experimentdauer näherten sich die Sauerstoffisotopenunterschiede der Gleichgewichtsfraktionierung an. Die Schwefelisotopensignatur verhielt sich ähnlich wie in den älteren Studien, sie zeigte eine grosse initiale kinetische Fraktionierung zwischen HSO_4^- und S^0 oder H_2S und näherte sich danach ebenfalls der Gleichgewichtsfraktionierung an. Die Laborexperimente belegen, dass die Ähnlichkeit der Sauerstoffisotopenzusammensetzung von HSO_4^- , produziert von der Disproportionierung von SO_2 bei North Su und dem Meerwassersulfat kein Zufall sind. Es zeigt viel mehr, dass die Disproportionierung von magmatischen SO_2 eine entscheidende Rolle in der Formung der Sauerstoffisotopenzusammensetzung des Meerwassersulfates spielen könnte, wobei die Sauerstoffisotopenzusammensetzung des Meerwassersulfates über geologische Zeiträume, an einen engen Bereich der Sauerstoffunterschiede relativ zu der Sauerstoffisotopenzusammensetzung des Meerwassers verankert wird.

Zusammenfassend, meine Dissertation zeigt, dass Sulfitspezierungen eine entscheidende Rolle für die Formung der Sauerstoffisotopenzusammensetzung von SO_4^{2-} während dem oxidativen Part des Schwefelkreislaufs spielen und dass diese Rolle immer in der Interpretation der Sauerstoffisotopensignatur des SO_4^{2-} berücksichtigt werden muss. Unsere neuen Erkenntnisse zu den Sauerstoffisotopenmuster während der Disproportionierung von SO_2 , offenbaren, dass dieser Prozess eine Art Anker für die Sauerstoffisotopenzusammensetzung des Meerwassersulfates ist.

1. General introduction

1.1. The sulfur cycle

Sulfur is a highly reactive element and exists at different oxidation states on our planet ranging from -II for hydrogen sulfide (H_2S) as the most reduced sulfur compound to +VI for sulfate (SO_4^{2-}) the most oxidized sulfur compound, which is in the modern O_2 atmosphere the most stable sulfur compound. Many scientists tried to describe the processes that lead from more reduced sulfur compounds to more oxidized sulfur compounds and *vice versa* in form of a cycle, the so-called sulfur cycle (Fig. 1.1, see Canfield, 2001 or Bottrell and Newton, 2006). Thanks to improved sampling devices and analytical methods and accompanying experimental approaches in laboratory experiments the knowledge about the sulfur processes in natural environments became more and more complex and thus today the sulfur cycle is known to involve many intermediate products and pathways. Sulfur compounds such as SO_4^{2-} can be reduced in anoxic environments by dissimilatory sulfate reduction to H_2S via various inorganic sulfur intermediates as well as sulfur enzyme complexes that have to be taken in account and which are not illustrated in the simplified scheme in Fig. 1.1. Some of the sulfur intermediates that are produced during the oxidative part of the sulfur cycle can be disproportionated which means they are split up into sulfur compounds with sulfur being at higher and lower oxidation state (Granger and Warren, 1969). This could also be the case for sulfur intermediates during the sulfate reduction, but as this would be an intracellular process there it is little information about this hypothetical process (Trithionate pathway, Akagi, 1995). The biogeochemical redox reactions depicted in Fig. 1.1 are an important part of the global biogeochemical sulfur cycle.

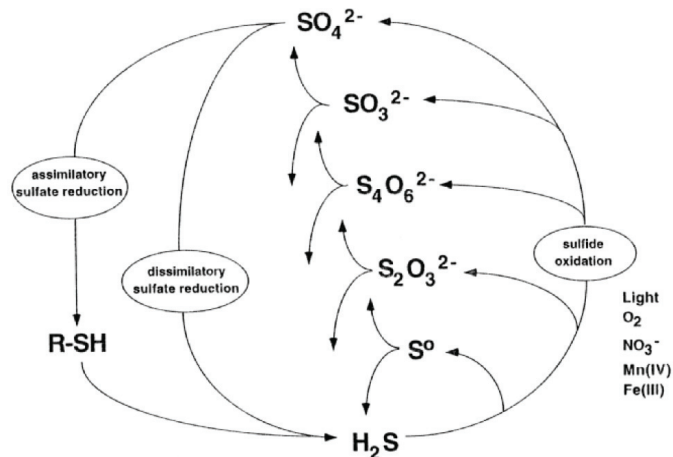


Fig. 1.1: Simplified scheme for cycling of sulfur with SO_4^{2-} (sulfur +VI) being reduced via assimilatory or dissimilatory sulfate reduction and H_2S (sulfur -II) is oxidized in the presence of oxidizing agents. Various sulfur intermediates are produced during the sulfur oxidation of more reduced sulfur compounds and can be disproportionated to sulfur compounds at higher and lower oxidation state (scheme taken from Canfield, 2001).

1.1.1. The global sulfur cycle: sources and sinks

Sulfur is constantly discharged into the ocean or atmosphere from the mantle in volcanically active areas at mid ocean ridges (MOR), above subduction zones or by the weathering of sulfur bearing minerals. At MOR settings tectonic plates drift apart from each other and new basaltic crust is formed in large amounts. During these melting processes sulfur compounds from the magma source are released into the crust where they will be mixed with hydrothermal fluids that discharge at focused spots in orifices or via diffuse venting along the MOR (Peters et al., 2010). Discharge of sulfur compound bearing hydrothermal fluids at focused spots is responsible for the formation of so-called black smokers or depending on the composition of the hydrothermal fluid grey and white smokers. The hydrothermal fluids discharged along the MORs contain high amounts (~ 1 to 5 mmol kg^{-1}) of reduced sulfur in form of H_2S (Charlou et al., 2000). The oxidation of H_2S serves chemolithotrophic organisms as important source of energy to fix carbon. Chemolithotrophic life could have evolved very early on Earth, in a time when no or little molecular oxygen (O_2) was present in the atmosphere because hydrothermal venting of so-called geofuels enabled microorganisms to live independent of sunlight through the coupling of production of organic compounds (reduction of carbon from carbonate) and oxidation of reduced geofuels. The discharge of sulfur compounds in volcanically active areas related to subduction zones is only well studied at terrestrial volcanoes which are often found on the island arcs or on the continental margins around the Pacific Ocean (“ring of fire”). Global estimates give a SO_2 flux of $1.5\text{-}50 \text{ Tg yr}^{-1}$ and a H_2S flux of $1\text{-}2.8 \text{ Tg yr}^{-1}$ (Von Glasow et al., 2009 and references therein). In subduction related volcanic settings emissions of H_2S and mainly sulfur dioxide (SO_2) were observed (Menyailov et al., 1986; Williams et al., 1990; Khokhar et al., 2005). The emission of SO_2 can affect the climate by acting as a cloud condensation nuclei and thereby increasing the Earth’s albedo (Wigley, 1989). Depending on the volcanic eruption style the volcanic plume can reach the stratosphere where SO_2 can affect the global climate for years, whereas at less vigorous eruptions the plume stays in the atmosphere and the SO_2 will be oxidized and rained out within days to weeks in form of acid rain (von Glasow et al., 2009). Notably, during the last few centuries anthropogenic emissions became a major source of SO_2 to the atmosphere. The anthropogenic contribution (-0.17 W m^{-2}) to total sulfate aerosol radiative forcing is in the same range as the emissions from volcanoes (-0.15 W m^{-2} ; Graf et al., 1998).

Another volcanically active setting related to subduction zones can be found in back-arc basins where the slab of the subducted plate induces a slab pull situation on the overlying plate which causes extensional stresses and the production of back-arc spreading centers with accompanying transform faults. Due to these tectonic features back-arc basins are volcanically very active allowing the existence of hydrothermal systems. In addition to the mantle as sulfur source there could be also a contribution of sulfur from the subducted plate. To date there are only few studies that investigated the sulfur chemistry in back-arc basin related hydrothermal sites. A recent study on a submarine volcano near the Mariana Arc by Butterfield and colleagues (2011) indicated that submarine volcanically active environments related to subduction zones might contribute significantly to global sulfur cycling. Butterfield et al. (2011) discovered vigorous venting white smokers where massive amounts of magmatic $\text{SO}_2(\text{aq})$ are

discharged into the seawater (concentrations up to 163 mmol kg^{-1}) and the authors raised the question if such hydrothermally active sites are representative for submarine arc settings, this could have an important impact on the global sulfur flux to the ocean. Chapter 4 describes a similar hydrothermal system with vigorous venting of a sulfur rich fluid in the back-arc Manus Basin, Papua New Guinea and the analyses at this hydrothermal system support the hypothesis of Butterfield et al. (2011).

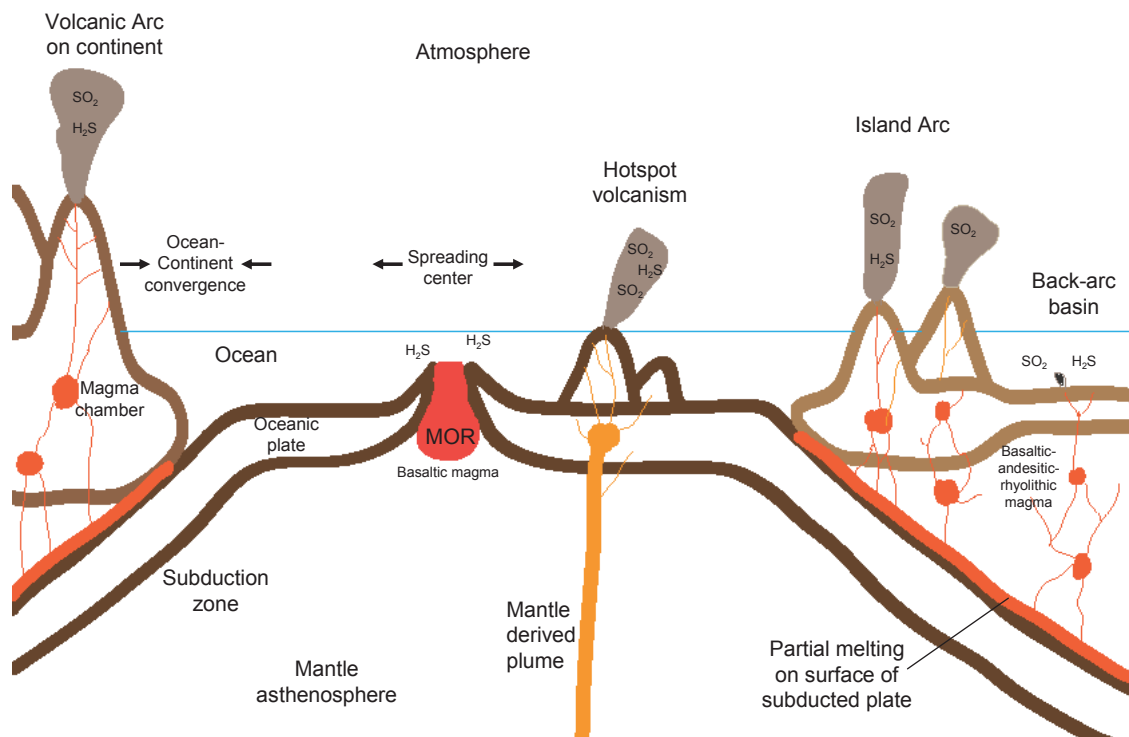


Fig. 1.2: Volcanic settings on Earth related to plate tectonics and their role as sulfur source for the exogenic sulfur cycle.

The third important sulfur source over geological time scales is the weathering of sulfur bearing minerals on the continents with approximately 100 Tg S yr^{-1} (see Bottrell and Newton, 2006). Thereby, massive amounts of sulfate minerals such as gypsum ($\text{CaSO}_4 \cdot 2\text{H}_2\text{O}$), anhydrite (CaSO_4), barite (BaSO_4) or celestite (SrSO_4) along with sedimentary sulfides (e.g. pyrite FeS_2) that were precipitated earlier in marine environments are dissolved during continuous erosion and chemical weathering of sedimentary rocks that have been uplifted by tectonic processes such as the collision of tectonic plates. Beside sedimentary sulfur bearing minerals, massive sulfide ore deposits (e.g. FeS_2 , FeS , $(\text{Zn,Fe})\text{S}$, PbS) can be found in terrestrial environments, that were formed prior in hydrothermally active systems (Ohmoto, 1996), and also igneous and metamorphic rock contain sulfur bearing mineral phases. Sulfate derived from the weathering of the continental rocks are transported via rivers into freshwater lakes and will be finally supplied to the ocean.

On the side of sulfur sinks in the global sulfur cycle are the precipitation of evaporites such as gypsum in enclosed basins (Babel, 2007 and references therein), the precipitation

of sulfate minerals (anhydrite) in hydrothermal systems (Craddock and Bach, 2010) and the precipitation of metal sulfides in anoxic sediments (Jørgensen et al., 1990) as well as in hydrothermal systems (Scott and Binns, 1995) that act as sinks during the global sulfur cycling (estimates in Bottrell and Newton, 2006).

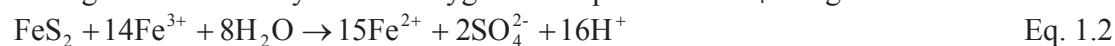
These different sources and sinks of sulfur compounds resupply diverse environments on our planet with various sulfur compounds of different oxidation states since billions of years and allow the existence of a most diverse range of microorganisms.

1.1.2. Oxidation of reduced sulfur compounds

The oxidation of reduced sulfur compounds can occur abiotically or biologically by sulfide oxidizing bacteria. The reduced sulfur compounds are most abundant in anoxic sediments with active sulfate reduction and in the hydrothermal systems where high amounts of H₂S or metal sulfides are discharged. Another place with high densities of sulfide minerals are active and former ore mining sites that provide an open access to chemical weathering and/or to sulfur oxidizing microorganisms, typically resulting in the rapid oxidation of H₂S to SO₄²⁻. In shallow waters such as in lakes, acid pools or in the shelf area of the oceans oxidation of reduced sulfur compounds can be carried out by photosynthetic green or purple sulfur bacteria (GSB and PSB, respectively; Martínez-Alonso et al., 2005). These photolithotrophic bacteria depend on the sunlight and on a source of reduced sulfur compounds (e.g. H₂S, S⁰, S₂O₃²⁻), such as decaying organic material or H₂S produced during active microbial sulfate reduction (Ghosh and Dam, 2009). Both GSB and PSB use the reduced sulfur compounds as electron donors for the fixation of CO₂ during the anoxygenic growth (Frigaard and Dahl, 2009). Studies on the enzyme system of sulfur oxidizing bacteria indicated that reduced sulfur compounds are oxidized via different pathways which involve different sulfur intermediates (Friedrich et al., 2005; Ghosh and Dam, 2009). Chemolithotrophic sulfur oxidizers such as *Beggiatoa spp.* (Schwedt et al., 2012), *Thiobacillus thiooxidans* (Schippers and Sand, 1999) or *Acidithiobacillus ferrooxidans* (Balci et al., 2007) oxidize reduced sulfur compounds independent of light, but require an oxidant, such as O₂, nitrate, manganese or iron oxides. In aqueous environments that contain both O₂ and ferric iron (Fe³⁺), which is typical for mining sites where acidophilic organism perform pyrite oxidation, the oxidation pathways may differ (Taylor et al., 1984a; Taylor et al., 1984b; Rimstidt and Vaughan, 2003; Balci et al., 2007). Both oxidation reactions with O₂ and Fe³⁺ produce protons, often causing extreme acidic conditions:



During the oxidation with O₂ via Eq. 1.1 seven oxygen atoms in the produced SO₄²⁻ molecules are derived from O₂ and one oxygen atom comes from the water source. During the oxidation by Fe³⁺ all oxygen in the produced SO₄²⁻ originates from water:



Although it appears that during the oxidation with Fe³⁺ a much more acidic environment is produced, this is not the case if oxidation of ferrous iron (Fe²⁺) to ferric iron with O₂ accompanies the process of Eq. 1.2:



The oxidation of ferrous iron (Fe^{2+}) in Eq. 1.3 is necessary to provide reaction Eq. 1.2 with Fe^{3+} and initializes a cycle where Fe^{3+} is reduced back to Fe^{2+} during the oxidation of reduced sulfur compounds and returns back into Eq. 1.3 (Stumm and Lee, 1961; Singer and Stumm, 1970). The experiments of Taylor and colleagues (1984b) already demonstrated that the relative contribution of each pathway varies strongly and in natural environments a mixture between both oxidation pathways is common. Although many studies investigated the oxidation of reduced sulfur compounds, the detailed oxidation mechanisms are still unclear. Only few studies (e.g. Granger and Warren, 1969; Schippers et al., 1996; Schippers and Sand, 1999; Rimstidt and Vaughan, 2003; Druschel and Borda, 2006) made the attempt to explain the oxidation mechanisms in more detail. The oxidation of reduced sulfur compounds is most probably a multi-step process involving many sulfur intermediates that might vary for the different oxidation pathways. Due to their high reactivity together with low abundances these inferred compounds are extremely difficult to detect. Schippers and colleagues (1996) postulated that thiosulfate ($\text{S}_2\text{O}_3^{2-}$) is the first intermediate that forms after the Fe^{3+} is attacking at low pH at the pyrite (FeS_2) surface, further polythionates (e.g. $\text{S}_4\text{O}_6^{2-}$) were detected, probably from the oxidation of $\text{S}_2\text{O}_3^{2-}$ by Fe^{3+} . Similar processes could occur also at higher pH with other polythionates such as trithionate ($\text{S}_3\text{O}_6^{2-}$) or pentathionate ($\text{S}_5\text{O}_6^{2-}$) and the $\text{S}_4\text{O}_6^{2-}$ could be hydrolyzed to the highly reactive disulfane-monosulfonic acid ($\text{S}_3\text{O}_3^{2-}$) which can further react to elemental sulfur (S_8) and SO_3^{2-} :



The pyrite leaching bacteria *Thiobacillus ferrooxidans* and *Leptospirillum ferrooxidans* carry Fe^{3+} ions in their exopolymer layer (Gehrke et al., 1995), most probably to attach their cells to the sulfide minerals and to detach the sulfur compounds from the mineral surface (Schippers et al., 1996). In another study two indirect oxidation mechanisms for metal sulfides were proposed both being initiated by the oxidative attack of Fe^{3+} on the surface of the mineral (Schippers and Sand, 1999). In one mechanism, the so-called thiosulfate mechanism, leaching of pyrite (FeS_2), molybdenum disulfide (MoS_2) or tungsten disulfide (WS_2) proceeds via the release of sulfur from the mineral as $\text{S}_2\text{O}_3^{2-}$, whereas in the second mechanism, the so-called polysulfide mechanism, polysulfides will be formed during the leaching of sphalerite (ZnS), chalcopyrite (CuFeS_2) or galena (PbS), with subsequent reaction to S_8 (Schippers and Sand, 1999). Rimstidt and Vaughan (2003) explain the pyrite oxidation with a three step model of which the three steps occur simultaneously. The first step is the cathodic reaction where an aqueous species such as $\text{O}_2(\text{aq})$ or Fe^{3+} attaches on the mineral surface to accept electrons at the Fe^{2+} site. The second step is an electron transport from the anodic site through the pyrite which acts as a semiconductor. The third step is the anodic reaction where the sulfide sulfur or disulfide sulfur gets oxidized to SO_4^{2-} via multiple steps. Due to the fact that only one or maximal two electrons can be transferred per oxidation step, many attempts have been undertaken to identify the involved intermediates (see references in Rimstidt and Vaughan, 2003). At the anodic site H_2O molecules will form complexes with OH^- being attached to the pyrite releasing electrons and protons. At a certain point in a complex reaction chain the Fe-S bond will be weakened so much that $\text{S}_2\text{O}_3^{2-}$ will be released into solution which decomposes quickly at acidic conditions to S^0 and sulfurous acid (Rimstidt and Vaughan, 2003):



Similar pathways are supposed in Druschel and Borda (2006), who consider a pathway where $S_2O_3^{2-}$ is detached from the mineral and reacts via Eq. 1.5 or via oxidation by Fe^{3+} to $S_4O_6^{2-}$ and a pathway where the Fe-S bond is stronger and SO_3^{2-} is detached instead which oxidizes rapidly to SO_4^{2-} . Druschel and Borda also evaluate the polysulfide pathway (after Schippers and Sand, 1999) and a third pathway which is driven by defects in the pyrite lattice or induced photochemically which increases the reactivity of the pyrite for the nucleophilic attack by water molecules (see Fig. 1.3).

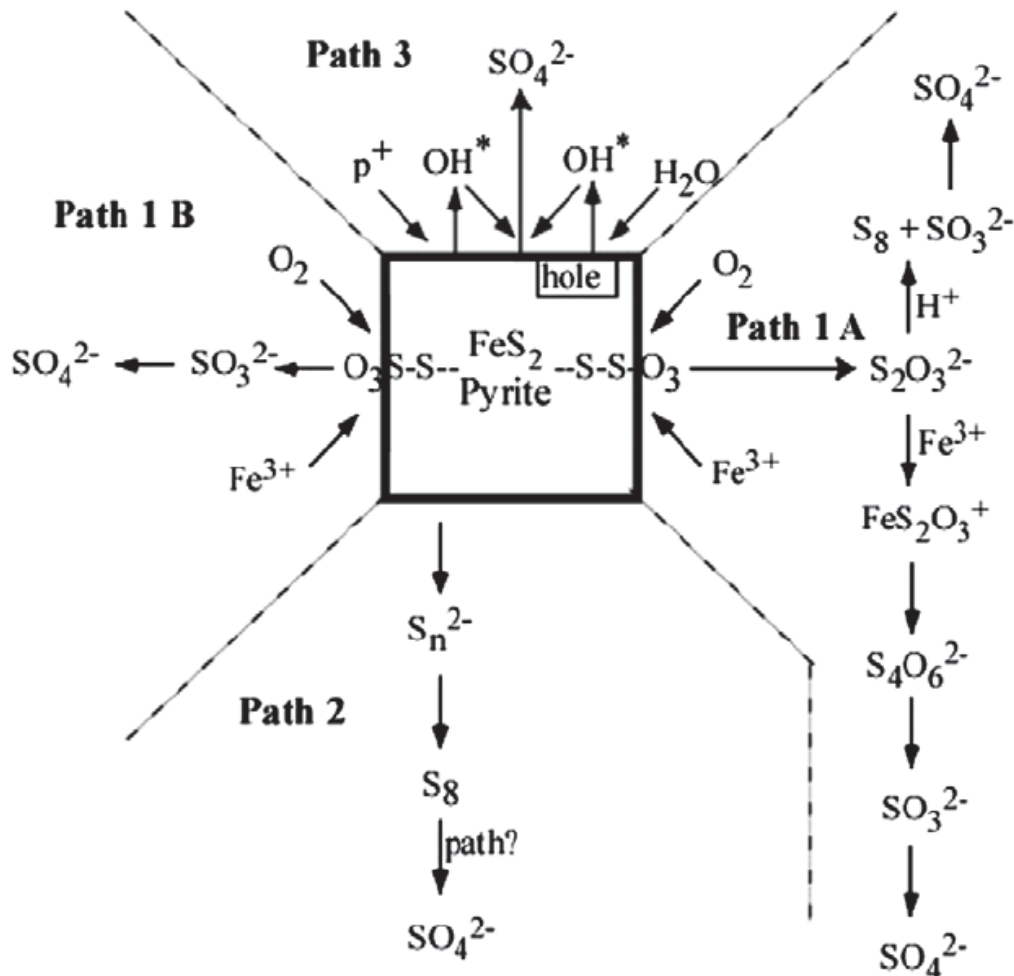


Fig. 1.3: Different oxidation pathways of pyrite described in Druschel and Borda (2006).

Despite all the efforts in the study of sulfide mineral oxidation pathways, it remains unclear at which hydrochemical conditions which oxidation pathway occurs, what sulfoxy intermediates play an important role and also the function and role of microorganisms remain unresolved. Sulfoxy intermediates such as $S_3O_6^{2-}$, $S_4O_6^{2-}$, $S_5O_6^{2-}$, $S_2O_3^{2-}$, $S_3O_3^{2-}$ and SO_3^{2-} are expected to be involved during the oxidation pathways (Schippers et al., 1996; Druschel and Borda, 2006), but better detection methods or further experimental studies are needed to determine the role of each sulfoxy intermediate. Microbiological studies continue to shed more and more light on the utilized oxidation

pathways by allowing for the identification of specific enzymes that are necessary to cope with certain sulfur compounds (see Ghosh and Dam, 2009). These studies in combination with stable isotope approaches and geochemical analyses using HPLC and X-ray absorption near edge structure (XANES) spectroscopy (Franz et al. 2009) might be the best approach to understand the mechanism of the oxidation of reduced sulfur compounds more in detail in the future.

1.1.3. Dissimilatory sulfate reduction (DSR)

Sulfate is the most abundant sulfur compound at the surface of the Earth which includes the oceans, sediments and freshwater. Many microorganisms have the ability to respire organic matter or H_2 by reducing SO_4^{2-} to gain energy for their growth in the absence of O_2 :



Energy yielding alternatives are needed in marine sediments where O_2 is rapidly depleted in the upper most part of the sediment column (Bethke et al., 2011). Beside the microbial reduction of metals (e.g. Mn, Fe) or nitrate (NO_3^-) dissimilatory sulfate reduction (DSR) is mainly responsible for the mineralization of organic matter in anoxic sediments at various places on Earth (Jørgensen, 1977; Jørgensen et al., 1990; Canfield et al., 1993; Jørgensen et al., 2001; Böttcher et al., 2004; Omoregie et al., 2009). The final product of the DSR is H_2S which is excreted from the cell either passively due to its volatility or actively because high concentrations of H_2S can be toxic. Most of the expelled H_2S will diffuse to the sediment surface where it is oxidized back to SO_4^{2-} in the presence of O_2 or other oxidants (approximately 90%, after Jørgensen, 1982); only a small percentage will be buried as pyrite and leave the loop of active sedimentary sulfur cycling. It is not only the global distribution but also the finding that DSR already occurred in the early Achaean that makes it such an important process for the mineralization of organic matter (Shen and Buick, 2004; Roerdink et al., 2012). Thus microbial sulfate reduction must have influenced the cycling of sulfur already since the early history of the Earth. The overall reactions of microbial sulfate reduction are well known (Eq. 1.6 and Eq. 1.7) but the detailed reaction mechanism and its consequences on the atomic properties of the sulfur compounds are much more complex and still a matter of debate. Today it is accepted that DSR is comprised of multiple, reversible enzymatic steps that occur inside the cell. Sulfate is taken up into the cell from the surrounding solution (step 1) and is activated with ATP (adenosine triphosphate) by ATP sulfurylase in the cytoplasm to the sulfur intermediate APS (adenosine 5'-phosphosulfate; step 2; Peck Jr., 1959). The APS is then reduced to SO_3^{2-} in step 3 incorporating two electrons during the enzymatic reduction catalyzed by APS reductase (Peck Jr., 1960; Peck Jr. and Stulberg, 1962; Fritz et al., 2002). The last step in DSR (Fig. 1.4) is the single step reduction of SO_3^{2-} to H_2S by sulfite reductase (step 4), but there are studies that proposed step 4 involves sulfoxy intermediates such as thiosulfate ($S_2O_3^{2-}$) and trithionate ($S_3O_6^{2-}$; Kemp and Thode, 1968; Kobayashi et al., 1969; Rees et al., 1973; Kobayashi et al., 1974; Fitz and Cypionka, 1990; Akagi, 1995). Additionally, the last step 4 in Fig. 1.3 is drawn as unidirectional (after Canfield, 2001), but isotope modeling approaches and previous studies with the sulfate reducing bacteria *Desulfobacter latus* revealed that step 4 could

be reversible as well (Brunner and Bernasconi, 2005; Eckert et al., 2011). Some degree of reversibility is certainly expected if the reduction from SO_3^{2-} to H_2S is a multistep reaction and involves sulfoxy intermediates such as $\text{S}_3\text{O}_6^{2-}$ and $\text{S}_2\text{O}_3^{2-}$ which are thought to form SO_3^{2-} during further reduction to H_2S (Kobayashi et al., 1969; Fitz and Cypionka, 1990; Akagi, 1995).

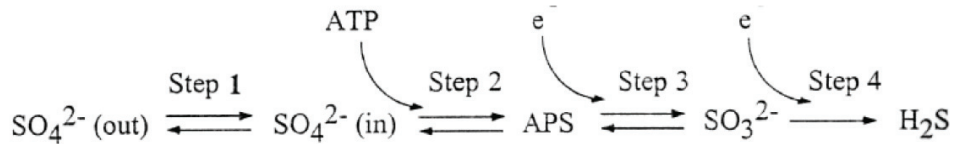


Fig. 1.4: Pathway of the stepwise enzymatic dissimilatory sulfate reduction (from Canfield, 2001).

Most of the findings on the mechanism of the DSR originate from physiological and enzyme based studies on pure cultures of *Desulfovibrio desulfuricans*, but meanwhile many other sulfate reducing organisms were cultured which are thought to perform DSR in the same way as *Desulfovibrio desulfuricans* (e.g. Davidson et al., 2009 (*Desulfotomaculum putei*); Eckert et al., 2011 (*Desulfobacter latus*)). A recent study Fritz and colleagues (2002) thoroughly investigated the molecular and catalytic properties during the third step in Fig. 1.4, the reduction from APS to SO_3^{2-} . They proposed that the APS reduction step by the APS reductase starts with FAD being reduced first and the N-5 of the FAD binding to the APS via a nucleophilic attack at the sulfur atom. When the FAD-APS intermediate is formed its electron structure is rearranged, AMP (adenosine monophosphate) released and the N(5)-sulfite adduct formed. The SO_3^{2-} is probably protonated and dissociates in form of bisulfite (HSO_3^-) from the oxidized FAD as illustrated in Fig. 1.5 (from Fritz et al., 2002):

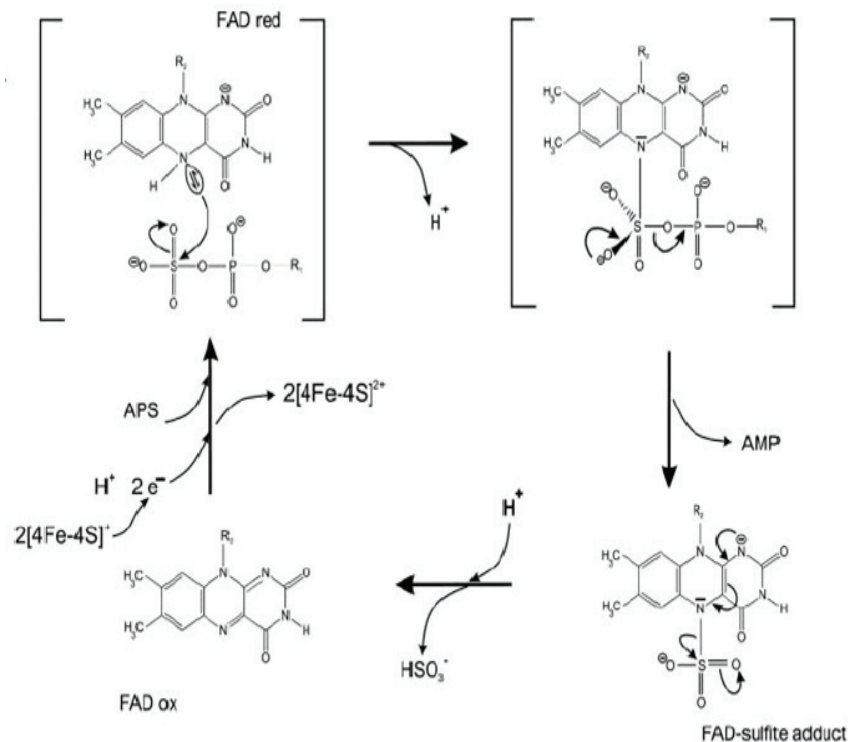


Fig. 1.5: Proposed mechanism of the reduction of APS by APS reductase during DSR (from Fritz et al., 2002).

During the reverse of step 3 the sulfite attaches first at the N-5 atom of the oxidized FAD, the negative charge of the sulfite will shift towards the FAD enabling the nucleophilic attack of the AMP on the sulfur atom of the FAD-sulfite complex (Fritz et al., 2002). Afterwards electrons will be rearranged and APS is freed from the FAD which is now reduced by two electrons. The authors further note that during the reduction or the oxidation step of APS two $[4Fe-4S]$ clusters in the APS reductase serve as transfer mechanism for the electrons from the protein surface to the FAD site and in the other direction, respectively. Interesting is that during the oxidation of SO_3^{2-} to APS the fourth oxygen atom is derived from the AMP. The AMP is a product from the APS and the APS is formed from the reaction of the cellular sulfate with ATP, whereas the ATP was formed from the reaction of adenosine diphosphate (ADP) with a phosphate molecule (Akagi, 1995; Canfield, 2001). Sulfate reducing bacteria can be found in various environments such as marine sediments, waste water basins or eutrophicated lakes where the excess in nutrient input from the industry or agriculture lead to anoxic environments. The produced H_2S can be used from sulfur oxidizing bacteria to dwell in the close proximity of the sulfate reducing bacteria if there is a potential oxidant such as ferric iron (Fe^{3+}) or if light is available for phototrophic H_2S oxidation. Active sulfur cycling can occur as well to a minor amount in the deep sediments as it was shown in the methane zone of marine sediments in the Aarhus Bay where H_2S produced from DSR is apparently oxidized back to SO_4^{2-} by Fe^{3+} to small but detectable concentrations. These small concentrations of SO_4^{2-} may allow sulfate reducers to dwell deep below the main sulfate zone and form the so-called cryptic sulfur cycle (Holmkvist et al., 2011).

1.1.4. Disproportionation of sulfur intermediates

The oxidation of the most reduced sulfur compound H₂S proceeds over S⁰ before it gets oxidized to sulfoxy compounds containing sulfur with a higher oxidation state. Some bacteria have the ability to process these intermediate sulfur compounds where the sulfur intermediate is disproportionated in the absence of an electron source to sulfur compounds with sulfur at higher and lower oxidation state. A study on the sulfate reducing strain *Desulfovibrio sulfodismutans* sp. nov. revealed that this bacteria can grow under anaerobic conditions at room temperature from the disproportionation of S₂O₃²⁻ or SO₃²⁻ after the following reactions (Bak and Pfennig, 1987):



Bak and Pfennig showed that also other sulfate reducers (*Desulfobacter curvatus*, *Desulfovibrio vulgaris*) can disproportionate sulfoxy intermediates and that this process might be more common in anaerobic sediments if sulfur intermediates are abundant. The finding that some sulfate reducers are able to perform the disproportionation of sulfoxy intermediates, which were produced prior abiotically or biologically by sulfur oxidizing bacteria, shows nicely the entanglement and complexity of sulfur cycling in natural environments. In case of the S₂O₃²⁻ the two sulfur atoms are at different oxidation state, the sulfonate (central sulfur atom) becomes SO₄²⁻ via SO₃²⁻ that is an intermediate in Eq. 1.8 and the sulfane (outer sulfur atom) which forms the H₂S (Uyama et al., 1985; Bak and Pfennig, 1987; Habicht et al., 1998). The first oxidation product of H₂S is S⁰ which was also shown to be disproportionated by certain bacteria in anoxic sediments (Thamdrup et al., 1993, Canfield and Thamdrup, 1994). In the presence of MnO₂ the disproportionation of S⁰ the growth of these bacteria was sustained which indicates that this process might be important in metal rich anoxic sediments.



During the disproportionation of S⁰ the S⁰ is constantly re-supplied by the H₂S oxidation by the MnO₂ that is meanwhile reduced to Mn²⁺ or by FeOOH that is reduced to Fe²⁺ (Thamdrup et al., 1993). The process of Eq. 10 can be performed as well by the sulfate reducing bacteria *Desulfocapsa thiozymogenes* and *Desulfobulbus propionicus* in the presence of iron hydroxides (FeCO₃, FeOOH), where during the experiments with *Desulfocapsa thiozymogenes* SO₃²⁻ is thought to occur as an intermediate (Böttcher et al., 2001; Böttcher et al., 2005). Disproportionation of sulfur compounds, especially the microbial disproportionation of SO₃²⁻ is hypothesized to have influenced global sulfur cycling at least since the Precambrian (Skyring and Donnelly, 1982; Bak and Pfennig, 1987). Skyring and Donnelly discussed the possible important role of SO₃²⁻ produced from volcanic exhalations during the Precambrian where H₂S was probably the most abundant sulfur species as the atmosphere was lacking O₂.

Considering the volcanic exhalation of sulfur gases such as H₂S or SO₂ it is necessary to discuss also the role of the abiotic disproportionation of SO₂. This process has been demonstrated experimentally (Oana and Ishikawa, 1966; Kusakabe et al., 2000) at temperatures between 150°C to 326°C and has been observed in nature at a submarine volcano in the southern Mariana Arc by Butterfield and colleagues (2011). Depending on

the redox potential of the solutions the abiotic disproportionation of SO_2 will produce S^0 or H_2S as reduced sulfur compound:



The production of S^0 via Eq. 1.11 occurs at higher redox potentials, low temperatures and high total sulfur concentrations. In contrast, the production of H_2S happens at lower redox potentials, high temperatures and low total sulfur concentrations (Kusakabe et al., 2000). The authors also showed that the disproportionation reaction involved HSO_3^- as intermediate which is the hydrolyzed form of SO_2 . In the hydrothermal fluids of the submarine volcano at the Mariana Arc extremely high concentrations of HSO_3^- were detected (up to 163 mmol kg^{-1}) and massive amounts of S^0 was found (Butterfield et al., 2011). The disproportionation of SO_2 at hydrothermal temperatures is the topic of chapter 4 where we show evidence that the disproportionation of magmatic SO_2 is significant for the global sulfur cycling on Earth.

Recently a new disproportionation pathway was discovered by Milucka and colleagues (2012) in a consortium of methanotrophic archaea (ANME-2) and sulfate reducing Deltaproteobacteria (DSS) during the anaerobic oxidation of methane (AOM). The authors postulate a model where the ANME-2 are thought to oxidize methane (CH_4) to CO_2 while reducing SO_4^{2-} mainly to S^0 which is partly used in the cell and to some extent exits somehow the cell. The exported S^0 will react with H_2S in the surrounding water which forms polysulfides, with one of them being disulfide (HS_2^-) that is taken up by the DSS which are closely associated to the ANME-2 and perform the disproportionation of HS_2^- (Milucka et al., 2012):



This is an important finding as this process could be widespread in natural environments where anaerobic conditions meet the presence of CH_4 such as often observed in marine sediments or at mud volcanoes at the seafloor. The findings by Milucka and colleagues revealed that the ANME-2 cells might perform AOM alone without the sulfate reducers; raising the question why the sulfate reducers are so attracted to the ANME cells and even forming consortia. One possible explanation is that if the bacteria are able to perform the disproportionation of HS_2^- ($\Delta G = -12.7 \text{ kJ mol}^{-1}$) and gain energy from it.

1.2. Stable isotope studies on sulfate

A widespread tool to identify biogeochemical processes in natural environments or in laboratory experiments is the application of stable isotope geochemistry. Most of the light elements possess more than one stable isotope that differ from each other only by the number of neutrons in their atomic nucleus whereas possessing identical numbers of protons and electrons. Due to the different amount of neutrons, the stable isotopes deviate from each other in their weight and in the strengths of chemical bonds formed with other elements. This leads to slight differences in their mobility and reactivity during biogeochemical processes. As consequence the stable isotopes will experience kinetic or equilibrium isotope fractionations during biogeochemical transformations. During kinetic processes the lighter isotope typically will preferentially accumulate in the product phase (although exceptions to this rule of thumb are known), leaving the substrate enriched in

the heavy isotope. If the process is reversible, which is usually the case during biogeochemical pathways also a kinetic isotope fractionation will occur in the opposite direction. If a process becomes fully reversible, i.e. reaches thermodynamic equilibrium, the stable isotope distribution will also approach an equilibrium, the so-called equilibrium isotope fractionation between two compounds of which the more stable compound will be enriched in the heavy isotope.

In Table 1.1 the natural abundance of the stable isotopes of oxygen and sulfur are listed, with ^{16}O and ^{32}S being the most abundant isotopes of the respective element. Usually the isotope ratio of a compound refers to the ratio between the second most abundant isotope and the most abundant isotope ($^{18}\text{O}/^{16}\text{O}$ and $^{34}\text{S}/^{32}\text{S}$, respectively). With improvements in isotope ratio mass spectrometry, it is now also possible to measure abundances of so-called minor isotopes ($^{17}\text{O}/^{16}\text{O}$, $^{33}\text{S}/^{32}\text{S}$ and $^{36}\text{S}/^{32}\text{S}$).

Table 1.1: Isotopic abundances and relative atomic masses of oxygen and sulfur (from Sharp, 2007)

Symbol	Atomic number	Mass number	Abundance (%)	Atomic weight ($^{12}\text{C} = 12$)
O	8	16	99.759	15.99491
		17	0.037	16.99914
		18	0.204	17.99916
S	16	32	95.0	31.97207
		33	0.76	32.97146
		34	4.22	33.96786
		36	0.014	35.96709

The stable isotope composition of a certain compound is commonly reported in the δ -notation, which gives the isotopic ratio of the designated compound relative to the isotope ratio of an international accepted standard. Typically, isotope compositions of oxygen and sulfur are reported as ‰ values. Oxygen isotope compositions ($\delta^{18}\text{O}$) are reported relative to Vienna Standard Mean Ocean Water (VSMOW) and sulfur isotope compositions ($\delta^{34}\text{S}$) are reported relative to Vienna Cañon Diablo Troilite (VCDT):

$$\delta^{18}\text{O} = \left(\frac{\left(\frac{^{18}\text{O}}{^{16}\text{O}} \right)^{\text{x}}}{\left(\frac{^{18}\text{O}}{^{16}\text{O}} \right)^{\text{std}}} - 1 \right) \cdot 10^3 \text{‰} \quad \text{and} \quad \delta^{34}\text{S} = \left(\frac{\left(\frac{^{34}\text{S}}{^{32}\text{S}} \right)^{\text{x}}}{\left(\frac{^{34}\text{S}}{^{32}\text{S}} \right)^{\text{std}}} - 1 \right) \cdot 10^3 \text{‰}$$

with x being the sample and std the element specific isotope standard. Further isotopic terminology used in this work is the isotopic difference Δ between two substances which is equal to the offset between the corresponding δ -values. If a process presumably leads to equilibrium isotope fractionation and if the equilibrium isotope fractionation is rather small, Δ is approximately equal to the isotopic enrichment factor ϵ which is directly related to the isotope fractionation factor α , as demonstrated in the following example for the difference between the isotope compositions of SO_4^{2-} and H_2O :

$$\Delta^{18}\text{O}_{\text{SO}_4^{2-}/\text{H}_2\text{O}} = \delta^{18}\text{O}_{\text{SO}_4^{2-}} - \delta^{18}\text{O}_{\text{H}_2\text{O}} \approx \epsilon^{18}\text{O}_{\text{SO}_4^{2-}/\text{H}_2\text{O}} \approx \ln \alpha^{18}\text{O}_{\text{SO}_4^{2-}/\text{H}_2\text{O}}$$

This here used isotope terminology is adapted from recent literature and takes recently recommended terminologies into account (Coplen, 2011).

Since the oxygenation of the atmosphere SO_4^{2-} is the most abundant form of sulfur compounds in natural environments on the Earth's surface. It can be produced via diverse oxidation pathways, from disproportionation or simply be residual SO_4^{2-} in sulfate reducing anaerobic environments. All these biogeochemical processes will leave a process specific isotope imprint in the isotope composition of the SO_4^{2-} which reflect specific kinetic and equilibrium isotope effects associated with the respective biogeochemical pathway (see Van Stempvoort and Krouse, 1994; Canfield, 2001). The SO_4^{2-} molecule is very inert and does not exchange its stable isotopes with the surrounding water or other sulfur compounds under most conditions. Isotope exchange occurs only in extreme environments such as in extremely acidic solutions or at very high temperatures (Lloyd, 1968). This makes the stable isotope composition of SO_4^{2-} an ideal tool for the identification of the various processes involved in sulfur cycling and due to its stability an excellent archive for the processes that occurred in the geological past.

The main focus of this work is on the oxygen isotope signature of SO_4^{2-} affected by sulfur cycling. In contrast to the stable sulfur isotope signatures caused by biogeochemical sulfur transformations, the oxygen isotope effects during sulfur cycling are under-investigated and our understanding of what causes the observed effects is still very patchy. In the following I will give an overview of the state of the art of some key observations about oxygen isotope fractionation during sulfur cycling.

Oxygen isotope patterns during the oxidation of reduced sulfur compounds:

The oxidation of reduced sulfur compounds such as pyrite, iron monosulfide, sphalerite or elemental sulfur can occur biologically or abiotically via oxidation by O_2 or Fe^{3+} . As the acid mine drainage (AMD) is a major concern because it pollutes the environment with dissolved heavy metals and sulfuric acid, a main focus of stable isotope studies on oxidative sulfur cycling was placed on the isotope effects during the oxidation of pyrite. There are two general oxidation reactions, the oxidation by air O_2 (Eq. 1.1) where most of the oxygen in the produced SO_4^{2-} is derived from O_2 and the oxidation by Fe^{3+} (Eq. 1.2) where all of the oxygen in the produced SO_4^{2-} is derived from H_2O . The fact that both oxygen sources have a very distinct oxygen isotope composition with the $\delta^{18}\text{O}$ of air being 23.5‰ (Kroopnick and Craig, 1972) and the $\delta^{18}\text{O}$ of meteoric water being usually at or below 0‰, allow the determination of the relative contribution of each oxidation pathway with a isotope mass balance (see Balci et al., 2007). Several authors performed laboratory experiments in the presence or absence of pyrite oxidizing bacteria with O_2 or Fe^{3+} as oxidant and tried to determine the relative contribution of each pathway at specific conditions as well as the oxygen isotope fractionation between the produced SO_4^{2-} and the corresponding oxygen sources ($\epsilon^{18}\text{O}_{\text{SO}_4\text{-O}_2}$ or $\epsilon^{18}\text{O}_{\text{SO}_4\text{-H}_2\text{O}}$, respectively) to understand better the sulfur oxidation mechanism in AMD environments. The outcome of these studies was interesting and frustrating at the same time because the relative contribution of each oxygen source varied in a wide range between the various studies (e.g. 68% H_2O oxygen contribution in Lloyd, 1967; 87% H_2O contribution in Balci et al., 2007), and the same was also the case for the determined oxygen isotope fractionation factors, with $\epsilon^{18}\text{O}_{\text{SO}_4\text{-H}_2\text{O}}$ in most experiments corresponding to inverse values or values close to 0‰ (see Lloyd, 1967: $\epsilon^{18}\text{O}_{\text{SO}_4\text{-O}_2} = -8.7\text{‰}$, $\epsilon^{18}\text{O}_{\text{SO}_4\text{-H}_2\text{O}} = 0.0\text{‰}$; Balci et al., 2007:

$\epsilon^{18}\text{O}_{\text{SO}_4\text{-O}_2} \approx -10\text{‰}$, $\epsilon^{18}\text{O}_{\text{SO}_4\text{-H}_2\text{O}} = 3.5\text{‰}$; Brabec et al., 2012: $\epsilon^{18}\text{O}_{\text{SO}_4\text{-H}_2\text{O}} = 5.6\text{‰}$). An inverse isotope fractionation means that the heavy ^{18}O is preferentially incorporated in the product.

These findings show that it is not possible to interpret the pyrite oxidation mechanism in natural environments just by measuring the oxygen isotope composition of formed HSO_4^- without considering additional biogeochemical analyses. However, they also raise the intriguing question how it is possible to produce an inverse isotope fractionation where the SO_4^{2-} seems to incorporate water oxygen which is more enriched in the heavy oxygen (^{18}O) and if there are different sulfoxy intermediates involved depending on the biochemical conditions in which the oxidation process occurs, which could be responsible for the varying oxygen source contributions due to their ability to exchange oxygen with the water.

Oxygen isotope patterns during the DSR:

With the exception of strongly acidic conditions or high temperatures, the HSO_4^- ion does not exchange its oxygen isotopes with water. Still, in environments known for active DSR, as it is the case in anaerobic marine sediments or in DSR experiments, the oxygen isotope composition of the residual SO_4^{2-} changes with increasing duration of sulfate reduction until it approaches a common plateau value that is approximately 29‰ (at 5°C, from Fritz et al., 1989) heavier as the oxygen isotope composition of the surrounding water. Mizutani and Rafter (1973) explained this dependence of the oxygen isotope composition of the residual SO_4^{2-} on the oxygen isotope composition of the water by indirect oxygen isotope exchange between an intermediate during the DSR and the water. Isotope model approaches such as by Brunner et al. (2005) explained the observed water dependence by oxygen exchange between the DSR intermediates APS and SO_3^{2-} with water. The oxygen isotope exchange between APS and water has been excluded in two recent studies (Brunner et al., 2012; Kohl et al., 2012) of which the former is also part of this thesis (see chapter 6), which leaves SO_3^{2-} as potential candidate for the observed oxygen isotope dependence of residual HSO_4^- on the oxygen isotope composition of water. In our oxygen isotope model (Brunner et al. 2012) we hypothesize that also adenosine monophosphate (AMP) might exchange oxygen with cell internal water and therefore could contribute to the observed oxygen isotope signature during DSR (Fig. 1.6, see also Turchyn et al., 2010). Additionally, oxygen exchange could occur via the APS production from the ATP that was formed during the reaction of ADP with a phosphate molecule in equilibrium with water (see section 1.1.3. of this dissertation; Coleman et al., 2005). The determination of the oxygen isotope equilibrium fractionation between sulfite and water, which was lacking so far, is essential to understand better the mechanisms that are responsible for the observed oxygen isotope patterns in the residual SO_4^{2-} during DSR.

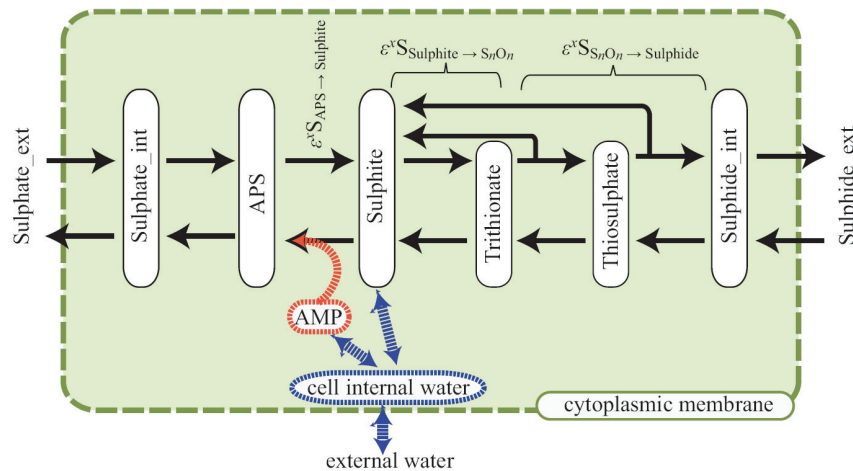


Fig. 1.6: General scheme of the stable isotope signature during the dissimilatory sulfate reduction, with AMP and SO_3^{2-} being suspected for exchanging oxygen with cell internal water (from Brunner et al., 2012).

Sulfur and oxygen isotope patterns during the disproportionation of sulfur intermediates:

Stable isotope studies revealed large sulfur isotope fractionations for sulfur disproportionation processes and have consequences for the interpretation of the isotope signature of sulfates in natural environments (see Canfield et al., 2001). The sulfur isotope effects by sulfur disproportionating microbes could be responsible for the observed large sulfur isotope differences between SO_4^{2-} and reduced sulfur compounds (e.g. pyrite) in natural environments, where sulfur isotope fractionations often exceed 50‰ with highest fractionations of 85‰ (Habicht and Canfield, 2001). However, large sulfur isotope offsets between SO_4^{2-} and H_2S can also be caused by dissimilatory sulfate reduction alone (Rudnicki et al, 2001; Wortmann et al., 2001; Brunner and Bernasconi, 2005; Canfield et al. 2010, Sim et al., 2011).

Also the oxygen isotope effects during sulfur disproportionation (Eq. 1.10) can be large. The oxygen isotope composition of SO_4^{2-} produced during S^0 disproportionation experiments with a pure culture of *Desulfocapsa thiozymogenes* and an enrichment culture “Kuhgraben” was enriched in the ^{18}O relative to the oxygen isotope composition of the water by 17.4‰ and by 16.6‰, respectively (Böttcher et al., 2001). The authors proposed that SO_3^{2-} might be formed as metabolic intermediate in the S^0 disproportionation and would cause the high oxygen isotope offset by approaching the isotope equilibrium fractionation between SO_3^{2-} and the surrounding water before its subsequent oxidation to SO_4^{2-} . Böttcher et al. (2005) performed further S^0 disproportionation experiments with a pure culture of the sulfate reducer *Desulfobulbus propionicus* and obtained an oxygen isotope fractionation between SO_4^{2-} and water of 21‰. This high fractionation was again explained as result of oxygen isotope exchange between a potential SO_3^{2-} intermediate and water. The slightly lower oxygen isotope fractionation in the experiments of Böttcher et al. (2001) could be explained by the higher disproportionation rates leaving the SO_3^{2-} less time to equilibrate with the water, whereas in the experiments of Böttcher et al. (2005) the SO_3^{2-} had more time to equilibrate its

oxygen with the water, but it could be explained as well by possible differences in the metabolism of the different bacteria.

In a study on the abiotic disproportionation of SO_2 at hydrothermal temperatures (Eq. 1.11 or Eq. 1.12), Kusakabe et al. (2000) measured the sulfur isotope fractionation during this process, observing a large initial kinetic fractionation between the sulfur isotope composition of the produced HSO_4^- and the more reduced form (H_2S or S^0 , respectively; Kusakabe et al., 2000). The authors did not measure the oxygen isotope composition of the produced HSO_4^- , but reported results from volcanically influenced lakes, showing a co-variation to the oxygen isotope composition of the respective water. A detailed study on the oxygen isotope fractionation during SO_2 disproportionation at hydrothermal temperatures is still missing, a gap that we filled with our field and experimental study (see chapter 4).

1.3. Sulfite species and its role as sulfoxy intermediate

The term sulfite has already been frequently mentioned in the introduction to sulfur cycling which is an indication that this sulfur compound must be a common intermediate. However, before the importance of sulfite as an intermediate during sulfur cycling can be discussed, it needs to be defined what sulfite is.

Sulfite is a pH dependent sulfur compound and forms different sulfite species at different pH conditions such as sulfite *sensu stricto* (SO_3^{2-}), bisulfite with its two isomers (HSO_3^- , SO_3H^-), pyrosulfite or metabisulfite ($\text{S}_2\text{O}_5^{2-}$) and the volatile sulfur dioxide (SO_2). The different sulfite species have in common that their sulfur atom is at an oxidation state of +IV. Some of the reactions that occur during the conversion of one sulfite species into another involve the incorporation of one oxygen atom from a H_2O molecule ($\text{SO}_2 + \text{H}_2\text{O} \leftrightarrow \text{HSO}_3^- + \text{H}^+$ and $2\text{HSO}_3^- \leftrightarrow \text{S}_2\text{O}_5^{2-} + \text{H}_2\text{O}$; see Betts and Voss, 1970; Horner and Connick, 2003). Consequences of these conversion reactions are that sulfite species rapidly exchange their oxygen isotopes with water. Especially at low pH where SO_2 is present the oxygen exchange is extremely rapid (Betts and Voss, 1970; Holt et al., 1983). At circum neutral pH the exchange kinetics are still fast, at pH of 8.9 it is a matter of minutes, at pH 10.5 oxygen exchange is in the range of some days and in the highly alkaline range at pH above 12.7 no oxygen exchange is observed even after 17 days (Betts and Voss, 1970). Although, the kinetics of the exchange reactions with sulfite species and water are well known, there is no detailed study on the oxygen isotope equilibrium fractionation between sulfite species and water. The study by Holt et al. (1983) is the only one that gives an estimate for the oxygen isotope equilibrium fractionation between gaseous SO_2 and water vapor which is approximately 24‰ at 22°C.

The fact that sulfite species in a broad pH range rapidly exchange their oxygen isotopes with the surrounding water as well as sulfite being often mentioned as being the final sulfoxy intermediate during the oxidation of reduced sulfur compounds makes it an important candidate as a shaper of the oxygen isotope composition of the produced SO_4^{2-} (Granger and Warren, 1969; Druschel and Borda, 2006; Brunner et al., 2008). Stable oxygen isotope studies in the laboratory or in natural environments already identified the role of the oxygen exchange rate between sulfite and water relative to the oxidation rate in shaping the oxygen isotope composition of sulfate (Hubbard et al., 2009; Kohl and Bao, 2011), but so far the oxygen isotope equilibrium fractionation between sulfite and water has not been determined. The lack of such studies is probably caused by the many

experimental challenges in the determination of equilibrium isotope fractionations between sulfite and water, challenges that we overcame in our study (chapter 2). Obtaining a value for the equilibrium isotope fractionation between sulfite and water is essential for the interpretation of results from sulfite oxidation experiments and for the determination of the process specific oxygen isotope effects (chapter 3).

1.4. Motivation and outline of the dissertation

The aim of this study is to contribute to a deeper understanding of the oxygen isotope signature of SO_4^{2-} during sulfur cycling. Especially, the role of SO_3^{2-} – often considered the final sulfoxy intermediate during the oxidative sulfur cycling – in shaping the oxygen isotope composition of SO_4^{2-} is still unclear. In contrast to the inert SO_4^{2-} molecule, sulfite rapidly exchanges its oxygen with water and might therefore strongly impact the oxygen isotope composition of SO_4^{2-} in natural environments. The disproportionation of magmatic SO_2 (which is also a sulfite species) in hydrothermal systems is probably an under-estimated source for SO_4^{2-} in the ocean. Its oxygen isotope signature could thus have a strong impact on the oxygen isotope composition of seawater sulfate. The outcome of this work shows that sulfite species play indeed an important role for the oxygen isotope composition of SO_4^{2-} and must be taken into account in isotope studies concerning the cycling of sulfur.

The thesis is structured as follows:

Overview of the manuscripts:

Chapter 2 “The oxygen isotope equilibrium fractionation between sulfite species and water”

Chapter 2 describes the pH dependence of sulfite species and the accompanied challenges that have to be taken into account when attempting to determine the oxygen isotope equilibrium fractionation. Sulfite species rapidly exchange their oxygen isotopes with water and at the same time sulfite was often mentioned as important sulfoxy intermediate during the oxidative and the reductive part of sulfur cycling. These properties make sulfite an important agent that can influence the oxygen isotope composition of SO_4^{2-} which is an inert sulfur compound that under most conditions does not exchange oxygen with water (see Lloyd, 1968; Chiba and Sakai, 1985). By performing experiments in distinctly labeled solutions at different pH and applying a complex oxygen isotope mass balance approach we could disentangle the oxygen isotope equilibrium fractionation between SO_3^{2-} and water and give a rough estimate for the oxygen isotope equilibrium fractionation between SO_2 and water.

Inigo A. Müller, Benjamin Brunner, Christian Breuer, Max Coleman and Wolfgang Bach. The manuscript is under review in *Geochimica et Cosmochimica Acta*.

Chapter 3 “Isotopic evidence of the pivotal role of sulfite oxidation in shaping the oxygen isotope signature of sulfate”

In this chapter we demonstrate that the range of oxygen isotope signatures of SO_4^{2-} from abiotic SO_3^{2-} oxidation experiments accommodates almost the entire range of oxygen isotope offsets between water and sulfate produced from the oxidation of reduced sulfur bearing minerals in natural environments. The chemical parameters of the experiments such as the presence and/or absence of the oxidizing agent (O_2 , Fe^{3+}) and the pH of the solution strongly influence the rate of oxygen exchange between sulfite species and water as well as the oxidation rate which is highest at circum neutral pH. In this chapter we provide evidence that SO_3^{2-} is the final sulfoxy intermediate during the oxidation of reduced sulfur compounds and therefore is of major importance for the oxygen isotope composition in the produced SO_4^{2-} .

Inigo A. Müller, Benjamin Brunner and Max Coleman.
The manuscript is under review in *Chemical Geology*.

Chapter 4 “The isotope signature of magmatic SO_2 disproportionation: A comparison between laboratory experiments and a hydrothermally active site in the Manus Basin, Papua New Guinea”

Chapter 4 discusses the role of the disproportionation of magmatic SO_2 in shaping the oxygen isotope composition of seawater sulfate. The scientific expedition SO-216 to the eastern Manus Basin, Papua New Guinea, revealed that this process is responsible for the elevated discharge of HSO_4^- and formation of large amounts of liquid S^0 . We report for the first time the $\delta^{34}\text{S}$ of 12.0‰ of the magmatic SO_2 source in a hydrothermal system at the seafloor. The isotope analyses of the hydrothermal site at North Su displayed a surprising similarity between the sulfur and oxygen isotope composition of discharged HSO_4^- and the isotope composition of seawater sulfate. To answer the question if the disproportionation of SO_2 could be at least partially responsible for the isotope composition of the modern seawater sulfate we performed laboratory experiments, where we SO_2 disproportionation at temperatures ranging from 150°C to 320°C. The initial kinetic isotope fractionation between HSO_4^- and the experiment solution is indeed in the range of the known oxygen isotope offset between seawater sulfate and seawater. Our study thus indicates that the disproportionation of magmatic SO_2 in hydrothermal systems related to subduction zones could play a significant role in shaping the oxygen isotope composition of seawater sulfate throughout Earth's history.

Inigo A. Müller, Benjamin Brunner, Thomas Max, Christian Breuer, Eoghan P. Reeves, Janis Thal, Stefano M. Bernasconi and Wolfgang Bach.
The manuscript is in preparation for submission to *Earth and Planetary Science Letters*.

Chapter 5 “Synthesis and outlook”

This chapter summarizes the role of sulfite species as final sulfoxy intermediate during the oxidation of reduced sulfur compounds on the oxygen isotope composition of SO_4^{2-} . The value for the oxygen isotope equilibrium fractionation between sulfite species and water is of importance to explain observed isotope effects during oxidation experiments of reduced sulfur compounds and give further hints for the interpretation of the DSR mediated oxygen isotope exchange in the residual SO_4^{2-} . The importance of the oxygen isotope signature of the disproportionation of magmatic SO_2 for the oxygen isotope composition of seawater sulfates over geological time scales has to be expanded by better quantification of the global contribution of magmatic SO_2 to the global sulfur cycle and by comparison with other geochemical tracers for the tectonic activity in the past to see if this is constant source or varies with time.

Chapter 6 “Appendix: The reversibility of dissimilatory sulphate reduction and the cell-internal multi-step reduction of sulphite to sulphide: insights from the oxygen isotope composition of sulphate”

During my PhD work I contributed to this study, which focuses on the interpretation of sulfur and oxygen isotope signatures of dissimilatory sulfate reduction (DSR) and the role of sulfite in this process by taking part in the writing process and by calculating oxygen and sulfur isotope mass balances. Dissimilatory sulfate reduction is one of the most important biochemical pathways to oxidize organic matter in anoxic environments using SO_4^{2-} as terminal electron acceptor. It is an enzymatically catalyzed reversible multistep pathway in the bacterial cell, leaving the residual SO_4^{2-} with a process specific isotope imprint. Whereas the sulfur isotope composition in the cell external residual SO_4^{2-} is gradually enriched in the heavy sulfur isotopes, the oxygen isotope composition approaches an “equilibrium isotope offset” with respect to the water. The sulfur isotope signature is explained by kinetic isotope fractionations during the enzymatic reversible reduction steps of DSR, but the oxygen isotope signature must be produced by a combination of kinetic isotope effects during the reversible reduction steps and oxygen isotope exchange between sulfoxy intermediates and cell internal water. This study is the first approach that tries to explain the isotope fractionation patterns of the DSR with a combined sulfur and oxygen isotope model, in which water oxygen can be introduced into the system via direct oxygen exchange between SO_3^{2-} and water and during the re-oxidation of SO_3^{2-} by the APS reductase from the AMP which is in equilibrium with the water. The isotope model shows that a multi isotope approach including the oxygen isotopes and major and minor sulfur isotopes (^{33}S , ^{34}S and ^{36}S) can help to explain the mechanisms during DSR more in detail. The isotope model is compatible with isotope studies on DSR but for studies that observed a sulfur isotope fractionation of +50‰ during the reduction from SO_3^{2-} to H_2S the model has to include at least two reduction steps in the reduction of SO_3^{2-} to H_2S (e.g. via $\text{S}_2\text{O}_3^{2-}$ or $\text{S}_3\text{O}_6^{2-}$). Further we can say from the model that rapid DSR mediated oxygen exchange correlates with large sulfur isotope fractionations and the opposite is the case with smaller sulfur isotope fractionations.

Benjamin Brunner, Florian Einsiedl, Gail L. Arnold, Inigo Müller, Stefanie Templer and Stefano M. Bernasconi: *Isotopes in Environmental and Health Studies* **48**, 33-54.

1.4. References

- Akagi J. M. (1995) Respiratory sulfate reduction. *In* Sulfate-Reducing Bacteria. LL Barton (ed) Plenum Press, New York, p 89-109.
- Babel M. (2007) Depositional environments of a salina-type evaporite basin recorded in the Badenian gypsum facies in the northern Carpathian Foredeep. *In* Schreiber, B. c., Lugli S. and Babel M. (eds) *Evaporites Through Space and Time*. Geological Society, London, Special Publications **285**, 107-142.
- Bak F. and Pfennig N. (1987) Chemolithotrophic growth of *Desulfovibrio sulfodismutans* sp. nov. by disproportionation of inorganic sulfur compounds. *Arch. Microbiol.* **147**, 184-189.
- Balci N., Shanks III W. C., Mayer B. and Mandernack K. W. (2007) Oxygen and sulfur isotope systematics of sulfate produced by bacterial and abiotic oxidation of pyrite. *Geochimica et Cosmochimica Acta* **71**, 3796-3811.
- Bethke C. M., Sanford R. A., Kirk M. F., Jin Q. and Flynn T. M. (2011) The thermodynamic ladder in geomicrobiology. *American Journal of Science* **311**, 183-210.
- Betts R. H. and Voss R. H. (1970) The kinetics on oxygen exchange between the sulfite ion and water. *Canadian Journal of Chemistry* **48**, 2035-2041.
- Böttcher M. E., Thamdrup B. and Vennemann T. W. (2001) Oxygen and sulfur isotope fractionation during anaerobic bacterial disproportionation of elemental sulfur. *Geochimica et Cosmochimica Acta* **65**, 1601-1609.
- Böttcher M. E., Khim B.-K., Suzuki A., Gehre M., Wortmann U. G. and Brumsack H.-J. (2004) Microbial sulfate reduction in deep sediments of the Southwest Pacific (ODP Leg 181, Sites 1119-1125): evidence from stable sulfur isotope fractionation and pore water modeling. *Marine Geology* **205**, 249-260.
- Böttcher M. E., Thamdrup B., Gehre M. and Theune A. (2005) $^{34}\text{S}/^{32}\text{S}$ and $^{18}\text{O}/^{16}\text{O}$ Fractionation During Sulfur Disproportionation by *Desulfobulbus propionicus*. *Geomicrobiology Journal* **22**, 219-226.
- Bottrell S. H. and Newton R. J. (2006) Reconstruction of changes in global sulfur cycling from marine sulfate isotopes. *Earth-Science Reviews* **75**, 59-83.
- Brabec M. Y., Lyons T. W. and Mandernack K. W. (2012) Oxygen and sulfur isotope fractionation during sulfide oxidation by anoxygenic phototrophic bacteria. *Geochimica et Cosmochimica Acta* **83**, 234-251.
- Brunner B. and Bernasconi S. M. (2005) A revised isotope fractionation model for dissimilatory sulfate reduction in sulfate reducing bacteria. *Geochimica et Cosmochimica Acta* **69**, 4759-4771.
- Brunner B., Bernasconi S. M., Kleikemper J. and Schroth M. H. (2005) A model for oxygen and sulfur isotope fractionation in sulfate during bacterial sulfate reduction processes. *Geochimica et Cosmochimica Acta* **69**, 4773-4785.

- Brunner B., Yu J.-Y., Mielke R. E., MacAskill J. A., Madzunkov S., McGenity T. J. and Coleman M. (2008) Different isotope and chemical patterns of pyrite oxidation related to lag and exponential growth phases of *Acidithiobacillus ferrooxidans* reveal a microbial growth strategy. *Earth and Planetary Science Letters* **270**, 63-72.
- Brunner B., Einsiedl F., Arnold G. L., Müller I., Templer S. and Bernasconi S. M. (2012) The reversibility of dissimilatory sulphate reduction and the cell-internal multi-step reduction of sulphite to sulphide: insights from the oxygen isotope composition of sulphate. *Isotopes in Environmental and Health Studies* **48**, 33-54.
- Butterfield D. A., Nakamura K., Takano B., Lilley M., Lupton J. E. and Resing J. A. (2011) High SO₂ flux, sulfur accumulation, and gas fractionation at an erupting submarine volcano. *Geology* **39**, 803-806.
- Canfield D. E., Jørgensen B. B., Fossing H., Glud R., Gundersen J., Ramsing N. B., Thamdrup B., Hansen J. W., Nielsen L. P. and Hall P. O. J. (1993) Pathways of organic carbon oxidation in three continental margin sediments. *Marine Geology* **113**, 27-40.
- Canfield D. E. and Thamdrup B. (1994) The Production of ³⁴S-Depleted Sulfide During Bacterial Disproportionation of Elemental Sulfur. *Science* **266**, 1973-1975.
- Canfield D. E. (2001) Biogeochemistry of Sulfur Isotopes. *Reviews in Mineralogy and Geochemistry* **43**, 607-636.
- Canfield D. E., Farquhar J. and Zerkle A. L. (2010) High isotope fractionations during sulfate reduction in a low-sulfate euxinic ocean analog. *Geology* **38**, 415-418.
- Charlou J. L., Donval J. P., Douville E., Jean-Baptiste P., Radford-Knoery J., Fouguet Y., Dapigny A. and Stievenard M. (2000) Compared geochemical signatures and the evolution of Menez Gwen (37°50'N) and Lucky Strike (37°17'N) hydrothermal fluids, south of the Azores Triple Junction on the Mid-Atlantic Ridge. *Chemical Geology* **171**, 49-75.
- Chiba, H. and Sakai, H. (1985) Oxygen isotope exchange rate between dissolved sulfate and water at hydrothermal temperatures. *Geochimica et Cosmochimica Acta* **49**, 993-1000.
- Coleman A. S., Blake R. E., Karl D. M., Fogel M. L. and Turekian K. K. (2005) Marine phosphate oxygen isotopes and organic matter remineralization in the oceans. *PNAS* **102**, 13023-13028.
- Coplen T. B. (2011) Guidelines and recommended terms for expression of stable-isotope-ratio and gas-ratio measurement results. *Rapid Commun. Mass Spectrom.* **25**, 2538-2560.
- Craddock P. R. and Bach W. (2010) Insights to magmatic-hydrothermal processes in the Manus back-arc basin as recorded by anhydrite. *Geochimica et Cosmochimica Acta* **74**, 5514-5536.
- Davidson M. M., Bisher M. E., Pratt L. M., Fong J., Southam G., Pfiffner S. M., Reches Z. and Onstott T. C. (2009) Sulfur Isotope Enrichment during Maintenance Metabolism in the Thermophilic Sulfate-Reducing Bacterium *Desulfotomaculum putei*. *Applied and Environmental Microbiology* **75**, 5621-5630.
- Druschel G. and Borda M. (2006) Comment on "Pyrite dissolution in acidic media" by M. Descostes, P. Vitorge, and C. Beaucaire. *Geochimica et Cosmochimica Acta* **70**, 5246-5250.

- Eckert T., Brunner B., Edwards E. A. and Wortmann U. G. (2011) Microbially mediated re-oxidation of sulfide during dissimilatory sulfate reduction by *Desulfobacter latus*. *Geochimica et Cosmochimica Acta* **75**, 3469-3485.
- Fitz R. M. and Cypionka H. (1990) Formation of thiosulfate and trithionate during sulfite reduction by washed cells of *Desulfovibrio desulfuricans*. *Arch. Microbiol.* **154**, 400-406.
- Franz B., Lichtenberg H., Hormes J., Dahl C. and Prange A. (2009) The speciation of soluble sulphur compounds in bacterial culture fluids by X-ray absorption near edge structure spectroscopy. *Environmental Technology* **30**, 1281-1289.
- Friedrich C. G., Bardischewsky F., Rother D., Qentmeier A. and Fischer J. (2005) Prokaryotic sulfur oxidation. *Current Opinion in Microbiology* **8**, 253-259.
- Frigaard N. U. and Dahl C. (2009) Sulfur metabolism in phototrophic sulfur bacteria. *Adv. Microb. Physiol.* **54**, 103-200.
- Fritz G., Büchert T. and Kroneck P. M. H. (2002) The Function of the [4Fe-4S] Clusters and FAD in Bacterial and Archaeal Adenylylsulfate Reductases: Evidence for flavin-catalyzed reduction of adenosine 5'-phosphosulfate. *The Journal of Biological Chemistry* **277**, 26066-26073.
- Fritz P., Basharmal G. M., Drimmie R. J., Ibsen J. and Qureshi R. M. (1989) Oxygen isotope exchange between sulphate and water during bacterial reduction of sulphate. *Chemical Geology (Isotope Geoscience Section)*, **79**, 99-105.
- Gehrke T., Hallmann R. and Sand W. (1995) Importance of exopolymers from *Thiobacillus ferrooxidans* and *Leptospirillum ferrooxidans* for bioleaching. Page 1-11 in T. Vargas, C. A. Jerez, J. V. Wiertz, and H. Toledo (ed.), Biohydrometallurgical processing. University of Chile, Santiago, Chile.
- Ghosh W. and Dam B. (2009) Biochemistry and molecular biology of lithotrophic sulfur oxidation by taxonomically and ecologically diverse bacteria and archaea. *FEMS Microbiol. Rev.* **33**, 999-1043.
- Graf H.-F., Langmann B. And Feichter J. (1998) The contribution of Earth degassing to the atmospheric sulfur budget. *Chemical Geology* **147**, 131-145.
- Granger H. C. and Warren C. C. (1969) Unstable Sulfur Compounds and the Origin of Roll-type Uranium Deposits. *Economic Geology* **64**, 160-171.
- Habicht K. S., Canfield D. E. and Rethmeier J. (1998) Sulfur isotope fractionation during bacterial reduction and disproportionation of thiosulfate and sulfite. *Geochimica et Cosmochimica Acta* **62**, 2585-2595.
- Habicht K. S. and Canfield D. E. (2001) Isotope fractionation by sulfate-reducing natural populations and the isotopic composition of sulfide in marine sediments. *Geology* **29**, 555-558.
- Holmkvist L., Ferdelman T. G. and Jørgensen B. B. (2011) A cryptic sulfur cycle driven by iron in the methane zone of marine sediment (Aarhus Bay, Denmark). *Geochimica et Cosmochimica Acta* **75**, 3581-3599.
- Holt B. D., Cunningham P. T., Engelkemeir A. G., Graczyk D. G. and Kumar R. (1983) Oxygen-18 study of nonaqueous-phase oxidation of sulfur dioxide. *Atmospheric Environment* **17**, 625-632.
- Horner D. A. and Connick R. E. (2003) Kinetics of Oxygen Exchange between the Two Isomers of Bisulfite Ion, Disulfite Ion ($S_2O_5^{2-}$), and Water As Studied by Oxygen-17 Nuclear Magnetic Resonance Spectroscopy. *Inorganic Chemistry* **42**, 1884-1894.

- Jørgensen B. B. (1977) The sulfur cycle of a coastal marine sediment (Limfjorden, Denmark). *Limnology and Oceanography* **22**, 814-832.
- Jørgensen B. B. (1982) Mineralization of organic matter in the sea bed—the role of sulphate reduction. *Nature* **296**, 643-645.
- Jørgensen B. B., Bang M. and Blackburn T. H. (1990) Anaerobic mineralization in marine sediments from the Baltic Sea-North Sea transition. *Marine Ecology Progress Series* **59**, 39-54.
- Jørgensen B. B., Weber A. and Zopfi J. (2001) Sulfate reduction and anaerobic methane oxidation in Black Sea sediments. *Deep-Sea Research I* **48**, 2097-2120.
- Kemp A. L. W. and Thode H. G. (1968) The mechanism of the bacterial reduction of sulphate and of sulphite from isotope fractionation studies. *Geochimica et Cosmochimica Acta* **32**, 71-91.
- Khokhar M. F., Frankenberg C., Van Roozendaal M., Beirle S., Kühl S., Richter A., Platt U. and Wagner T. (2005) Satellite observations of atmospheric SO₂ from volcanic eruptions during the time-period of 1996-2002. *Advances in Space Research* **36**, 879-887.
- Kobayashi K., Seki Y. and Ishimoto M. (1969) Intermediary formation of trithionate in sulfite reduction by a sulfate-reducing bacterium. *The Journal of Biochemistry* **65**, 155-157.
- Kobayashi K., Seki Y. and Ishimoto M. (1974) Biochemical Studies on Sulfate-reducing Bacteria XIII. Sulfite Reductase from *Desulfovibrio vulgaris*—Mechanism of Trithionate, Thiosulfate, and Sulfide Formation and Enzymatic Properties. *The Journal of Biochemistry* **75**, 519-529.
- Kohl I. and Bao H. (2011) Triple-oxygen-isotope determination of molecular oxygen incorporation in sulfate produced during abiotic pyrite oxidation (pH = 2-11). *Geochimica et Cosmochimica Acta* **75**, 1785-1798.
- Kohl I. E., Asatryan R. and Bao H. (2012) No oxygen isotope exchange between water and APS-sulfate at surface temperature: Evidence from quantum chemical modeling and triple-oxygen isotope experiments. *Geochimica et Cosmochimica Acta* **95**, 106-118.
- Kroopnick P. and Craig H. (1972) Atmospheric Oxygen: Isotopic Composition and Solubility Fractionation. *Science* **175**, 54-55.
- Kusakabe M., Komoda Y., Takano B. and Abiko T. (2000) Sulfur isotopic effects in the disproportionation reaction of sulfur dioxide in hydrothermal fluids: implications for the $\delta^{34}\text{S}$ variations of dissolved bisulfate and elemental sulfur from active crater lakes. *Journal of Volcanology and Geothermal Research* **97**, 287-307.
- Lloyd R. M. (1967) Oxygen-18 Composition of Oceanic Sulfate. *Science* **156**, 1228-1231.
- Lloyd R. M. (1968) Oxygen Isotope Behavior in the Sulfate-Water System. *Journal of Geophysical Research* **73**, 6099-6110.
- Martínez-Alonso M., Van Bleijswijk J., Gaju N. and Muyzer G. (2005) Diversity of anoxygenic phototrophic sulfur bacteria in the microbial mats of the Ebro Delta: a combined morphological and molecular approach. *FEMS Microbiology Ecology* **52**, 339-350.
- Menyailov I. A., Nikitina L. P., Shapar V. N. and Pilipenko V. P. (1986) Temperature increase and chemical change of fumarolic gases at Momotombo Volcano,

- Nicaragua in 1982-1985: Are these indicators of a possible eruption? *Journal of Geophysical Research* **91**, 12199-12214.
- Milucka J., Ferdelman T. G., Polerecky L., Franzke D., Wegener G., Schmid M., Lieberwirth I., Wagner M., Widdel F. and Kuypers M. M. M. (2012) Zero-valent sulphur is a key intermediate in marine methane oxidation. *Nature* **491**, 541-546.
- Mizutani Y. and Rafter A. T. (1973) Isotopic behaviour of sulphate oxygen in the bacterial reduction of sulphate. *Geochemical Journal* **6**, 183-191.
- Oana S. and Ishikawa H. (1966) Sulfur isotopic fractionation between sulfur and sulfuric acid in the hydrothermal solution of sulfur dioxide. *Geochemical Journal* **1**, 45-50.
- Ohmoto H. (1996) Formation of volcanogenic massive sulfide deposits: The Kuroko perspective. *Ore Geology Reviews* **10**, 135-177.
- Omorgie E. O., Niemann H., Mastalerz V., de Lange G. J., Stadnitskaia A., Mascle J., Foucher J.-P. and Boetius A. (2009) Microbial methane oxidation and sulfate reduction at cold seeps of the deep Eastern Mediterranean Sea. *Marine Geology* **261**, 114-127.
- Peck Jr. H. D. (1959) The ATP-dependent reduction of sulfate with hydrogen in extracts of *Desulfovibrio desulfuricans*. *Biochemistry* **45**, 701-708.
- Peck Jr. H. D. (1960) Adenosine 5'-phosphosulfate as an intermediate in the oxidation of thiosulfate by *Thiobacillus thioparus*. *Biochemistry* **46**, 1053-1057.
- Peck Jr. H. D. (1961) Evidence for the reversibility of the reaction catalyzed by adenosine 5'-phosphosulfate reductase. *Biochim. Biophys. Acta* **49**, 621-624.
- Peck Jr. H. D. (1962) V. Comparative metabolism of inorganic sulfur compounds in microorganisms. *Microbiol. Mol. Biol. Rev.* **26**, 67-94.
- Peck Jr. H. D. and Stulberg M. P. (1962) O¹⁸ studies on the mechanism of sulfate formation and phosphorylation in extracts of *Thiobacillus thioparus*. *The Journal of Biological Chemistry* **237**, 1648-1652.
- Rees C. E. (1973) A steady-state model for sulphur isotope fractionation in bacterial reduction processes. *Geochimica et Cosmochimica Acta* **37**, 1141-1162.
- Peters M., Strauss H., Farquhar J., Ockert C., Eickmann B. and Jost C. L. (2010) Sulfur cycling at the Mid-Atlantic Ridge: A multiple sulfur isotope approach. *Chemical Geology* **269**, 180-196.
- Rimstidt J. D. and Vaughan D. J. (2003) Pyrite oxidation: A state-of-the-art assessment of the reaction mechanism. *Geochimica et Cosmochimica Acta* **67**, 873-880.
- Roerdink D. L., Mason P. R. D., Farquhar J. and Reimer T. (2012) Multiple sulfur isotopes in Paleoarchean barites identify an important role for microbial sulfate reduction in the early marine environment. *Earth and Planetary Science Letters* **331-332**, 177-186.
- Rudnicki M. D., Elderfield H. and Spiro B. (2001) Fractionation of sulfur isotopes during bacterial sulfate reduction in deep ocean sediments at elevated temperatures. *Geochimica et Cosmochimica Acta* **65**, 777-789.
- Schippers A., Jozsa P.-G. and Sand W. (1996) Sulfur Chemistry in Bacterial Leaching of Pyrite. *Applied and Environmental Microbiology* **62**, 3424-3431.
- Schippers A. and Sand W. (1999) Bacterial Leaching of Metal Sulfides Proceeds by Two Indirect Mechanisms via Thiosulfate or via Polysulfides and Sulfur. *Applied and Environmental Microbiology* **65**, 319-321.

- Schwedt A., Kreuzmann A.-C., Polerecky L. and Schulz-Vogt H. (2012) Sulfur respiration in a marine chemolithoautotrophic *Beggiatoa* strain. *Frontiers in Microbiology* (Microbial Physiology and Metabolism) **2**, 1-8.
- Scott S. D. and Binns R. A. (1995) Hydrothermal processes and contrasting styles of mineralization in the western Woodlark and eastern Manus basins of the western Pacific. From Parson L. M., Walker C. L. and Dixon D. R. (eds), *Hydrothermal Vents and Processes*, Geological Society Special Publication **87**, 191-205.
- Sharp Z. (2007) Principles of stable isotope geochemistry. Pearson Education, Inc.
- Shen Y. and Buick R. (2004) The antiquity of microbial sulfate reduction. *Earth-Science Reviews* **64**, 243-273.
- Sim M. S., Ono S., Donovan K., Templer S. and Bosak T. (2011) Effect of electron donors on the fractionation of sulfur isotopes by a marine *Desulfovibrio* sp. *Geochimica et Cosmochimica Acta* **75**, 4244-4259.
- Singer P. C. and Stumm W. (1970) Acidic Mine Drainage: The Rate-Determining Step. *Science* **2**, 1121-1123.
- Skyring G. W. and Donnelly T. H. (1982) Precambrian sulfur isotopes and a possible role for sulfite in the evolution of biological sulfate reduction. *Precambrian Research* **17**, 41-61.
- Stumm W. and Lee G. F. (1961) Oxygenation of Ferrous Iron. *Industrial and Engineering Chemistry* **53**, 143-146.
- Taylor B. E., Wheeler M. C. and Nordstrom D. K. (1984a) Isotope composition of sulphate in acid mine drainage as measure of bacterial oxidation. *Nature* **308**, 538-541.
- Taylor B. E., Wheeler M. C. and Nordstrom D. K. (1984b) Stable isotope geochemistry of acid mine drainage: Experimental oxidation of pyrite. *Geochimica et Cosmochimica Acta* **48**, 2669-2678.
- Thamdrup B., Finster K., Würgler Hansen J. and Bak F. (1993) Bacterial Disproportionation of Elemental Sulfur Coupled to Chemical Reduction of Iron or Manganese. *Applied and Environmental Microbiology* **59**, 101-108.
- Turchyn A. V., Brüchert V., Lyons T. W., Engel G. S., Balci N., Schrag D. P. and Brunner B. (2010) Kinetic oxygen isotope effects during dissimilatory sulfate reduction: A combined theoretical and experimental approach. *Geochimica et Cosmochimica Acta* **74**, 2011-2024.
- Uyama F., Chiba H., Kusakabe M. and Sakai H. (1985) Sulfur isotope exchange reaction in the aqueous system: thiosulfate-sulfide-sulfate at hydrothermal temperature. *Geochem. J.* **19**, 301-315.
- Van Stempvoort D. R. and Krouse H. R. (1994) Controls of $\delta^{18}\text{O}$ in Sulfate. in Environmental Geochemistry of Sulfide Oxidation, Alpers C. N., Blowes D. W., Eds. (American Chemical Society, Washington, DC, pp. 446-480.
- Von Glasow R., Bobrowski N. and Kern C. (2009) The effects of volcanic eruptions on atmospheric chemistry. *Chemical Geology* **263**, 131-142.
- Wigley T. M. L. (1989) Possible climate change due to SO_2 -derived cloud condensation nuclei. *Nature* **339**, 365-367.
- Williams S. N., Sturchio N. C., Calvache M. L. V., Mendez R. F., Londoño A. C. and García N. P. (1990) Sulfur dioxide from Nevado del Ruiz volcano, Colombia:

- total flux and isotopic constraints on its origin. *Journal of Volcanology and Geothermal Research* **42**, 53-68.
- Wortmann U. G., Bernasconi S. M. and Böttcher M. E. (2001) Hypersulfidic Deep Biosphere Indicates Extreme Sulfur Isotope Fractionation During Single-Step Microbial Sulfate Reduction. *Geology* **29**, 647-650.
- Wortmann U. G., Chernyavsky B., Bernasconi S. M., Brunner B., Böttcher M. E. and Swart P. K. (2007) Oxygen isotope biogeochemistry of pore water sulfate in the deep biosphere: Dominance of isotope exchange reactions with ambient water during microbial sulfate reduction (ODP Site 1130). *Geochimica et Cosmochimica Acta* **71**, 4221-4232.

2. The oxygen isotope equilibrium fractionation between sulfite species and water

Inigo A. Müller^{a,b,*}, Benjamin Brunner^a, Christian Breuer^{b,c}, Max Coleman^{d,e} and Wolfgang Bach^{b,c}

^aBiogeochemistry Department, Max Planck Institute for Marine Microbiology, Celsiusstrasse 1, 28359 Bremen, Germany

^bMARUM-Center for Marine Environmental Sciences, University of Bremen, Leobener Strasse, 28359 Bremen, Germany

^cDepartment of Geosciences, University of Bremen, Klagenfurter Strasse, 28359 Bremen, Germany

^dPlanetary Surface Instruments Group, NASA Jet Propulsion Laboratory, California Institute of Technology, 4800 Oak Grove Drive, Pasadena, CA 91109, USA

^eNASA Astrobiology Institute

*Corresponding author: imueller@mpi-bremen.de; Tel.: 0049 4212028 638

2.1. Abstract

Sulfite is an important sulfoxy intermediate in oxidative and reductive sulfur cycling in the marine and terrestrial environment. Aqueous sulfite exists as different sulfite species, such as dissolved sulfur dioxide (SO₂), bisulfite (HSO₃⁻), pyrosulfite (S₂O₅²⁻) and sulfite *sensu stricto* (SO₃²⁻), whereas their relative abundance in solution depends on the pH. Conversion of one species into another is rapid and involves in many cases incorporation of oxygen from or release of oxygen to water (e.g. SO₂ + H₂O ↔ HSO₃⁻ + H⁺) resulting in rapid oxygen isotope exchange between sulfite species and water. Consequently, the oxygen isotope composition of sulfite is expected to be strongly dependent on the oxygen isotope composition of water, unlike sulfate which does not spontaneously exchange oxygen isotopes with water under most conditions (Lloyd, 1968). Thus, sulfate preserves the oxygen isotope signature created by oxidative and reductive sulfur cycling that proceeds over sulfite as intermediate. For the understanding and interpretation of the sulfate oxygen isotope composition, it is pivotal to understand the isotope effects caused by oxygen isotope exchange between sulfite and water. The value for the oxygen isotope equilibrium fractionation between sulfite in solution and water is poorly constrained. One reason for the lack of accurate information on the equilibrium isotope fractionation between sulfite and water are technical difficulties in extraction of sulfite from solution for oxygen isotope analysis.

To overcome these challenges, anoxic isotope equilibration experiments were performed with dissolved sodium sulfite in solutions with distinct oxygen isotope signatures. Sulfite was precipitated using two different agents, barium chloride and silver nitrate. The experiments were performed at pH 1.5, 6.3, 6.6, and 9.7 to investigate how sulfite species distribution affects the oxygen isotope equilibrium fractionation between sulfite and water.

From the experiments at very low pH where SO_2 is the dominant sulfite species, a rough estimate for the oxygen isotope equilibrium fractionation factor between the aqueous SO_2 and water ($\epsilon^{\text{EQ}}_{\text{SO}_2 \leftrightarrow \text{H}_2\text{O}}$) with a value of approximately 37.0‰ at 22°C was determined. From near neutral and high pH experiments a more firm estimate for the oxygen isotope equilibrium fractionation between sulfite and water ($\epsilon^{\text{EQ}}_{\text{SO}_3^{2-} \leftrightarrow \text{H}_2\text{O}}$) of 15.2±0.7‰ at 22°C was found.

Our results provide new insights into the oxygen isotope fractionation during reductive and oxidative sulfur cycling. They demonstrate that isotope exchange between sulfite and water during dissimilatory sulfate reduction (DSR) alone cannot be responsible for the apparent oxygen isotope equilibrium fractionation between sulfate and water mediated by DSR. Our estimates also provide a basis for tracing and quantifying the transformation of sulfoxy intermediates during the oxidation of reduced sulfur compounds to sulfate.

2.2. Introduction

2.2.1. The role of sulfite in shaping the oxygen isotope composition of sulfate

Due to its reactivity, sulfite is not abundant in the environment. It is released into the environment as SO_2 by magmatic processes such as the degassing of SO_2 from hydrothermal systems at the seafloor or from volcanically active terrestrial environments where it can undergo disproportionation to sulfate and reduced sulfur compounds (Butterfield et al., 2011; Kusakabe et al., 2000). An important anthropogenic source of SO_2 released into the atmosphere is the burning of fossil fuels (e.g. coal, oil, gas, wood and gasoline), which is one of the causes for acid rain (Holt et al., 1981; Pham et al., 1996; Quinn, 1989; Zhao et al., 1988).

Despite its scarceness in the environment, sulfite is assumed to be an important sulfoxy intermediate in reductive and oxidative sulfur cycling. It is an intermediate in dissimilatory sulfate reduction (DSR), where sulfate is used as electron acceptor in the oxidation of organic matter (Brunner and Bernasconi, 2005; Brunner et al., 2005; Brunner et al., 2012; Fritz et al., 2002; Mizutani and Rafter, 1973; Peck Jr., 1962; Peck Jr. and Stulberg, 1962; Turchyn et al., 2010). Sulfite is also thought to be an important intermediate during the oxidation of reduced sulfur compounds (e.g. H_2S , HS^- , FeS_2 , FeS) and elemental S which exist in high abundance under reducing conditions in marine sediments at the seafloor or in ore deposits (Schippers et al., 1996). These reduced sulfur compounds can be oxidized by microorganisms or abiotically where molecular oxygen (O_2) or ferric iron (Fe^{3+}) are used as oxidants. Oxidative and reductive sulfur cycling leaves imprints in the oxygen isotope composition of sulfate, an ion that does not

spontaneously exchange oxygen isotopes with water unless exposed to extremely high temperatures and extremely low pH (Chiba and Sakai, 1985; Lloyd, 1968). Therefore, the oxygen isotope composition of sulfate has been used to investigate sulfur oxidation (e.g. Balci et al., 2007; Balci et al., 2012; Böttcher et al., 2001; Böttcher et al., 2005; Brabec et al., 2012; Brunner et al., 2008; Kohl and Bao, 2011; Lloyd, 1967; Lloyd, 1968), DSR (Fritz et al., 1989; Mizutani and Rafter, 1973; Wortmann et al., 2007) as well as past and present reductive and oxidative sulfur cycling on Earth (Bottrell et al., 2009; Bottrell and Newton, 2006; Pirllet et al., 2010; Riedinger et al., 2010; Turchyn and Schrag, 2004). Unlike sulfate, sulfite easily exchanges its oxygen isotopes with ambient water, and due to its importance as intermediate in oxidative and reductive sulfur cycling, it is very likely that the isotope effects associated with this isotope exchange process are pivotal in shaping the isotope signature of sulfate. So far, the equilibrium isotope effect for oxygen isotope exchange between sulfite and water has not been determined accurately, only a preliminary estimate exists (~11.5‰, Brunner et al., 2006).

2.2.2. Species-dependent oxygen isotope exchange between sulfite and water

In aqueous solutions, sulfite exists in the form of different sulfur species which have in common that the sulfur atom has an oxidation state of +IV. Simon and Waldmann (1955 and 1956) investigated the characteristics of sulfite species in aqueous solutions (reaction 2.1, 2.2 and 2.3) and their dependence on the pH, as well as the total concentration of sulfite species. They observed that SO₂ in solution forms bisulfite ions (HSO₃⁻, reaction 2.1) with sulfurous acid (H₂SO₃) as a hypothetical intermediate. However, H₂SO₃ as species so far has not been detected in aqueous solutions (Sülzle et al., 1988). Simon and Waldmann (1955 and 1956) observed that bisulfite forms sulfite *sensu stricto* (SO₃²⁻) and another proton via reaction 2.2 and described a reaction where two HSO₃⁻ ions react to form pyrosulfite (S₂O₅²⁻) and water (Eq. 2.3). All abbreviations in the text are listed in Table 2.1 with short explanation.



and



By now, the reactions between sulfite species have been studied in more detail, and the kinetics of oxygen exchange between water and sulfite species are fairly well constrained (see Horner and Connick, 2003 and references discussed therein) for example by measuring the frequency dependence of the attenuation of sound waves in sulfur dioxide solutions (Eigen et al., 1961), by experiments with ¹⁸O tracers (Betts and Voss, 1970 and Betts and Libich, 1970) or with relaxation measurements by ¹⁷O nuclear magnetic resonance spectroscopy (Connick et al., 1982; Horner and Connick, 1986; Horner and Connick, 2003). Betts and Voss (1970) determined the kinetics of the sulfite water exchange (Eq. 1) with ¹⁸O as stable isotope tracer and by mass spectrometry. Horner and Connick (1982 and 2003) evaluated the equilibrium constants for the isomerization of the bisulfite ion (Eq. 2.4) as well as the kinetics between the isomers of bisulfite, the disulfite ion (pyrosulfite S₂O₅²⁻) and water (Eq. 2.3) by studying the characteristics of these sulfite species in solution with oxygen-17 nuclear magnetic resonance spectroscopy.



With the help of equilibrium constants (e.g. from Horner and Connick, 2003) and information on the total sulfite concentration it is possible to quantitatively predict the sulfite species distribution in an aqueous solution as a function of pH. Figure 1 depicts such a distribution for a total sulfite concentration of 0.02 M – the concentration chosen for the experiments in our study – and is based on equilibrium constants for equations 2.1, 2.2, 2.3 ($Q_1 = 10^{-1.37}$ m, $Q_2 = 10^{-6.34}$ m, $Q_3 = 0.082 \text{ M}^{-1}$) where the differences between molal (m) and molar (M) units is considered to be unimportant compared to uncertainties in the rate constant values (Horner and Connick, 2003), the constant for the water dissociation ($\text{p}Q_{\text{W}} = 13.79$), and on the equilibrium constant for the dissociation of sodium sulfite ion ($\text{NaSO}_3^- = \text{Na}^+ + \text{SO}_3^{2-}$, $\log K = 0.83$, from Visual MINTEQ database 2008).

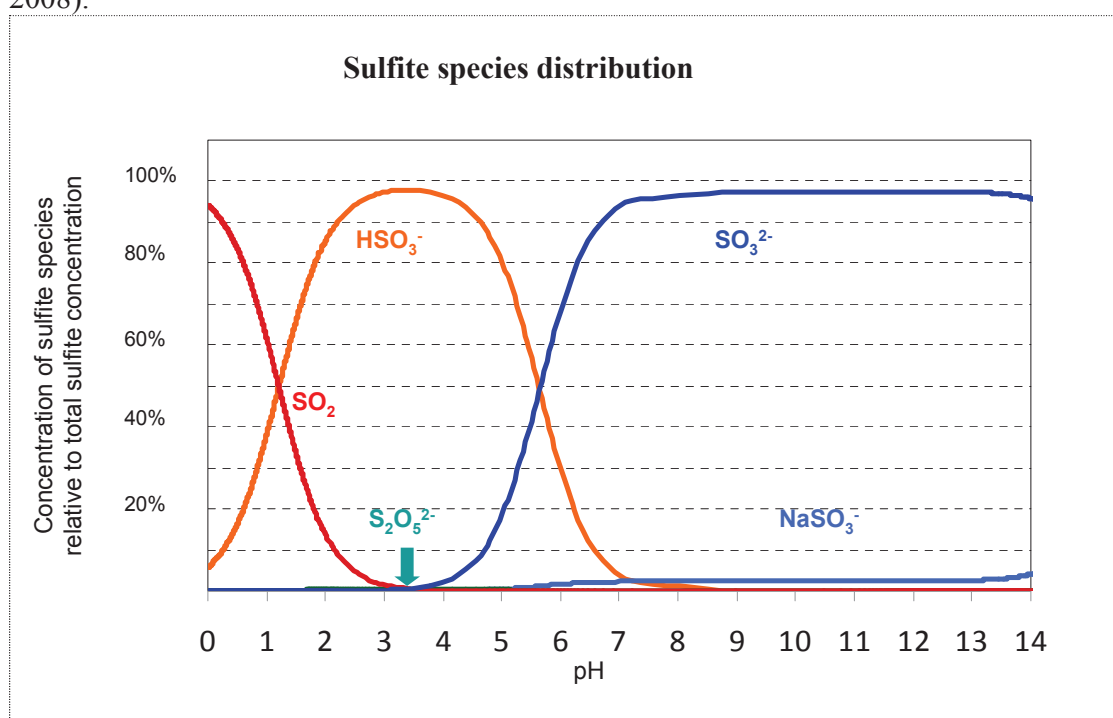


Fig. 2.1: pH dependent sulfite species distribution in a solution with a total sulfite concentration of 0.02 M: Below pH 1 sulfur dioxide (SO₂) dominates, between pH 1.5 and pH 6 the sum of the two bisulfite isomers (HSO₃⁻, SO₃H⁻). The amount of S₂O₅²⁻ is very small. In the alkaline pH range SO₃²⁻ dominates and there are minor amounts of NaSO₃⁻. The sulfite speciation was calculated with the software Geochemist Workbench using equilibrium constants from Horner and Connick (2003).

2.2.3. Precipitation of sulfite salts for subsequent oxygen isotope analysis and determination of isotope fractionation between sulfite and water

Even though the kinetic behavior of sulfite species in aqueous solutions has been explored in detail, reliable information on the oxygen isotope equilibrium fractionation between sulfite species and water is lacking so far. One reason for the lack of this data is the technical difficulty of extracting sulfite species from solution for oxygen isotope analysis. The experimental challenge arises from the fact that typically more than one sulfite species coexist in solution (Fig. 2.1) causing extraction techniques such as

precipitation of sulfite as barium sulfite or silver sulfite to induce conversion of all sulfite species, (i.e. SO_2 and $\text{S}_2\text{O}_5^{2-}$) to SO_3^{2-} , via equations 2.1 – 2.4. The oxygen isotope signature of the precipitated sulfite salt cannot be directly attributed to an equilibrium isotope fractionation between a certain sulfite species and water for two reasons: First, each sulfite species is expected to possess an individual oxygen isotope equilibrium fractionation with water which could vary for the different sulfite species, and second, the wholesale conversion of all sulfite species to SO_3^{2-} is likely to induce incorporation of additional oxygen from water and kinetic oxygen isotope effects. Furthermore, the precipitated sulfite salts such as BaSO_3 can be strongly hygroscopic, resulting in uptake of water vapor from the air, which typically introduces oxygen with a much lighter isotopic composition than the isotope composition of the sample.

To overcome these challenges and to determine the effective oxygen isotope equilibrium fractionation between different sulfite species and water, replicate oxygen isotope equilibration experiments were performed in water with three distinct isotope compositions of which sulfite was collected as two different sulfite salts (BaSO_3 and Ag_2SO_3). For each sulfite salt, four aliquots were precipitated by addition of isotopically distinct precipitation solutions (barium chloride and silver chloride solution, respectively). This approach allows disentangling isotope effects caused by the precipitation process from the actual equilibrium isotope effects. The comparison between the results obtained from different sulfite salts helped assessing the reliability of different sulfite precipitation strategies.

2.3. Methods

To determine the oxygen isotope equilibrium fractionation between dissolved sulfite species and water three prerequisites must be fulfilled: First, the experimental/technical challenges related to the collection of samples for isotope analysis must be identified, secondly, experimental approaches to overcome these challenges must be established, and thirdly, an isotope mass balance that considers all relevant factors affecting the oxygen isotope composition of the precipitates in our experiments must be developed.

2.3.1. Experiment challenges and approaches on how to cope with them

The following isotope effects during the conversion of sulfite species into sulfite salt have an impact on the experimental results:

- The conversion of SO_2 and $\text{S}_2\text{O}_5^{2-}$ into HSO_3^- (Eq. 2.1 and Eq. 2.3) involves incorporation of oxygen from water, which includes kinetic oxygen isotope fractionation with respect to sulfite species and with respect to water.
- The conversion of HSO_3^- into SO_3^{2-} (Eq. 2.2) during the precipitation as sulfite salt involves kinetic oxygen isotope fractionation with respect to HSO_3^- .
- The precipitation of SO_3^{2-} as a salt (Ag_2SO_3 and BaSO_3) involves kinetic oxygen isotope fractionation, and probably equilibrium isotope fractionation between the solid phase and dissolved SO_3^{2-} .
- Sulfite salts may incorporate considerable amounts of water molecules during precipitation in their structure, also known for BaSO_4 minerals (“lattice water”; see

Neagle and Rochester, 1988; Walton and Walden, 1946a; Walton and Walden, 1946b).

- Rapid oxygen isotope exchange between sulfite species and water can overprint kinetic isotope effects during the conversion of one sulfite species to another. For example, SO_2 could become enriched in ^{18}O during the conversion of SO_2 to BaSO_3 due to preferential conversion of SO_2 depleted in ^{18}O to SO_3^{2-} . This enrichment could be overprinted by rapid oxygen isotope exchange between SO_2 and water (i.e. the oxygen isotope composition from SO_2 would be no longer quantitatively converted to sulfite).
- Precipitated sulfite salts can be hygroscopic and thus incorporate water from air with entirely different oxygen isotope composition.
- Oxidation of sulfite to sulfate stops oxygen isotope exchange and leaves strong O isotope imprints.

Experimental approaches to cope with these challenges involve:

- A rapid shift of the sample solution pH (e.g. by addition of NaOH solution) to strongly basic conditions induces the conversion of sulfite species to SO_3^{2-} which efficiently stops oxygen isotope exchange between sulfite species and water. This approach has some trade-offs: i) high pH solutions are not suitable for the precipitation of sulfite salts with cations that easily form hydroxides, for example addition of Ag^+ induces precipitation of AgOH , ii) the treatment with a base may facilitate incorporation of water oxygen into crystal lattice, iii) salts precipitated in the presence of a strong base could be more hygroscopic.
- Using pH conditions and sulfite concentrations where one or two species dominate limits number of unknowns for subsequent isotope mass balance calculations. We chose a total concentration of sulfite of 0.02 M combined with two different pH settings: very low pH (pH 1.5, SO_2 and HSO_3^- dominate) and slightly acid to basic solutions (pH 6.3 to 9.7, HSO_3^- and/or SO_3^{2-} dominate). Under these conditions $\text{S}_2\text{O}_5^{2-}$ occurs only in very low proportions (Fig. 2.1). Consequences for the isotope mass balance are as follows: i) $\text{S}_2\text{O}_5^{2-}$ can be neglected, ii) due to the similarity of the molecular structure of the two bisulfite isomers (HSO_3^- , SO_3H^-) and SO_3^{2-} we expect that their equilibrium isotope effects relative to water are similar. Therefore we treat the oxygen equilibrium isotope effects for these three species as identical.
- Cations that induce precipitation of sulfite salts with lower solubility products than others may cause a more rapid and quantitative conversion of sulfite species to the respective salt. Thereby oxygen isotope exchange between sulfite and water during precipitation would be suppressed. We used Ag^+ and Ba^{2+} to test this possibility. An additional benefit of using different cations as agents for salt precipitation is that some salts may also be less hygroscopic than others.
- Cleaning of the precipitated sulfite salts with acetone which may diminish the amount of incorporated precipitation water and accelerates the drying procedure of precipitated salts (limits oxygen isotope exchange between water and sulfite from salt during drying).
- Using precipitation solutions with different isotope compositions allows quantifying of the amount of oxygen incorporated from water during the precipitation stage. This value can be compared to the theoretical oxygen incorporation which is expected to result from the conversion of SO_2 and $\text{S}_2\text{O}_5^{2-}$. Much larger values than anticipated are

indicative of ongoing oxygen isotope exchange during the precipitation process, and thus provide information on how reliable the estimates for equilibrium isotope fractionation are (because kinetic isotope effects with respect to sulfite species that exchange oxygen isotopes with water cannot be fully accounted for).

- Using different experimental waters allows to assess if there is an external contaminant (e.g. water taken up from water vapor in case of hygroscopic sulfite salts) or if there is an internal contaminant (e.g. sulfate derived from sulfite oxidation in an early stage of the experiment or sulfate that contaminated the Na_2SO_3 starting material) and also allows correction for such a contaminant. Furthermore, using different waters means “different travel distances” for isotope equilibration – if all offsets are in the same range, there is a good indication that the samples truly reached isotope equilibrium with water.
- The experiments need to be carried out under anoxic conditions to prevent oxidation of sulfite.

2.3.2. Equilibrium experiments

Oxygen-18 labeled experiment solutions:

For the equilibration experiments, water with three different oxygen isotope compositions ($\delta^{18}\text{O}_{\text{H}_2\text{O}_{\text{exp}}}$ of -7.7‰, 28.1‰ and 64.6‰) were prepared by mixing de-ionized water (18 M Ω , abbreviated as MQ) with appropriate amounts of water consisting of 98% ^{18}O (NUKEM GmbH). This range of isotope values was chosen to obtain a considerable spread in isotope compositions, which is still in a range where results from isotope measurements can be considered to be reliable.

Preparation of sulfite equilibration experiments:

Glass flasks (Duran glass bottles, volume 290 ml) were filled with 250 ml of experimental solutions which leaves approximately 40 ml headspace once the flask is sealed with a rubber stopper. The flasks were purged with oxygen-free nitrogen gas (N_2) for 30 minutes to obtain anoxic conditions. Meanwhile 0.63 g sodium sulfite (Na_2SO_3 from Fluka, $M_{\text{R}} = 126.04 \text{ g mol}^{-1}$) was weighed into small plastic tubes (1.5 ml microtubes), ready to add to the experiment flasks. To prevent contamination with oxygen from air, the experiment flasks and microtubes filled with Na_2SO_3 powder were placed in a plastic glove bag with a N_2 atmosphere (purged twice with N_2 gas before closing the glove bag gas tight; see Fig. 2.2). Inside the glove bag the experiment solutions were purged again for 5 minutes with N_2 gas, before adding the Na_2SO_3 powder and immediately sealing the flasks with rubber stoppers.

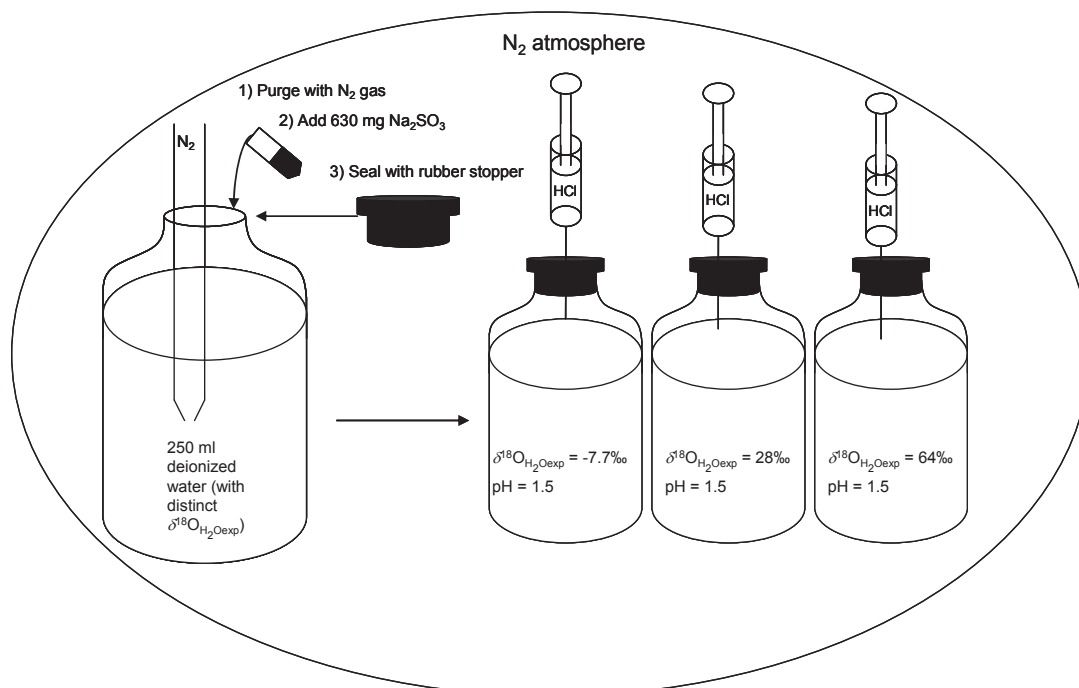


Fig. 2.2: Preparation of experiment solutions in a glove bag with N_2 atmosphere to prevent contamination with air. Each of the isotopically distinct experiment solutions was purged first with N_2 gas. Subsequently Na_2SO_3 was added, and the bottles were sealed immediately with rubber stoppers. For the experiments at very low pH, the pH was adjusted by injecting 6 M HCl with a syringe through the rubber stopper.

Adjusting the pH of the equilibrium experiments:

The experiments were adjusted to low pH with hydrochloric acid, experiments near neutral pH with acetate buffer solutions and for the high pH experiments solely by adding Na_2SO_3 into the solutions. Low pH experiments were prepared by injecting 2 ml 6 M HCl through the rubber stopper of the experiment flasks inside the glove bag, to avoid loss of gaseous SO_2 which is produced at this low pH (see Fig. 2.1). The experiments close to neutral pH were performed in 40 mM acetate buffer solution prepared by adding 0.94 g sodium acetate trihydrate ($M_R = 136.1 \text{ g mol}^{-1}$) and 222 μl acetic acid ($M_R = 60.05 \text{ g mol}^{-1}$) to the labeled experiment solutions. By shaking the sealed experiment flasks, the Na_2SO_3 is immediately dissolved. The pH was measured with a pH electrode (pH-Meter 766 Calimatic from Knick) with accuracy of less than 0.09 pH units.

Experiment duration:

The experiments with low pH were equilibrated for one day, the experiments near neutral pH for two days and experiments at higher pH were equilibrated for three days to ensure that the oxygen of the sulfite species was in equilibrium with the surrounding water. Over the time of equilibration, the experiment flasks were kept inside the glove bag under a N_2 atmosphere.

2.3.3. Precipitation of sulfite salts with isotopically distinct precipitation solutions and with different cations (Ag^+ , Ba^{2+})

Precipitation with isotopically distinct solutions enables us to calculate the amount of incorporated water oxygen during the precipitation of sulfite salts.

Oxygen-18 labeled solutions for precipitation:

For the precipitation, water with four different oxygen isotope compositions ($\delta^{18}\text{O}_{\text{H}_2\text{O}_{\text{psoln}}}$ of -7.7‰, 48‰, 162‰ and 212‰) were prepared by mixing MQ water with appropriate amounts of water consisting of 98% of ^{18}O .

Precipitation solutions:

Three sets of precipitation solutions were prepared: i) Precipitation solutions with silver nitrate (for experiments at pH 6.3 and 6.6) were prepared by dissolving AgNO_3 ($M_R = 169.87 \text{ g mol}^{-1}$, AppliChem) in the four isotopically distinct solutions to a final concentration of 70 mM. ii) A second set of precipitation solutions with barium chloride (for experiments at pH 6.3 and 9.7) was prepared by dissolving $\text{BaCl}_2 \cdot 2\text{H}_2\text{O}$ ($M_R = 244.26 \text{ g mol}^{-1}$, Sigma Aldrich) in isotopically distinct solutions to a concentration of 50 mM. iii) A third set of precipitation solutions with barium (for experiments at pH 1.5 and 6.6) was prepared by dissolving $\text{BaCl}_2 \cdot 2\text{H}_2\text{O}$ and sodium hydroxide (NaOH , $M_R = 39.9 \text{ g mol}^{-1}$) in the isotopically distinct solutions to a concentration of 50 mM and 100 mM, respectively. The addition of NaOH to the precipitation solutions induces rapid conversion of sulfite (all species) in solution to SO_3^{2-} , and efficiently stops any further oxygen isotope exchange between sulfite and water. This approach is feasible with barium solutions, but not applicable to silver nitrate solutions, because silver would precipitate as silver hydroxide (AgOH) and silver oxide (Ag_2O) in alkaline solutions (Biedermann and Sillén, 1960). All precipitation solutions were purged with N_2 , sealed with rubber stoppers and placed inside the glove bag together with the experiment solutions.

Precipitation of sulfite salts:

Sulfite rapidly oxidizes in the presence of air (highest oxidation rate at pH 6.5; Zhang and Millero, 1991), thus also the precipitation of sulfite salts was carried out under a N_2 atmosphere in the glove bag. Aliquots (5 ml) of the precipitation solutions were distributed into plastic centrifuge tubes (Sarstedt, 15 ml). After preloading tubes with precipitation solutions the experiment flasks were opened and 5 ml of sample solution was transferred with a pipette into each of the four isotopically distinct precipitation solutions (Fig. 2.3). The isotope composition of the final precipitation mixture in which the salts were precipitated resulted in mixing 5 ml of an experimental solution ($\delta^{18}\text{O}_{\text{H}_2\text{O}_{\text{exp}}}$) with 5 ml of the precipitation solution ($\delta^{18}\text{O}_{\text{H}_2\text{O}_{\text{psoln}}}$) resulting in 10 ml of a precipitation mixture ($\delta^{18}\text{O}_{\text{H}_2\text{O}_{\text{mix}}}$).

Collection of sulfite salts:

After adding the sulfite solution to the precipitation solutions, the centrifuge tubes were capped and immediately transferred to a centrifuge outside the glove bag. The tubes were centrifuged at 2000 rpm for five minutes. Subsequently the supernatant was decanted and

5 ml of acetone was added (after Betts and Libich, 1970). The samples were mixed with the acetone by vigorous shaking of the centrifuge tubes followed by centrifugation at 2000 rpm for five minutes, and decanting of the acetone supernatant. This step was repeated once more, before drying the precipitates in an oven for two days at 50°C. Initially, a few selected samples were freeze dried instead of oven dried, but as both methods yielded identical results all precipitates were subsequently dried in the oven.

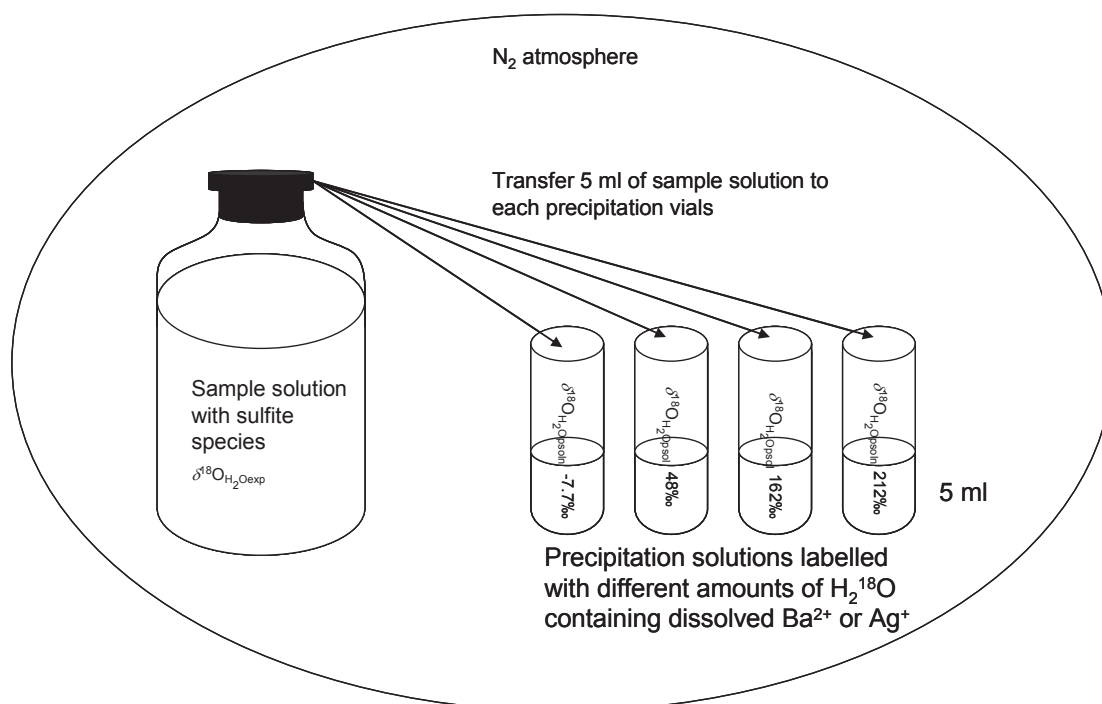


Fig. 2.3: Precipitation of sulfite: The precipitation was done in N_2 atmosphere to prevent contamination with air. Plastic tubes were preloaded with 5 ml of the precipitation solutions (containing Ag^+ or Ba^{2+} , respectively) and then 5 ml of the sulfite solution was added, the plastic tubes closed, shaken and taken out of the glove bag for subsequent centrifugation.

Trapping of laboratory water vapor:

Water vapor is a potential contaminant in hygroscopic sulfite precipitates. To determine the oxygen isotope composition of water vapor in our laboratory we used a cooling coil ($T = -27^\circ\text{C}$) in a closed vessel and collected the formed ice that accumulated at the coil. To accumulate enough ice for isotope measurements we had to open the lid of the vessel several times so that fresh water vapor could enter and subsequently condense during closed phases.

2.3.4. Stable isotope measurements

The oxygen isotope compositions of the precipitates were measured by isotope ratio mass spectrometry (IRMS) by a Finnigan DELTA^{plus} mass spectrometer coupled to a thermochemical reduction device (TC/EA Finnigan). In brief, the precipitates were weighed (BaSO₃ between 0.3 – 0.4 mg and Ag₂SO₃ between 0.6 – 0.8 mg) into silver cups which were loaded into an auto sampler coupled the TC/EA. In the TC/EA the samples were reduced at 1450°C in the presence of carbon. The evolved CO gas was carried through a gas chromatography column and analyzed by continuous flow isotope mass spectrometry. The isotope results are reported in the standard δ -notation where the isotope ratio ($R = {}^{18}\text{O}/{}^{16}\text{O}$) of the sample is compared to the ratio of the Vienna Standard Mean Ocean Water (VSMOW), i.e. $\delta^{18}\text{O} = (R_{\text{sample}}/R_{\text{VSMOW}} - 1) \times 10^3\text{‰}$. Measurements were calibrated using standards NBS 127 ($\delta^{18}\text{O} = 8.7\text{‰}$), SO-5 ($\delta^{18}\text{O} = 12\text{‰}$) and SO-6 ($\delta^{18}\text{O} = -11.3\text{‰}$). The reproducibility based on repeated measurements of the standards is less than 0.5‰ (1 σ).

The oxygen isotope composition of water samples was determined with two different sampling devices: i) with a Cavity Ringdown Mass spectrometer (Los Gatos Research LGR DLT-100) and ii) with a Thermo Fisher Scientific® Delta V Plus IRMS. For measurements at the DLT-100, a small amount of liquid sample was injected into a heated septum port of the liquid auto sampler where it quickly vaporized and transported into a 25 cm laser cell. Here, the relative molecular abundances of ²H¹H¹⁶O, ¹H¹H¹⁸O, and ¹H¹H¹⁶O are determined at a wavelength of 1390 nm and converted into atomic ratios of ²H/¹H and ¹⁸O/¹⁶O. The obtained ratios are then converted by post-processing to the δ -scale with respect to VSMOW. Each sample was measured 10 times, the first four measurements were discarded because of potential memory effects, the average of the last six measurements yields the value for the isotope composition of the sample. The reproducibility for the DLT-100 measurements is typically less than 0.3‰ (1 σ).

Analyses with the Thermo Fisher Scientific® Delta V Plus mass spectrometer were carried out with the CO₂ equilibration method. Sample solutions from the experiments at high pH were acidified with small amounts of phosphorous pentoxide (P₄O₁₀), to prevent trapping of CO₂ gas in the sample solutions. From each sample, 200 μ l aliquots were transferred into gas tight glass vials with a volume of approximately 12 ml, afterwards the vials were purged with a mixture of 0.5% CO₂ in He gas. The samples were gently shaken for 18 hours allowing isotope equilibrium between sample water and CO₂ gas. After equilibration, small amounts of the gas were transferred via a Gas Bench device (Finnigan) to the IRMS. The system was calibrated with the international reference waters SMOW, GISP and SLAP and the oxygen isotope ratios are reported in the δ -notation relative to VSMOW. The reproducibility of the measurements based on repeated measurements of standards is less than 0.1‰ (1 σ).

The oxygen isotope composition of the same water samples show almost identical values with the two distinct measurement devices, with offsets smaller than 0.2‰. The isotope composition of the precipitation solution was calculated from the known amounts of mixing components (actual mol amounts of isotopologues in 5 ml of experiment solution and in 5 ml of precipitation solution) and their measured isotope compositions. The reported standard deviations are isotope values determined by using linear regression calculated for 95% confidence limits.

2.3.5. Isotope mass balances for the determination of the oxygen isotope equilibrium fractionation between dissolved sulfite and water

The relative amount of SO_2 , HSO_3^- , SO_3H^- , $\text{S}_2\text{O}_5^{2-}$, SO_3^{2-} , NaSO_3^- in solution depends on the pH (Fig. 2.1). Each of the species has a specific but constant oxygen isotope equilibrium fractionation relative to water. Mass balances for the amount of sulfur and oxygen of sulfite in solution can be written as follows:

$$[\text{Sulfite}_{\text{sulfur}}] = [\text{SO}_2] + [\text{HSO}_3^-] + [\text{SO}_3\text{H}^-] + 2 \cdot [\text{S}_2\text{O}_5^{2-}] + [\text{SO}_3^{2-}] + [\text{NaSO}_3^-] \quad \text{Eq. 2.5}$$

and

$$[\text{Sulfite}_{\text{oxygen}}] = 2 \cdot [\text{SO}_2] + 3 \cdot [\text{HSO}_3^-] + 3 \cdot [\text{SO}_3\text{H}^-] + 5 \cdot [\text{S}_2\text{O}_5^{2-}] + 3 \cdot [\text{SO}_3^{2-}] + 3 \cdot [\text{NaSO}_3^-] \quad \text{Eq. 2.6}$$

where expressions in [] refer to concentrations (for abbreviations, see Table 2.1 in 2.8. Appendices).

In our experiments, the concentrations of $\text{S}_2\text{O}_5^{2-}$ and NaSO_3^- are very small (Fig 2.1). Therefore, we can neglect these two species in our mass balance considerations.

$$[\text{Sulfite}_{\text{sulfur}}] = [\text{SO}_2] + [\text{HSO}_3^-] + [\text{SO}_3\text{H}^-] + [\text{SO}_3^{2-}] \quad \text{Eq. 2.7}$$

$$[\text{Sulfite}_{\text{oxygen}}] = 2 \cdot [\text{SO}_2] + 3 \cdot [\text{HSO}_3^-] + 3 \cdot [\text{SO}_3\text{H}^-] + 3 \cdot [\text{SO}_3^{2-}] \quad \text{Eq. 2.8}$$

The amount of oxygen of a sulfite precipitate can be calculated using a mass balance. The derived mass balance includes water oxygen that was incorporated during the conversion of sulfite species into SO_3^{2-} , water that was incorporated into the crystal lattice during the precipitation, and oxygen from contaminants (abbreviated as cont; i.e. oxygen from water vapor due to hygroscopic properties of sulfite salts).

$$[\text{Prec}_{\text{oxygen}}] = 3 \cdot [\text{SO}_2] + 3 \cdot [\text{HSO}_3^-] + 3 \cdot [\text{SO}_3\text{H}^-] + 3 \cdot [\text{SO}_3^{2-}] + [\text{H}_2\text{O}_{\text{mix incorp}}] + [\text{cont}] \quad \text{Eq. 2.9}$$

Based on the oxygen mass balance of the precipitate, we can derive an isotope mass balance for sulfite precipitates.

$$[\text{Prec}_{\text{oxygen}}] \cdot \delta^{18}\text{O}_{\text{prec}} = 3 \cdot [\text{SO}_2] \cdot \left(\frac{2}{3} \cdot \delta^{18}\text{O}_{\text{SO}_2} + \frac{1}{3} \cdot \left(\delta^{18}\text{O}_{\text{H}_2\text{O}_{\text{mix}}} + \varepsilon_{\text{H}_2\text{O} \setminus \text{SO}_2 \rightarrow \text{HSO}_3^-} \right) \right) + 3 \cdot [\text{HSO}_3^-] \cdot \delta^{18}\text{O}_{\text{HSO}_3^-} + 3 \cdot [\text{SO}_3\text{H}^-] \cdot \delta^{18}\text{O}_{\text{SO}_3\text{H}^-} + 3 \cdot [\text{SO}_3^{2-}] \cdot \delta^{18}\text{O}_{\text{SO}_3^{2-}} + [\text{H}_2\text{O}_{\text{mix incorp}}] \cdot \delta^{18}\text{O}_{\text{H}_2\text{O}_{\text{mix}}} + [\text{cont}] \cdot \delta^{18}\text{O}_{\text{cont}} \quad \text{Eq. 2.10}$$

where $\delta^{18}\text{O}_{\text{prec}}$ refers to the oxygen isotope composition of the precipitate, $\delta^{18}\text{O}_{\text{cont}}$ to the oxygen isotope composition of the contaminant, $\text{H}_2\text{O}_{\text{mix incorp}}$ designates water molecules from the precipitation mixture that are incorporated in the sulfite salt during precipitation

and $\epsilon_{\text{H}_2\text{O}\backslash\text{SO}_2\rightarrow\text{HSO}_3^-}$ designates the kinetic fractionation of water oxygen that is incorporated when SO_2 reacts with water to HSO_3^- (Eq. 2.1).

This isotope mass balance is based on the assumption that there is either no isotope effect for conversion of one sulfite species to another (e.g. no isotope discrimination between remaining SO_2 and SO_2 that is converted to SO_3^{2-}), or that there is a quantitative conversion of all sulfite species without simultaneous oxygen isotope exchange with water. If simultaneous oxygen isotope exchange with water occurs during the conversion of sulfite into the sulfite precipitate a quantitative conversion of all sulfite species would not suffice to justify the above assumption. In this case, estimates for equilibrium isotope fractionations based on Eq. 2.10 have to be considered with caution, as they might be biased by ignoring kinetic isotope effects resulting from the transformation of one sulfite species into another.

Equation 2.10 can be further simplified: due to the similar structure of the molecules of both bisulfite isomers (HSO_3^- , SO_3H^-) and SO_3^{2-} we expect the oxygen isotope fractionation with water to be similar for the three sulfite species, and consequently use only one equilibrium oxygen isotope fractionation for the bisulfites and SO_3^{2-} with respect to water.

$$\begin{aligned} & [\text{Prec}_{\text{oxygen}}] \cdot \delta^{18}\text{O}_{\text{prec}} = \\ & 3 \cdot [\text{SO}_2] \cdot \left(\frac{2}{3} \cdot \delta^{18}\text{O}_{\text{SO}_2} + \frac{1}{3} \cdot \left(\delta^{18}\text{O}_{\text{H}_2\text{Omix}} + \epsilon_{\text{H}_2\text{O}\backslash\text{SO}_2\rightarrow\text{HSO}_3^-} \right) \right) \\ & + 3 \cdot \left([\text{HSO}_3^-] + [\text{SO}_3\text{H}^-] + [\text{SO}_3^{2-}] \right) \delta^{18}\text{O}_{\text{SO}_3^{2-}} \\ & + [\text{H}_2\text{O}_{\text{mix incorp}}] \cdot \delta^{18}\text{O}_{\text{H}_2\text{Omix}} + [\text{cont}] \cdot \delta^{18}\text{O}_{\text{cont}} \end{aligned}$$

Eq. 2.11

The oxygen isotope composition of the similar molecules (HSO_3^- , SO_3H^- and SO_3^{2-}) is designated as $\delta^{18}\text{O}_{\text{SO}_3^{2-}}$. Considering that oxygen isotope exchange may happen during the precipitation (which would, as discussed above, have a negative impact on the reliability of estimates for equilibrium isotope fractionation), we have to introduce quantities for sulfite species that are in original conditions (e.g. $[\text{SO}_2]_{\text{orig}}$) and quantities for sulfite species that that have exchanged isotopes during the precipitation procedure (e.g. $[\text{SO}_2]_{\text{exchanged}}$):

$$\begin{aligned} & [\text{Prec}_{\text{oxygen}}] \cdot \delta^{18}\text{O}_{\text{prec}} = \\ & 3 \cdot [\text{SO}_2]_{\text{orig}} \cdot \left(\frac{2}{3} \cdot \left(\delta^{18}\text{O}_{\text{H}_2\text{Oexp}} + \epsilon_{\text{SO}_2\leftrightarrow\text{H}_2\text{O}}^{\text{EQ}} \right) + \frac{1}{3} \cdot \left(\delta^{18}\text{O}_{\text{H}_2\text{Omix}} + \epsilon_{\text{H}_2\text{O}\backslash\text{SO}_2\rightarrow\text{HSO}_3^-} \right) \right) \\ & + 3 \cdot [\text{SO}_2]_{\text{exchanged}} \cdot \left(\frac{2}{3} \cdot \left(\delta^{18}\text{O}_{\text{H}_2\text{Omix}} + \epsilon_{\text{SO}_2\leftrightarrow\text{H}_2\text{O}}^{\text{EQ}} \right) + \frac{1}{3} \cdot \left(\delta^{18}\text{O}_{\text{H}_2\text{Omix}} + \epsilon_{\text{H}_2\text{O}\backslash\text{SO}_2\rightarrow\text{HSO}_3^-} \right) \right) \\ & + 3 \cdot \left\{ [\text{HSO}_3^-] + [\text{SO}_3\text{H}^-] + [\text{SO}_3^{2-}] \right\}_{\text{orig}} \cdot \left(\delta^{18}\text{O}_{\text{H}_2\text{Oexp}} + \epsilon_{\text{SO}_3^{2-}\leftrightarrow\text{H}_2\text{O}}^{\text{EQ}} \right) \\ & + 3 \cdot \left\{ [\text{HSO}_3^-] + [\text{SO}_3\text{H}^-] + [\text{SO}_3^{2-}] \right\}_{\text{exchanged}} \cdot \left(\delta^{18}\text{O}_{\text{H}_2\text{Omix}} + \epsilon_{\text{SO}_3^{2-}\leftrightarrow\text{H}_2\text{O}}^{\text{EQ}} \right) \\ & + [\text{H}_2\text{O}_{\text{mix incorp}}] \cdot \delta^{18}\text{O}_{\text{H}_2\text{Omix}} + [\text{cont}] \cdot \delta^{18}\text{O}_{\text{cont}} \end{aligned}$$

Eq. 2.12

In Eq. 2.12, $\varepsilon^{\text{EQ}}_{\text{SO}_2 \leftrightarrow \text{H}_2\text{O}}$ and $\varepsilon^{\text{EQ}}_{\text{SO}_3^{2-} \leftrightarrow \text{H}_2\text{O}}$ represent the oxygen isotope equilibrium fractionation between dissolved SO_2 and water, and between SO_3^{2-} and water, respectively. We use $\{\}$ to indicate that all terms within these parentheses possess the same property, which is defined as subscript right of the parenthesis, e.g. $\{\}_{\text{orig}}$. Division of Eq. 2.12 by $[\text{Prec}_{\text{oxygen}}]$ results in:

$$\begin{aligned} \delta^{18}\text{O}_{\text{prec}} = & \frac{[\text{SO}_2]_{\text{orig}}}{[\text{Prec}_{\text{oxygen}}]} \cdot \left(2 \cdot \left(\delta^{18}\text{O}_{\text{H}_2\text{O}} + \varepsilon^{\text{EQ}}_{\text{SO}_2 \leftrightarrow \text{H}_2\text{O}} \right) + \left(\delta^{18}\text{O}_{\text{H}_2\text{Omix}} + \varepsilon_{\text{H}_2\text{O}/\text{SO}_2 \rightarrow \text{HSO}_3^-} \right) \right) \\ & + \frac{[\text{SO}_2]_{\text{exchanged}}}{[\text{Prec}_{\text{oxygen}}]} \cdot \left(2 \cdot \left(\delta^{18}\text{O}_{\text{H}_2\text{Omix}} + \varepsilon^{\text{EQ}}_{\text{SO}_2 \leftrightarrow \text{H}_2\text{O}} \right) + \left(\delta^{18}\text{O}_{\text{H}_2\text{Omix}} + \varepsilon_{\text{H}_2\text{O}/\text{SO}_2 \rightarrow \text{HSO}_3^-} \right) \right) \\ & + 3 \cdot \frac{\left\{ [\text{HSO}_3^-] + [\text{SO}_3\text{H}^-] + [\text{SO}_3^{2-}] \right\}_{\text{orig}}}{[\text{Prec}_{\text{oxygen}}]} \cdot \left(\delta^{18}\text{O}_{\text{H}_2\text{O}} + \varepsilon^{\text{EQ}}_{\text{SO}_3^{2-} \leftrightarrow \text{H}_2\text{O}} \right) \\ & + 3 \cdot \frac{\left\{ [\text{HSO}_3^-] + [\text{SO}_3\text{H}^-] + [\text{SO}_3^{2-}] \right\}_{\text{exchanged}}}{[\text{Prec}_{\text{oxygen}}]} \cdot \left(\delta^{18}\text{O}_{\text{H}_2\text{Omix}} + \varepsilon^{\text{EQ}}_{\text{SO}_3^{2-} \leftrightarrow \text{H}_2\text{O}} \right) \\ & + \frac{[\text{H}_2\text{O}_{\text{mix incorp}}]}{[\text{Prec}_{\text{oxygen}}]} \cdot \delta^{18}\text{O}_{\text{H}_2\text{Omix}} + \frac{[\text{cont}]}{[\text{Prec}_{\text{oxygen}}]} \cdot \delta^{18}\text{O}_{\text{cont}} \end{aligned}$$

Eq. 2.13

Eq. 2.13 is rewritten in a simplified form:

$$\begin{aligned} \delta^{18}\text{O}_{\text{prec}} = & a_1 \cdot \left(2 \cdot \left(\delta^{18}\text{O}_{\text{H}_2\text{Oexp}} + \varepsilon^{\text{EQ}}_{\text{SO}_2 \leftrightarrow \text{H}_2\text{O}} \right) + \left(\delta^{18}\text{O}_{\text{H}_2\text{Omix}} + \varepsilon_{\text{H}_2\text{O}/\text{SO}_2 \rightarrow \text{HSO}_3^-} \right) \right) \\ & + a_2 \cdot \left(2 \cdot \left(\delta^{18}\text{O}_{\text{H}_2\text{Omix}} + \varepsilon^{\text{EQ}}_{\text{SO}_2 \leftrightarrow \text{H}_2\text{O}} \right) + \left(\delta^{18}\text{O}_{\text{H}_2\text{Omix}} + \varepsilon_{\text{H}_2\text{O}/\text{SO}_2 \rightarrow \text{HSO}_3^-} \right) \right) \\ & + 3 \cdot b_1 \cdot \left(\delta^{18}\text{O}_{\text{H}_2\text{Oexp}} + \varepsilon^{\text{EQ}}_{\text{SO}_3^{2-} \leftrightarrow \text{H}_2\text{O}} \right) \\ & + 3 \cdot b_2 \cdot \left(\delta^{18}\text{O}_{\text{H}_2\text{Omix}} + \varepsilon^{\text{EQ}}_{\text{SO}_3^{2-} \leftrightarrow \text{H}_2\text{O}} \right) \\ & + c \cdot \delta^{18}\text{O}_{\text{H}_2\text{Omix}} + d \cdot \delta^{18}\text{O}_{\text{cont}} \end{aligned}$$

With

$$a_1 = \frac{[\text{SO}_2]_{\text{orig}}}{[\text{Prec}_{\text{oxygen}}]}$$

$$a_2 = \frac{[\text{SO}_2]_{\text{exchanged}}}{[\text{Prec}_{\text{oxygen}}]}$$

$$b_1 = \frac{\{[\text{HSO}_3^-] + [\text{SO}_3\text{H}^-] + [\text{SO}_3^{2-}]\}_{\text{orig}}}{[\text{Prec}_{\text{oxygen}}]}$$

$$b_2 = \frac{\{[\text{HSO}_3^-] + [\text{SO}_3\text{H}^-] + [\text{SO}_3^{2-}]\}_{\text{exchanged}}}{[\text{Prec}_{\text{oxygen}}]}$$

$$c = \frac{[\text{H}_2\text{O}_{\text{prec incorp}}]}{[\text{Prec}_{\text{oxygen}}]}$$

$$d = \frac{[\text{cont}]}{[\text{Prec}_{\text{oxygen}}]}$$

and

$$1 = 3 \cdot (a_1 + a_2) + 3 \cdot (b_1 + b_2) + c + d$$

Eq. 2.14

The expression $1=3 \cdot (a_1+a_2)+3 \cdot (b_1+b_2)+c+d$ results from the division of Eq. 2.12 by $[\text{Prec}_{\text{oxygen}}]$ which normalizes all oxygen contributions to $\text{Prec}_{\text{oxygen}}$. We can rearrange Eq. 2.14 to

$$\begin{aligned} \delta^{18}\text{O}_{\text{prec}} = & (2 \cdot a_1 + 3 \cdot b_1) \cdot \delta^{18}\text{O}_{\text{H}_2\text{Oexp}} \\ & + (a_1 + 3 \cdot a_2 + 3 \cdot b_2 + c) \cdot \delta^{18}\text{O}_{\text{H}_2\text{Omix}} \\ & + 2 \cdot (a_1 + a_2) \cdot \varepsilon_{\text{SO}_2 \leftrightarrow \text{H}_2\text{O}}^{\text{EQ}} \\ & + (a_1 + a_2) \cdot \varepsilon_{\text{H}_2\text{O} \setminus \text{SO}_2 \rightarrow \text{HSO}_3^-} \\ & + 3 \cdot (b_1 + b_2) \cdot \varepsilon_{\text{SO}_3^{2-} \leftrightarrow \text{H}_2\text{O}}^{\text{EQ}} \\ & + d \cdot \delta^{18}\text{O}_{\text{cont}} \end{aligned}$$

Eq. 2.15

and rewrite Eq. 2.15 as:

$$\begin{aligned} \delta^{18}\text{O}_{\text{prec}} = & k \cdot \delta^{18}\text{O}_{\text{H}_2\text{Oexp}} + m \cdot \delta^{18}\text{O}_{\text{H}_2\text{Omix}} \\ & + 2 \cdot (a_1 + a_2) \cdot \varepsilon_{\text{SO}_2 \leftrightarrow \text{H}_2\text{O}}^{\text{EQ}} + (a_1 + a_2) \cdot \varepsilon_{\text{H}_2\text{O} \setminus \text{SO}_2 \rightarrow \text{HSO}_3^-} \\ & + 3 \cdot (b_1 + b_2) \cdot \varepsilon_{\text{SO}_3^{2-} \leftrightarrow \text{H}_2\text{O}}^{\text{EQ}} + d \cdot \delta^{18}\text{O}_{\text{cont}} \end{aligned}$$

with:

$$k = 2 \cdot a_1 + 3 \cdot b_1$$

$$m = a_1 + 3 \cdot a_2 + 3 \cdot b_2 + c$$

Eq. 2.16

The value of m is a measure of how much water was incorporated into the sulfite salt during the precipitation procedure, whereas the value of k is a measure of how much water in the sulfite salt originates from the experiment solution. The values of $\delta^{18}\text{O}_{\text{prec}}$, $\delta^{18}\text{O}_{\text{H}_2\text{Oexp}}$ and $\delta^{18}\text{O}_{\text{H}_2\text{Omix}}$ can be experimentally accessed. Consequently, m can be determined from experiments where the isotope composition of experimental water ($\delta^{18}\text{O}_{\text{H}_2\text{Oexp}}$) is kept constant and the isotope composition of the precipitation mixture ($\delta^{18}\text{O}_{\text{H}_2\text{Omix}}$) is varied via graphical determination of the slope of the regression line in a $\delta^{18}\text{O}_{\text{prec}}$ vs. $\delta^{18}\text{O}_{\text{H}_2\text{Omix}}$ plot (for an example, see Fig. 2.4a). Once the value of m is determined by the above procedure, Eq. 2.16 can be rearranged to:

$$\begin{aligned} \delta^{18}\text{O}_{\text{prec}} - m \cdot \delta^{18}\text{O}_{\text{H}_2\text{Omix}} &= k \cdot \delta^{18}\text{O}_{\text{H}_2\text{Oexp}} \\ &+ 2 \cdot (a_1 + a_2) \cdot \varepsilon_{\text{SO}_2 \leftrightarrow \text{H}_2\text{O}}^{\text{EQ}} + (a_1 + a_2) \cdot \varepsilon_{\text{H}_2\text{O} \cdot \text{SO}_2 \rightarrow \text{HSO}_3^-} + 3 \cdot (b_1 + b_2) \cdot \varepsilon_{\text{SO}_3^{2-} \leftrightarrow \text{H}_2\text{O}}^{\text{EQ}} + d \cdot \delta^{18}\text{O}_{\text{cont}} \end{aligned} \quad \text{Eq. 2.17}$$

Thus, the value of k can be determined by the slope of a regression line in a $(\delta^{18}\text{O}_{\text{prec}} - m \cdot \delta^{18}\text{O}_{\text{H}_2\text{Omix}})$ vs. $\delta^{18}\text{O}_{\text{H}_2\text{Oexp}}$ plot, whereas the intercept of the regression line at $\delta^{18}\text{O}_{\text{H}_2\text{Oexp}} = 0$ corresponds to the constant term in Eq. 2.17. This term is composed of the isotope effects, the isotope composition of the contaminant and their relative contributions (Fig. 2.4b).

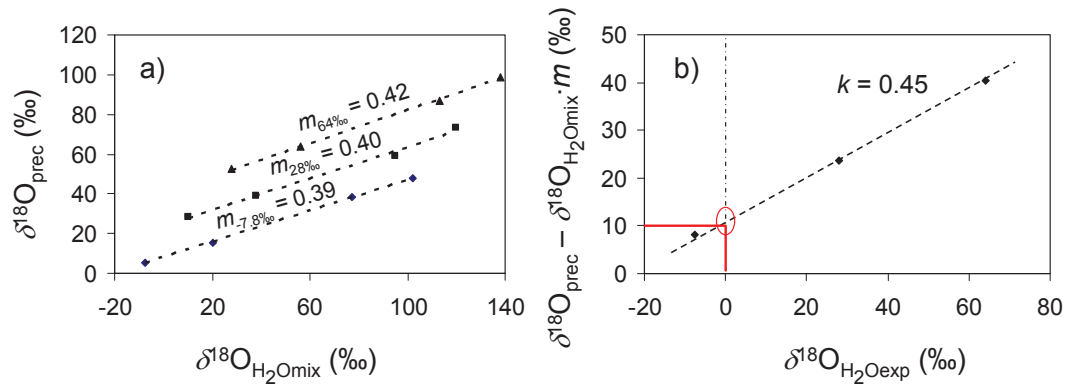


Fig. 2.4: Determination of m , k and the invariant terms in Eq. 2.17.

2.4a): The slope of the obtained regression lines is equal to the amount of incorporated oxygen derived from precipitation mixture (m) for each of the three isotopically distinct experiment solutions.

2.4b): The slope of the regression line corresponds to the relative amount of oxygen in the precipitates derived from the experiment solution (k) is obtained by plotting the difference between the isotope composition of the precipitate ($\delta^{18}\text{O}_{\text{prec}}$) and the average of the precipitation mix ($\delta^{18}\text{O}_{\text{H}_2\text{Omix}}$) times m (determined in 2.4a) on the y axis against the $\delta^{18}\text{O}_{\text{H}_2\text{Oexp}}$ on the x axis. The intercept of the regression line with the y axis where $\delta^{18}\text{O}_{\text{H}_2\text{Oexp}}$ is zero (red circle) corresponds to the value of the invariant terms in Eq. 2.17 (for this example we plotted data from the experiment at pH 1.5 where sulfite was precipitated as BaSO_3).

If experiment solution and precipitation solution were the only oxygen sources available (i.e. no contaminant, $d = 0$), the sum of k and m would always be 1. Consequently, the value of d can be determined:

$$d = 1 - (k + m) \quad \text{Eq. 2.18}$$

Obviously, knowledge of the values of $\delta^{18}\text{O}_{\text{prec}}$, $\delta^{18}\text{O}_{\text{H}_2\text{Oexp}}$, $\delta^{18}\text{O}_{\text{H}_2\text{Omix}}$, m , k , and d is insufficient to determine the remaining unknown parameters in Eq. 2.17 (i.e. a_1 , a_2 , b_1 , b_2 , $\varepsilon^{\text{EQ}}_{\text{SO}_2 \leftrightarrow \text{H}_2\text{O}}$, $\varepsilon^{\text{EQ}}_{\text{SO}_3^{2-} \leftrightarrow \text{H}_2\text{O}}$, $\varepsilon_{\text{H}_2\text{O} \setminus \text{SO}_2 \rightarrow \text{HSO}_3^-}$, $\delta^{18}\text{O}_{\text{cont}}$). However, it is possible to further simplify the above isotope mass balance by performing experiments under specific conditions such as different pH conditions where some sulfite species can be excluded (e.g. SO_2 does not occur at circum-neutral or high pH), or by applying precipitation techniques that rapidly and quantitatively convert sulfite species, thereby minimizing the effect of simultaneous oxygen isotope exchange with ambient water (e.g. by adding NaOH or by using cations with very low solubility product).

2.4. Results and conclusions

In the first part of this section we assess the appropriateness of different sulfite conversion/precipitation techniques. The second part of the section is devoted to the calculation of estimates for $\varepsilon^{\text{EQ}}_{\text{SO}_3^{2-} \leftrightarrow \text{H}_2\text{O}}$ and $\varepsilon^{\text{EQ}}_{\text{SO}_2 \leftrightarrow \text{H}_2\text{O}}$. The measured isotope values are reported in Table 2.2 (in 2.8. Appendices).

2.4.1. Comparison between different precipitation agents (Ba^{2+} and Ag^+) and differences between precipitation at constant pH and with pH shift (with NaOH)

How much oxygen isotope exchange occurs between sulfite species and water during the precipitation of sulfite salts is of major interest, because calculations in this study are based on the assumption that such an exchange is of minor importance. Therefore, we first compare values of m for experiments that were carried out at a pH of 6.3 (no SO_2 species expected, Fig 2.1), where sulfite salts were precipitated with different solutions containing either Ba^{2+} or Ag^+ . For each experiment four isotopically distinct precipitation solutions were used, allowing for the graphic determination of m (Fig. 2.5). The experiments with Ag^+ as precipitation agent yielded a relative precipitation mixture oxygen incorporation of $m_{\text{Ag}^+} = 0.48 \pm 0.01$; a value much smaller than the experiments where sulfite was precipitated with Ba^{2+} ($m_{\text{Ba}^{2+}} = 0.90 \pm 0.01$).

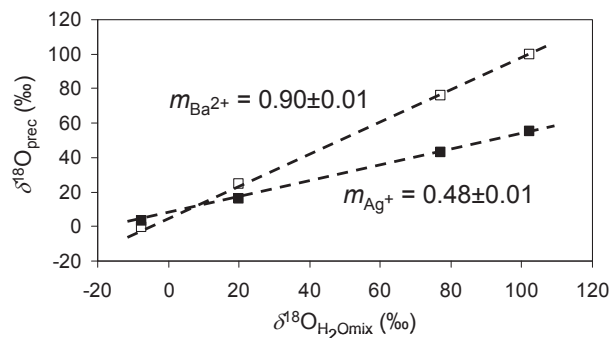


Fig. 2.5: Comparison between precipitation agents Ba^{2+} (hollow squares) and Ag^+ (filled squares) during precipitation of sulfite species without shifting the pH: The relative amount of oxygen from the precipitation mixture (m) in the respective sulfite salt for the experiments with silver is with 0.48 ± 0.01 half as large as for the experiments precipitated with barium ($m = 0.90 \pm 0.01$).

From this observation it is evident that much more oxygen isotope exchange between sulfite and water occurs during the precipitation of sulfite as BaSO_3 than during the precipitation of sulfite as Ag_2SO_3 . This difference may be attributed to the higher solubility of BaSO_3 compared to Ag_2SO_3 (BaSO_3 : $K_{\text{sp}} = 5.0 \times 10^{-10}$; Ag_2SO_3 : $K_{\text{sp}} = 1.5 \times 10^{-14}$; at 25°C from Lide, 1998), which might result in a more sluggish precipitation of BaSO_3 than Ag_2SO_3 . Precipitation of sulfite species with Ba^{2+} without shifting the pH is thus not suitable for the determination of the oxygen isotope equilibrium fractionation between sulfite and water. However, as an alternative, BaSO_3 may be precipitated after shifting the pH of the sulfite solution to higher values, where no oxygen isotope exchange between sulfite and water occurs. Unfortunately, this procedure is not applicable with silver solutions as precipitation agents, as silver would precipitate as silver hydroxide (AgOH) and silver oxide (Ag_2O) in alkaline solutions (Biedermann and Sillén, 1960). We, therefore, compared the m values for the precipitation of sulfite salts from an experiment solution at pH 6.6 (no SO_2 species expected, Fig 2.1), which were in one case precipitated with Ba^{2+} after the pH of the solution was shifted to high values and in the other case were directly precipitated by adding a solution containing Ag^+ . The comparison of the obtained m values shows that there is much less oxygen incorporation from the precipitation mixture when the precipitation solution is shifted to high pH and sulfite is subsequently precipitated as BaSO_3 salt ($m_{\text{Ba}^{2+}} = 0.03 \pm 0.01$) compared to the direct precipitation with Ag^+ ($m_{\text{Ag}^+} = 0.43 \pm 0.01$; Fig. 2.6).

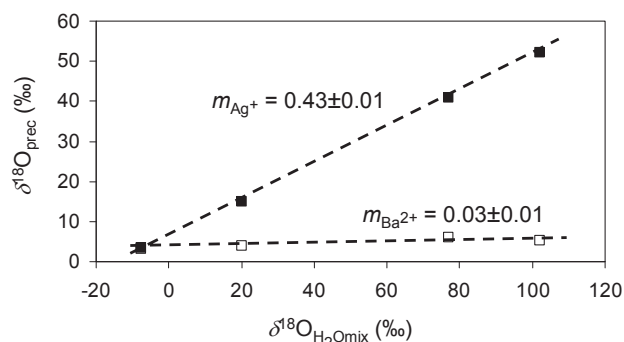


Fig. 2.6: Comparison between experiments at pH 6.6 for different precipitation techniques: Sulfite was either precipitated with silver solutions (filled squares) or precipitated with $\text{Ba}^{2+}/\text{NaOH}$ solutions (hollow squares) accompanied by a strong pH shift. The oxygen incorporation from the precipitation mixture is much lower in the experiments where we shifted the pH during precipitation ($m_{\text{Ba}^{2+}} = 0.03 \pm 0.01$).

We hypothesize that the observed 3% oxygen contribution from the precipitation solution in the BaSO_3 salt may represent entrained precipitation solution in the barium precipitate rather than actual isotope exchange between sulfite and water during sulfite precipitation at high pH. Such lattice water was observed for barium sulfate, where a group of three water molecules can substitute one molecule of barium sulfate and/or hydroxyl groups are occluded in the structure of the salt (Neagle and Rochester, 1988; Walton and Walden, 1946a; Walton and Walden, 1946b). Still, the small value for m demonstrates that the approach to precipitate sulfite by the combined use of $\text{NaOH}/\text{Ba}^{2+}$, is a reliable procedure that immediately stops isotope exchange between sulfite species at

circum-neutral to high pH values, and should allow for an accurate determination of the oxygen isotope equilibrium fractionation between sulfite species and the experiment solution.

2.4.2. Oxygen isotope equilibrium fractionation between sulfite and water in barium sulfite precipitates BaSO₃

Experiments at pH 6.6 and 9.7 were chosen to determine $\varepsilon^{\text{EQ}}_{\text{SO}_3^{2-} \leftrightarrow \text{H}_2\text{O}}$ because under these conditions SO₂ does not exist in solution and the parameters a_1 and a_2 become zero. It can be further assumed that the contribution of the precipitation mixture is solely caused by entrainment of water into the salt crystal, and not due to isotope exchange between sulfite and water. This assumption is based on the observation that oxygen isotope exchange between sulfite and water is extremely slow at pH 9.7 and because NaOH was added to the experiment carried out at pH 6.6 to shift the pH to a high value during the precipitation of BaSO₃. Consequently the parameter b_2 becomes zero and c equals m . Equation 2.16 can thus be rewritten as:

$$\begin{aligned} \delta^{18}\text{O}_{\text{prec}} &= 3 \cdot b_1 \cdot \left(\delta^{18}\text{O}_{\text{H}_2\text{Oexp}} + \varepsilon^{\text{EQ}}_{\text{SO}_3^{2-} \leftrightarrow \text{H}_2\text{O}} \right) + c \cdot \delta^{18}\text{O}_{\text{H}_2\text{Omix}} + d \cdot \delta^{18}\text{O}_{\text{cont}} \\ &= k \cdot \delta^{18}\text{O}_{\text{H}_2\text{Oexp}} + m \cdot \delta^{18}\text{O}_{\text{H}_2\text{Omix}} + k \cdot \varepsilon^{\text{EQ}}_{\text{SO}_3^{2-} \leftrightarrow \text{H}_2\text{O}} + (1 - k - m) \cdot \delta^{18}\text{O}_{\text{cont}} \end{aligned}$$

with:

$$k = 3 \cdot b_1$$

$$m = c$$

$$d = 1 - (k + m)$$

Eq. 2.19

For both experiments, the m value – which is equal to that part of oxygen in the precipitate which originates from the precipitation mixture – is so small ($m_{\text{pH } 6.6} = 0.03 \pm 0.01$; $m_{\text{pH } 9.7} = 0.04 \pm 0.02$) that oxygen exchange between sulfite species and the precipitation mixture can be excluded. The values obtained for the contribution of experiment solution are $k_{\text{pH } 6.6} = 0.86 \pm 0.00$ and $k_{\text{pH } 9.7} = 0.77 \pm 0.01$, from which we can estimate the relative oxygen contribution of the contaminant ($d = 1 - (k + m)$) in the precipitates of experiments at pH 6.6 to be approximately 0.11 (11%) and in the precipitates of experiments at pH 9.7 to be approximately 0.18 (18%). In the case that k would be equal to one and all oxygen in the precipitate would be derived from the experiment solution, the contribution of $\delta^{18}\text{O}_{\text{cont}}$ would become zero and the constant equal to the equilibrium fractionation $\varepsilon^{\text{EQ}}_{\text{SO}_3^{2-} \leftrightarrow \text{H}_2\text{O}}$. In experiments at pH 6.6 and pH 9.7 k is less than one and at the same time slightly different. Therefore, we can determine the values for $\varepsilon^{\text{EQ}}_{\text{SO}_3^{2-} \leftrightarrow \text{H}_2\text{O}}$ and $\delta^{18}\text{O}_{\text{cont}}$ by comparing the results of both experiments graphically with each other. For the comparison, we rearrange Eq. 2.19 for the two experimental pH solutions, where for each pH all terms with the exception of the equilibrium fractionation and $\delta^{18}\text{O}_{\text{cont}}$ are assumed to be constant:

$$\frac{\left\{ \delta^{18}\text{O}_{\text{prec}} - k \cdot \delta^{18}\text{O}_{\text{H}_2\text{Oexp}} - m \cdot \delta^{18}\text{O}_{\text{H}_2\text{Omix}} \right\}_{\text{pH } 6.6}}{\left\{ k \right\}_{\text{pH } 6.6}} = \varepsilon^{\text{EQ}}_{\text{SO}_3^{2-} \leftrightarrow \text{H}_2\text{O}} + \frac{\left\{ (1 - k - m) \right\}_{\text{pH } 6.6}}{\left\{ k \right\}_{\text{pH } 6.6}} \cdot \delta^{18}\text{O}_{\text{cont}}$$

and

$$\frac{\{\delta^{18}\text{O}_{\text{prec}} - k \cdot \delta^{18}\text{O}_{\text{H}_2\text{Oexp}} - m \cdot \delta^{18}\text{O}_{\text{H}_2\text{Omix}}\}_{\text{pH}_{9.7}}}{\{k\}_{\text{pH}_{9.7}}} = \varepsilon_{\text{SO}_3^{2-} \leftrightarrow \text{H}_2\text{O}}^{\text{EQ}} + \frac{\{(1-k-m)\}_{\text{pH}_{9.7}}}{\{k\}_{\text{pH}_{9.7}}} \cdot \delta^{18}\text{O}_{\text{cont}}$$

Eq. 2.20

By plotting the results of the three isotopically distinct experimental solutions of two pH experiments on the same plot, we can draw a regression line through all the points and extrapolate the line to the intercept with the y axis where k is equal to one and as consequence $d = 0$. Thus, the values of the two unknowns can be determined graphically where $\varepsilon_{\text{SO}_3^{2-} \leftrightarrow \text{H}_2\text{O}}^{\text{EQ}}$ corresponds to the intercept of the regression line with the y axis and $\delta^{18}\text{O}_{\text{cont}}$ corresponds to the slope of the regression line (Fig. 2.7). The value for the oxygen isotope equilibrium fractionation between sulfite and water is $\varepsilon_{\text{SO}_3^{2-} \leftrightarrow \text{H}_2\text{O}}^{\text{EQ}} = 15.2 \pm 0.7\text{‰}$ and the value of the oxygen isotope composition of the contaminant source is approximately $\delta^{18}\text{O}_{\text{cont}} = -28.7 \pm 3.6\text{‰}$ (see Fig. 2.7). As shown below, the oxygen isotope composition of the contaminant is almost identical to values of water vapor measured in the laboratory.

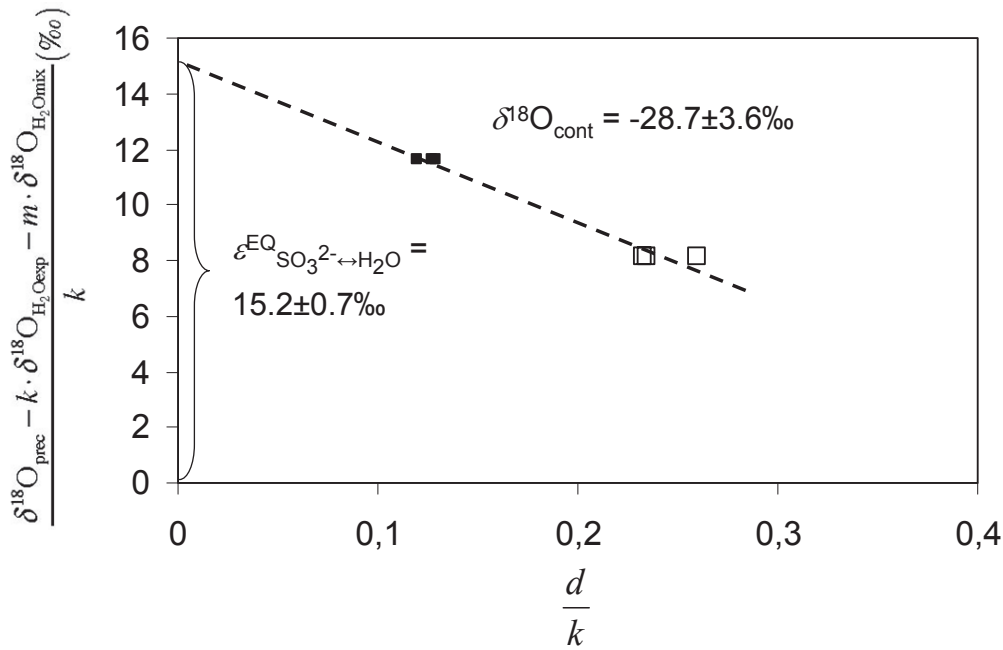


Fig. 2.7: Graphical determination of the oxygen isotope equilibrium fractionation between sulfite and water ($\varepsilon_{\text{SO}_3^{2-} \leftrightarrow \text{H}_2\text{O}}^{\text{EQ}}$) according to Eq. 2.20: The intercept between the regression line and the y axis is equal to $\varepsilon_{\text{SO}_3^{2-} \leftrightarrow \text{H}_2\text{O}}^{\text{EQ}}$ and the slope of the regression line is equal to the oxygen isotope composition of the contaminant ($\delta^{18}\text{O}_{\text{cont}} = -28.7 \pm 3.6\text{‰}$). The data used in the graph are from the experiments at pH 6.6 (black squares) and 9.7 (hollow squares), where dissolved sulfite was precipitated as BaSO_3 .

Isotope composition of water vapor in the laboratory:

The oxygen isotope composition of the collected water ($\delta^{18}\text{O}_{\text{vapor}}$) was $-27.5 \pm 0.3\text{‰}$ which is close to the value obtained for the contaminant in our BaSO_3 precipitates ($\delta^{18}\text{O}_{\text{cont}} = -28.7 \pm 3.6\text{‰}$).

Comparison of the oxygen isotope equilibrium fractionations between sulfite and water determined from silver sulfite precipitates:

The experiments at pH 6.3 and 6.6 where sulfite was precipitated as Ag_2SO_3 through the addition of AgNO_3 (no addition of NaOH to avoid co-precipitation of AgOH) can be used to obtain another estimate for $\epsilon^{\text{EQ}}_{\text{SO}_3^{2-} \leftrightarrow \text{H}_2\text{O}}$, which is independent of the precipitation technique for BaSO_3 . The estimate for $\epsilon^{\text{EQ}}_{\text{SO}_3^{2-} \leftrightarrow \text{H}_2\text{O}}$ based on Ag_2SO_3 precipitates has to be considered less reliable than the values obtained by shifting the pH with NaOH and precipitation as BaSO_3 , as ongoing oxygen isotope exchange between sulfite and water during the precipitation of Ag_2SO_3 can obscure kinetic isotope effects (i.e. preferred precipitation of isotopically light/heavy sulfite species). Still, the value for $\epsilon^{\text{EQ}}_{\text{SO}_3^{2-} \leftrightarrow \text{H}_2\text{O}}$ by the Ag_2SO_3 method should not deviate strongly from the value obtained with BaSO_3 because a large kinetic isotope effects during the precipitation of Ag_2SO_3 is not expected (i.e. no chemical bonds are broken). We can simplify Eq. 2.16 by assuming that no SO_2 exists at pH 6.3 and 6.6 (Fig. 2.1) and by considering the entrainment of precipitation water into Ag_2SO_3 precipitates minor compared to the portion of the oxygen in Ag_2SO_3 that was contributed by oxygen isotope exchange between sulfite and water during the precipitation (i.e. $c = 0$):

$$\begin{aligned} \delta^{18}\text{O}_{\text{prec}} &= 3 \cdot b_1 \cdot \left(\delta^{18}\text{O}_{\text{H}_2\text{Oexp}} + \epsilon^{\text{EQ}}_{\text{SO}_3^{2-} \leftrightarrow \text{H}_2\text{O}} \right) + 3 \cdot b_2 \cdot \left(\delta^{18}\text{O}_{\text{H}_2\text{Omix}} + \epsilon^{\text{EQ}}_{\text{SO}_3^{2-} \leftrightarrow \text{H}_2\text{O}} \right) + d \cdot \delta^{18}\text{O}_{\text{cont}} \\ &= k \cdot \delta^{18}\text{O}_{\text{H}_2\text{Oexp}} + m \cdot \delta^{18}\text{O}_{\text{H}_2\text{Omix}} + (k + m) \cdot \epsilon^{\text{EQ}}_{\text{SO}_3^{2-} \leftrightarrow \text{H}_2\text{O}} + d \cdot \delta^{18}\text{O}_{\text{cont}} \end{aligned}$$

with:

$$k = 3 \cdot b_1$$

$$m = 3 \cdot b_2$$

$$d = 1 - (k + m)$$

Eq. 2.21

The graphically determined values for the experiment at pH 6.3 are $m = 0.48 \pm 0.01$ and $k = 0.58 \pm 0.04$ ($d = -0.06$) and for pH 6.6, $m = 0.43 \pm 0.01$ and $k = 0.57 \pm 0.03$ ($d = 0.01$). The small values for d (sum of k and m close to 1) show that, unlike for BaSO_3 , there is no contaminant in Ag_2SO_3 . This allows us to set $d = 0$ in Eq. 2.21:

$$\delta^{18}\text{O}_{\text{prec}} - m \cdot \delta^{18}\text{O}_{\text{H}_2\text{Omix}} = k \cdot \delta^{18}\text{O}_{\text{H}_2\text{Oexp}} + \epsilon^{\text{EQ}}_{\text{SO}_3^{2-} \leftrightarrow \text{H}_2\text{O}} \quad \text{Eq. 2.22}$$

Equation 2.22 can be used to graphically determine the value for $\epsilon^{\text{EQ}}_{\text{SO}_3^{2-} \leftrightarrow \text{H}_2\text{O}}$ of $10.9 \pm 0.9\text{‰}$ (Fig. 2.8). This value obtained from Ag_2SO_3 precipitates is approximately 4.3‰ lighter than the value from the BaSO_3 ($15.2 \pm 0.7\text{‰}$.) This lighter value is likely due to normal kinetic isotope effects (isotopically light sulfite species are preferred) during precipitation of sulfite which are obscured by the ongoing oxygen exchange of the dissolved sulfite with the precipitation solution.

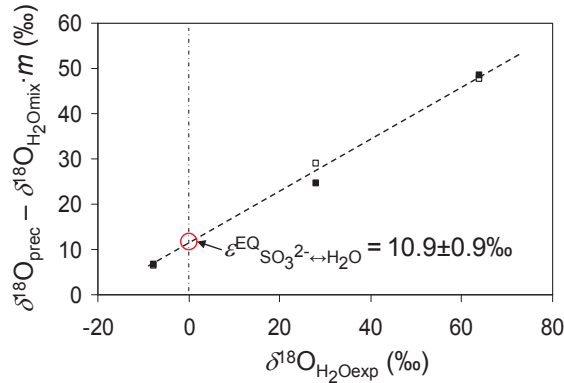


Fig. 2.8: Graphical determination of the oxygen isotope equilibrium fractionation between sulfite and water from Ag_2SO_3 precipitates from experiments at pH 6.3 and 6.6: In case of the experiments with silver, there is no contamination with water vapor; therefore, the oxygen isotope equilibrium fractionation between sulfite and water can be determined graphically after Eq. 2.22 where $\delta^{18}\text{O}_{\text{H}_2\text{Oexp}} = 0$.

2.4.3. Determination of the oxygen isotope equilibrium fractionation between dissolved SO_2 and water from experiments at pH 1.5

In the experiments at pH 1.5 the amounts of HSO_3^- and SO_2 in solution are approximately identical (Fig. 2.1). For the precipitation of BaSO_3 , NaOH was used to rapidly shift the pH of the experiment solution to higher values where no oxygen isotope exchange between sulfite and water occurs. From the experiments carried out at pH 6.6, it is known that this approach is likely effective for sulfite species such as HSO_3^- , SO_3H^- and SO_3^{2-} . From this we deduce that our precipitation technique will suppress isotope exchange between precipitation water and those species (i.e. $b_2 = 0$), however we cannot infer that this is also the case for SO_2 . Therefore, Eq. 2.16 can only be slightly simplified:

$$\delta^{18}\text{O}_{\text{prec}} = k \cdot \delta^{18}\text{O}_{\text{H}_2\text{Omix}} + m \cdot \delta^{18}\text{O}_{\text{H}_2\text{Oexp}} + 2 \cdot (a_1 + a_2) \cdot \epsilon_{\text{SO}_2 \leftrightarrow \text{H}_2\text{O}}^{\text{EQ}} + (a_1 + a_2) \cdot \epsilon_{\text{H}_2\text{O}/\text{SO}_2 \rightarrow \text{HSO}_3^-} + 3 \cdot b_1 \cdot \epsilon_{\text{SO}_3^{2-} \leftrightarrow \text{H}_2\text{O}}^{\text{EQ}} + d \cdot \delta^{18}\text{O}_{\text{cont}}$$

with:

$$k = 2 \cdot a_1 + 3 \cdot b_1$$

$$m = a_1 + 3 \cdot a_2 + c$$

$$d = 1 - (k - m)$$

Eq. 2.23

The graphically determined values for k and m (Fig. 2.4) are 0.45 ± 0.01 and 0.40 ± 0.01 , respectively, resulting in an estimate for d of 0.15 (15% contaminant), which is comparable to our other experiments with BaSO_3 as precipitate. In order to solve Eq. 2.23, the results from the experiment at pH 6.6 can be used as estimates (i.e. $c = 0.03$, $\delta^{18}\text{O}_{\text{cont}} = -28.7 \pm 3.6\text{‰}$, $\epsilon_{\text{SO}_3^{2-} \leftrightarrow \text{H}_2\text{O}}^{\text{EQ}} = 15.2 \pm 0.7\text{‰}$). We can explore the ratio between HSO_3^- and SO_2 for the case that the entire SO_2 pool exchanged its oxygen with water during the precipitation, i.e. where $a_1 = 0$.

The equations for k and m from above are simplified ($k = 3 \cdot b_1$ and $m = 3 \cdot a_2 + c$) and the ratio between HSO_3^- and SO_2 becomes:

$$\frac{k}{m - c} = \frac{0.45}{0.37} \quad \text{Eq. 2.24}$$

This ratio (55% HSO_3^- to 45% SO_2 when normalized to 100%) corresponds to a pH of 1.3 in the pH dependent species distribution of sulfite species (Fig. 2.1), which is close to the measured pH in the experiment solution of 1.5. If we were to choose a slightly higher ratio between HSO_3^- and SO_2 that is closer to the predicted ratio at pH 1.5 (Fig. 2.1) the value for a_1 would become negative, which is impossible. Choosing a lower ratio between HSO_3^- and SO_2 would yield values for a_1 that are larger than zero, but would require a pH lower than 1.3, thus even further away from the measured pH of 1.5. We attribute the difference between the pH estimate derived from Eq. 2.24 and the actually measured pH to uncertainties in the equilibrium constants used in the sulfite species distribution that result in a large uncertainty for the ratio between HSO_3^- and SO_2 because concentration gradients are very steep in this pH range (Fig. 2.1). Therefore, it can be concluded that almost the entire pool of SO_2 exchanged oxygen isotopes with the solution during the precipitation of BaSO_3 , confirming that isotope exchange at very low pH via Eq. 2.1 is extremely rapid and implying that it cannot be immediately stopped by addition of NaOH. Assuming that $a_1 = 0$, the unknown parameters in Eq. 2.23 can be separated:

$$\frac{\delta^{18}\text{O}_{\text{prec}} - m \cdot \delta^{18}\text{O}_{\text{H}_2\text{Omix}} - 3 \cdot b_1 \cdot \varepsilon_{\text{SO}_3^{2-} \leftrightarrow \text{H}_2\text{O}}^{\text{EQ}} - d \cdot \delta^{18}\text{O}_{\text{cont}}}{a_1 + a_2} = \frac{k}{a_1 + a_2} \cdot \delta^{18}\text{O}_{\text{H}_2\text{Oexp}} + 2 \cdot \varepsilon_{\text{SO}_2 \leftrightarrow \text{H}_2\text{O}}^{\text{EQ}} + \varepsilon_{\text{H}_2\text{O} \setminus \text{SO}_2 \rightarrow \text{HSO}_3^-}$$

Eq. 2.25

The value of $2 \cdot \varepsilon_{\text{SO}_2 \leftrightarrow \text{H}_2\text{O}}^{\text{EQ}} + \varepsilon_{\text{H}_2\text{O} \setminus \text{SO}_2 \rightarrow \text{HSO}_3^-}$ can be determined graphically ($74.0 \pm 1.7\%$, Fig. 2.9). We cannot disentangle the potential kinetic isotope fractionation that oxygen undergoes, which is incorporated from the precipitation mixture during the conversion of SO_2 to HSO_3^- ($\varepsilon_{\text{H}_2\text{O} \setminus \text{SO}_2 \rightarrow \text{HSO}_3^-}$), from the equilibrium isotope fractionation between SO_2 and H_2O ($\varepsilon_{\text{SO}_2 \leftrightarrow \text{H}_2\text{O}}^{\text{EQ}}$). Furthermore, we have to acknowledge that – analogous to the precipitation experiments with silver nitrate – a kinetic isotope effect could be imposed on the oxygen isotope composition of SO_2 that is being converted to HSO_3^- ($\varepsilon_{\text{SO}_2 \setminus \text{H}_2\text{O} \rightarrow \text{HSO}_3^-}$) that cannot be excluded from our isotope mass balance. To obtain at least a rough estimate of $\varepsilon_{\text{SO}_2 \leftrightarrow \text{H}_2\text{O}}^{\text{EQ}}$ it can be assumed that these kinetic isotope fractionations are small compared to the equilibrium isotope fractionation and can be set equal to zero. With these assumptions, the calculated oxygen isotope equilibrium fractionation between dissolved SO_2 and water is approximately 37.0‰. We can compare this value for $\varepsilon_{\text{SO}_2 \leftrightarrow \text{H}_2\text{O}}^{\text{EQ}}$ to the study on oxygen isotope fractionation on the oxygen exchange between gaseous SO_2 and water vapor by Holt et al. (1983), who observed an isotope fractionation of approximately 24‰ at 22°C. Our value for the oxygen isotope equilibrium fractionation between aqueous SO_2 and water is approximately 13‰ higher than the equilibrium fractionation for gaseous SO_2 and water vapor. If we were to use smaller values for the $[\text{HSO}_3^-]/[\text{SO}_2]$ ratio (which would imply a pH-dependent species distribution that differs strongly from our calculations, see Fig. 2.1), we would obtain

only slightly smaller values for $\varepsilon^{\text{EQ}}_{\text{SO}_2 \leftrightarrow \text{H}_2\text{O}}$ that would not resolve the discrepancy between our findings and the value determined by Holt et al. (1983). Ignoring the large uncertainties involved, it might be possible that a part of this discrepancy is due to a higher stability of aqueous SO_2 compared to gaseous SO_2 as there is a fairly strong association of hydrated SO_2 with high abundance water molecules, forming stronger hydrogen bonds than hydrated CO_2 (Moin et al., 2011) or attributed to the aforementioned kinetic isotope effects. However, in the case of the latter, one needs to consider that inverse kinetic isotope effects (preferred use of H_2O and SO_2 enriched in ^{18}O) would need to be postulated to explain the difference between our findings and the results by Holt et al. (1983).

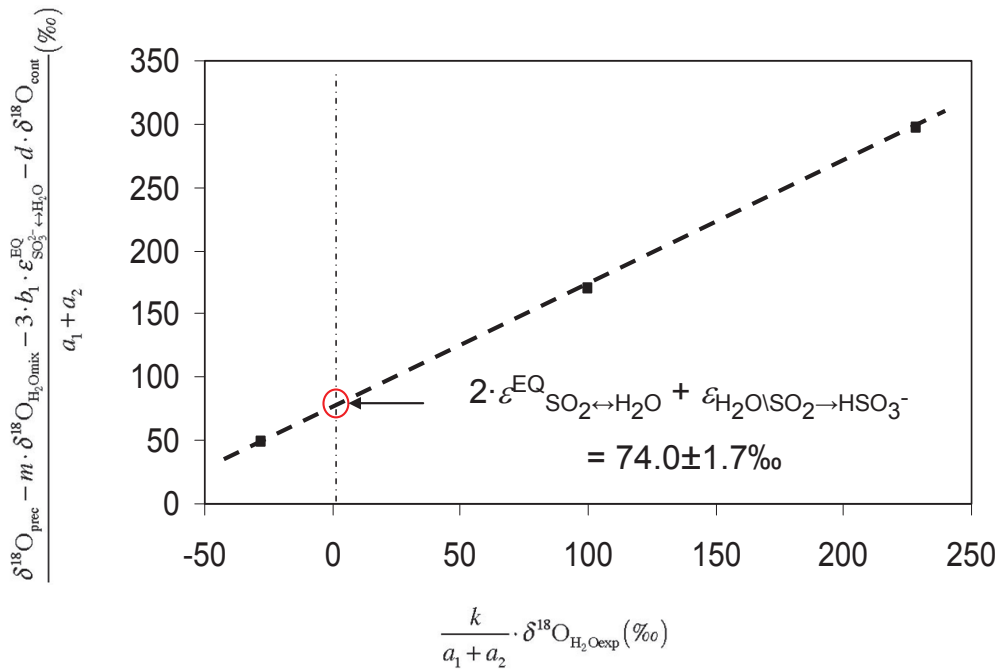


Fig. 2.9: Graphical determination of the oxygen isotope fractionation between SO_2 and water from experiments at pH 1.5: The red circle indicates the constant term from Eq. 2.25 which corresponds to twice $\varepsilon^{\text{EQ}}_{\text{SO}_2 \leftrightarrow \text{H}_2\text{O}}$ plus a kinetic isotope effect for the water oxygen incorporation during the conversion of SO_2 to HSO_3^- ($\varepsilon_{\text{H}_2\text{O} \setminus \text{SO}_2 \rightarrow \text{HSO}_3^-}$).

2.4.4. Implications of the obtained oxygen isotope equilibrium fractionation values

Oxygen isotope exchange between sulfite and water is often considered to have a major impact on the oxygen isotope signatures of sulfate affected by oxidative and reductive sulfur cycling. We were able to determine the oxygen isotope equilibrium fractionation between sulfite (HSO_3^- , SO_3H^- , SO_3^{2-} , NaSO_3^-) and water of $\varepsilon^{\text{EQ}}_{\text{SO}_3^{2-} \leftrightarrow \text{H}_2\text{O}} = 15.2 \pm 0.7\text{‰}$ and also to provide a rough estimate for the oxygen isotope fractionation between dissolved sulfur dioxide and water ($\varepsilon^{\text{EQ}}_{\text{SO}_2 \leftrightarrow \text{H}_2\text{O}} = 37.0\text{‰}$). These values are of importance for a better understanding of the oxygen isotope signature in residual sulfate during dissimilatory sulfate reduction (DSR) as well as for the understanding of the oxygen isotope signatures in sulfate produced during oxidative processes.

During DSR, where sulfate is reduced over intermediates such as adenosine 5'-phosphosulfate (APS) and sulfite to sulfide, the oxygen isotope composition in the residual sulfate is dependent on the oxygen isotope composition of the surrounding water (Mizutani and Rafter, 1973) despite the fact that sulfate does not exchange directly its oxygen with the water (Chiba and Sakai, 1985; Lloyd, 1968). This observation is generally explained as a result of DSR-mediated equilibrium oxygen isotope fractionation between residual sulfate and the water driving the oxygen isotope composition of sulfate towards a constant value of approximately 23‰ (Zeebe, 2010) to 26‰ (Fritz et al., 1989) at 22°C. This mechanism was intensively investigated both by experimental studies as well as modeling approaches (Blake et al., 2006; Brunner and Bernasconi, 2005; Brunner et al., 2005; Brunner et al., 2012; Fritz et al., 1989; Turchyn et al., 2010; Wortmann et al., 2007). It is assumed that the oxygen isotope fractionation observed during DSR results from reversible enzymatic steps during sulfate reduction, enabling the oxidation of sulfoxy intermediates that rapidly exchange oxygen isotopes with ambient water back to sulfate. Sulfite is considered to be an important intermediate in DSR and is known to rapidly exchange oxygen isotopes with water, unlike the more oxidized sulfoxy anions in DSR, such as APS or cell-internal sulfate (Brunner et al. 2012, Kohl et al., 2012).

The value of 15.2‰ obtained for $\epsilon^{\text{EQ}}_{\text{SO}_3^{2-} \leftrightarrow \text{H}_2\text{O}}$ is much smaller than the estimates for DSR-mediated isotope equilibrium between sulfate and water (23‰, Zeebe, 2010; 26‰, Fritz et al., 1989). Oxygen isotope exchange between sulfite and water alone therefore cannot be responsible for the oxygen isotope fractionation during DSR and highlights the importance of the isotope effects related to the back oxidation of sulfite to APS, which involves the incorporation of oxygen from adenosine monophosphate (AMP) (Peck, 1962; Peck and Stulberg, 1962; Fritz et al. 2002; Wortmann et al., 2007; Brunner et al., 2012). However, our finding that there may be a much higher oxygen isotope equilibrium fractionation between SO_2 and water of $\epsilon^{\text{EQ}}_{\text{SO}_2 \leftrightarrow \text{H}_2\text{O}} = 37.0\text{‰}$ adds a slight twist to these considerations, as it highlights that different sulfite species may have strongly different isotope equilibrium values. In this respect, $\text{S}_2\text{O}_5^{2-}$ is of interest, because, unlike SO_2 , it can exist at circum-neutral conditions that are physiologically relevant. As $\text{S}_2\text{O}_5^{2-}$ existed only in extremely small quantities in our experiments, we could not determine an equilibrium isotope fractionation for this species. In biological systems, low abundance of a species does not imply its unimportance, and it is interesting to note that $\text{S}_2\text{O}_5^{2-}$ has been considered as a potential alternative to SO_3^{2-} in DSR (Woolfolk, 1962).

Our results will also be useful for the study of oxidative sulfur cycling of reduced sulfur compounds, which operate depending on environmental conditions, such as pH, over various abiotic and biochemical pathways with a multitude of distinct sulfoxy intermediates. Many of these pathways have in common that in a chain of oxidation steps sulfite is the final sulfoxy intermediate before the oxidation to the final product sulfate. Knowledge of the effective value of $\epsilon^{\text{EQ}}_{\text{SO}_3^{2-} \leftrightarrow \text{H}_2\text{O}}$ and having an approximate estimate of $\epsilon^{\text{EQ}}_{\text{SO}_2 \leftrightarrow \text{H}_2\text{O}}$ will enable a more quantitative interpretation of the oxygen isotope signature of sulfate produced from oxidative sulfur cycling.

2.5. Conclusions

We performed experiments with dissolved sulfite species to determine the oxygen isotope equilibrium fractionation factor between dissolved sulfite and water. The experimentally most feasible way to determine the oxygen isotope equilibrium values was to add NaOH which shifts the pH to values higher than 12, thereby overcoming the challenges of ongoing oxygen isotope exchange between sulfite and water during the precipitation of sulfite salts. This procedure, however, comes at a price; precipitated BaSO_3 salts are strongly hygroscopic and the effects of the contamination through uptake of water vapor have to be resolved by mathematical treatments and corrections after data generation. Silver sulfite salts do not show this hygroscopic behavior, but silver nitrate solutions cannot be used at high pH because of co-precipitation of AgOH with Ag_2SO_3 . The methods tested and applied in our research are transferable to the determination of the oxygen isotope equilibrium fractionation between water and oxyanions other than sulfite, where similar challenges as for the precipitation of sulfite for oxygen isotope analysis exist, e.g. nitrite, or selenite.

We determined a rough estimate for the oxygen isotope equilibrium fractionation between SO_2 and water at low pH of $\epsilon^{\text{EQ}}_{\text{SO}_2 \leftrightarrow \text{H}_2\text{O}} = 37.0\text{‰}$ and a more firm estimate for the oxygen isotope equilibrium between SO_3^{2-} and water at circum neutral pH of $\epsilon^{\text{EQ}}_{\text{SO}_3^{2-} \leftrightarrow \text{H}_2\text{O}} = 15.2\text{‰}$. With increasing pH, HSO_3^- and SO_3^{2-} become more abundant. As SO_2 disappears from the sulfite system, the overall oxygen exchange between water and sulfite is still rapid, but not as rapid as in the presence of SO_2 . At very high pH (>12) only SO_3^{2-} and some NaSO_3^- will be present in solution, as consequence oxygen isotope exchange between sulfite and water is extremely slow. Under these conditions, oxygen isotope disequilibria between sulfite and water will be retained (Fig. 2.10).

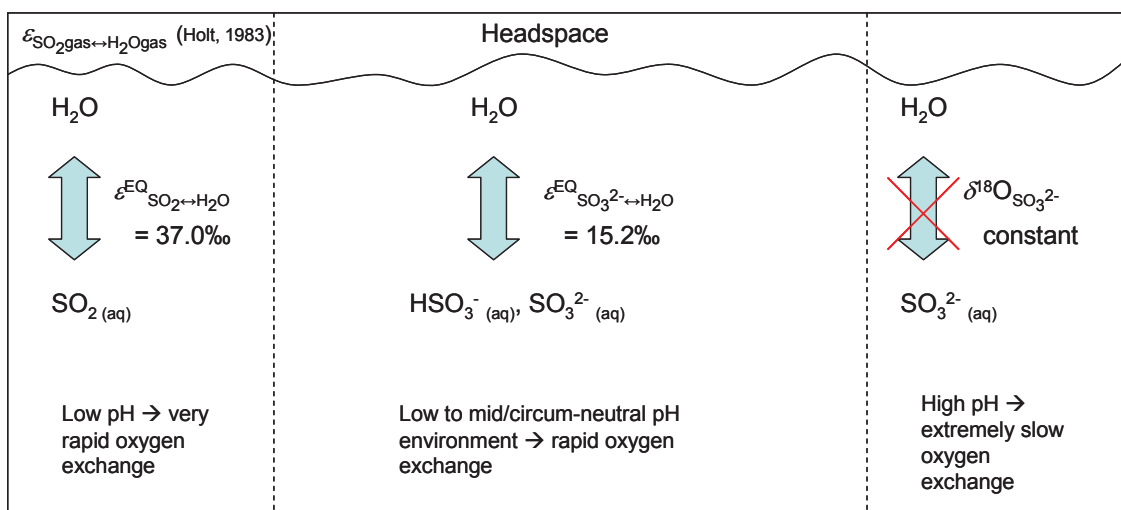


Fig. 2.10: Oxygen isotope exchange scenarios at different pH conditions: The equilibrium fractionation between sulfite and water of 15.2‰ is rapidly obtained at intermediate pH range where HSO_3^- and SO_3^{2-} are the dominant sulfite species in solution. In experiments at extreme low pH where SO_2 becomes more abundant, oxygen exchange is the most rapid and the oxygen isotope equilibrium between SO_2 and water of 37.0‰ could be determined. In case the pH is high, probably above 12, oxygen exchange is not measurable anymore and the oxygen isotope composition of sulfite will retain its pre-existing isotope value.

2.6. Acknowledgments

The authors thank T.G. Ferdelman and M.M.M. Kuypers for supporting this study, T. Max for crucial help with the mass spectrometer and assistance in the laboratory. We thank S.M. Bernasconi for the isotopic analysis and support as well as A.V. Turchyn for inspiring discussions and valuable advice. This project would not have been possible without the financial support provided by MARUM (Center for Marine Environmental Sciences) and the Max Planck Society. The contribution of M.C. was carried out at the Jet Propulsion Laboratory (JPL), California Institute of Technology, under contract with the National Aeronautics and Space Administration (NASA), with support from the NASA Astrobiology Institute (NAI-WARC).

2.7. References

- Balci N., Shanks III W. C., Mayer B. and Mandernack K. W. (2007) Oxygen and sulfur isotope systematics of sulfate produced by bacterial and abiotic oxidation of pyrite. *Geochimica et Cosmochimica Acta* **71**, 3796-3811.
- Balci N., Mayer B., Shanks III W. C. and Mandernack K. W. (2012) Oxygen and sulfur isotope systematics of sulfate produced during abiotic and bacterial oxidation of sphalerite and elemental sulfur. *Geochimica et Cosmochimica Acta* **77**, 335-351.
- Betts R. H. and Libich S. (1970) ^{18}O Transfer in the System Thiosulfate-Sulfite-Water: an Example of a Set of Consecutive Reversible First Order Rate Processes. *Canadian Journal of Chemistry* **49**, 180-186.
- Betts R. H. and Voss R. H. (1970) The kinetics of oxygen exchange between the sulfite ion and water. *Canadian Journal of Chemistry* **48**, 2035-2041.
- Biedermann G. and Sillén L. G. (1960) Studies on the Hydrolysis of Metal Ions. Part 30. A Critical Survey of the Solubility Equilibria of Ag_2O . *Acta Chemica Scandinavia* **14**, 717-725.
- Blake R. E., Surkov A. V., Böttcher M. E., Ferdelman T. G. and Jørgensen B. B. (2006) 7. Oxygen Isotope Composition of Dissolved Sulfate in Deep-Sea Sediments: Eastern Equatorial Pacific Ocean. *Jørgensen, B.B., D'Hondt, S.L., and Miller, D.J. (Eds.), Proc. ODP, Sci. Results* **201**, 1-23.
- Böttcher M. E., Thamdrup B. and Vennemann T. W. (2001) Oxygen and sulfur isotope fractionation during anaerobic bacterial disproportionation of elemental sulfur. *Geochimica et Cosmochimica Acta* **65**, 1601-1609.
- Böttcher M. E., Thamdrup B., Gehre M. and Theune A. (2005) $^{34}\text{S}/^{32}\text{S}$ and $^{18}\text{O}/^{16}\text{O}$ Fractionation During Sulfur Disproportionation by *Desulfobulbus propionicus*. *Geomicrobiology Journal* **22**, 219-226.
- Bottrell S. H. and Newton R. J. (2006) Reconstruction of changes in global sulfur cycling from marine sulfate isotopes. *Earth-Science Reviews* **75**, 59-83.
- Bottrell S. H., Mortimer R. J. G., Davies I. M., Harvey S. M. and Krom M. D. (2009) Sulphur cycling in organic-rich marine sediments from a Scottish fjord. *Sedimentology* **56**, 1159-1173.
- Brabec M. Y., Lyons T. W. and Mandernack K. W. (2012) Oxygen and sulfur isotope fractionation during sulfide oxidation by anoxygenic phototrophic bacteria. *Geochimica et Cosmochimica Acta* **83**, 234-251.

- Brunner B., Bernasconi S. M., Kleikemper J. and Schroth M. H. (2005) A model for oxygen and sulfur isotope fractionation in sulfate during bacterial sulfate reduction processes. *Geochimica et Cosmochimica Acta* **69**, 4773-4785.
- Brunner B. and Bernasconi S. M. (2005) A revised isotope fractionation model for dissimilatory sulfate reduction in sulfate reducing bacteria. *Geochimica et Cosmochimica Acta* **69**, 4759-4771.
- Brunner B., Mielke R. E. and Coleman M. (2006) Abiotic oxygen isotope equilibrium fractionation between sulfite and water. *Eos Trans. AGU* **87** (52), Fall Meet. Suppl. Abstract V11C-0601.
- Brunner B., Yu J-Y., Mielke, R. E., MacAskill J. A., Madzunkov S., McGenity T. J. and Coleman M. (2008) Different isotope and chemical patterns of pyrite oxidation related to lag and exponential growth phases of *Acidithiobacillus ferrooxidans* reveal a microbial growth strategy. *Earth and Planetary Science Letters* **270**, 63-72.
- Brunner B., Einsiedl F., Arnold G. L., Müller I., Templer S. and Bernasconi S. M. (2012) The reversibility of dissimilatory sulphate reduction and the cell-internal multi-step reduction of sulphite to sulphide: insights from the oxygen isotope composition of sulphate. *Isotopes in Environmental and Health Studies* **48**, 33-54.
- Butterfield D. A., Nakamura K., Takano B., Lilley M. D., Lupton J. E., Resing J. A. and Roe K. K. (2011) High SO₂ flux, sulfur accumulation, and gas fractionation at an erupting submarine volcano. *Geology* **39**, 803-806.
- Chiba H. and Sakai H. (1985) Oxygen isotope exchange rate between dissolved sulfate and water at hydrothermal temperatures. *Geochimica et Cosmochimica Acta* **49**, 993-1000.
- Connick R. E., Tam T. M. and Deuster E. V. (1982) Equilibrium constant for the dimerization of bisulfite ion to form disulfite(2-)ion. *Inorg. Chem.* **21**, 103-107.
- Eigen M., Kustin K. and Maass G. (1961) Die Geschwindigkeit der Hydratation von SO₂ in wäßriger Lösung. *Zeitschrift für Physikalische Chemie Neue Folge* **30**, 130-136.
- Fritz G., Büchert T. and Kroneck P. M. H. (2002) The Function of the [4Fe-4S] Clusters and FAD in Bacterial and Archaeal Adenylylsulfate Reductases. Evidence for flavin-catalyzed reduction of adenosine 5'-phosphosulfate. *The Journal of Biological Chemistry* **277**, 26066-26073.
- Fritz P., Basharmal G. M., Drimmie R. J., Ibsen J. and Qureshi R. M. (1989) Oxygen isotope exchange between sulphate and water during bacterial reduction of sulphate. *Chemical Geology (Isotope Geoscience Section)*, **79**, 99-105.
- Holt B. D., Kumar R. and Cunningham P. T. (1981) Oxygen-18 study of the aqueous-phase oxidation of sulfur dioxide. *Atmospheric Environment* **15**, 557-566.
- Holt B. D., Cunningham P. T., Engelkemeir A. G., Graczyk D. G. and Kumar R. (1983) Oxygen-18 study of nonaqueous-phase oxidation of sulfur dioxide. *Atmospheric Environment* **17**, 625-632.
- Horner D. A. and Connick R. E. (1986) Equilibrium Quotient for the Isomerization of Bisulfite Ion from HSO₃⁻ to SO₃H⁻. *Inorg. Chem.* **25**, 2414-2417.
- Horner D. A. and Connick R. E. (2003) Kinetics of Oxygen Exchange between the Two Isomers of Bisulfite Ion, Disulfite Ion (S₂O₅²⁻), and Water As Studied by Oxygen-17 Nuclear Magnetic Resonance Spectroscopy. *Inorg. Chem.* **42**, 1884-1894.

- Kohl I. and Bao H. (2011) Triple-oxygen-isotope determination of molecular oxygen incorporation in sulfate produced during abiotic pyrite oxidation (pH = 2-11). *Geochimica et Cosmochimica Acta* **75**, 1785-1798.
- Kohl I. E., Asatryan R. and Bao H. (2012) No oxygen isotope exchange between water and APS-sulfate at surface temperature: Evidence from quantum chemical modeling and triple-oxygen isotope experiments. *Geochimica et Cosmochimica Acta* **95**, 106-118.
- Kusakabe M., Komoda Y., Takano B. and Abiko T. (2000) Sulfur isotopic effects in the disproportionation reaction of sulfur dioxide in hydrothermal fluids: implications for the $\delta^{34}\text{S}$ variations of dissolved bisulfate and elemental sulfur from active crater lakes. *Journal of Volcanology and Geothermal Research* **97**, 287-307.
- Lide D. R. (Ed.), Handbook of Chemistry and Physics, 79th edn., 1998-1999, CRC Press, Boca Raton, FL, 1998.
- Lloyd R. M. (1967) Oxygen-18 Composition of Oceanic Sulfate. *Science* **156**, 1228-1231.
- Lloyd R. M. (1968) Oxygen Isotope Behavior in the Sulfate-Water System. *Journal of Geophysical Research* **73**, 6099-6110.
- Mizutani Y. and Rafter A. T. (1973) Isotopic behaviour of sulphate oxygen in the bacterial reduction of sulphate. *Geochemical Journal* **6**, 183-191.
- Moin S. T., Lim L. H. V., Hofer T. S., Randolph B. R. and Rode B. M. (2011) Sulfur Dioxide in Water: Structure and Dynamics Studied by an Ab Initio Quantum Mechanical Charge Field Molecular Dynamics Simulation. *Inorganic Chemistry* **50**, 3379-3386.
- Neagle W. and Rochester C. H. (1988) Infrared and Gravimetric Studies of the Adsorption of Water on Barium Sulphate. *J. Chem. Soc.* **84**, 3625-3632.
- Peck Jr. H. D. (1962) V. Comparative Metabolism of Inorganic Sulfur Compounds in Microorganisms. *Microbiol. Mol. Biol. Rev.* **26(1)**, 67-94.
- Peck Jr. H. D. and Stulberg M. P. (1962) O¹⁸ Studies on the Mechanism of Sulfate Formation and Phosphorylation in Extracts of *Thiobacillus thioparus*. *The Journal of Biological Chemistry* **237**, 1648-1652.
- Pham M., Müller J.-F., Brasseur G. P., Granier C. and Mégie G. (1996) A 3D model study of the global sulphur cycle: contributions of anthropogenic and biogenic sources. *Atmospheric Environment* **30**, 1815-1822.
- Pirlet H., Wehrmann L. M., Brunner B., Frank N., Dewanckele J., Rooij D. V., Foubert A., Swennen R., Naudts L., Boone M., Cnudde V. and Henriët J. P. (2010) Diagenetic formation of gypsum and dolomite in a cold-water coral mound in the Porcupine Seabight, off Ireland. *Sedimentology* **57**, 786-805.
- Quinn M.-L. (1989) Early smelter sites: a neglected chapter in the history and geography of acid rain in the United States. *Atmospheric Environment* **23**, 1281-1292.
- Riedinger N., Brunner B., Formolo M. J., Solomon E., Kasten S., Strasser M. and Ferdelman T. G. (2010) Oxidative sulfur cycling in the deep biosphere of the Nankai Trough, Japan. *Geology* **38**, 851-854.
- Schippers A., Jozsa P.-G., and Sand W. (1996) Sulfur Chemistry in Bacterial Leaching of Pyrite. *Applied and Environmental Microbiology* **62**, 3424-3431.
- Simon A. and Waldmann K. (1955) Wäßrige Disulfit-(Pyrosulfit-)Lösungen und ihr Verhalten in Abhängigkeit von Konzentrationen und Alkalisierungsgrad. *Zeitschrift für anorganische und allgemeine Chemie* **281**, 113-134.

- Simon A. and Waldmann K. (1956) Über die Ionen der Schwefligen Säure in wäßriger Lösung. *Zeitschrift für anorganische und allgemeine Chemie* **283**, 359-364.
- Sülzle D., Verhoeven M., Terlouw J. K. and Schwarz H. (1988) Generation and Characterization of Sulfurous Acid (H₂SO₃) and of Its Radical Cation as Stable Species in the Gas Phase. *Angew. Chem. Int. Ed. Engl.* **27**, 1533-1534.
- Turchyn A. V. and Schrag D. P. (2004) Oxygen Isotope Constraints on the Sulfur Cycle over the Past 10 Million Years. *Science* **303**, 2004-2007.
- Turchyn A. V., Brüchert V., Lyons T. W., Engel G. S., Balci N., Schrag D. P. and Brunner B. (2010) Kinetic oxygen isotope effects during dissimilatory sulfate reduction: A combined theoretical and experimental approach. *Geochimica et Cosmochimica Acta* **74**, 2011-2024.
- Walton G. and Walden Jr. G. H. (1946a) The Contamination of Precipitated Barium Sulfate by Univalent Cations. *Journal of the American Chemical Society* **68**, 1742-1750.
- Walton G. and Walden Jr. G. H. (1946b) The Nature of the Variable Hydration of Precipitated Barium Sulfate. *Journal of the American Chemical Society* **68**, 1750-1753.
- Woolfolk C. A., 1962. Reduction of inorganic compounds with molecular hydrogen by *Micrococcus Lactilyticus*. II: Stoichiometry with inorganic sulfur compounds. *J. Bacteriol.* **84**, 659-668.
- Wortmann U. G., Chernyavsky B., Bernasconi S. M., Brunner B., Böttcher M. E. and Swart P. K. (2007) Oxygen isotope biogeochemistry of pore water sulfate in the deep biosphere: Dominance of isotope exchange reactions with ambient water during microbial sulfate reduction (ODP Site 1130). *Geochimica et Cosmochimica Acta* **71**, 4221-4232.
- Zeebe R. E. (2010) A new value for the stable oxygen isotope fractionation between dissolved sulfate ion and water. *Geochimica et Cosmochimica Acta* **74**, 818-828.
- Zhang J.-Z. and Millero F. J. (1991) The rate of sulfite oxidation in seawater. *Geochimica et Cosmochimica Acta* **55**, 677-685.
- Zhao D., Xjong J., Xu Y. and Chan W. H. (1988) Acid rain in Southwestern China. *Atmospheric Environment* **22**, 349-358.

2.8. Appendices

SO ₂	Sulfur dioxide
HSO ₃ ⁻ /SO ₃ H ⁻	Bisulfite isomers
S ₂ O ₅ ²⁻	Pyrosulfite or metabisulfite
SO ₃ ²⁻	Sulfite <i>sensu stricto</i>
H ₂ SO ₃	Sulfurous acid
NaSO ₃ ⁻	Sodium sulfite ion
$\epsilon^{EQ}_{SO_2 \leftrightarrow H_2O}$	Oxygen isotope equilibrium fractionation between SO ₂ and water
$\epsilon^{EQ}_{SO_3^{2-} \leftrightarrow H_2O}$	Oxygen isotope equilibrium fractionation between SO ₃ ²⁻ and water
O ₂	Molecular oxygen
Fe ³⁺	Ferric iron
DSR	Dissimilatory Sulfate Reduction
BaSO ₃	Barium sulfite
Ag ₂ SO ₃	Silver sulfite
AgOH	Silver hydroxide
NaOH	Sodium hydroxide
Na ₂ SO ₃	Sodium sulfite
$\delta^{18}O_{H_2O_{exp}}$	Oxygen isotope composition of experiment solution
$\delta^{18}O_{H_2O_{psoln}}$	Oxygen isotope composition of precipitation solution
$\delta^{18}O_{H_2O_{mix}}$	Oxygen isotope composition of precipitation mixture
Ag ₂ O	Silver oxide
[Sulfite _{sulfur}]	Total concentration of sulfite sulfur
[Sulfite _{oxygen}]	Total concentration of oxygen from sulfite species
[Prec _{oxygen}]	Total concentration of oxygen in precipitated sulfite salt
[H ₂ O _{mix incorp}]	Concentration of oxygen from precipitation mixture entrained in precipitated sulfite salt
[cont]	Concentration of oxygen from contaminant entrained in precipitated sulfite salt
$\delta^{18}O_{SO_3^{2-}}$	Oxygen isotope composition of sulfite
[SO ₂] _{orig}	Oxygen concentration of SO ₂ in equilibrium with experiment solution
[SO ₂] _{exchanged}	Oxygen concentration of SO ₂ in equilibrium with precipitation solution
$\delta^{18}O_{prec}$	Oxygen isotope composition of precipitated sulfite salt
[H ₂ O _{incorp}]	H ₂ O molecules incorporated in precipitated sulfite salt
([HSO ₃ ⁻]+[SO ₃ H ⁻]+[SO ₃ ²⁻]) orig or exchanged	Oxygen concentration from similar sulfite molecules in equilibrium with experiment solution or with precipitation mixture, respectively
<i>a</i> ₁	Relative amount of SO ₂ in equilibrium with experiment solution

a_2	Relative amount of SO ₂ in equilibrium with precipitation mixture
b_1	Relative amount of (HSO ₃ ⁻ , SO ₃ H ⁻ , SO ₃ ²⁻) in equilibrium with experiment solution
b_2	Relative amount of (HSO ₃ ⁻ , SO ₃ H ⁻ , SO ₃ ²⁻) in equilibrium with precipitation mixture
c	Relative amount of entrained H ₂ O molecules from precipitation solution
d	Relative amount of entrained contaminant molecules
$\delta^{18}\text{O}_{\text{cont}}$	Oxygen isotope composition of contaminant
k	Relative amount of oxygen in the precipitated sulfite salt which originates from experiment solution
m	Relative amount of oxygen in the precipitated sulfite salt which originates from precipitation mixture
$\delta^{18}\text{O}_{\text{vapor}}$	Oxygen isotope composition of water vapor
$\varepsilon_{\text{H}_2\text{O}\backslash\text{SO}_2\rightarrow\text{HSO}_3^-}$	Kinetic isotope effect for water oxygen during conversion of SO ₂ to HSO ₃ ⁻
$\varepsilon_{\text{SO}_2\backslash\text{H}_2\text{O}\rightarrow\text{HSO}_3^-}$	Kinetic isotope effect for SO ₂ during conversion to HSO ₃ ⁻
APS	Adenosine 5'-phosphosulfate
AMP	Adenosine monophosphate

Table 2.2

Experiment description	pH	$\delta^{18}\text{O}$ sample solution (‰)	$\delta^{18}\text{O}$ precipitation solution (‰)	$\delta^{18}\text{O}$ precipitate (‰)	Experiment description	pH	$\delta^{18}\text{O}$ sample solution (‰)	$\delta^{18}\text{O}$ precipitation solution (‰)	$\delta^{18}\text{O}$ precipitate (‰)
1) Oxygen isotope values of experiments precipitated as BaSO_3 at constant pH (at 295°K)	6.31	-7.7	-7.7	-0.5	4) Oxygen isotope values of experiments precipitated as Ag_2SO_3 at constant pH (at 295°K)	6.31	-7.7	-7.7	3.0
			20.1	24.7				20.1	16.0
			77.1	75.8				77.1	43.2
			102.1	100.1				102.1	55.0
	6.38	28	10.1	15.3		6.38	28	10.1	30.3
			38	39.8		38		44.1	
			95	91.0		95		74.1	
			120	114.8		120		87.3	
	6.36	64	28.1	31.7		6.36	64	28.1	61.9
			56	57.6		56		72.7	
			113	107.8		113		99.6	
			138	130.2		138		110.8	
2) Oxygen isotope values of experiments precipitated as BaSO_3 with pH shift (at 295°K)	6.70	-7.7	-7.7	3.1	5) Oxygen isotope values of experiments precipitated as Ag_2SO_3 at constant pH (at 295°K)	6.70	-7.7	-7.7	3.4
			20.1	4.0				20.1	14.8
			77.1	5.9				77.1	41.0
			102.1	5.4				102.1	52.2
	6.60	28	10.1	34.2		6.60	28	10.1	32.6
			38	35.3		38		43.9	
			95	36.8		95		66.3	
			120	36.9		120		74.8	
	6.53	64	28.1	65.9		6.53	64	28.1	60.5
			56	67.8		56		72.8	
			113	69.0		113		99.1	
			138	69.7		138		110.1	
3) Oxygen isotope values of experiments precipitated as BaSO_3 at constant pH (at 295°K)	9.76	-7.7	-7.7	1.8	6) Oxygen isotope values of experiments precipitated as BaSO_3 with pH shift (at 295°K)	1.57	-7.7	-7.7	5.3
			20.1	-1.3				20.1	15.6
			77.1	4.0				77.1	38.3
			102.1	3.2				102.1	47.6
	9.72	28	10.1	28.3		1.54	28	10.1	28.2
			38	28.7		38		39.0	
			95	33.6		95		59.2	
			120	32.8		120		73.4	
	9.76	64	28.1	56.7		1.51	64	28.1	52.5
			56	58.7		56		63.7	
			113	62.7		113		87.1	
			138	61.4		138		98.9	

3. Isotopic evidence of the pivotal role of sulfite oxidation in shaping the oxygen isotope signature of sulfate

Inigo A. Müller^{a,b,*}, Benjamin Brunner^a and Max Coleman^{c,d}

^aBiogeochemistry Department, Max Planck Institute for Marine Microbiology, Celsiusstrasse 1, 28359 Bremen, Germany

^bMARUM—Center for Marine Environmental Sciences, University of Bremen, Leobener Strasse, 28359 Bremen, Germany

^cPlanetary Surface Instruments Group, NASA Jet Propulsion Laboratory, California Institute of Technology, 4800 Oak Grove Drive, Pasadena, CA 91109, USA

^dNASA Astrobiology Institute

*Corresponding author: imueller@mpi-bremen.de; Tel.: 0049 4212028 638; Fax: 0049 4212028 690

3.1. Abstract

The oxygen isotope composition of sulfate serves as an archive of past oxidative sulfur cycling. It carries information about the oxidants as well as the biochemical pathways involved in the oxidation of reduced sulfur compounds, as oxygen sources can be traced by their distinct oxygen isotope composition. Studies on the aerobic oxidation of reduced sulfur compounds (e.g. H₂S, HS⁻, FeS₂, FeS, Fe₃S₄ and elemental S) have shown varying relative contributions of oxygen from dissolved molecular oxygen (O₂) and water (H₂O). These discrepancies are likely due to slight differences in the production and consumption rate of sulfoxo intermediates which can exchange oxygen isotopes with water. Sulfite is often considered to be the final sulfoxo intermediate in the oxidation of reduced sulfur compounds to sulfate. Therefore, it is assumed that sulfite species (e.g. SO₃²⁻, HSO₃⁻, S₂O₅²⁻, SO₂), and their respective residence time play a crucial role in the oxygen isotope signature of produced sulfate. However, data on the oxygen isotope signature of sulfate derived from sulfite oxidation are scarce.

We performed experiments to assess the oxygen isotope effects of abiotic oxidation of sulfite under different pH conditions (pH 1, 4.9 and 13.3) to study the influence of varying pH on the oxygen isotope signature of produced sulfate during the oxidation by O₂ or ferric iron (Fe³⁺). These parameters impact the relative contribution of oxygen from water and O₂ to the produced sulfate, and control the competition between the rate of oxygen isotope exchange between sulfite and water and the sulfite oxidation rate. There is a striking overlap in the range of oxygen isotope compositions of sulfate from our experiments at different chemical conditions with the variations in

the oxygen isotope composition of sulfate derived from oxidative processes in the environment. We obtained $\Delta^{18}\text{O}_{\text{SO}_4\text{-H}_2\text{O}}$ from 5.9‰ up to 17.6‰ (anaerobic oxidation with Fe^{3+} and oxidation at low pH with O_2 as sole oxidant, respectively), a range which, for example, compares well with the $\Delta^{18}\text{O}_{\text{SO}_4\text{-H}_2\text{O}}$ values from 3.9‰ to 13.6‰ from a study on acid mine drainage from the Río Tinto by Hubbard et al. (2009). This implies that oxygen isotope effects during sulfite oxidation largely control the isotope signature of sulfate derived from the oxidation of sulfur compounds. However, our results also indicate that preexisting non-equilibrium isotope signatures of sulfite are likely partially preserved in the final sulfate product under many environmental conditions.

Our findings contribute to a better understanding of the isotope effects that occur during oxidative sulfur cycling. For example, positive isotope offsets between the oxygen isotope composition of sulfate and water observed in anoxic pyrite oxidation experiments with Fe^{3+} as the sole oxidizing agent can now be explained by the interplay of the rate of oxygen exchange between sulfite and water, driving the isotope composition towards isotope equilibrium fractionation between sulfite and water (positive offset) and normal isotope effects (negative offset) during sulfite oxidation.

3.2. Introduction

3.2.1. Tracing of biogeochemical sulfur cycling by oxygen isotopes of sulfate

Sulfate is highly abundant in the ocean (~28 mM) and is an extremely important electron acceptor for microbial re-mineralization of organic matter in anoxic marine sediments where other electron acceptors such as O_2 , nitrate or metal oxides are rapidly depleted (Jørgensen, 1977; Canfield et al., 1993; Thamdrup et al., 1994; Holmkvist et al., 2011). Microbes can use sulfate to oxidize organic matter via dissimilatory sulfate reduction where sulfate serves as terminal electron acceptor in the oxidation of organic matter. Reduced sulfur compounds such as dissolved sulfide (HS^- , H_2S) or sulfide minerals (e.g., FeS_2 , Fe_3S_4 , FeS) can then be oxidized back to sulfate if they become exposed to O_2 or other oxidized compounds, for example in the case where dissolved sulfide diffuses towards the sediment-water interface or when previously anoxic sediments become oxic due to environmental changes (e.g. Ku et al., 1999; Pirlet et al., 2010; Ziegenbalg 2010; Lindtke et al., 2011; Pfeffer et al., 2012; Pirlet et al., 2012; Schwedt et al., 2012). The oxygen isotope composition of sulfate can serve as an archive for such processes, as it does not spontaneously exchange oxygen isotopes with ambient water under natural conditions, with the exception of extreme environments with elevated temperatures and very low pH (Lloyd, 1968; Chiba and Sakai, 1985; Tichomirowa and Junghans, 2009). Peculiarly, to some degree, the oxygen isotope composition of sulfate is nevertheless dependent on the oxygen isotope composition of the surrounding water because abiotic and microbial reductive and oxidative sulfur cycling enables indirect oxygen isotopes exchange between sulfate and water. Many biochemical processes are known to alter the oxygen isotope composition of sulfate, including dissimilatory sulfate reduction

(Mizutani and Rafter, 1973; Fritz et al., 1989; Brunner et al., 2005; Brunner et al., 2012), oxidation of reduced sulfur compounds such as pyrite, sulfide or elemental sulfur (Lloyd, 1967; Lloyd, 1968; Taylor et al., 1984a; Taylor et al., 1984b; Van Stempvoort and Krouse, 1994; Balci et al., 2007; Brunner et al., 2008; Oba and Poulson, 2009a; Tichomirowa and Junghans, 2009; Heidel and Tichomirowa, 2010; Heidel and Tichomirowa, 2011; Kohl and Bao, 2011; Balci et al., 2012; Brabec et al., 2012), and disproportionation of elemental sulfur (Böttcher et al., 2001; Böttcher et al., 2005). Thus, the oxygen isotope composition of sulfate carries information about biochemical pathways and about the oxygen sources – typically H₂O or O₂ but could also include oxygen bearing compounds such as other sulfoxy anions, nitrate or phosphate – involved in sulfur cycling. Understanding and recognition of the oxygen isotope fingerprints caused by different biochemical processes is pivotal for a meaningful interpretation of oxygen isotope signature of sulfate from environmental samples and laboratory experiments.

3.2.2. The role of sulfite as intermediate in oxidative and reductive S-cycling

Sulfite is a sulfoxy intermediate that exists in the form of different species, including sulfite *sensu stricto* (SO₃²⁻), bisulfite (HSO₃⁻), pyrosulfite/metabisulfite (S₂O₅²⁻), and sulfur dioxide (SO₂). The relative abundance of these species is pH dependent (Betts and Voss, 1970; Horner and Connick, 2003; Müller et al., *subm.*): SO₃²⁻ is most abundant at pH higher than 7, HSO₃⁻ is highly abundant between pH 1-7 and SO₂ is most abundant at pH below 1. Pyrosulfite exists only in minor amounts between pH 1-7 where HSO₃⁻ is the dominant sulfite species. For convenience, in the following, we use the expression sulfite as a general term for all sulfite species in solution.

Sulfite is assumed to be an important intermediate in sulfate reduction, being the first reduced sulfur species in the stepwise reduction of sulfate to sulfite (Peck, 1962; Peck and Stulberg, 1962; Fritz et al., 2002). In oxidative sulfur cycling a number of different sulfoxy intermediates is involved, such as thiosulfate (S₂O₃²⁻), polythionates (S_xO₆²⁻) or sulfite (SO₃²⁻) (Lloyd, 1967; Sada et al., 1987; Xu and Schoonen, 1995; Schippers et al., 1996; Schippers and Jørgensen, 2001; Druschel et al., 2003; Rimstidt and Vaughan, 2003; Druschel and Borda, 2006; Hubbard et al., 2009; Kohl and Bao, 2011). The mechanisms during oxidation of reduced sulfur compounds are not understood in detail, however, it is evident that more than one oxidation pathway exists (Rimstidt and Vaughan, 2003; Druschel and Borda, 2006). Still, sulfite is considered to be of special importance, because it is thought that for many biochemical pathways, the last step of the oxidation of sulfur compounds to sulfate proceeds via oxidation of sulfite to sulfate (Brunner et al., 2008 and references therein).

3.2.3. Potential pivotal role of sulfite for oxygen isotope composition of sulfate from oxidation of reduced sulfur compounds

Unlike sulfate, sulfite is known to exchange oxygen isotopes quickly with ambient water. Thus it is possible that the oxygen isotope signature of sulfite is reset by rapid isotope exchange with water, and that therefore, only the oxidation of sulfite to sulfate is important for establishing the isotope composition of sulfate. Such a mode of function for

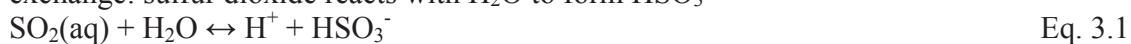
sulfite has previously been postulated for the oxygen isotope effects during partially reversible dissimilatory sulfate reduction (Brunner et al., 2012), but has not been considered for the multitude of biochemical reactions during oxidative sulfur cycling despite the ubiquity of sulfite as an intermediate in such processes. The question becomes if the oxygen isotope effects during sulfite oxidation are responsible, or at least compatible, with the oxygen isotope effects observed for the oxygen isotope patterns during the oxidation of reduced sulfur compounds.

Studies on the oxygen isotope effects during oxidative sulfur cycling include reduced sulfur compounds such as H_2S , HS^- , sulfide minerals like pyrite (FeS_2), iron monosulfide (FeS) or sphalerite ($(\text{Zn,Fe})\text{S}$) and elemental sulfur (S^0) (Lloyd, 1967; Lloyd, 1968; Taylor et al., 1984a; Taylor et al., 1984b; Balci et al., 2007; Brunner et al., 2008; Oba and Poulson, 2009a; Tichomirowa and Junghans, 2009; Heidel and Tichomirowa, 2010; Heidel and Tichomirowa, 2011; Kohl and Bao, 2011; Balci et al., 2012; Brabec et al., 2012). For the oxidation of such compounds a considerable range of oxygen isotope effects has been reported, both for isotope fractionation factors, as well as for differences in the relative amount of oxygen derived from H_2O and O_2 in the produced sulfate. For example, a wide range for the contribution of oxygen from H_2O to sulfate during pyrite oxidation has been observed (Lloyd, 1967: 68%; Taylor et al., 1984b: 23-100%; Balci et al., 2007: 87%; Tichomirowa and Junghans, 2009: 50-80%; Heidel and Tichomirowa, 2010: 91%; Kohl and Bao, 2011: 71-79%). The oxygen isotope fractionation factors reported in the aforementioned studies cover a wide range of inverse values (i.e. produced sulfate is enriched in ^{18}O relative to H_2O) for oxidation experiments with Fe^{3+} as sole oxidizing agent ($\epsilon^{18}\text{O}_{\text{SO}_4-\text{H}_2\text{O}}$ between 2.3‰ to 8.2‰. Also in the case of oxidation of reduced sulfur compounds with O_2 the fractionations vary widely ($\epsilon^{18}\text{O}_{\text{SO}_4-\text{O}_2}$ between -4.3‰ to -11.4‰; Lloyd, 1968; Taylor et al., 1984b; Balci et al., 2007), however, unlike the fractionation between sulfate and water, the fractionations between sulfate and O_2 appear to be normal isotope effects (i.e. O_2 derived oxygen in the produced sulfate is depleted in ^{18}O relative to O_2).

3.2.4. Isotope effects during sulfite oxidation

Oxygen isotope equilibrium fractionation between sulfite and water:

Oxygen exchange between sulfite species and water leads to the partial or full expression of an equilibrium isotope effect between sulfite and water (e.g. Holt et al., 1983; Müller et al., *subm.*). Two interspecies reactions probably are responsible for the isotope exchange: sulfur dioxide reacts with H_2O to form HSO_3^-



and $\text{S}_2\text{O}_5^{2-}$ reacts with H_2O to form two molecules of HSO_3^-



At 22°C, the equilibrium isotope fractionation between H_2O and the species HSO_3^- and SO_3^{2-} ($\epsilon^{\text{EQ}}_{\text{SO}_3^{2-}\leftrightarrow\text{H}_2\text{O}}$) is approximately 15.2‰ (Müller et al., *subm.*), whereas the equilibrium isotope fractionation between SO_2 in solution and ambient H_2O ($\epsilon^{\text{EQ}}_{\text{SO}_2\leftrightarrow\text{H}_2\text{O}}$) is approximately 37.0‰ (Müller et al., *subm.*). Currently, there is no estimate for the oxygen isotope equilibrium fractionation between $\text{S}_2\text{O}_5^{2-}$ and H_2O . However, unlike HSO_3^- , $\text{S}_2\text{O}_5^{2-}$ often only exists in very small concentrations (Müller et al., *subm.*). Therefore, we do not consider this species in our study.

Competition between sulfite oxidation rate and rate of oxygen isotope exchange between sulfite and water:

When studying isotope effects during sulfite oxidation, the fact that isotope exchange between residual sulfite and water continues during the oxidation reaction must be considered. The competition between the sulfite oxidation rate and the rate of oxygen isotope exchange between sulfite and H₂O is an important factor for the oxygen isotope composition of produced sulfate, as it controls if any pre-existing isotope composition of sulfite (i.e. sulfite derived from the oxidation of more reduced sulfoxy intermediates) is preserved, or if the oxygen isotope equilibrium fractionation between sulfite and water is fully expressed. The pH and the presence of Fe²⁺ or Fe³⁺ have a strong effect on the competition between the rates of sulfite oxidation and isotope exchange with H₂O. The pH controls the oxygen exchange rate between sulfite and water (Betts and Voss, 1970; Holt et al., 1981; Connick et al., 1982; Horner and Connick, 1986; Horner and Connick, 2003; Müller et al., *subm.*) with most rapid rates at low pH, where SO₂ is the most abundant sulfite species in solution (Holt et al., 1981), and slowest rates at high pH (extremely slow above pH of 12.7; Betts and Voss, 1970). The pH and the presence of Fe²⁺ or Fe³⁺ also influence sulfite oxidation rates. Zhang and Millero (1991) studied the oxidation of sulfite at different pH conditions and the influence of the presence of dissolved metals. Their work showed that the oxidation with molecular oxygen is fastest at pH 6.5 and decreased at higher or lower pH. This implies that HSO₃⁻ and SO₃²⁻ are the likely substrates for the actual oxidation, implying that also under acidic conditions, the oxidation of SO₂ proceeds over bisulfite and does not affect SO₂ directly, a mechanism that was previously postulated by Holt et al. (1981). Furthermore, Zhang and Millero (1991) demonstrated that presence of Fe²⁺ or Fe³⁺ strongly accelerates the oxidation of sulfite to sulfate.

Main abiotic pathways of sulfite oxidation:

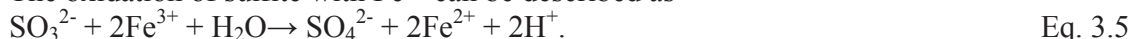
There are two main abiotic pathways for sulfite oxidation (Fig. 3.1): first the oxidation of sulfite with O₂ in solution (O₂(aq)) and secondly the oxidation of sulfite with Fe³⁺. The oxidation of sulfite with O₂(aq) is represented by the following two equations, where the first equation describes the continuous exchange of gaseous O₂ in the headspace of an experiment with O₂(aq)



and the second equation describes the actual consumption of O₂(aq) during the oxidation of sulfite



The oxidation of sulfite with Fe³⁺ can be described as



The oxidation of sulfite with Fe³⁺ can be sustained by oxidation of Fe²⁺ with O₂, according to



The sum of Eq. 3.5 and Eq. 3.6 results in a net reaction equal to Eq. 3.4, however, and most importantly, the oxygen source for sulfite oxidation to sulfate in the case of Eq. 3.4 is O₂, whereas the oxygen source in Eq. 3.5 is H₂O. Depending on environmental conditions such as the pH, the abiotic reaction presented in Eq. 3.6 can be slow, a reason why in natural environments it is often catalyzed by microbes, that gain energy through

this reaction at acidic to neutral pH (Stumm and Lee, 1961; Espejo et al., 1988; Smith et al., 1988; James and Ferris, 2004; Oba and Poulson, 2009b).

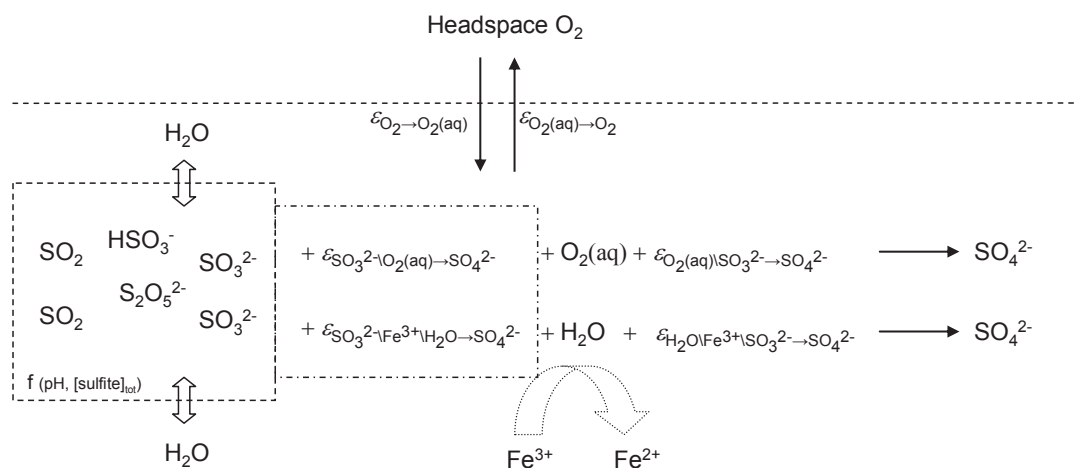


Fig. 3.1: Abiotic sulfite oxidation pathways and respective isotope effects

Sulfite speciation depends on pH and the total sulfite concentration (box on the left), whereas the rate of oxygen isotope exchange with water mainly depends on pH. Sulfate is produced from equilibrated or partially equilibrated sulfite either by oxidation with O₂, or by oxidation with Fe³⁺, the latter leading to incorporation of water oxygen. Both oxidation reactions compete with each other and both pathways have their specific oxygen isotope effects.

Isotope effects during the oxidation of sulfite to sulfate:

The isotope effects during sulfite oxidation can be categorized into two main groups: 1) oxygen isotope effects during oxygen isotope exchange between sulfite and water, 2) kinetic oxygen isotope effects during the oxidation of sulfite, which will be specific for different oxidants (O₂ in Eq. 3.4 or Fe³⁺ in Eq. 3.5; abbreviations of all terms are listed in Table 3.1 in the appendix of this chapter). Furthermore, any system wherein the isotope effects during the oxidation of sulfite to sulfate can be studied typically consists of a sulfite and oxidant (i.e. O₂(aq) and/or Fe³⁺) containing aqueous solution, which is in contact with a gas-phase (here referred to as headspace) that may contain oxidants that can be in exchange with dissolved oxidants (i.e. O₂). Thus, kinetic and/or isotope exchange effects related to transfer of O₂ from and to the headspace need to be considered, and in systems that contain both O₂ and Fe²⁺ or Fe³⁺ kinetic oxygen isotope effects related to the oxidation of Fe²⁺ to Fe³⁺ with O₂ (Eq. 3.6) need to be taken into account. Sulfite exists in solution as several species, and it is possible that different species become directly oxidized (which would yield species-specific isotope effects). For simplicity, we only consider the isotope composition of SO₃²⁻ (which encompasses bisulfite and sulfite ions) in this study. We base this simplification on the observation that sulfite oxidation rates are highest in the pH range of 5.5 to 7.5 (Zhang and Millero, 1991), where sulfite is the dominating species, and infer that oxidation of other sulfite species, such as SO₂, proceed as well over SO₃²⁻ or HSO₃⁻ as intermediates.

We can describe the isotope effects during sulfite oxidation by the following mass balances:

Mass balance and isotope mass balance of molecular oxygen in headspace:

$$\frac{d}{dt}O_2 = -f_{O_2 \rightarrow O_2(aq)} + f_{O_2(aq) \rightarrow O_2} \quad \text{Eq. 3.7}$$

$$\frac{d}{dt}(O_2 \cdot \delta O_2) = -f_{O_2 \rightarrow O_2(aq)} \cdot (\delta O_2 + \varepsilon_{O_2 \rightarrow O_2(aq)}) + f_{O_2(aq) \rightarrow O_2} \cdot (\delta O_2(aq) + \varepsilon_{O_2(aq) \rightarrow O_2}) \quad \text{Eq. 3.8}$$

where $f_{O_2 \rightarrow O_2(aq)}$ and $f_{O_2(aq) \rightarrow O_2}$ designate the fluxes between O_2 in the headspace and O_2 in the aqueous phase. The oxygen isotope effects related to these fluxes are designated as $\varepsilon_{O_2 \rightarrow O_2(aq)}$ and $\varepsilon_{O_2(aq) \rightarrow O_2}$, the oxygen isotope composition of O_2 from the headspace is designated as δO_2 , whereas the oxygen isotope composition of $O_2(aq)$ is designated as $\delta O_2(aq)$.

Mass balance and isotope mass balance of molecular oxygen in solution:

$$\frac{d}{dt}O_2(aq) = +f_{O_2 \rightarrow O_2(aq)} - f_{O_2(aq) \rightarrow O_2} - f_{O_2(aq)SO_3^{2-} \rightarrow SO_4^{2-}} - f_{O_2(aq)Fe^{2+} \rightarrow Fe^{3+}} \quad \text{Eq. 3.9}$$

$$\begin{aligned} \frac{d}{dt}(O_2(aq) \cdot \delta O_2(aq)) = & \frac{d}{dt}O_2(aq) \cdot \delta O_2(aq) + O_2(aq) \cdot \frac{d}{dt}\delta O_2(aq) = \\ & +f_{O_2 \rightarrow O_2(aq)} \cdot (\delta O_2 + \varepsilon_{O_2 \rightarrow O_2(aq)}) - f_{O_2(aq) \rightarrow O_2} \cdot (\delta O_2(aq) + \varepsilon_{O_2(aq) \rightarrow O_2}) \\ & - f_{O_2(aq)SO_3^{2-} \rightarrow SO_4^{2-}} \cdot (\delta O_2(aq) + \varepsilon_{O_2(aq)SO_3^{2-} \rightarrow SO_4^{2-}}) - f_{O_2(aq)Fe^{2+} \rightarrow Fe^{3+}} \cdot (\delta O_2(aq) + \varepsilon_{O_2(aq)Fe^{2+} \rightarrow Fe^{3+}}) \end{aligned} \quad \text{Eq. 3.10}$$

where $f_{O_2(aq)SO_3^{2-} \rightarrow SO_4^{2-}}$ and $f_{O_2(aq)Fe^{2+} \rightarrow Fe^{3+}}$ designate the fluxes for consumption of $O_2(aq)$ via oxidation of sulfite to sulfate and via oxidation of Fe^{2+} to Fe^{3+} , respectively, with $\varepsilon_{O_2(aq)SO_3^{2-} \rightarrow SO_4^{2-}}$ and $\varepsilon_{O_2(aq)Fe^{2+} \rightarrow Fe^{3+}}$ being the corresponding isotope effects. An experimentally accessible value is the oxygen isotope fractionation relative to O_2 remaining in the headspace of an experiment ($\varepsilon_{O_2\text{consumption}}$), which results from the combination of fluxes and isotope effects described in Eq. 3.9 and Eq. 3.10.

Mass balance of ferrous iron:

$$\frac{d}{dt}Fe^{2+} = +f_{Fe^{3+}SO_3^{2-}H_2O \rightarrow SO_4^{2-}} - f_{O_2(aq)Fe^{2+} \rightarrow Fe^{3+}}, \quad \text{Eq. 3.11}$$

where $f_{Fe^{3+}SO_3^{2-}H_2O \rightarrow SO_4^{2-}}$ and $f_{O_2(aq)Fe^{2+} \rightarrow Fe^{3+}}$ designate the fluxes for production of Fe^{2+} via Fe^{3+} reduction during the oxidation of sulfite to SO_4^{2-} and for the consumption of Fe^{2+} via oxidation to Fe^{3+} by $O_2(aq)$.

Mass balance of ferric iron

$$\frac{d}{dt}Fe^{3+} = -f_{Fe^{3+}SO_3^{2-}H_2O \rightarrow SO_4^{2-}} + f_{O_2(aq)Fe^{2+} \rightarrow Fe^{3+}} \quad \text{Eq. 3.12}$$

where the fluxes are designated as for Fe^{2+} but with opposite prefix.

Mass balance and isotope mass balance for sulfite

$$\frac{d}{dt}SO_3^{2-} = -f_{SO_3^{2-}O_2(aq) \rightarrow SO_4^{2-}} - f_{SO_3^{2-}Fe^{3+}H_2O \rightarrow SO_4^{2-}} \quad \text{Eq. 3.13}$$

$$\begin{aligned}
\frac{d}{dt}(\text{SO}_3^{2-} \cdot \delta\text{SO}_3^{2-}) = & \\
& -f_{\text{SO}_3^{2-} \leftrightarrow \text{H}_2\text{O}} \cdot (\delta\text{SO}_3^{2-} - (\delta\text{H}_2\text{O} + \varepsilon_{\text{SO}_3^{2-} \leftrightarrow \text{H}_2\text{O}}^{\text{EQ}})) - f_{\text{SO}_3^{2-} \setminus \text{O}_2(\text{aq}) \rightarrow \text{SO}_4^{2-}} \cdot (\delta\text{SO}_3^{2-} + \varepsilon_{\text{SO}_3^{2-} \setminus \text{O}_2(\text{aq}) \rightarrow \text{SO}_4^{2-}}) \\
& -f_{\text{SO}_3^{2-} \setminus \text{Fe}^{3+} \setminus \text{H}_2\text{O} \rightarrow \text{SO}_4^{2-}} \cdot (\delta\text{SO}_3^{2-} + \varepsilon_{\text{SO}_3^{2-} \setminus \text{Fe}^{3+} \setminus \text{H}_2\text{O} \rightarrow \text{SO}_4^{2-}})
\end{aligned}$$

Eq. 3.14

where $f_{\text{SO}_3^{2-} \setminus \text{O}_2(\text{aq}) \rightarrow \text{SO}_4^{2-}}$ and $f_{\text{SO}_3^{2-} \setminus \text{Fe}^{3+} \setminus \text{H}_2\text{O} \rightarrow \text{SO}_4^{2-}}$ designate the fluxes for sulfite consumption during oxidation to SO_4^{2-} with $\text{O}_2(\text{aq})$ or Fe^{3+} as oxidant and the isotope effects related to the isotope discrimination during consumption of sulfite by direct oxidation with $\text{O}_2(\text{aq})$ designated as $\varepsilon_{\text{SO}_3^{2-} \setminus \text{O}_2(\text{aq}) \rightarrow \text{SO}_4^{2-}}$ and the isotope effect related to oxidation with Fe^{3+} designated as $\varepsilon_{\text{SO}_3^{2-} \setminus \text{Fe}^{3+} \setminus \text{H}_2\text{O} \rightarrow \text{SO}_4^{2-}}$. The oxygen exchange between sulfite and water ($f_{\text{SO}_3^{2-} \leftrightarrow \text{H}_2\text{O}}$) with the corresponding oxygen isotope equilibrium fractionation ($\varepsilon_{\text{SO}_3^{2-} \leftrightarrow \text{H}_2\text{O}}^{\text{EQ}}$) enables the oxygen isotope composition of sulfite (δSO_3^{2-}) to be in equilibrium with the water.

Mass balance and isotope mass balance for sulfate

$$\begin{aligned}
\frac{d}{dt}\text{SO}_4^{2-} = & +f_{\text{SO}_3^{2-} \setminus \text{O}_2(\text{aq}) \rightarrow \text{SO}_4^{2-}} + f_{\text{SO}_3^{2-} \setminus \text{Fe}^{3+} \setminus \text{H}_2\text{O} \rightarrow \text{SO}_4^{2-}} & \text{Eq. 3.15} \\
\frac{d}{dt}(\text{SO}_4^{2-} \cdot \delta\text{SO}_4^{2-}) = & \\
& +f_{\text{SO}_3^{2-} \setminus \text{O}_2(\text{aq}) \rightarrow \text{SO}_4^{2-}} \cdot \left(\frac{3}{4} \cdot (\delta\text{SO}_3^{2-} + \varepsilon_{\text{SO}_3^{2-} \setminus \text{O}_2(\text{aq}) \rightarrow \text{SO}_4^{2-}}) + \frac{1}{4} \cdot (\delta\text{O}_2(\text{aq}) + \varepsilon_{\text{O}_2(\text{aq}) \setminus \text{SO}_3^{2-} \rightarrow \text{SO}_4^{2-}}) \right) \\
& +f_{\text{SO}_3^{2-} \setminus \text{Fe}^{3+} \setminus \text{H}_2\text{O} \rightarrow \text{SO}_4^{2-}} \cdot \left(\frac{3}{4} \cdot (\delta\text{SO}_3^{2-} + \varepsilon_{\text{SO}_3^{2-} \setminus \text{Fe}^{3+} \setminus \text{H}_2\text{O} \rightarrow \text{SO}_4^{2-}}) + \frac{1}{4} \cdot (\delta\text{H}_2\text{O} + \varepsilon_{\text{H}_2\text{O} \setminus \text{Fe}^{3+} \setminus \text{SO}_3^{2-} \rightarrow \text{SO}_4^{2-}}) \right)
\end{aligned}$$

Eq. 3.16

where $f_{\text{SO}_3^{2-} \setminus \text{O}_2(\text{aq}) \rightarrow \text{SO}_4^{2-}}$ and $f_{\text{SO}_3^{2-} \setminus \text{Fe}^{3+} \setminus \text{H}_2\text{O} \rightarrow \text{SO}_4^{2-}}$ designate the fluxes of SO_4^{2-} produced via direct oxidation of sulfite by $\text{O}_2(\text{aq})$ or via indirect oxidation of sulfite with Fe^{3+} as oxidant where the additional oxygen comes from H_2O . The oxygen isotope composition of SO_4^{2-} (δSO_4^{2-}) is affected by the relative fluxes of the two oxidation pathways, the isotope compositions of the various reactants and the corresponding isotope effects. Beside the isotope effect for the consumption of sulfite during the oxidation with $\text{O}_2(\text{aq})$ to SO_4^{2-} (Eq. 3.4) there is an additional isotope discrimination during consumption of $\text{O}_2(\text{aq})$ designated as $\varepsilon_{\text{SO}_3^{2-} \setminus \text{O}_2(\text{aq}) \rightarrow \text{SO}_4^{2-}}$. For the oxidation of sulfite with Fe^{3+} (Eq. 3.5), in addition to isotope effects related to the isotope discrimination during consumption of sulfite by oxidation with Fe^{3+} , also the isotope effects related to the isotope discrimination during consumption of H_2O for the oxidation of sulfite with Fe^{3+} ($\varepsilon_{\text{H}_2\text{O} \setminus \text{Fe}^{3+} \setminus \text{SO}_3^{2-} \rightarrow \text{SO}_4^{2-}}$) needs to be considered.

So far, there are no data available on the aforementioned kinetic isotope effects, with the exception of a study that determined the isotope effect of O_2 consumption from the headspace of a sulfite oxidation experiment (Oba and Poulson, 2009a) which corresponds to the combined kinetic isotope effects of oxygen transfer from headspace in and out of solution and isotope fractionation during the consumption of $\text{O}_2(\text{aq})$, i.e. $\varepsilon_{\text{O}_2\text{consumption}}$.

Parameters affecting the isotope composition of sulfate produced by sulfite oxidation:

In summary, many parameters are likely to have an impact on the oxygen isotope composition of sulfate produced by sulfite oxidation (Fig. 3.1):

- oxygen isotope composition of sulfite,
 - oxygen isotope composition of water,
 - oxygen isotope composition of O₂ in headspace and aqueous solution,
 - availability of other compounds that may serve as oxidants or electron shuttles (i.e. Fe²⁺, Fe³⁺)
 - kinetic and equilibrium isotope effects
 - rate of sulfite oxidation (a function of pH and temperature)
- and
- rate of oxygen isotope exchange between sulfite and H₂O (a function of pH and temperature).

3.2.5 Aim of this study

With sulfite oxidation being the final step in the conversion of reduced sulfur compounds to sulfate there is little doubt that this step may be pivotal in shaping the oxygen isotope signature of produced sulfate. However, very little is known about the isotope effects related to this step, and on how they depend on environmental parameters, such as the pH, as well as on how they depend on the presence/absence of oxidants and electron shuttles (Fe²⁺, Fe³⁺, O₂). With this study, we aim to fill this gap in knowledge. We report the results from abiotic sulfite oxidation experiments that were carried out under different pH conditions (pH 1, 4.9 and 13.3) and in presence/absence of Fe²⁺, Fe³⁺ and O₂. Our results provide a step towards a more detailed mechanistic understanding of the abiotic oxidation of sulfite, and help exploring the question if the oxygen isotope effects during sulfite oxidation are responsible, or at least compatible, with the oxygen isotope effects observed during the oxidation of reduced sulfur compounds.

We note that in natural systems where chemical reactions are often mediated by microbes, reaction kinetics will differ from abiotic experiments. To out-compete abiotic reactions microbes have either to operate faster (enzymatically catalyzed reactions) or inhibit the abiotic process (e.g. spatially separating the reactants by formation of a biofilm). However, it is not possible to differentiate the extent or significance of biotic processes without first establishing the abiotic effects. Special care was taken that our experimental systems were sterile and that the reagent preparation methods ensured sterility. Furthermore, the starting concentration of sulfite in the experiments was higher than 100 mM, a concentration that is toxic for most organisms (Sugio et al., 1992; Sugio et al., 1994).

3.3. Methods

3.3.1. Experimental approaches based on isotope mass balance considerations

For the determination of the isotope fractionation factors, and relative contribution of O₂ vs. Fe³⁺ to sulfite oxidation, experimental approaches are needed that allow isolation of a specific group of parameters such as experiments where either O₂ or Fe³⁺ as oxidants can

be excluded, and experiments where the isotope composition of sulfite can be predicted or controlled. The latter can be achieved by equilibration of sulfite prior to the oxidation with water that has an oxygen isotope composition identical to the isotope composition of the experimental solution. The isotope composition of sulfite then becomes:

$$\delta\text{SO}_3^{2-} = \delta\text{SO}_3^{2-}(\text{EQ}) = \delta\text{H}_2\text{O} + \varepsilon_{\text{SO}_3^{2-} \leftrightarrow \text{H}_2\text{O}}^{\text{EQ}} \quad \text{Eq. 3.17}$$

In cases where the oxygen isotope exchange rate between sulfite and water is much larger than other fluxes affecting the sulfite pool, this isotope composition is maintained throughout the experiment.

Experimentally easily accessible isotope values are the isotope composition of water, of oxygen in the headspace, and the oxygen isotope composition of produced sulfate. Here, we first consider the effect of a large reservoir of O_2 or the situation where O_2 is continuously resupplied to the headspace. A consequence of this situation is that the amount of $\text{O}_2(\text{aq})$ and $\delta\text{O}_2(\text{aq})$ will also quickly reach a constant value. Consequently, the derivative after the time of the product of $\text{O}_2(\text{aq})$ and $\delta\text{O}_2(\text{aq})$ becomes zero and Eq. 3.10 can be solved for the steady state oxygen isotope composition of $\text{O}_2(\text{aq})$:

$$\begin{aligned} \delta\text{O}_2(\text{aq})_{\text{steady state}} = & \\ & \frac{f_{\text{O}_2(\text{aq}) \rightarrow \text{O}_2} \cdot \varepsilon_{\text{O}_2(\text{aq}) \rightarrow \text{O}_2} + f_{\text{O}_2(\text{aq})\text{SO}_3^{2-} \rightarrow \text{SO}_4^{2-}} \cdot \varepsilon_{\text{O}_2(\text{aq})\text{SO}_3^{2-} \rightarrow \text{SO}_4^{2-}} + f_{\text{O}_2(\text{aq})\text{Fe}^{2+} \rightarrow \text{Fe}^{3+}} \cdot \varepsilon_{\text{O}_2(\text{aq})\text{Fe}^{2+} \rightarrow \text{Fe}^{3+}}}{f_{\text{O}_2 \rightarrow \text{O}_2(\text{aq})}} \end{aligned} \quad \text{Eq. 3.18}$$

Equation 3.18 highlights the fact that the oxygen isotope composition of $\text{O}_2(\text{aq})$ depends on the isotope fractionations related to $\text{O}_2(\text{aq})$ consumption, oxygen exchange between aqueous phase and headspace, and on the corresponding flux sizes as well as on the isotope composition of O_2 in the headspace. It is now possible to calculate the oxygen isotope composition of $\text{O}_2(\text{aq})$ that is being consumed due to oxidative processes (considering only the isotope effects related to the consumption of aqueous oxygen to form sulfate and ferric iron):

$$\begin{aligned} \delta\text{O}_2(\text{aq})_{\text{steady state}} \langle \text{consumed by oxidative processes} \rangle = & \\ & \frac{\left(f_{\text{O}_2(\text{aq})\text{SO}_3^{2-} \rightarrow \text{SO}_4^{2-}} \cdot \left(\delta\text{O}_2(\text{aq})_{\text{steady state}} + \varepsilon_{\text{O}_2(\text{aq})\text{SO}_3^{2-} \rightarrow \text{SO}_4^{2-}} \right) \right)}{f_{\text{O}_2(\text{aq})\text{SO}_3^{2-} \rightarrow \text{SO}_4^{2-}} + f_{\text{O}_2(\text{aq})\text{Fe}^{2+} \rightarrow \text{Fe}^{3+}}} \\ & + \frac{\left(f_{\text{O}_2(\text{aq})\text{Fe}^{2+} \rightarrow \text{Fe}^{3+}} \cdot \left(\delta\text{O}_2(\text{aq})_{\text{steady state}} + \varepsilon_{\text{O}_2(\text{aq})\text{Fe}^{2+} \rightarrow \text{Fe}^{3+}} \right) \right)}{f_{\text{O}_2(\text{aq})\text{SO}_3^{2-} \rightarrow \text{SO}_4^{2-}} + f_{\text{O}_2(\text{aq})\text{Fe}^{2+} \rightarrow \text{Fe}^{3+}}} \\ \delta\text{O}_2(\text{aq})_{\text{steady state}} + & \frac{f_{\text{O}_2(\text{aq})\text{SO}_3^{2-} \rightarrow \text{SO}_4^{2-}} \cdot \varepsilon_{\text{O}_2(\text{aq})\text{SO}_3^{2-} \rightarrow \text{SO}_4^{2-}} + f_{\text{O}_2(\text{aq})\text{Fe}^{2+} \rightarrow \text{Fe}^{3+}} \cdot \varepsilon_{\text{O}_2(\text{aq})\text{Fe}^{2+} \rightarrow \text{Fe}^{3+}}}{f_{\text{O}_2(\text{aq})\text{SO}_3^{2-} \rightarrow \text{SO}_4^{2-}} + f_{\text{O}_2(\text{aq})\text{Fe}^{2+} \rightarrow \text{Fe}^{3+}}} \end{aligned} \quad \text{Eq. 3.19}$$

Substituting $\delta\text{O}_2(\text{aq})_{\text{steady state}}$ in Eq. 3.19 with Eq. 3.18 results in
 $\delta\text{O}_2(\text{aq})_{\text{steady state}}$ (consumed by oxidative processes) =

$$\begin{aligned} & \delta\text{O}_2 + \varepsilon_{\text{O}_2 \rightarrow \text{O}_2(\text{aq})} \\ & \frac{f_{\text{O}_2(\text{aq}) \rightarrow \text{O}_2} \cdot \varepsilon_{\text{O}_2(\text{aq}) \rightarrow \text{O}_2} + f_{\text{O}_2(\text{aq})\text{SO}_3^{2-} \rightarrow \text{SO}_4^{2-}} \cdot \varepsilon_{\text{O}_2(\text{aq})\text{SO}_3^{2-} \rightarrow \text{SO}_4^{2-}} + f_{\text{O}_2(\text{aq})\text{Fe}^{2+} \rightarrow \text{Fe}^{3+}} \cdot \varepsilon_{\text{O}_2(\text{aq})\text{Fe}^{2+} \rightarrow \text{Fe}^{3+}}}{f_{\text{O}_2 \rightarrow \text{O}_2(\text{aq})}} \\ & + \frac{f_{\text{O}_2(\text{aq})\text{SO}_3^{2-} \rightarrow \text{SO}_4^{2-}} \cdot \varepsilon_{\text{O}_2(\text{aq})\text{SO}_3^{2-} \rightarrow \text{SO}_4^{2-}} + f_{\text{O}_2(\text{aq})\text{Fe}^{2+} \rightarrow \text{Fe}^{3+}} \cdot \varepsilon_{\text{O}_2(\text{aq})\text{Fe}^{2+} \rightarrow \text{Fe}^{3+}}}{f_{\text{O}_2(\text{aq})\text{SO}_3^{2-} \rightarrow \text{SO}_4^{2-}} + f_{\text{O}_2(\text{aq})\text{Fe}^{2+} \rightarrow \text{Fe}^{3+}}} \\ & = \delta\text{O}_2 + \varepsilon_{\text{O}_2 \text{ consumption}} \end{aligned}$$

Eq. 3.20

with the total isotope effect related to oxygen consumption from the headspace defined as:

$$\begin{aligned} \varepsilon_{\text{O}_2 \text{ consumption}} & = \\ & \varepsilon_{\text{O}_2 \rightarrow \text{O}_2(\text{aq})} \\ & \frac{f_{\text{O}_2(\text{aq}) \rightarrow \text{O}_2} \cdot \varepsilon_{\text{O}_2(\text{aq}) \rightarrow \text{O}_2} + f_{\text{O}_2(\text{aq})\text{SO}_3^{2-} \rightarrow \text{SO}_4^{2-}} \cdot \varepsilon_{\text{O}_2(\text{aq})\text{SO}_3^{2-} \rightarrow \text{SO}_4^{2-}} + f_{\text{O}_2(\text{aq})\text{Fe}^{2+} \rightarrow \text{Fe}^{3+}} \cdot \varepsilon_{\text{O}_2(\text{aq})\text{Fe}^{2+} \rightarrow \text{Fe}^{3+}}}{f_{\text{O}_2 \rightarrow \text{O}_2(\text{aq})}} \\ & + \frac{f_{\text{O}_2(\text{aq})\text{SO}_3^{2-} \rightarrow \text{SO}_4^{2-}} \cdot \varepsilon_{\text{O}_2(\text{aq})\text{SO}_3^{2-} \rightarrow \text{SO}_4^{2-}} + f_{\text{O}_2(\text{aq})\text{Fe}^{2+} \rightarrow \text{Fe}^{3+}} \cdot \varepsilon_{\text{O}_2(\text{aq})\text{Fe}^{2+} \rightarrow \text{Fe}^{3+}}}{f_{\text{O}_2(\text{aq})\text{SO}_3^{2-} \rightarrow \text{SO}_4^{2-}} + f_{\text{O}_2(\text{aq})\text{Fe}^{2+} \rightarrow \text{Fe}^{3+}}} \end{aligned}$$

Eq. 3.21

Equation 3.21 shows that $\varepsilon_{\text{O}_2 \text{ consumption}}$ depends also on the isotope effects for O_2 exchange between aqueous and gaseous phase – thus this value is not a constant in the sense of a kinetic isotope fractionation for a well defined unidirectional reaction. The value of $\varepsilon_{\text{O}_2 \text{ consumption}}$ can be estimated based on experiments with a closed headspace, where the amount of residual O_2 in equilibrium with $\text{O}_2(\text{aq})$ and its isotope composition can be monitored. This allows for the determination of the isotope effect related to oxygen consumption by a Rayleigh distillation approach. In such an experiment, the assumption of a steady state oxygen isotope composition on pool size of $\text{O}_2(\text{aq})$ are no longer given. However, as long as the amount of oxygen in the headspace is large and diffusion of oxygen in and out of the solution is fast which the case is during the early stage of experiments, such an approximation is valid.

In the case where both conditions, such as constant isotope composition of sulfite and large pool of O₂, are given, also the isotope composition of produced sulfate becomes constant:

$$\begin{aligned} \delta\text{SO}_4^{2-} = & \frac{3}{4} \cdot \left(\delta\text{H}_2\text{O} + \varepsilon_{\text{SO}_3^{2-} \leftrightarrow \text{H}_2\text{O}}^{\text{EQ}} \right) \\ & \left(+ f_{\text{O}_2(\text{aq})\text{SO}_3^{2-} \rightarrow \text{SO}_4^{2-}} \cdot \left(\frac{3}{4} \cdot \varepsilon_{\text{SO}_3^{2-} \setminus \text{O}_2(\text{aq}) \rightarrow \text{SO}_4^{2-}} + \frac{1}{4} \cdot \left(\delta\text{O}_2(\text{aq}) + \varepsilon_{\text{O}_2(\text{aq})\text{SO}_3^{2-} \rightarrow \text{SO}_4^{2-}} \right) \right) \right) \\ & + \frac{\left(+ f_{\text{Fe}^{3+}\text{SO}_3^{2-}\text{H}_2\text{O} \rightarrow \text{SO}_4^{2-}} \cdot \left(\frac{3}{4} \cdot \varepsilon_{\text{SO}_3^{2-} \setminus \text{Fe}^{3+}\text{H}_2\text{O} \rightarrow \text{SO}_4^{2-}} + \frac{1}{4} \cdot \left(\delta\text{H}_2\text{O} + \varepsilon_{\text{H}_2\text{O}\text{Fe}^{3+}\text{SO}_3^{2-} \rightarrow \text{SO}_4^{2-}} \right) \right) \right)}{f_{\text{O}_2(\text{aq})\text{SO}_3^{2-} \rightarrow \text{SO}_4^{2-}} + f_{\text{Fe}^{3+}\text{SO}_3^{2-}\text{H}_2\text{O} \rightarrow \text{SO}_4^{2-}}} \end{aligned} \quad \text{Eq. 3.22}$$

Attributing Y to the fraction of oxidation by Fe³⁺ and $(1-Y)$ to the fraction of oxidation by O₂, we can reformulate equation 3.22 to:

$$\begin{aligned} \delta\text{SO}_4^{2-} = & (1-Y) \cdot \frac{1}{4} \cdot \delta\text{O}_2(\text{aq}) + (1-Y) \cdot \left(\frac{3}{4} \cdot \varepsilon_{\text{SO}_3^{2-} \setminus \text{O}_2(\text{aq}) \rightarrow \text{SO}_4^{2-}} + \frac{1}{4} \cdot \varepsilon_{\text{O}_2(\text{aq})\text{SO}_3^{2-} \rightarrow \text{SO}_4^{2-}} \right) \\ & + \left(\frac{3}{4} + Y \cdot \frac{1}{4} \right) \cdot \delta\text{H}_2\text{O} + \frac{3}{4} \cdot \varepsilon_{\text{SO}_3^{2-} \leftrightarrow \text{H}_2\text{O}}^{\text{EQ}} + Y \cdot \left(\frac{3}{4} \cdot \varepsilon_{\text{SO}_3^{2-} \setminus \text{Fe}^{3+}\text{H}_2\text{O} \rightarrow \text{SO}_4^{2-}} + \frac{1}{4} \cdot \varepsilon_{\text{H}_2\text{O}\text{Fe}^{3+}\text{SO}_3^{2-} \rightarrow \text{SO}_4^{2-}} \right) \end{aligned} \quad \text{Eq. 3.23}$$

The above equation shows that the value for Y can be determined by performing sulfite oxidation experiments by varying the $\delta\text{H}_2\text{O}$ and by varying δO_2 , respectively. With this approach the contribution ($1-Y$ and Y , respectively) of oxygen from O₂(aq) and H₂O can be assessed independently. If the value for Y does not agree between the approach with varying the $\delta\text{H}_2\text{O}$ and the approach with varying δO_2 it has to be concluded that one of the prerequisites that allow for the simplifications in Eq. 3.22/3.23 is not met. The here presented determination of the relative contribution of different oxygen sources presented here is similar to the interpretation of oxygen isotope patterns during pyrite oxidation (Lloyd, 1967; Van Stempvoort and Krouse, 1994; Balci et al., 2007; Tichomirowa and Junghans, 2009; Heidel and Tichomirowa, 2010; Heidel and Tichomirowa, 2011; Balci et al., 2012). There, a general oxygen isotope mass balance model, which was introduced by Lloyd in 1967 and further modified by Van Stempvoort and Krouse (1994) and by Balci et al. (2007) is applied:

$$\delta^{18}\text{O}_{\text{SO}_4^{2-}} = X (\delta^{18}\text{O}_{\text{H}_2\text{O}} + \varepsilon^{18}\text{O}_{\text{SO}_4-\text{H}_2\text{O}}) + (1-X) (\delta^{18}\text{O}_{\text{O}_2} + \varepsilon^{18}\text{O}_{\text{SO}_4-\text{O}_2}), \quad \text{Eq. 3.24}$$

where X corresponds to the total fraction of oxygen derived from a water source and $(1-X)$ corresponds to the total fraction of oxygen derived from O₂. The isotope enrichment factors $\varepsilon^{18}\text{O}_{\text{SO}_4-\text{H}_2\text{O}}$ and $\varepsilon^{18}\text{O}_{\text{SO}_4-\text{O}_2}$ refer to the difference in the isotope composition of the oxygen source and the isotope composition of oxygen that was incorporated into sulfate derived from the respective source. Thus, the enrichment factors may refer to a sequence of isotope fractionations, and not to a single fractionation step.

The relationship between Y (Eq. 3.23) and X (Eq. 3.24) is as follows:

$$X = \left(\frac{3}{4} + Y \cdot \frac{1}{4} \right) \Rightarrow 4 \cdot X = 3 + Y$$

and

$$(1 - X) = (1 - Y) \cdot \frac{1}{4} \Rightarrow 4 - 4 \cdot X = 1 - Y \Rightarrow 4 \cdot X = 3 + Y$$

Eq. 3.25

For example, when only oxygen from O_2 contributes to the oxidation of sulfite that was previously equilibrated with H_2O , Y becomes zero, which corresponds to $X = 3/4$. When only oxygen from H_2O contributes to the oxidation of sulfite that was previously equilibrated with H_2O , Y becomes one, which corresponds to $X = 1$.

We can now consider further simplifications of the isotope budgets that result from adjusting experimental parameters: If O_2 is omitted in the experiments (i.e. $Y = 1$), Eq. 3.23 simplifies to:

$$\delta SO_4^{2-} \text{ (no } O_2) = \delta H_2O + \frac{3}{4} \cdot \epsilon_{SO_3^{2-} \leftrightarrow H_2O}^{EQ} + \frac{3}{4} \cdot \epsilon_{SO_3^{2-} \setminus Fe^{3+} \setminus H_2O \rightarrow SO_4^{2-}} + \frac{1}{4} \cdot \epsilon_{H_2O \setminus Fe^{3+} \setminus SO_3^{2-} \rightarrow SO_4^{2-}} \quad \text{Eq. 3.26}$$

If Fe^{2+} and Fe^{3+} are omitted in the experiments (i.e. $Y = 0$), Eq. 23 simplifies to:

$$\delta SO_4^{2-} \text{ (noFe)} = \frac{3}{4} \cdot \delta H_2O + \frac{1}{4} \cdot \delta O_2 \text{ (aq)} + \frac{3}{4} \cdot \epsilon_{SO_3^{2-} \leftrightarrow H_2O}^{EQ} + \frac{3}{4} \cdot \epsilon_{SO_3^{2-} \setminus O_2 \text{ (aq)} \rightarrow SO_4^{2-}} + \frac{1}{4} \cdot \epsilon_{O_2 \text{ (aq)} \setminus SO_3^{2-} \rightarrow SO_4^{2-}} \quad \text{Eq. 3.27}$$

This allows us to substitute the unknown parameters $\delta O_2 \text{ (aq)}$ and $\epsilon_{O_2 \text{ (aq)} \setminus SO_3^{2-} \rightarrow SO_4^{2-}}$ with the experimentally accessible parameters for the consumption of O_2 from the headspace (Eq. 3.20), because in a Fe^{2+} and Fe^{3+} free experiment, only the oxidation of sulfite to sulfate acts as sink for O_2 :

$$\delta SO_4^{2-} \text{ (noFe)} = \frac{3}{4} \cdot \delta H_2O + \frac{1}{4} \cdot \delta O_2 + \frac{1}{4} \cdot \epsilon_{O_2 \text{ consumption (noFe)}} + \frac{3}{4} \cdot \epsilon_{SO_3^{2-} \leftrightarrow H_2O}^{EQ} + \frac{3}{4} \cdot \epsilon_{SO_3^{2-} \setminus O_2 \text{ (aq)} \rightarrow SO_4^{2-}} \quad \text{Eq. 3.28}$$

Furthermore, Eq. 3.21 simplifies to:

$$\epsilon_{O_2 \text{ consumption (noFe)}} = \frac{f_{O_2 \text{ (aq)} \rightarrow O_2} \cdot \epsilon_{O_2 \text{ (aq)} \rightarrow O_2} + f_{O_2 \text{ (aq)} \setminus SO_3^{2-} \rightarrow SO_4^{2-}} \cdot \epsilon_{O_2 \text{ (aq)} \setminus SO_3^{2-} \rightarrow SO_4^{2-}}}{f_{O_2 \rightarrow O_2 \text{ (aq)}}} + \epsilon_{O_2 \text{ (aq)} \setminus SO_3^{2-} \rightarrow SO_4^{2-}} \quad \text{Eq. 3.29}$$

and Eq. 3.20 simplifies to:

$$\delta O_2 \text{ (aq)}_{\text{steady state (noFe)}} = \delta O_2 + \epsilon_{O_2 \rightarrow O_2 \text{ (aq)}} + \epsilon_{O_2 \text{ (aq)} \setminus SO_3^{2-} \rightarrow SO_4^{2-}} + \frac{f_{O_2 \text{ (aq)} \rightarrow O_2} \cdot \epsilon_{O_2 \text{ (aq)} \rightarrow O_2} + f_{O_2 \text{ (aq)} \setminus SO_3^{2-} \rightarrow SO_4^{2-}} \cdot \epsilon_{O_2 \text{ (aq)} \setminus SO_3^{2-} \rightarrow SO_4^{2-}}}{f_{O_2 \rightarrow O_2 \text{ (aq)}}}$$

Eq. 3.30

With the equations above and the corresponding experimental conditions it is possible to disentangle some of the kinetic fractionation effects that occur during the oxidation of sulfite to sulfate. If dissolved iron species (Fe^{2+} , Fe^{3+}) are omitted in experiments and the value for $\epsilon_{O_2 \text{ consumption (noFe)}}$ is experimentally determined, Eq. 3.28 can be used to determine the kinetic fractionation factor for the consumption of SO_3^{2-} during the

oxidation with dissolved O_2 ($\epsilon_{SO_3^{2-}O_2(aq) \rightarrow SO_4^{2-}}$). From Eq. 3.26 it is possible to determine the kinetic isotope effects for the oxidation of sulfite by Fe^{3+} if O_2 is omitted in the experiments. Thereby, the determined kinetic isotope effect can be attributed to $\frac{3}{4}$ to the isotope effect for the consumption of sulfite during oxidation to sulfate by Fe^{3+} ($\epsilon_{SO_3^{2-}Fe^{3+}H_2O \rightarrow SO_4^{2-}}$) and to $\frac{1}{4}$ to the isotope effect for the consumption of water molecules which are the oxygen source of the additional oxygen atom ($\epsilon_{H_2OFe^{3+}SO_3^{2-} \rightarrow SO_4^{2-}}$). For Eq. 3.26 or 3.28 to become applicable it has first to be verified that sulfite is in oxygen isotope equilibrium with water and that the final oxygen atom added during the oxidation comes from H_2O or $O_2(aq)$, respectively. Based on the above derived isotope mass balance considerations derived above we performed six experiments (A, B1, B2, B3, C and D) to

- investigate under which conditions sulfite oxidation rates are fast enough to compete with oxygen isotope exchange between sulfite and water, creating isotope disequilibrium,
 - disentangle the isotope fractionation factors which occur during abiotic oxidation of sulfite to sulfate
- and
- determine the range of oxygen isotope values of sulfate produced from sulfite oxidation in a situation where water and O_2 have a natural abundance isotope composition, for a direct comparison to sulfates from the environment.

Experiment A:

Experiment A is a sulfite oxidation experiment performed with a limited oxygen headspace in absence of ferric and ferrous iron where the concentration of the residual O_2 in the headspace and the isotope composition of O_2 , H_2O and sulfate are monitored. Due to the absence of iron species the isotope fractionation for O_2 consumed during oxidation of SO_3^{2-} ($\epsilon_{O_2\text{consumption}(noFe)}$) can be determined. This allows to subsequently determine the kinetic fractionation for the consumption of sulfite molecules during the abiotic oxidation of sulfite by O_2 ($\epsilon_{SO_3^{2-}O_2(aq) \rightarrow SO_4^{2-}}$).

Experiments B1, B2, B3:

Experiments B1, B2 and B3 are sulfite oxidation experiments with a large oxygen headspace in absence of ferric and ferrous iron at three different pH conditions (pH 1, 4.9 and 13.3). They serve to test if O_2 is solely incorporated into SO_4^{2-} or if some oxygen from O_2 ends up in water. This test is necessary to show that all consumed O_2 is used for the SO_3^{2-} oxidation to validate Eq. 3.28, which is used in the interpretation of the results from experiment A. The value for $\epsilon_{SO_3^{2-}O_2(aq) \rightarrow SO_4^{2-}}$ calculated in experiment A can then be used to determine the value of $\epsilon_{O_2\text{consumption}(noFe)}$ in experiments B1, B2 and B3. Performing the experiments at different pH conditions enables us to detect potential sulfite-isotope disequilibrium effects, resulting from sulfite oxidation rate out-competing oxygen exchange between sulfite and water.

Experiment C:

Experiment C is a sulfite oxidation experiment with dissolved Fe^{3+} as sole oxidant (i.e. in absence of O_2) at a low pH. This experiment serves to test if H_2O is indeed the sole oxygen source in the produced SO_4^{2-} and to determine the kinetic isotope effects during anoxic sulfite oxidation (sum of $\frac{3}{4} \epsilon_{\text{SO}_3^{2-}\text{-Fe}^{3+}\text{-H}_2\text{O}\rightarrow\text{SO}_4^{2-}}$ and $\frac{1}{4} \epsilon_{\text{H}_2\text{O}\text{-Fe}^{3+}\text{-SO}_3^{2-}\rightarrow\text{SO}_4^{2-}}$). As the end-member situations (Fe-free vs. O_2 free) of experiments B1 and C are likely uncommon in natural environments, experiment D was carried out.

Experiment D:

Experiment D was performed with an O_2 headspace and in presence of dissolved Fe^{2+} . This experiment mimics a situation akin to an acid mine drainage system, where two possible oxygen sources (H_2O and O_2) contribute to the produced SO_4^{2-} , with the restriction that the O_2 concentration in the headspace (100%) of our experiment is much higher than in Earth's atmosphere (~21%) and that concentrations of Fe^{2+} in the environment can vary strongly. This experiment helps to elucidate if sulfite oxidation proceeds in oxygen isotope disequilibrium under these conditions. Furthermore, the isotope signature of produced sulfate can be compared to environmental studies.

3.3.2. Experimental setup*Preparation of isotopically labeled water:*

Isotopically distinct water (-7.7‰, 48‰, 162‰) was produced by injecting appropriate amounts of water consisting of 98% ^{18}O (NUKEM GmbH) to de-ionized water (18M Ω , abbreviated as MQ).

Preparation of stock solutions:

Sulfite stock solutions were prepared in plastic syringes in a nitrogen (N_2) atmosphere by dissolving anhydrous sodium sulfite (6 g of Na_2SO_3 , $M_R = 126.04 \text{ g mol}^{-1}$, Fluka) in 50 ml of isotopically labeled water (corresponding to isotope composition of the experimental solutions). Prior to sulfite addition, the water was purged for 20 minutes with N_2 gas to expel oxygen. Subsequent to the addition of Na_2SO_3 to water 10 ml of 6 M hydrochloric acid (HCl) were added to the sulfite solution. Care was taken to minimize the loss of sulfur dioxide gas (SO_2) produced by the acidification of the sulfite solution. Before further use, sulfite stock solutions were kept in the plastic syringes in N_2 atmosphere for in minimum an hour to ensure complete oxygen isotope exchange between sulfite and water. Due to the large addition of Na_2SO_3 , the oxygen isotope composition of the stock solutions can deviate from the experimental solutions, with a large impact on strongly labeled solutions. The oxygen isotope composition of the sulfite stock solutions ($\delta\text{H}_2\text{O}_{\text{stock}}$) was calculated from the known amount and isotope composition of oxygen from Na_2SO_3 and the experimental solutions ($\text{H}_2\text{O}_{\text{exp}}$) according to

$$\delta\text{H}_2\text{O}_{\text{stock}} = \frac{(\text{O}_{\text{Na}_2\text{SO}_3} \langle \text{mol} \rangle \cdot \delta\text{Na}_2\text{SO}_3 + \text{O}_{\text{H}_2\text{O}_{\text{exp}}} \langle \text{mol} \rangle \cdot \delta\text{H}_2\text{O}_{\text{exp}})}{(\text{O}_{\text{Na}_2\text{SO}_3} \langle \text{mol} \rangle + \text{O}_{\text{H}_2\text{O}_{\text{exp}}} \langle \text{mol} \rangle)} \quad \text{Eq. 3.31}$$

Preparation of experimental solutions:

The experimental solutions were prepared in glass containers with the isotopically labeled water adjusted to the specific pH. The following buffers were used to stabilize solutions at a specific pH: HCl (pH 1), acetic acid (glacial pure) + sodium acetate trihydrate (pH 4.9) and KCl + NaOH (pH 13.3). The exact amount of experiment solution for the specific experiments (A-D) is given in the respective experimental descriptions.

Experiment containers and headspace:

Duran bottles with total volume of 2300 ml were used as experiment containers. The main port of the experiment container was sealed with a gas tight rubber stopper and afterwards, the container was purged for approximately 8 minutes with O₂ gas (oxygen N48, AIR LIQUIDE) through the side port (see Fig. 3.2). The small side port is sealed with PTFE/Silicone septa to prevent contamination with air and at the same time to allow sampling with gas tight syringes over the duration of the experiment.

For the approach with isotopically distinct O₂ we prepared the experiments as following. Each set of experiments contains three containers with distinct oxygen isotope composition in the headspace. To obtain the different isotope compositions, we injected different amounts of ¹⁸O spiked O₂ (oxygen gas, 99% ¹⁸O spike from ISOTEC) in two of the three experiment containers. In all three containers we used unlabeled de-ionized MQ water.

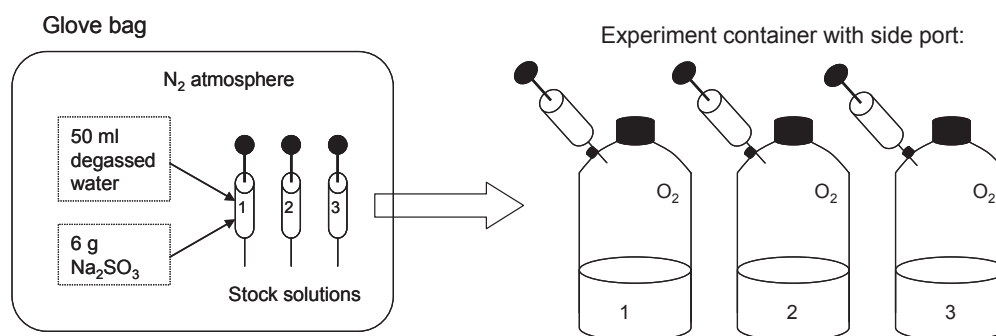


Fig. 3.2: Preparation of sulfite stock solution in a glove bag with a N₂ atmosphere and subsequent injection of the stock solution through the septum of the side port into the experiment containers.

3.3.3. Setup of different experiments (A-D)

All experiments were performed in the laboratory at 22°C and the experimental solutions were kept in constant motion during the whole time to accelerate uptake of headspace O₂ into solution. Experiment C with Fe³⁺ and in absence of O₂ was kept in motion with a magnetic stirrer to keep the solution well mixed.

Experiment A with limited headspace oxygen and without iron species:

Two containers (volume of 2300 ml) were filled with 960 ml of experimental solution buffered at pH 4.9. Compared to the other experiments the volume of the headspace was much smaller and due to that O₂ was consumed almost quantitatively during the course of the experiment. The main port was sealed with a rubber stopper with an attached oxygen microsensors (Revsbech et al., 1983; Revsbech, 1989) for continuous monitoring of the

oxygen concentration in the headspace (see Fig. 3.3). After installing the oxygen microsensors, we purged the headspace with O₂ gas (oxygen N48, AIR LIQUIDE) over the small side port (Fig. 3.3) which was subsequently sealed. We injected a total of 14 g of Na₂SO₃ partitioned in two syringes containing 50 ml acetate buffer solution, which corresponds to a starting concentration in the experiment of approximately 0.105 M.

We sampled aliquots for concentration measurements of sulfite, sulfate, and for the oxygen isotope composition analyses of sulfate, O₂ and water (δSO_4^{2-} , δO_2 and $\delta\text{H}_2\text{O}_{\text{exp}}$). By monitoring the concentration of O₂ in the headspace and δO_2 we can determine the oxygen isotope fractionation during consumption of O₂ for the oxidation of sulfite to sulfate using the closed system Rayleigh equation (after Mariotti et al., 1981).

$$\varepsilon_{\text{O}_2, \text{consumption}(\text{noFe})} \cdot \ln f = \ln \left[\frac{\delta\text{O}_2(t)+1}{\delta\text{O}_2(t_0)+1} \right] \cdot 1000\text{‰} \quad \text{Eq. 3.32}$$

with f being the concentration of O₂ at time t relative to the starting concentration at t_0 , and δO_2 being the measured oxygen isotope composition of the headspace O₂ at time t and at t_0 . The duration of experiment A was four days.

Experiment container with oxygen microsensors:

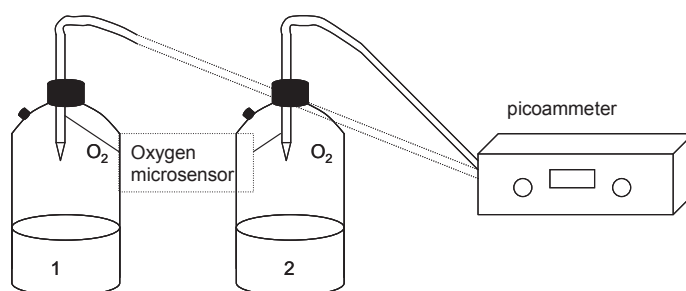


Fig. 3.3: Setup of experiment A with the oxygen microsensors penetrating a gas tight rubber stopper to monitor the oxygen concentration in the headspace during the experiment. The picoammeter measures the electron current from the microsensors and transfers the data over an interface to the computer.

Experiment B1, B2 and B3 with large oxygen headspace and without iron species:

The experiments were prepared using 390 ml of experimental solutions with a different pH for each container, leaving a O₂ headspace corresponding to approximately 78 mmol O₂ which is far in excess of the oxygen needed for the oxidation of subsequently added sulfite (6 to 7.5 g of Na₂SO₃, corresponding to 47.6 to 59.5 mmol of sulfite). To start the experiment, we injected the 50 ml of sulfite stock solution from a syringe through the side port into the experiment bottles (see Fig. 3.2). In all three experiments we started with a total amount of 440 ml water per bottle and 6 g of Na₂SO₃ in experiment B2 and B3 and 7.5 g Na₂SO₃ in experiment B1.

B1: This experiment was performed at pH 1 with two sets of experiments. In the first set we performed the experiments in isotopically distinct water but constant isotope composition of the O₂ in the headspace to determine the water oxygen contribution in the produced sulfate (Y) after Eq. 3.23. The other set of experiments was performed in isotopically identical water but with three isotopically distinct O₂ in the headspace to

determine the contribution of O_2 in the produced sulfate ($1-Y$) after Eq. 3.23. The experiment duration lasted approximately 14 days due to slow oxidation.

B2: The experiment was performed at pH 4.9 in three isotopically distinct experimental solutions to determine the water oxygen incorporation Y after Eq. 3.23. The oxidation reaction at this pH is much faster than in experiment B1 and the experiment lasted approximately four days.

B3: Experiment B3 was performed at a high pH 13.3 in isotopically identical MQ water but with isotopically distinct O_2 in the headspace. The sulfite stock solutions were prepared in acidified de-ionized water to ensure full oxygen exchange with the water before it was added to the experimental solution buffered at pH 13.3 where no oxygen exchange between sulfite and water occurs (Betts and Voss, 1970, Horner and Connick 2003). From this experiment we can determine the direct O_2 contribution to produced sulfate ($1 - Y$). Oxidation of sulfite at such a high pH is similarly slow as for the low pH (experiment B1) when no iron species are present; the experiment lasted approximately 14 days.

Experiment C with Fe^{3+} as sole oxidizing agent:

Experiments with ferric iron as oxidant were performed at pH 1 using three isotopically distinct acid KCl + HCl buffer solutions that prevent precipitation of Fe^{3+} (oxyhydr)oxides. The experiments were performed in Duran bottles with 500 ml volume with a headspace of approximately 50 ml and prepared in N_2 atmosphere. Fe^{3+} is dissolved as anhydrous $FeCl_3$ ($M_R = 162.2 \text{ g mol}^{-1}$) to final concentrations of 0.111 M. The sulfite stock solutions were injected through a Teflon sealing. The starting sulfite concentration in the total of 450 ml experimental solution was approximately 0.105 M and the experiment lasted 14 days to ensure complete oxidation of SO_3^{2-} .

Experiment D in the presence of large O_2 headspace and dissolved Fe^{2+} :

Two sets of experiment D were performed with dissolved Fe^{2+} and with O_2 in the headspace at pH 1 to investigate the relative contributions of the two oxygen sources (H_2O and O_2) when both oxidizing agents are present. The pH of the experiment was low to prevent the extremely fast oxidation that would occur at neutral pH. Fe^{2+} was dissolved in form of 12 g iron(II)chloride tetrahydrate ($M_R = 198.81 \text{ g mol}^{-1}$) in 35 ml acidified de-ionized water under N_2 atmosphere (total Fe^{2+} concentration of 134 mM). The Fe^{2+} and sulfite stock solutions were injected in the experiment containers immediately after each other. One set of the experiment had isotopically distinct solutions while keeping the oxygen isotope composition of the O_2 constant and another set of experiments had isotopically distinct O_2 in the headspace while keeping the oxygen isotope composition of the water constant; the experiment duration was 11 days.

3.3.4. Measurements

Hydrochemistry (pH and concentrations of O_2 , SO_4^{2-} , SO_3^{2-}):

The concentrations of sulfite, sulfate and the pH were measured in aliquots (7 ml) taken during the course of the experiments. The pH was measured with pH indicator strips (MACHEREY-NAGEL) during the experiment and after termination of the experiment with a pH electrode (pH-Meter 766 Calimatic from Knick, accuracy better 0.09 pH units).

In experiment A we measured the O₂ concentration in the headspace of the experiment with oxygen microsensors prepared in our institute as previously described (Revsbech et al., 1983; Revsbech, 1989; Ebert and Brune, 1997). Oxygen measurements with microsensors are based on current measurements induced by the electrochemical reduction of oxygen at the sensor electrode with a rate proportional to its concentration. The oxygen sensor works based on oxygen diffusion through a silicone membrane to a sensing gold cathode and has additionally a guard silver cathode which prevents diffusion of oxygen from the internal electrolyte towards the sensor tip and thus stabilizes the measuring signal (Revsbech et al., 1983; Revsbech, 1989; Ebert and Brune, 1997). The flux of electrons from an internal Ag/AgCl anode needed for the reduction process produces an electron current which is measured with a picoammeter outside the experiment container (Fig. 3.3). We applied a two point calibration, where 21% O₂ saturation corresponds to the detected value of laboratory air and 0% to the O₂ concentration that was measured in de-ionized water purged with nitrogen gas.

Samples for sulfate concentration measurements by ion chromatography (IC) were first acidified with 6 M HCl, then purged with N₂ to strip out gaseous SO₂, and afterwards strongly diluted with MQ water for subsequent IC measurements. The sulfate concentrations were used to calculate the oxidation rates of sulfite.

Oxygen isotope analyses of H₂O:

The measurements of the oxygen isotope composition of the experiment solutions were carried out with the CO₂ equilibration method (Epstein and Mayeda, 1953; Nelson, 2000) followed by isotope analysis with an isotope ratio mass spectrometer (IRMS, Thermo Fisher Scientific® Delta V Plus). Sample solutions from the experiments at high pH were acidified with small amounts of phosphorous pentoxide (P₄O₁₀), to prevent trapping of CO₂ gas in the sample solutions. From each sample, 200 µl aliquots were transferred into gas tight glass vials with a volume of approximately 12 ml, afterwards the vials were purged with He containing 0.5% CO₂. The samples were gently shaken for 18 hours allowing isotope equilibration between sample water and CO₂ gas. After equilibration, small amounts of the gas were transferred via a Gas Bench device (Finnigan) to the IRMS. The system was calibrated with the reference waters SMOW, GISP and SLAP and the oxygen isotope ratios are reported in the δ-notation relative to the Vienna Standard Mean Ocean Water (VSMOW), i.e. $\delta^{18}\text{O} = (R_{\text{sample}}/R_{\text{VSMOW}} - 1) \times 1000\text{‰}$. The reproducibility of the measurements based on repeated measurements of standards is less than 0.1‰ (1σ).

Oxygen isotope analyses of SO₄²⁻:

Aliquots for sulfate isotope analysis were strongly acidified with 6 M HCl and purged for 20 minutes with N₂ gas to expel sulfur dioxide, which is produced upon acidification from the residual sulfite in the solution. The sulfate is subsequently precipitated as BaSO₄ by adding a filtered barium hydroxide (Ba(OH)₂) solution, centrifuged and rinsed two times with MQ water to minimize potential contamination with hydroxides. The oxygen isotope composition of the precipitates was measured with a Finnigan DELTA^{plus} IRMS coupled to a thermochemical reduction device (TC/EA Finnigan), where samples (0.3 – 0.4 mg in silver cups) are reduced at 1450°C in presence of carbon to CO gas. The isotope data are reported in the standard δ-notation relative to VSMOW. Measurements were calibrated using standards NBS 127 (δ¹⁸O = 8.7‰), SO-5 (δ¹⁸O = 12‰) and SO-6

($\delta^{18}\text{O} = -11.3\text{‰}$). The reproducibility based on repeated measurements of the standards is less than 0.5‰ (1σ). The standard deviation of our sulfate samples range between 0.2‰ (1σ) for samples from unlabeled experiments to 1.4‰ (1σ) for samples from experiments which were strongly labeled.

Oxygen isotope analyses of O₂:

The oxygen isotope composition of O₂ was measured with the same TC/EA-IRMS setup as for the analysis of the oxygen isotope composition of the sulfate samples. We collected O₂ from the headspace of the experiment containers with a gas tight glass syringe. The syringe was purged three times before taking the sample. For storage, the gas was injected into 13 ml glass vials that were prefilled with helium and sealed with rubber stoppers. To measure the isotope composition of oxygen gas samples with the IRMS, we attached an injection port in the helium stream of the system. The gas samples were injected through the injection port and carried by the He stream through a water trap into the reactor of the TC/EA where it was reduced to CO gas which was analyzed for its isotope composition by the IRMS (see Brunner et al., 2008). The oxygen isotope composition of the samples was obtained by comparing the obtained isotope ratio to repeated injections of oxygen gas (oxygen N48, AIR LIQUIDE; $\delta\text{O}_{2(\text{ref})} = 14.6\text{‰}$), which was calibrated with the internal solid standards NBS 127 ($\delta^{18}\text{O} = 8.7\text{‰}$), SO-5 ($\delta^{18}\text{O} = 12\text{‰}$) and SO-6 ($\delta^{18}\text{O} = -11.3\text{‰}$) and expressed in δ notation relative to VSMOW. The δO_2 values reported in our study are always an average of several time points (three to six) with the standard deviation ranging between 0.5‰ (1σ) for samples from unlabeled headspace to 1.5‰ (1σ) for samples from experiments with a strongly labeled headspace.

3.3.5. Determination of Y, isotope enrichment factors and isotope offsets

We determined the relative oxygen source contributions of water and O₂ based on the isotope mass balance of Eq. 3.23. The total water oxygen contribution can be determined graphically from the slope of a linear regression by plotting the measured δSO_4^{2-} against the isotopically distinct $\delta\text{H}_2\text{O}_{\text{exp}}$ of the same experiment. From the slope we can further deduce the amount of water oxygen that is incorporated only during the final oxidation step (Y) by assuming that sulfite fully equilibrated its isotopes with water prior to sulfite oxidation (i.e. slope = $3/4 + Y \cdot 1/4$) and obtain an estimate for the O₂ oxygen contribution during the final oxidation step (1-Y). The O₂ contribution to produced sulfate can also be determined directly, because the total O₂ contribution (1-Y) * 1/4 from Eq. 3.23 is equal to the slope of a linear regression when we plot the δSO_4^{2-} of one experiment against the isotopically distinct δO_2 . For the determination of the relative oxygen source contribution we omitted the first sampling points in the time series because those sulfate samples are prone to artifacts caused by high sulfite concentrations which may not be quantitatively removed with our acidification procedure and lead to erroneous isotope values in the sulfate. The error of the contribution of each oxygen source was calculated by error propagation from the error on the slope of the regression line (Anova, 95% confidence level).

The isotope enrichment factors and isotope offsets between the isotope composition of sulfate and water ($\Delta^{18}\text{O}_{\text{SO}_4-\text{H}_2\text{O}}$) were calculated from the isotope data of experiments without ¹⁸O spike in water or O₂. Using data (marked in bold in Table 3.3) from

experiments that were carried out close to natural abundance avoids artifacts that potentially result due to small contaminations of isotopically spiked samples with contaminants that have a natural abundance isotope composition. To compare the $\Delta^{18}\text{O}_{\text{SO}_4\text{-H}_2\text{O}}$ of our experiments to reported observed isotope offsets from natural environments or experiments it must be noted that the δO_2 in our experiments was between 6.8‰ and 12.6‰ for non-spiked experiments, whereas the δO_2 of air is approximately 23.5‰ (Kroopnick and Craig, 1972). For a realistic comparison between our data and data from the literature the $\Delta^{18}\text{O}_{\text{SO}_4\text{-H}_2\text{O}}$ from our experiments (A, B1, B2, B3 and D) needs to be adjusted to the oxygen isotope composition of air. This is achieved by subtracting the known O_2 contribution from our isotope mass balances times δO_2 from our measured δSO_4^{2-} and by adding the same amount of O_2 times the oxygen isotope composition of air (i.e. 23.5‰; Kroopnick and Craig, 1972):

$$\delta\text{SO}_4^{2-}(\text{air}) = \delta\text{SO}_4^{2-} - \frac{1}{4} \cdot (1 - Y) \cdot \delta\text{O}_2 + \frac{1}{4} \cdot (1 - Y) \cdot \delta\text{O}_2(\text{air}) \quad \text{Eq. 3.33}$$

To obtain $\Delta^{18}\text{O}_{\text{SO}_4\text{-H}_2\text{O}}$ (Table 3.3) the oxygen isotope composition of the experimental solution was subtracted from $\delta\text{SO}_4^{2-}(\text{air})$. We note that under disequilibrium conditions, the isotope composition of sulfite from natural abundance experiments deviates slightly from the theoretical isotope equilibrium value expected for isotope exchange with the experimental solutions, however, this is also likely for sulfite that is produced as intermediate in the oxidation of sulfur compounds to sulfate. Thus, comparisons of $\Delta^{18}\text{O}_{\text{SO}_4\text{-H}_2\text{O}}$ have to be considered as not fully quantitative. Error estimates (1σ) for isotope enrichment factors and $\Delta^{18}\text{O}_{\text{SO}_4\text{-H}_2\text{O}}$ were based on error propagation of uncertainties of isotope measurements and error estimates for Y .

3.4. Results and discussion

3.4.1. Hydrochemistry

The measured sulfate concentrations scatter and sometimes exceed the maximum sulfate concentration that can be expected based on initial SO_3^{2-} concentrations. These inaccuracies probably resulted from the strong dilution of sample aliquots for concentration measurements, which was necessary because of high sulfate concentrations that were too high for direct analysis by IC. To partially correct for these inaccuracies in the determination of sulfite oxidation rates, SO_4^{2-} concentrations had to be normalized to the expected final SO_4^{2-} concentration based on initial SO_3^{2-} concentrations. We determined the rate constant k for the oxidation of sulfite which is second order with respect to the SO_3^{2-} concentration (sum of all sulfite species) and half or zero order with respect to oxygen when O_2 is present or absent, respectively (equation 3.7 in Zhang and Millero, 1991). By plotting the negative derivative of the SO_3^{2-} concentration derived by subtracting the calculated SO_4^{2-} concentrations from the initial SO_3^{2-} concentrations against the square of the SO_3^{2-} concentration times $[\text{O}_2]^{0.5}$, whereas the slope is equal to k , the rate constant for sulfite oxidation. The concentration of $\text{O}_2(\text{aq})$ was calculated with Henry's law, assuming that k_{H} (Henry coefficient for water) is approximately $769.2 \text{ L atm mol}^{-1}$ at 25°C and the partial pressure of O_2 is 1 atm which reveals a concentration of $0.0013 \text{ M O}_2(\text{aq})$ in the experiments with O_2 in excess. In experiment A we could

calculate the actual O_2 pressure in the headspace via the ideal gas law from the actual O_2 concentration that we monitored with the microsensors (see Table 3.4) and determine from that the concentration of $O_2(aq)$ during the experiment. The calculation of $O_2(aq)$ concentrations might involve errors but they are accurate enough for our oxidation rate calculations. For the experiment C which was performed in absence of O_2 we determined the oxidation rate by plotting the negative derivative of the SO_3^{2-} concentration against the square of the SO_3^{2-} concentration to determine k from the slope of the graph. The logarithm of the oxidation rates k are listed in Table 3.2, less negative rates represent faster sulfite oxidation. Because of the aforementioned uncertainties, the determined oxidation rates should only be used to qualitatively assess the connection between oxidation rates, pH, and presence/absence of ferric/ferrous iron in our experiments (Table 3.2).

Table 3.2

Hydrochemistry of the abiotic sulfite oxidation experiments (at 22°C)					
Experiment description	pH	SO_3^{2-} (mM) initial	Oxidation rate (log k) ($M^{-1} \text{ min}^{-1}$)	Fe^{2+} (mM) initial	Fe^{3+} (mM) initial
A	4.90	104.8	-0.739±0.079		
B1	1.13	136.0	-1.601±0.080		
B2	4.88	108.0	1.059±0.024		
B3	13.36	108.0	-1.015±0.037		
C	1.00	100.7	0.288±0.080		105.8
D	0.90	105.0	-0.590±0.059	134.0	

Highest sulfite oxidation rates were observed in experiment B2 which was performed at pH 4.88 and in the absence of dissolved iron species. Slowest oxidation rates occurred in experiment B1 which was performed at a pH of approximately 1 and in the absence of dissolved iron species. Experiments C and D with Fe^{2+} or Fe^{3+} in solution were performed at a similar pH to experiment B1 but the oxidation rates were one order of magnitude higher (see Table 3.2). Dissolved iron species obviously accelerate the oxidation process drastically. The oxidation rate in experiment C is likely faster than in experiment D because the oxidizing agent Fe^{3+} is already present from beginning whereas in experiment D, Fe^{2+} first has to be oxidized with O_2 to Fe^{3+} (Eq. 3.6). The oxidation rate of sulfite in experiment B3, which was performed under strongly alkaline conditions (pH 13.3), is slower than in experiment B2 and the experiments with dissolved iron (C and D) but faster than in experiment B1. Despite the fact that experiment A was performed at a similar pH to that in experiment B2 (4.9 and 4.88, respectively), the oxidation rate in experiment A was more than 60 times slower (Table 3.2). We attribute this discrepancy to the smaller amount of O_2 in the headspace of experiment A (i.e. sulfite oxidation rate being dependent on sulfite and $O_2(aq)$ concentrations). In general, our observations confirm that sulfite oxidation rates are highest at circum neutral pH and/or in presence of

dissolved iron species and decrease at lower and higher pH and/or with restricted iron availability, an observation consistent with the study by Zhang and Millero (1991), who reported highest oxidation rates at pH 6.5 and a decrease towards lower and higher pH and higher oxidation rates in presence of Fe^{2+} and Fe^{3+} . However, our oxidation rates are much lower than oxidation rates determined by Zhang and Millero (1991) who obtained an oxidation rate at pH 4.79 of $\log k$ equal to 2.29 (k in $\text{M}^{-1} \text{min}^{-1}$) whereas in our experiment B2 at similar pH we obtained only a $\log k$ equal to 1.06 (Table 3.2). The reason for this large discrepancy is that their experiments were performed in seawater and ours in de-ionized water, a similar observation has been reported already by Hitchens and Towne (1936). Zhang and Millero (1991) investigated also the effect of salinity at pH 8.2 and 25°C and obtained a value of 0.97 for $\log k$ at a minimal salinity of 0.17 but a much higher rate of 2.87 at a salinity of 35.06. If we apply this difference to the oxidation rate measurements of Zhang and Millero (1991) at pH 4.79 we would obtain $\log k$ values that are in the same range as the value we obtained in experiment B2.

The fast oxidation rates at medium pH and in the presence of iron species likely affect the oxygen isotope signature in the produced sulfate, because the sulfite species in solution have less time to equilibrate oxygen isotopes with the surrounding water and therefore might retain their original oxygen isotope composition.

3.4.2. Isotopes

Relative contribution of oxygen from H_2O and O_2 :

A series of sulfite oxidation experiments with water or O_2 with different oxygen isotope compositions allows determination of the relative contributions of oxygen from these two sources. The sum of the two contributions is expected to be one as long as sulfite completely equilibrates oxygen isotopes with water prior to oxidation. Deviations from unity can thus be considered as an expression of non-equilibrium conditions or as a result of kinetic isotope fractionation strongly affecting one of the pools considered, i.e. O_2 . Our sulfite stock solutions were prepared in a way (acidification) that sulfite was in isotope equilibrium with water which had the same oxygen isotope composition as the experimental solution. However, it must be remembered that Na_2SO_3 salt has an oxygen isotope composition of 1‰, which is different from the oxygen isotope compositions of the water we used. This difference and the addition of hydrochloric acid in the stock solutions (with an estimated $\delta^{18}\text{O}_{\text{HCl}}$ of -8‰) can cause differences between the oxygen isotope compositions of the sulfite stock solution ($\delta\text{H}_2\text{O}_{\text{stock}}$) and the solution in the experiment container ($\delta\text{H}_2\text{O}_{\text{exp}}$; see Table 3.3). Since oxidation rates are very fast at circum-neutral pH or in presence of dissolved iron species, it is possible that sulfite preserves the isotope signature of the sulfite stock solution instead of attaining isotope equilibrium with the experimental solution. Therefore, the graphical determination of the relative contribution of oxygen from water in the produced sulfate needs to be carried out twice, once in a δSO_4^{2-} vs. $\delta\text{H}_2\text{O}_{\text{exp}}$ and once in a δSO_4^{2-} vs. $\delta\text{H}_2\text{O}_{\text{stock}}$ plot. Comparison of the relative contribution of oxygen from O_2 , determined from a δSO_4^{2-} vs. δO_2 then reveals if the competition between the rates of oxygen isotope exchange between sulfite and water and the rate of sulfite oxidation created disequilibrium conditions.

Table 3.3

Oxygen isotope compositions of all experiments performed at 22°C (in ‰)							
Experiment description	pH	$\delta\text{H}_2\text{O}_{\text{exp}}^*$	$\delta\text{H}_2\text{O}_{\text{stock}}^*$	δSO_4^{2-*}	δO_2^*	$\delta\text{SO}_4^{2-}(\text{air})$	$\Delta^{18}\text{O}_{\text{SO}_4\text{-H}_2\text{O}}$
A	4.90	-7.8	-7.3	3.2	11.0	6.2	14.0
	4.90	-7.8	-7.3	23.8	95.7		
B1	1.13	-7.7	-7.3	6.0	6.3	9.9	17.6
	0.91	47.1	41.7	41.6	7.4		
	0.92	159.3	142.5	134.4	10.3		
	1.13	-7.7	-7.3	17.7	48.7		
	1.13	-7.7	-7.3	27.3	86.0		
B2	4.88	-7.4	-7.0	3.4	(11.0)	6.4	13.8
	4.88	47.2	44.9	43.2	(11.0)		
	4.88	159.0	151.3	124.3	(11.0)		
B3	13.36	-7.8	-7.3	4.2	10.3	7.4	15.2
	13.36	-7.8	-7.3	22.2	78.8		
	13.36	-7.8	-7.3	33.3	127.8		
C	1.03	-7.7	-7.3	-1.7	-	-	5.9
	1.02	47.0	45.0	49.5	-		
	0.97	159.1	152.2	154.0	-		
D	0.90	-7.7	-7.3	2.3	12.6	4.5	12.1
	0.90	46.3	37.8	39.7	12.3		
	0.90	156.7	130.1	116.8	13.0		
	0.86	-7.7	-7.3	1.9	12.5	4.2	11.8
	0.86	-7.7	-7.3	14.9	78.4		
	0.86	-7.7	-7.3	25.2	129.0		

* Bold numbers were used for calculations of isotope effects.

() Numbers in brackets are estimates by using isotope values of other experiments with same O_2 .

$\delta\text{SO}_4^{2-}(\text{air})$ is the oxygen composition of sulfate adjusted to the oxygen isotope composition of air ($\delta^{18}\text{O}(\text{air}) = 23.5\text{‰}$; Kroopnick and Craig, 1972) and $\Delta^{18}\text{O}_{\text{SO}_4\text{-H}_2\text{O}}$ is relative to the oxygen isotope composition of the experiment solutions.

Sulfite oxidation experiments with O₂ as sole oxidizing agent (A, B1, B2 and B3; Table 3.3):

Experiment A:

This experiment was performed in two experiment containers with isotopically identical experimental solutions at pH 4.9 but isotopically distinct O₂ in a limited headspace. Due to the low amount of O₂ in the headspace, the δO_2 changed (Table 3.4). Therefore, a graphical evaluation of the relative contribution of oxygen from O₂ in the oxidation of sulfite to sulfate could be made only by using the isotope composition of O₂ at the beginning of the experiment. We found a contribution of $24\pm 0\%$ of O₂ oxygen in the produced sulfate (Fig. 3.4, Table 3.3), indicating that all oxygen in the oxidation of sulfite to sulfate comes from O₂.

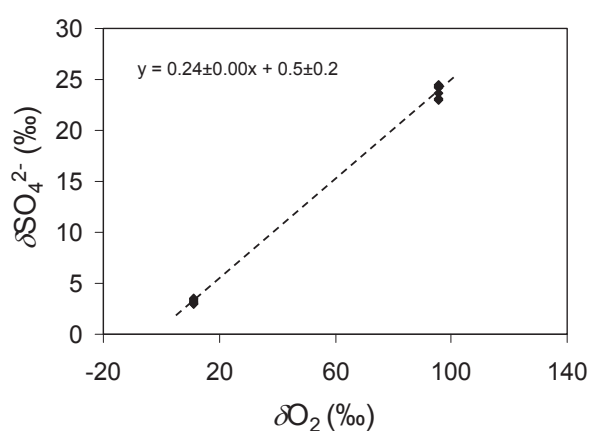


Fig. 3.4: Determination of the relative oxygen source contribution from O₂ in experiment A with O₂ as sole oxidizing agent at pH 4.9 with isotopically distinct O₂ in the headspace.

Table 3.4

Data of experiment A for Rayleigh approach at pH 4.90 and 22°C							
Experiment description	Time (min)	δO_2 (‰)	O ₂ concentr. (% of air)	Experiment description	Time (min)	δO_2 (‰)	O ₂ concentr. (% of air)
Experiment A without ¹⁸ O O ₂ spike	11	11.0	410.8	Experiment A with ¹⁸ O O ₂ spike	5	95.7	661.9
	947	4.8	115.3		926	77.7	224.1
	1344	5.7	82.8		1308	77.7	175.1
	2203	-0.6	44.9		2167	64.6	100.2
	2863	-6.8	28.8		2827	44.6	71.9
	3655	-7.3	17.4		3620	39.0	51.0
	5736	-25.8	10.0		5822	40.0	45.5

Experiment B1:

For experiment B1, which was carried out at pH 1.13, pH 0.91 and pH 0.92, the graphically determined contributions of oxygen from water amounted to $87\pm 3\%$ for the comparison between δSO_4^{2-} and $\delta\text{H}_2\text{O}_{\text{stock}}$ and to $78\pm 2\%$ for the comparison between δSO_4^{2-} and $\delta\text{H}_2\text{O}_{\text{exp}}$ (Fig. 3.5a). The oxygen contribution of oxygen from O_2 was found to be $27\pm 0\%$ (Fig. 3.5b). Whereas the sum of oxygen contribution from O_2 and experimental water yields $105\pm 3\%$, the sum of oxygen contribution from O_2 and stock solution yields $114\pm 2\%$, indicating that sulfite fully equilibrated its oxygen isotopes with experimental water prior to oxidation (i.e. 105% being more close to the expected 100%). We attribute the slight mismatch between the contributions from O_2 and experimental water to analytical difficulties encountered during the isotope analysis of O_2 , which manifested themselves by a high variability in replicate oxygen isotope measurements due to entrainment of air which contaminated the measurements. Measurements affected by considerable air contamination could be detected by mass spectrometry as a large peak of N_2 preceding the CO peak and were omitted in our study.

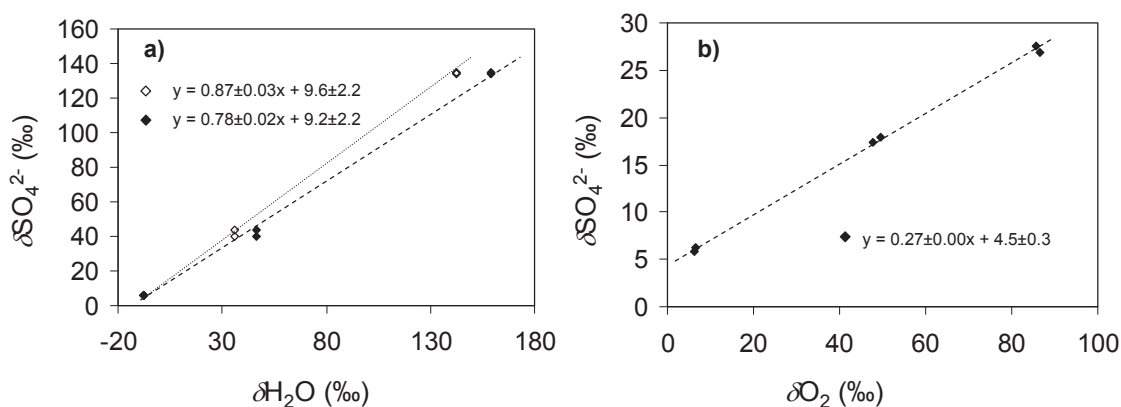


Fig. 3.5: Determination of the relative oxygen source contribution in experiment B1 with O_2 as sole oxidizing agent at pH 1. The δSO_4^{2-} is plotted against the isotopically distinct stock solutions (empty squares) as well as against the experimental solutions (filled squares) in a) and against the δO_2 from the experiment set with isotopically distinct O_2 in the headspace in b).

Experiment B2:

In the experiments at pH 4.88 we obtain a value for the slope of $76\pm 1\%$ oxygen contribution relative to the stock solutions and $73\pm 1\%$ oxygen contribution relative to the experimental solutions (Fig. 3.6), whereas the contribution of oxygen from O_2 was found to be 24% in experiment A, which was carried out at the same pH. The 100% oxygen mass balance between oxygen derived from stock solution and O_2 thus indicates that opposite to the lower pH conditions in experiment B1, oxygen isotope exchange between water and sulfite is slow compared to the sulfite oxidation rate at this pH, i.e. that disequilibrium conditions prevail, where sulfite species retain their oxygen isotope composition to some degree.

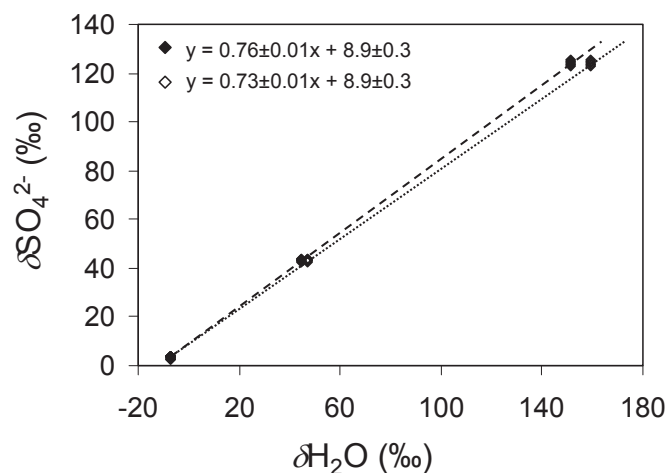


Fig. 3.6: Determination of the relative oxygen source contribution in experiment B2 with O_2 as sole oxidizing agent at pH 4.9. The δSO_4^{2-} is plotted against δH_2O_{exp} or δH_2O_{stock} , respectively, to determine the total water oxygen contribution in the produced sulfate from the slope: (◆) data plotted against the oxygen isotope composition of the sulfite stock solutions and (◇) data plotted against the oxygen isotope composition of the experimental solutions.

Experiment B3:

The experiment at pH 13.36 was only performed with isotopically distinct O_2 in the headspace and in identical solutions, because it is known that oxygen exchange between sulfite and water is extremely slow in this high pH range (Betts and Voss, 1970, Horner and Connick, 1986; Horner and Connick 2003). We found that oxygen from O_2 contributes $25 \pm 0\%$ to the sulfate produced from sulfite (Fig. 3.7).

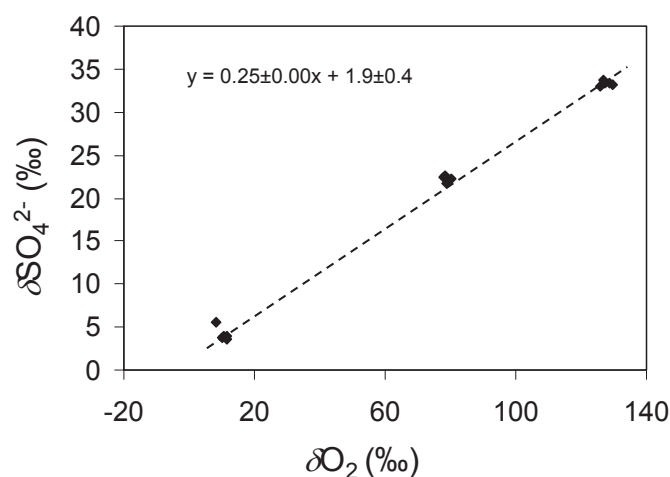


Fig. 3.7: Determination of the relative oxygen source contribution in experiment B3 with O_2 as sole oxidizing agent at pH 13.3.

Experiment C:

The anoxic experiments with Fe^{3+} as the oxidant in isotopically distinct water at pH 1 show $98\pm 1\%$ water oxygen contribution in the produced sulfate from stock solutions, and only $93\pm 1\%$ from the experimental solutions (Fig. 3.8), indicating that sulfite oxidation is more rapid than isotope exchange between sulfite and water, creating disequilibrium conditions. Even though the pH is as low as in experiment B1, the oxidation rate is much faster due to the presence of iron species (Table 3.2; Zhang and Millero, 1991). The small discrepancy to the expected 100% water oxygen incorporation could either be due to uncertainties in the measurements or caused by a small contamination with air during the course of the experiment.

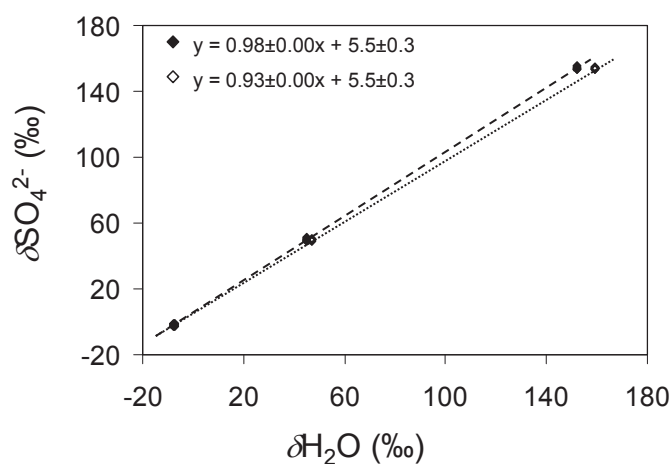


Fig. 3.8: Oxygen isotope results of experiment C with Fe^{3+} at pH 1. The $\delta^{18}\text{O}_{\text{SO}_4}$ is plotted against the $\delta^{18}\text{O}_{\text{H}_2\text{O}}$ of isotopically distinct solutions: (◆) data plotted against the oxygen isotope composition of the sulfite stock solutions and (◇) data plotted against the oxygen isotope composition of the experimental solutions.

Experiment D:

The experiments with O_2 and dissolved Fe^{2+} were performed at pH below 1, one set of experiments with isotopically distinct water and one set of experiments with isotopically distinct O_2 in the headspace (Table 3.3). The slope of the δSO_4^{2-} vs. δO_2 plot corresponds to a $20\pm 1\%$ oxygen contribution in the produced sulfate from O_2 (Fig. 3.9b). Therefore, approximately 80% of the oxygen should be derived from water. This result is consistent with the observed oxygen contribution from the stock solution ($83\pm 0\%$) whereas the contribution of oxygen from experimental water ($70\pm 0\%$) would strongly underestimate the oxygen contribution from water (Fig. 3.9a). Obviously, fast oxidation rates in the presence of dissolved iron species (even though initially present in the reduced, ferrous form) out-compete oxygen isotope exchange between sulfite and water, creating disequilibrium conditions. The small discrepancy between oxygen contribution from O_2 and from stock solution ($103\pm 1\%$), could be due to the fact that experiments with distinct δO_2 were performed at slightly more acidic conditions (Table 3.3). Such conditions cause slower oxidation of Fe^{2+} and may therefore, lead to a slightly higher direct O_2 oxygen contribution in produced sulfate.

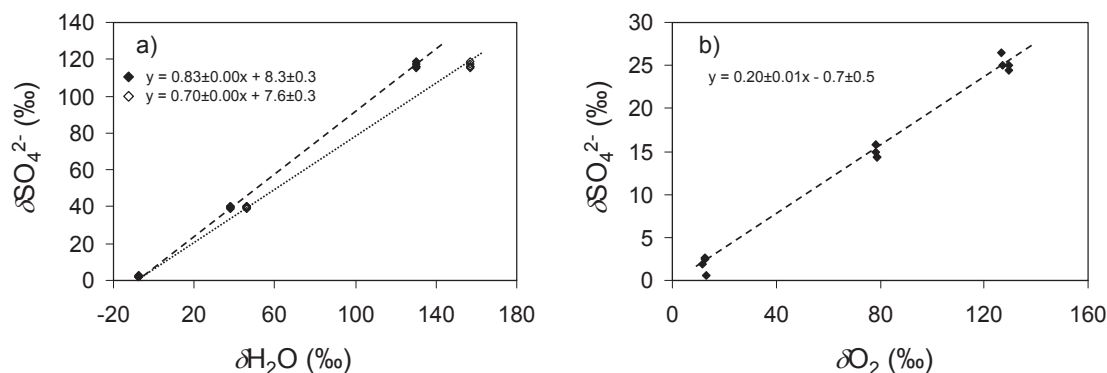


Fig. 3.9: Oxygen isotope results of sulfite oxidation experiments with Fe^{2+} and O_2 at pH 0.9. The δSO_4^{2-} is plotted against the $\delta\text{H}_2\text{O}$ of isotopically distinct solutions in a) and against the δO_2 values from experiments with isotopically distinct O_2 in the headspace in b). The plot with the $\delta\text{H}_2\text{O}$ shows two slopes: (\blacklozenge) data plotted against the oxygen isotope composition of the sulfite stock solutions and (\diamond) data plotted against the oxygen isotope composition of the experimental solutions.

In summary, the results from experiments A, B1, B2 and B3 where only O_2 was used as oxidizing agent strongly indicate that under such conditions the oxygen for the oxidation of sulfite to sulfate is derived to 100% from O_2 , i.e. that there is no oxygen isotope transfer from the O_2 pool to water. If Fe^{3+} is the only available oxidant, 100% of final oxygen in the produced sulfate is derived from water (experiment C), whereas in a experiment containing Fe^{2+} in solution and O_2 in the headspace the contribution of oxygen to sulfate was a mixture of 20% O_2 and 80% water. We deduce from our results that at slightly acid to neutral pH, and in the presence of iron species, sulfite oxidation rates will out-compete oxygen isotope exchange between sulfite and water (Exp. A, B2, B3, C, D). Under these conditions any preexisting non-equilibrium sulfite isotope signature will be partly conserved in the isotope composition of produced sulfate.

Kinetic isotope effects during sulfite oxidation:

Experiment A and B: Oxygen isotope fractionation during sulfite oxidation by O_2

The kinetic fractionation of O_2 consumption $\varepsilon_{\text{O}_2\text{consumption}(\text{noFe})}$ during the oxidation process from experiment A can be determined by a closed-system Rayleigh approach (Eq. 3.32; Fig. 3.10, Table 3.4). We found a value for $\varepsilon_{\text{O}_2\text{consumption}(\text{noFe})}$ of $7.1 \pm 0.9\text{‰}$ in experiments without $^{18}\text{O}_2$ spike ($\delta\text{O}_{2(t0)} = 11.0\text{‰}$), which is somewhat surprising because it implies that in our experiments, O_2 enriched in ^{18}O was preferentially consumed (an apparent inverse isotope effect). This finding is corroborated by an inverse $\varepsilon_{\text{O}_2\text{consumption}(\text{noFe})}$ of $18.9 \pm 1.1\text{‰}$ for the experiment where we used a $^{18}\text{O}_2$ spike ($\delta\text{O}_{2(t0)} = 95.7\text{‰}$). A larger $\varepsilon_{\text{O}_2\text{consumption}(\text{noFe})}$ for the isotopically labeled O_2 is expected, as isotope discrimination is more strongly expressed for spiked O_2 (^{18}O - ^{18}O bond) compared to non-spiked O_2 (^{16}O - ^{18}O bond). Our results, however do not agree with the result from Oba and Poulson (2009a) who determined an oxygen isotope fractionation of -3‰ for O_2 consumption during sulfite oxidation. Oba and Poulson (2009a) used a lower concentration of sulfite (0.02 M) in their experiment, which was carried out at neutral pH. Probably, the different isotope fractionations result from a different ratio of fluxes involved in the consumption

of O_2 from the headspace (e.g. Eq. 3.29), such as the diffusion of O_2 into and out of the experimental solution, and the actual consumption of aqueous O_2 during sulfite oxidation. For example, it is known that gaseous O_2 enriched in ^{18}O preferentially diffuses into water (Benson and Krause, 1980), whereas the actual consumption of O_2 may be associated with a normal kinetic isotope effect. If O_2 consumption in our experiments was more rapid than in the study of Oba and Poulson (2009a) then it is possible that the normal isotope effect related to O_2 consumption was suppressed (quantitative consumption), leading to the expression of an inverse isotope effect, related to preferential uptake of ^{18}O enriched O_2 from the headspace into water. The significantly lower sulfite oxidation rate for experiment A compared to experiment B2 (Table 3.2) supports the hypothesis that availability of aqueous O_2 may have been much more restricted than in the experiments with a larger O_2 headspace. This finding highlights the fact that the availability of O_2 both in experimental and natural sulfite oxidation not only affects the relative contributions of oxygen from H_2O and O_2 to produced sulfate, but may also have a massive impact on the oxygen isotope signature of the oxygen incorporated from O_2 into sulfate.

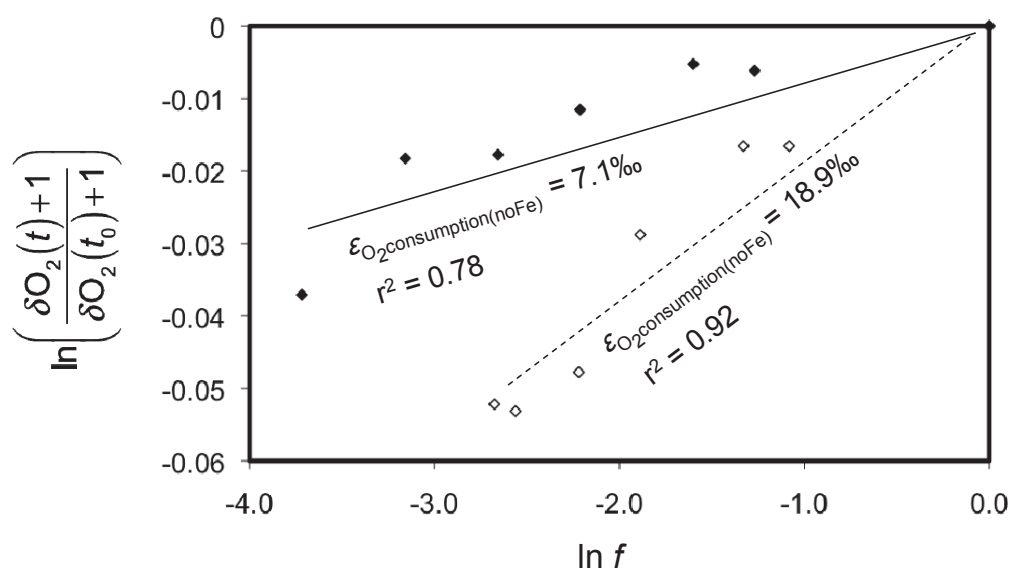


Fig. 3.10: Rayleigh plot of the logarithm of the oxygen isotope composition of O_2 at time t divided by the oxygen isotope composition of O_2 at t_0 against the logarithm of the O_2 concentration at t relative to the starting concentration at t_0 . The slope is equal to $\epsilon_{O_2\text{consumption(noFe)}}$. (◆) are results from the experiment where we started with $\delta O_2(t_0) = 11.0\text{‰}$ and (◇) are results from the experiment with ^{18}O spike in the headspace where we started with $\delta O_2(t_0) = 95.7\text{‰}$.

Since the contribution of O_2 oxygen in the oxidation of sulfite to sulfate was found to be 100%, we can use a simplified oxygen isotope mass balance (Eq. 3.28) to determine the kinetic isotope effects for the oxidation of sulfite with O_2 as sole oxidizing agent. The values of the oxygen isotope equilibrium fractionation between sulfite and water ($\epsilon_{SO_3^{2-} \leftrightarrow H_2O}^{EQ} = 15.2\text{‰}$; Müller et al., *subm.*) and for $\epsilon_{O_2\text{consumption(noFe)}}$ are known, leaving

the oxygen isotope effect for sulfite consumption ($\varepsilon_{\text{SO}_3^{2-}\text{-O}_2(\text{aq})\rightarrow\text{SO}_4^{2-}}$) the only undetermined isotope enrichment factor:

$$\varepsilon_{\text{SO}_3^{2-}\text{-O}_2(\text{aq})\rightarrow\text{SO}_4^{2-}} = \frac{1}{3} \cdot \left(4 \cdot \delta\text{SO}_4^{2-}(\text{noFe}) - 3 \cdot \delta\text{H}_2\text{O} - \delta\text{O}_2 - 3 \cdot \varepsilon_{\text{SO}_3^{2-}\leftrightarrow\text{H}_2\text{O}}^{\text{EQ}} - \varepsilon_{\text{O}_2\text{consumption}(\text{noFe})} \right) \quad \text{Eq. 3.34}$$

Although the sulfite oxidation rate in experiment A was considerably smaller (64 times, Table 3.2) than for experiment B2 that was carried out at a similar pH and where we observe that the sulfite oxidation rate out-competes isotope exchange between sulfite and water, we cannot exclude the possibility that isotope disequilibrium conditions also prevail in experiment A. Therefore, we use the isotope composition of the sulfite stock solution for $\delta\text{H}_2\text{O}$ (because of incomplete isotope exchange; $-7.3 \pm 0.1\text{‰}$ instead of $-7.8 \pm 0.1\text{‰}$, Table 3.3) in Eq. 3.34. Furthermore, in cases where isotope exchange between sulfite and water does not fully out-compete sulfite oxidation, isotope fractionation in residual sulfite (for $\varepsilon_{\text{SO}_3^{2-}\text{-O}_2(\text{aq})\rightarrow\text{SO}_4^{2-}}$) is expected to be expressed, with the consequence that the isotope composition of sulfite cannot *a priori* be considered constant over the course of the experiments. This scenario holds true for experiments B2 and B3 (disequilibrium conditions observed), and is likely for experiment A. However, the isotope composition of sulfate used for our calculations, which would in such a case describe a Rayleigh trend typical for an accumulating product, shows little change in an early stage of the experiment. Consequently, as the time series of the measured sulfate isotope compositions of A, B2 and B3 did not show any trend we can neglect this potential effect. Therefore, we can use the $\delta\text{SO}_4^{2-}(\text{noFe})$ ($3.2 \pm 0.2\text{‰}$) of each time point of the experiment and the δO_2 from the initial stage of the experiments carried out with unlabeled compounds in Eq. 3.33 (Table 3.3). This ensures that there is little impact of the closed system approach (Rayleigh trend for δO_2) and that larger errors typically associated with isotope labels (e.g. a much bigger effect of contaminations) are avoided. The kinetic oxygen isotope fractionation factors obtained for the consumption of sulfite molecules during oxidation to sulfate by O_2 ($\varepsilon_{\text{SO}_3^{2-}\text{-O}_2(\text{aq})\rightarrow\text{SO}_4^{2-}} = -9.7 \pm 0.3\text{‰}$) shows that sulfite molecules depleted in ^{18}O are preferentially oxidized.

Unlike $\varepsilon_{\text{O}_2\text{consumption}(\text{noFe})}$, which results from an entire suite of fractionation factors and flux ratios, $\varepsilon_{\text{SO}_3^{2-}\text{-O}_2(\text{aq})\rightarrow\text{SO}_4^{2-}}$ can be considered as result of a single reaction. Therefore, its value can be considered to be more robust, i.e. less dependent on the kinetics of other ongoing reactions. For this reason, we assume in the following that $\varepsilon_{\text{SO}_3^{2-}\text{-O}_2(\text{aq})\rightarrow\text{SO}_4^{2-}}$ can be treated as kinetic isotope fractionation that remains constant for all investigated sulfite oxidation experiments. Consequently, we can use the value obtained for $\varepsilon_{\text{SO}_3^{2-}\text{-O}_2(\text{aq})\rightarrow\text{SO}_4^{2-}}$ to determine the value of $\varepsilon_{\text{O}_2\text{consumption}(\text{noFe})}$ in experiments B1, B2 and B3. Equation 3.28 becomes:

$$\varepsilon_{\text{O}_2\text{consumption}(\text{noFe})} = 4 \cdot \delta\text{SO}_4^{2-}(\text{noFe}) - 3 \cdot \delta\text{H}_2\text{O} - \delta\text{O}_2 - 3 \cdot \varepsilon_{\text{SO}_3^{2-}\leftrightarrow\text{H}_2\text{O}}^{\text{EQ}} - 3 \cdot \varepsilon_{\text{SO}_3^{2-}\text{-O}_2\rightarrow\text{SO}_4^{2-}} \quad \text{Eq. 3.35}$$

For experiment B2, which was carried at a pH similar to that of experiment A, the oxidation rate is very rapid, i.e. we can use the value of $\delta\text{H}_2\text{O}_{\text{stock}}$ (Table 3.3). Experiment B3 was performed at higher pH where the oxidation rate is slower but still out-competes oxygen exchange between sulfite and water so that we can use as well the value of $\delta\text{H}_2\text{O}_{\text{stock}}$. However, this is not the case for experiment B1, where isotope exchange between sulfite and water out-competes sulfite oxidation. Thus, we use the value of

$\delta\text{H}_2\text{O}_{\text{exp}}$ for experiment B1. As for experiment A, we only consider data from experiments that were carried out close to the natural abundance isotope composition of water and O_2 (Table 3.3; values in bold). The values obtained for $\epsilon_{\text{O}_2\text{consumption}(\text{noFe})}$ are $23.3\pm 2.9\text{‰}$, $7.2\pm 2.1\text{‰}$, and $11.7\pm 4.3\text{‰}$ (if we exclude an outlying data point in experiment B3, the result would be $9.8\pm 0.8\text{‰}$) for experiment B1, B2, and B3, respectively. Of these inverse isotope effects only the value of experiment B2 is consistent with the isotope effect from experiment A ($\epsilon_{\text{O}_2\text{consumption}(\text{noFe})}$ of $7.1\pm 0.9\text{‰}$) which was performed at identical pH. In case of experiment B3 the inverse isotope effect is slightly larger and in case of experiment B1 the value is much larger. The range of values obtained for $\epsilon_{\text{O}_2\text{consumption}(\text{noFe})}$ could be attributed to differences in the O_2 exchange fluxes between headspace and aqueous phase relative to the rate of consumption of aqueous O_2 . However, the good match between experiment A and B2 – despite the significantly larger oxidation rate (Table 3.2) – indicates that additional factors may play a role. In the case of B1 it can be hypothesized that $\epsilon_{\text{SO}_3^{2-}\text{-O}_2(\text{aq})\rightarrow\text{SO}_4^{2-}}$ is suppressed (i.e. much smaller than -9.7‰) because the oxidation of SO_2 and HSO_3^- may proceed over a very small pool of SO_3^{2-} as the reaction of SO_2 to HSO_3^- via Eq. 3.1 is much slower than the subsequent sulfite oxidation.

It is tempting to use the inverse fractionations obtained for $\epsilon_{\text{O}_2\text{consumption}(\text{noFe})}$ in experiments B1, B2 and B3 as an argument for an inverse isotope effect during O_2 consumption, however such a reasoning would be circular, because these values were calculated using $\epsilon_{\text{SO}_3^{2-}\text{-O}_2(\text{aq})\rightarrow\text{SO}_4^{2-}}$ from experiment A, which was determined by using the inverse value for $\epsilon_{\text{O}_2\text{consumption}(\text{noFe})}$ in the respective experiment. If, alternatively, we use the value of -3‰ for $\epsilon_{\text{O}_2\text{consumption}(\text{noFe})}$ determined by Oba and Poulson (2009a) to determine $\epsilon_{\text{SO}_3^{2-}\text{-O}_2(\text{aq})\rightarrow\text{SO}_4^{2-}}$ in experiments A, B1, B2 and B3 we obtain values for $\epsilon_{\text{SO}_3^{2-}\text{-O}_2(\text{aq})\rightarrow\text{SO}_4^{2-}}$ of $-6.3\pm 0.3\text{‰}$, $-1.2\pm 1.0\text{‰}$, $-6.3\pm 0.7\text{‰}$ and $-5.4\pm 0.3\text{‰}$, respectively (Eq. 3.34). These values are very similar to each other with the exception of experiment B1 with only -1.2‰ . As hypothesized above, this smaller fractionation factor might be due to the high abundance of SO_2 and low abundance of SO_3^{2-} at pH 1.13, leading to the suppression of $\epsilon_{\text{SO}_3^{2-}\text{-O}_2(\text{aq})\rightarrow\text{SO}_4^{2-}}$.

The above considerations show that there is a large uncertainty with respect to the value of $\epsilon_{\text{O}_2\text{consumption}(\text{noFe})}$, and that there is the potential that this value varies greatly because it is influenced by many parameters. The value for $\epsilon_{\text{SO}_3^{2-}\text{-O}_2(\text{aq})\rightarrow\text{SO}_4^{2-}}$ appears to be more robust, being in the range of -5.4‰ to -9.7‰ . If the pH is very low, there is the potential that $\epsilon_{\text{SO}_3^{2-}\text{-O}_2(\text{aq})\rightarrow\text{SO}_4^{2-}}$ becomes suppressed due to quantitative conversion of newly formed SO_3^{2-} .

Experiment C: Oxygen isotope fractionation during oxidation of sulfite to sulfate by Fe^{3+}

From the isotope mass balance of experiment C we know that approximately 100% of the oxygen in the produced sulfate is derived from the water and that sulfite oxidation out-competes oxygen isotope exchange between sulfite and water. We can apply the simplified oxygen isotope mass balance from Eq. 3.26 to determine the total oxygen isotope fractionation effects for sulfite oxidation in absence of O_2 :

$$\frac{3}{4} \cdot \varepsilon_{\text{SO}_3^{2-} \setminus \text{Fe}^{3+} \setminus \text{H}_2\text{O} \rightarrow \text{SO}_4^{2-}} + \frac{1}{4} \cdot \varepsilon_{\text{H}_2\text{O} \setminus \text{Fe}^{3+} \setminus \text{SO}_3^{2-} \rightarrow \text{SO}_4^{2-}} = \delta \text{SO}_4^{2-} (\text{noO}_2) - \delta \text{H}_2\text{O}_{\text{stock}} - \frac{3}{4} \cdot \varepsilon_{\text{SO}_3^{2-} \leftrightarrow \text{H}_2\text{O}}^{\text{EQ}} \quad \text{Eq. 3.36}$$

Although the non-equilibrium conditions could result in a non-steady isotope composition of sulfite, we did not observe a distinct trend in the isotope composition of the accumulating sulfate product. As for experiments B2 and B3, we can therefore assume that this effect can be neglected. Using the values from the isotopically unlabeled experiment ($\delta \text{H}_2\text{O}_{\text{stock}} = -7.3 \pm 0.1\%$ and $\delta \text{SO}_4^{2-} (\text{noO}_2) = -1.7 \pm 0.7\%$) we find a kinetic isotope effect of $-5.8 \pm 0.7\%$. This kinetic isotope effect is a combination of $\frac{3}{4}$ the kinetic fractionation of sulfite molecules ($\varepsilon_{\text{SO}_3^{2-} \setminus \text{Fe}^{3+} \setminus \text{H}_2\text{O} \rightarrow \text{SO}_4^{2-}}$) and $\frac{1}{4}$ the kinetic fractionation of oxygen which is incorporated from water ($\varepsilon_{\text{H}_2\text{O} \setminus \text{Fe}^{3+} \setminus \text{SO}_3^{2-} \rightarrow \text{SO}_4^{2-}}$) and cannot be further separated with our approach. The fact that we did not observe a trend in the isotope composition of sulfate (accumulated product), implies that $\varepsilon_{\text{SO}_3^{2-} \setminus \text{Fe}^{3+} \setminus \text{H}_2\text{O} \rightarrow \text{SO}_4^{2-}}$ cannot be very large, and as consequence, also $\varepsilon_{\text{H}_2\text{O} \setminus \text{Fe}^{3+} \setminus \text{SO}_3^{2-} \rightarrow \text{SO}_4^{2-}}$ cannot be very large.

Experiment D: Comparison of the isotope offset between O_2 and the oxygen isotope composition in sulfate derived from $\text{O}_2(\text{aq})$ to the isotope effects for the O_2 consumption of experiments performed in absence of iron ($\varepsilon_{\text{O}_2 \text{consumption}(\text{noFe})}$)

In the experiment with O_2 and Fe^{2+} in solution, the oxidation proceeds via both oxidation pathways (Eq. 3.4-3.5) and O_2 is not only consumed for the oxidation of sulfite, but also for the oxidation of Fe^{2+} to Fe^{3+} . It is not possible to disentangle all the fractionation factors involved because there are three unknowns ($\delta \text{O}_2(\text{aq})$, $\varepsilon_{\text{O}_2(\text{aq}) \setminus \text{SO}_3^{2-} \rightarrow \text{SO}_4^{2-}}$, $\varepsilon_{\text{O}_2(\text{aq}) \setminus \text{Fe}^{2+} \rightarrow \text{Fe}^{3+}}$) for essentially one isotope mass balance (Eq. 3.23). Consequently, we cannot determine $\varepsilon_{\text{O}_2 \text{consumption}}$. However, we can calculate the isotope offset between O_2 in the headspace of the experiment and the oxygen isotope composition in sulfate that was derived from O_2 , which should, at least to some extent, be comparable to $\varepsilon_{\text{O}_2 \text{consumption}(\text{noFe})}$. Equation 3.23 is re-arranged to:

$$\begin{aligned} \delta \text{O}_2(\text{aq}) + \varepsilon_{\text{O}_2(\text{aq}) \setminus \text{SO}_3^{2-} \rightarrow \text{SO}_4^{2-}} - \delta \text{O}_2 = \\ \frac{4}{(1-Y)} \cdot \delta \text{SO}_4^{2-} - \delta \text{O}_2 - \frac{(3+Y)}{(1-Y)} \cdot \delta \text{H}_2\text{O}_{\text{stock}} - \frac{3}{(1-Y)} \cdot \varepsilon_{\text{SO}_3^{2-} \leftrightarrow \text{H}_2\text{O}}^{\text{EQ}} \\ - 3 \cdot \varepsilon_{\text{SO}_3^{2-} \setminus \text{O}_2(\text{aq}) \rightarrow \text{SO}_4^{2-}} - \frac{4Y}{(1-Y)} \cdot \left(\frac{3}{4} \cdot \varepsilon_{\text{SO}_3^{2-} \setminus \text{Fe}^{3+} \setminus \text{H}_2\text{O} \rightarrow \text{SO}_4^{2-}} + \frac{1}{4} \cdot \varepsilon_{\text{H}_2\text{O} \setminus \text{Fe}^{3+} \setminus \text{SO}_3^{2-} \rightarrow \text{SO}_4^{2-}} \right) \end{aligned} \quad \text{Eq. 3.37}$$

This offset can be determined by using the relative oxygen source contribution in SO_4^{2-} from experiment D (Y), as well as the kinetic fractionation for sulfite molecules during oxidation of sulfite by O_2 ($\varepsilon_{\text{SO}_3^{2-} \setminus \text{O}_2(\text{aq}) \rightarrow \text{SO}_4^{2-}}$) and the kinetic isotope effects of anoxic sulfite oxidation ($\frac{3}{4} \varepsilon_{\text{SO}_3^{2-} \setminus \text{Fe}^{3+} \setminus \text{H}_2\text{O} \rightarrow \text{SO}_4^{2-}}$ and $\frac{1}{4} \varepsilon_{\text{H}_2\text{O} \setminus \text{Fe}^{3+} \setminus \text{SO}_3^{2-} \rightarrow \text{SO}_4^{2-}}$) determined in experiments A and C, respectively. We used the following estimates: $Y = 0.2$, $\varepsilon_{\text{SO}_3^{2-} \setminus \text{O}_2(\text{aq}) \rightarrow \text{SO}_4^{2-}} = -9.7\%$, $\varepsilon_{\text{SO}_3^{2-} \leftrightarrow \text{H}_2\text{O}}^{\text{EQ}} = 15.2\%$, and $\frac{3}{4} \varepsilon_{\text{SO}_3^{2-} \setminus \text{Fe}^{3+} \setminus \text{H}_2\text{O} \rightarrow \text{SO}_4^{2-}} + \frac{1}{4} \varepsilon_{\text{H}_2\text{O} \setminus \text{Fe}^{3+} \setminus \text{SO}_3^{2-} \rightarrow \text{SO}_4^{2-}} = -5.8\%$. Experiment D proceeded under disequilibrium conditions, thus we use the isotope composition of $\delta \text{H}_2\text{O}_{\text{stock}}$ for this calculation. Similar to experiments B2, B3 and C, the isotope composition of sulfate (accumulating product) did

not change during the course of the experiment, implying that we can use the above equation despite the disequilibrium conditions. As for the calculation of the kinetic isotope effects in the other experiments, we only consider data that are close to natural abundance isotope compositions (Table 3.3). The offset between the isotope composition of $O_2(aq)$ that was consumed during the sulfate production and the actual isotope composition of O_2 in the headspace is $6.2 \pm 1.2\%$, which is comparable to the inverse isotope fractionation for $\epsilon_{O_2 \text{consumption}(noFe)}$ ($7.1 \pm 0.9\%$) determined in experiment A. The slightly smaller offset could be due to the isotope effects related to O_2 consumption for the oxidation of Fe^{2+} . Oba and Poulson (2009b) observed normal isotope fractionation (-4.5% to -11.6%) for the consumption of O_2 during Fe^{2+} oxidation. Such an additional normal isotope effect for the O_2 consumption during Fe^{2+} oxidation could result in the smaller inverse fractionation factor for O_2 consumption in experiment D.

3.4.3. Comparison to results from studies on biological oxidation of sulfur compounds

It is generally assumed that sulfite is often the last intermediate sulfur pool in the oxidation of reduced sulfur compounds to sulfate. However, evidence from an isotope geochemical perspective for this assumption is scarce, and the question whether the oxygen isotope effects during sulfite oxidation are responsible or at least compatible with the oxygen isotope effects during oxidation of reduced sulfur compounds has yet not been answered. Here, we address this question by comparing the results obtained from our un-spiked experiments to studies on the isotope signature of the oxidation of reduced sulfur compounds.

We observed that experiments A, B2, B3, C and D operated at disequilibrium conditions, where the rate of sulfite oxidation was sufficiently high to compete with oxygen isotope exchange between sulfite and water. Under such conditions, the oxygen isotope signature of sulfite is – at least to some degree – preserved in the oxygen isotope signature of produced sulfate. Consequently, in a stepwise oxidation of reduced sulfur compounds to sulfate with sulfite as intermediate, there is a high potential that the oxygen isotope imprints in the formation of sulfite are retained in the final product sulfate. This finding agrees with the observations of Kohl and Bao (2011), who determined the contribution of O_2 into the produced sulfate with triple oxygen isotope labeling experiments in a study on abiotic pyrite oxidation. Kohl and Bao (2011) found that the oxygen isotope contribution of O_2 to sulfate can be higher than 25% and concluded that sulfoxy intermediates that are subsequently oxidized to sulfite can already contain oxygen from O_2 (i.e. from preceding oxidation steps), a signature that can be preserved under conditions where sulfite oxidation is rapid compared to oxygen isotope exchange between sulfite and water.

A comparison of the oxygen isotope offsets between produced sulfate and water ($\Delta^{18}O_{SO_4-H_2O}$; Table 3.3) for sulfite oxidation and the $\Delta^{18}O_{SO_4-H_2O}$ for the oxidation of other, more reduced sulfur compounds (e.g. elemental sulfur, pyrite, sulfide, sphalerite) from the literature corroborates the likeliness that sulfite is a key intermediate in sulfur oxidation pathways. A quantitative comparison can be done for experiments carried out in the absence of O_2 (no influence of the δO_2 on the final result). We observe a $\Delta^{18}O_{SO_4-H_2O}$ of $5.9 \pm 0.7\%$ (experiment C, Table 3.3) which is in the range of observed

inverse kinetic oxygen isotope fractionation factors ($\epsilon^{18}\text{O}_{\text{SO}_4\text{-H}_2\text{O}}$ of 2.3‰ to 8.2‰) in oxidation studies (abiotically and biologically mediated) with reduced sulfur compounds in absence of O_2 (e.g. Taylor et al., 1984b; van Everdingen and Krouse, 1985; Balci et al., 2007; Heidel and Tichomirowa, 2011; Balci et al., 2012; Brabec et al., 2012). For a comparison to environmental data, we adjusted the $\Delta^{18}\text{O}_{\text{SO}_4\text{-H}_2\text{O}}$ for experiments where O_2 was present to the δO_2 of air, $\sim 23.5\text{‰}$ (Kroopnick and Craig, 1972) after Eq. 3.33 (Table 3.3). With $17.6\pm 1.3\text{‰}$ the $\Delta^{18}\text{O}_{\text{SO}_4\text{-H}_2\text{O}}$ was highest in experiment B1 (pH 1, O_2 only oxidant) – likely because sulfite species had enough time to attain isotope equilibrium with the experimental solution and because oxygen from O_2 , which is enriched in ^{18}O compared to the experimental solution was the sole oxidant. Other experiments with O_2 as oxidant at medium to higher pH (Exp A, B2, B3) as well as experiment D (pH 0.9) with Fe^{2+} and O_2 yielded $\Delta^{18}\text{O}_{\text{SO}_4\text{-H}_2\text{O}}$ of $14.0\pm 0.2\text{‰}$, $13.8\pm 0.6\text{‰}$, $15.2\pm 0.9\text{‰}$ (if we exclude an outlying data point in experiment B3, the result would be $14.8\pm 0.2\text{‰}$) and $12.1\pm 0.2\text{‰}$, respectively. Thus, all of the experiments in presence of O_2 showed significantly larger values for $\Delta^{18}\text{O}_{\text{SO}_4\text{-H}_2\text{O}}$ than the O_2 free experiment C (Fe^{3+} as oxidant). The range of $\Delta^{18}\text{O}_{\text{SO}_4\text{-H}_2\text{O}}$ for the abiotic oxidation of sulfite to sulfate (5.9‰ to 17.6‰) covers the narrow range of $\Delta^{18}\text{O}_{\text{SO}_4\text{-H}_2\text{O}}$ of 9 to 11‰ attributed to sulfide weathering in the Mackenzie River system in Canada (Calmels et al., 2007) and is similar to the range of observations ($\Delta^{18}\text{O}_{\text{SO}_4\text{-H}_2\text{O}}$ values from 3.9‰ to 13.6‰) from a study on acid mine drainage at the Río Tinto by Hubbard et al. (2009). In agreement with our observations, Hubbard et al. (2009) attributed large $\Delta^{18}\text{O}_{\text{SO}_4\text{-H}_2\text{O}}$ to situations where sulfite reaches isotopic equilibrium with the surrounding water before it gets oxidized by atmospheric oxygen. Brunner et al. (2008) observed a change from large $\Delta^{18}\text{O}_{\text{SO}_4\text{-H}_2\text{O}}$ ($\sim 11\text{‰}$ to 13‰) during the lag phase of pyrite leaching by *Acidithiobacillus ferrooxidans* (*Af*) to small $\Delta^{18}\text{O}_{\text{SO}_4\text{-H}_2\text{O}}$ ($\sim 0\text{‰}$ to 1‰) during the main stage of pyrite leaching. The change was attributed to a switch in metabolic pathways/growth strategy of *Af*, triggering a switch from relatively slow sulfite consumption in presence of O_2 to a rapid sulfite consumption in presence of Fe^{3+} (Brunner et al., 2008). The large $\Delta^{18}\text{O}_{\text{SO}_4\text{-H}_2\text{O}}$ during the lag phase would thus be caused by oxygen isotope exchange between sulfite and water as well as incorporation of oxygen from air into sulfate during sulfite oxidation (potentially in combination with an isotope effect caused by degassing of SO_2 ; Brunner et al., 2008), whereas the small $\Delta^{18}\text{O}_{\text{SO}_4\text{-H}_2\text{O}}$ is caused by rapid sulfite oxidation with Fe^{3+} . Thus, also the observations by Brunner et al. (2008) are consistent with our experimental results.

3.5. Conclusions

Our study demonstrates that the oxygen isotope fractionation during sulfite oxidation accommodates almost the entire range of observed oxygen isotope signatures of sulfate. The observed range of isotope fractionation results from different pH conditions and the presence/absence of different oxidizing agents (e.g. O_2 , Fe^{3+}). These findings corroborate that sulfite is indeed in many cases the final sulfoxy intermediate during the oxidation of sulfur compounds to sulfate. Moreover, our findings show that isotope fractionation during this final oxidation step has a dominant impact on the oxygen isotope composition of produced sulfate.

Given that isotope fractionation during sulfite oxidation is shaping the oxygen isotope signature of sulfate produced via oxidation of sulfur compounds (Fig. 3.11), we can draw the following conclusions:

- The observation of an apparently inverse isotope fractionation (positive $\Delta^{18}\text{O}_{\text{SO}_4\text{-H}_2\text{O}}$) for oxidation of sulfur compounds to sulfate is not caused by inverse kinetic isotope fractionation. It is due to equilibrium isotope fractionation between sulfite and water ($\epsilon^{\text{EQ}}_{\text{SO}_3^{2-}\leftrightarrow\text{H}_2\text{O}} = 15.2\%$; Müller et al., *subm.*), and can be enhanced by incorporation of oxygen from O_2 .
- Kinetic oxygen isotope effects directly attributable to kinetic processes during sulfite oxidation are normal. The consumption of sulfite by oxidation with O_2 is associated with an isotope effect ($\epsilon_{\text{SO}_3^{2-}\text{-O}_2(\text{aq})\rightarrow\text{SO}_4^{2-}}$) in the range between -5.4% to -9.7% and becomes even smaller under low pH conditions. The oxidation of sulfite by Fe^{3+} is associated with an isotope effect of -5.8% , which is composed of $\frac{3}{4}$ the kinetic fractionation of sulfite molecules ($\epsilon_{\text{SO}_3^{2-}\text{-Fe}^{3+}\text{-H}_2\text{O}\rightarrow\text{SO}_4^{2-}}$) and $\frac{1}{4}$ the kinetic fractionation of oxygen, which is incorporated from water ($\epsilon_{\text{H}_2\text{O}\text{-Fe}^{3+}\text{-SO}_3^{2-}\rightarrow\text{SO}_4^{2-}}$).
- The isotope effect for oxygen consumption ($\epsilon_{\text{O}_2\text{consumption}}$) is likely highly variable and may range from an inverse isotope fractionation to a normal isotope fractionation, depending on the flux balance for aqueous O_2 . This makes oxygen isotope exchange between aqueous and gaseous phase a crucial parameter for the overall observed isotope fractionation, necessitating assessment of these fluxes both in environmental studies as well as experimental work.
- The oxygen isotope effects are very sensitive to pH conditions and the presence or absence of oxidants such as Fe^{3+} or O_2 . These parameters control the competition between the rate of sulfite oxidation and the rate of oxygen isotope exchange with water, and thereby, to what extent preexisting isotope signatures of sulfite (i.e. from preceding oxidation steps) are retained in the oxygen isotopes of produced sulfate. They also control the relative amount of oxygen incorporation into sulfate from O_2 vs. H_2O .

Our findings on the oxygen isotope signature of abiotic sulfite oxidation provide a key to a better mechanistic understanding of the oxidation of reduced sulfur compounds to sulfate.

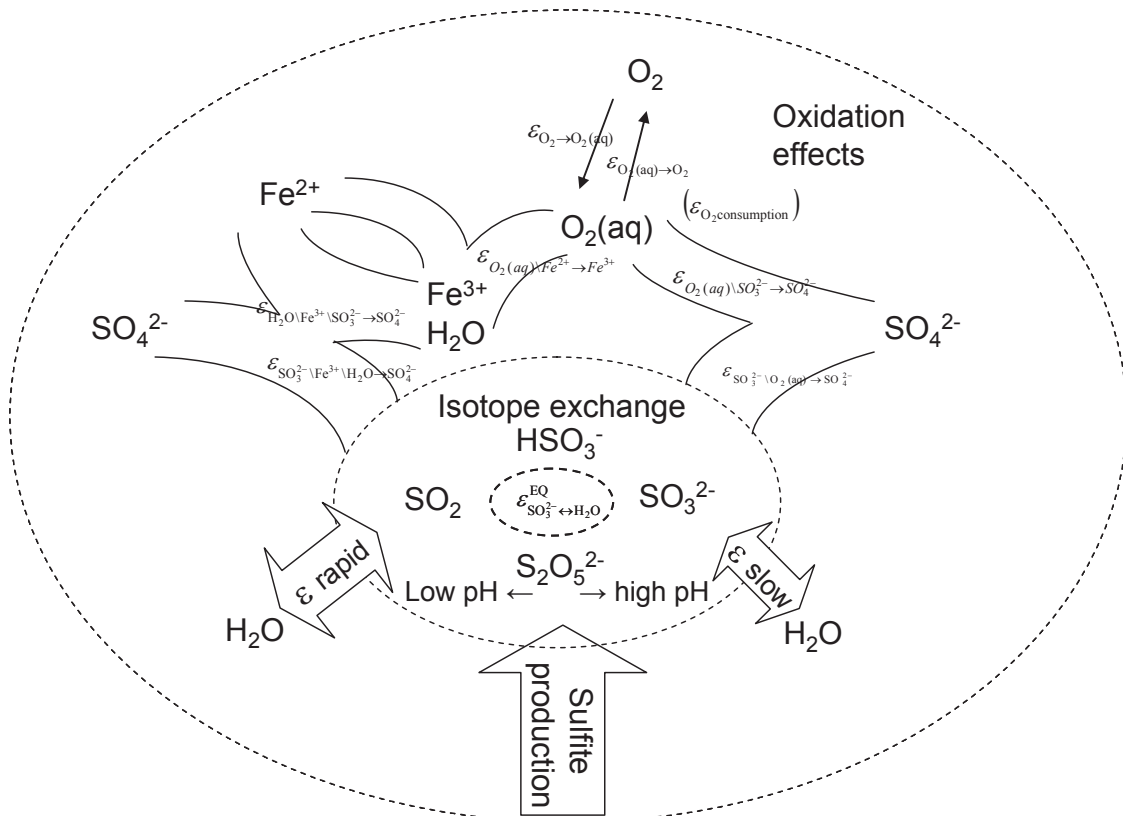


Fig. 3.11: General scheme of the oxygen isotope effects during the oxidation of sulfite to sulfate. Sulfite species exchange their oxygen with the surrounding water depending on the pH more or less rapidly. Sulfite partly or totally equilibrated with the water is oxidized by dissolved O_2 to sulfate (on right side) or by Fe^{3+} with water oxygen to sulfate (on left side). During the oxidation by Fe^{3+} we could determine a normal kinetic fractionation effect comprised of $\frac{3}{4} \epsilon_{\text{SO}_3^{2-} \setminus \text{Fe}^{3+} \setminus \text{H}_2\text{O} \rightarrow \text{SO}_4^{2-}}$ and $\frac{1}{4} \epsilon_{\text{H}_2\text{O} \setminus \text{Fe}^{3+} \setminus \text{SO}_3^{2-} \rightarrow \text{SO}_4^{2-}}$. The same holds partly for the oxidation by O_2 , in our experiment where we calculated a normal fractionation effect for $\epsilon_{\text{SO}_3^{2-} \setminus \text{O}_2(\text{aq}) \rightarrow \text{SO}_4^{2-}}$, but an inverse for $\epsilon_{\text{O}_2 \text{ consumption}}$ in experiments without iron in solution.

3.6. Acknowledgments

We would like to acknowledge T. Max for the help with the mass spectrometer, P. Stief for the introduction in application of oxygen microsensors and A.V. Turchyn and N. Balci for inspiring discussions. The authors thank S.M. Bernasconi for isotope analysis, W. Bach and T.G. Ferdelman for their support and the Max Planck Society as well as the MARUM for funding of this work. The contribution of M.C. was carried out at the NASA Jet Propulsion Laboratory (JPL), California Institute of Technology, under contract with the National Aeronautics and Space Administration (NASA), with support from the NASA Astrobiology Institute (NAI-WARC).

3.7. References

Balci N., Shanks III W. C., Mayer B. and Mandernack K. W. (2007) Oxygen and sulfur isotope systematics of sulfate produced by bacterial and abiotic oxidation of pyrite. *Geochimica et Cosmochimica Acta* **71**, 3796-3811.

- Balci N., Mayer B., Shanks III W. C. and Mandernack K. W. (2012) Oxygen and sulfur isotope systematics of sulfate produced during abiotic and bacterial oxidation of sphalerite and elemental sulfur. *Geochimica et Cosmochimica Acta* **77**, 335-351.
- Benson B. B. and Krause Jr. D. (1980) The concentration and isotopic fractionation of gases dissolved in freshwater in equilibrium with the atmosphere. 1. *Oxygen. Limnol. Oceanogr.* **25**(4), 662-671.
- Betts R. H. and Voss R. H. (1970) The kinetics of oxygen exchange between the sulfite ion and water. *Canadian Journal of Chemistry* **48**, 2035-2041.
- Böttcher M. E., Thamdrup B. and Vennemann T. W. (2001) Oxygen and sulfur isotope fractionation during anaerobic bacterial disproportionation of elemental sulfur. *Geochimica et Cosmochimica Acta* **65**, 1601-1609.
- Böttcher M. E., Thamdrup B., Gehre M. and Theune A. (2005) $^{34}\text{S}/^{32}\text{S}$ and $^{18}\text{O}/^{16}\text{O}$ Fractionation During Sulfur Disproportionation by *Desulfobulbus propionicus*. *Geomicrobiology Journal* **22**, 219-226.
- Brabec M. Y., Lyons T. W. and Mandernack K. W. (2012) Oxygen and sulfur isotope fractionation during sulfide oxidation by anoxygenic phototrophic bacteria. *Geochimica et Cosmochimica Acta* **83**, 234-251.
- Brunner B., Bernasconi S. M., Kleikemper J. and Schroth M. H. (2005) A model for oxygen and sulfur isotope fractionation in sulfate during bacterial sulfate reduction processes. *Geochimica et Cosmochimica Acta* **69**, 4773-4785.
- Brunner B., Yu J.-Y., Mielke R. E., MacAskill J. A., Madzunkov S., McGenity T. J. and Coleman M. (2008) Different isotope and chemical patterns of pyrite oxidation related to lag and exponential growth phases of *Acidithiobacillus ferrooxidans* reveal a microbial growth strategy. *Earth and Planetary Science Letters* **270**, 63-72.
- Brunner B., Einsiedl F., Arnold G. L., Müller I., Templer S. and Bernasconi S. M. (2012) The reversibility of dissimilatory sulphate reduction and the cell-internal multi-step reduction of sulphite to sulphide: insights from the oxygen isotope composition of sulphate. *Isotopes in Environmental and Health Studies* **48**, 33-54.
- Canfield D. E., Jørgensen B. B., Fossing H., Glud R., Gundersen J., Ramsing N. B., Thamdrup B., Hansen J. W., Nielsen L. P. and Hall P. O. J. (1993) Pathways of organic carbon oxidation in three continental margin sediments. *Marine Geology* **113**, 27-40.
- Chiba H. and Sakai H. (1985) Oxygen isotope exchange rate between dissolved sulfate and water at hydrothermal temperatures. *Geochimica et Cosmochimica Acta* **49**, 993-1000.
- Connick R. E., Tam T. M. and Deuster E. V. (1982) Equilibrium constant for the dimerization of bisulfite ion to form $\text{S}_2\text{O}_5^{2-}$. *Inorg. Chem.* **21**, 103-107.
- Druschel G. K., Schoonen M. A. A., Nordstrom D. K., Ball J. W., Xu Y. and Cohn C. A. (2003) Sulfur geochemistry of hydrothermal waters in Yellowstone National Park, Wyoming, USA. III. An anion-exchange resin technique for sampling and preservation of sulfoxyanions in natural waters. *Geochem. Trans.* **4**, 12-19.
- Druschel G. and Borda M. (2006) Comment on "Pyrite dissolution in acidic media" by M. Descostes, P. Vitorge, and C. Beaucaire. *Geochimica et Cosmochimica Acta* **70**, 5246-5250.

- Ebert A. and Brune A. (1997) Hydrogen Concentration Profiles at the Oxic-Anoxic Interface: a Microsensor Study of the Hindgut of the Wood-Feeding Lower Termite *Reticulitermes flavipes* (Kollar). *Applied and Environmental Microbiology* **63**, 4039-4046.
- Epstein S. and Mayeda T. (1953) Variation of O¹⁸ content of waters from natural sources. *Geochimica et Cosmochimica Acta* **4**, 213-224.
- Espejo R. T., Escobar B., Jedlicky E., Uribe P. and Badilla-Ohlbaum R. (1988) Oxidation of Ferrous Iron and Elemental Sulfur by *Thiobacillus ferrooxidans*. *Applied and Environmental Microbiology* **54**(7), 1694-1699.
- Fritz G., Büchert T. and Kroneck P. M. H. (2002) The Function of the [4Fe-4S] Clusters and FAD in Bacterial and Archaeal Adenylylsulfate Reductases. Evidence for flavin-catalyzed reduction of adenosine 5'-phosphosulfate. *The Journal of Biological Chemistry* **277**, 26066-26073.
- Fritz P., Basharmal G. M., Drimmie R. J., Ibsen J. and Qureshi R. M. (1989) Oxygen isotope exchange between sulphate and water during bacterial reduction of sulphate. *Chemical Geology (Isotope Geoscience Section)* **79**, 99-105.
- Heidel C. and Tichomirowa M. (2010) The role of dissolved molecular oxygen in abiotic pyrite oxidation under acid pH conditions - Experiments with ¹⁸O-enriched molecular oxygen. *Applied Geochemistry* **25**, 1664-1675.
- Heidel C. and Tichomirowa M. (2011) The isotopic composition of sulfate from anaerobic and low oxygen pyrite oxidation experiments with ferric iron - New insights into oxidation mechanisms. *Chemical Geology* **281**, 305-316.
- Hitchens R. M. and Towne R. W. (1936) The rate of reaction of sodium sulfite with oxygen dissolved in water. *Proc. Amer. Soc. Testing Mater.* **36**, 687-696.
- Holmkvist L., Kamyshny Jr. A., Vogt C., Vamvakopoulos K., Ferdelman T. G. and Jørgensen B. B. (2011) Sulfate reduction below the sulfate-methane transition in Black Sea sediments. *Deep-Sea Research I* **58**, 493-504.
- Holt B. D., Kumar R. and Cunningham P. T. (1981) Oxygen-18 study of the aqueous-phase oxidation of sulfur dioxide. *Atmospheric Environment* **15**, 557-566.
- Holt B. D., Cunningham P. T., Engelkemeir A. G., Graczyk D. G. and Kumar R. (1983) Oxygen-18 study of nonaqueous-phase oxidation of sulfur dioxide. *Atmospheric Environment* **17**, 625-632.
- Horner D. A. and Connick R. E. (1986) Equilibrium Quotient for the Isomerization of Bisulfite Ion from HSO₃⁻ to SO₃H⁻. *Inorg. Chem.* **25**, 2414-2417.
- Horner D. A. and Connick R. E. (2003) Kinetics of Oxygen Exchange between the Two Isomers of Bisulfite Ion, Disulfite Ion (S₂O₅²⁻), and Water As Studied by Oxygen-17 Nuclear Magnetic Resonance Spectroscopy. *Inorg. Chem.* **42**, 1884-1894.
- Hubbard C. G., Black S. and Coleman M. L. (2009) Aqueous geochemistry and oxygen isotope compositions of acid mine drainage from the Río Tinto, SW Spain, highlight inconsistencies in current models. *Chemical Geology* **265**, 321-334.
- James R. E. and Ferris F.G. (2004) Evidence for microbial-mediated iron oxidation at a neutrophilic groundwater spring. *Chemical Geology* **212**, 301-311.
- Jørgensen B. B. (1977) The sulfur cycle of a coastal marine sediment (Limfjorden, Denmark). *Limnology and Oceanography* **22**, 814-832.

- Kohl I. and Bao H. (2011) Triple-oxygen-isotope determination of molecular oxygen incorporation in sulfate produced during abiotic pyrite oxidation (pH = 2-11). *Geochimica et Cosmochimica Acta* **75**, 1785-1798.
- Kroopnick P. and Craig H. (1972) Atmospheric Oxygen: Isotopic Composition and Solubility Fractionation. *Science* **175**, 54-55.
- Ku T. C. W., Walter L. M., Coleman M. L., Blake R. E. and Martini A. M. (1999) Coupling between sulfur cycling and syndepositional carbonate dissolution: Evidence from oxygen and sulfur isotope composition of pore water sulfate, South Florida Platform, USA. *Geochimica et Cosmochimica Acta* **63**, 2529-2546.
- Lindtke J., Ziegenbalg S. B., Brunner B., Rouchy J. M., Pierre C. and Peckmann J. (2011) Authigenesis of native sulphur and dolomite in a lacustrine evaporitic setting (Hellín basin, Late Miocene, SE Spain). *Geol. Mag.* **148**, 655-669.
- Lloyd R. M. (1967) Oxygen-18 Composition of Oceanic Sulfate. *Science* **156**, 1228-1231.
- Lloyd R. M. (1968) Oxygen Isotope Behavior in the Sulfate-Water System. *Journal of Geophysical Research* **73**, 6099-6110.
- Mariotti A., Germon J. C., Hubert P., Kaiser P., Letolle R., Tardieux A. and Tardieux P. (1981) Experimental determination of nitrogen kinetic isotope fractionation: some principles; illustration for the denitrification and nitrification processes. *Plant and Soil* **62**, 413-430.
- Mizutani Y. and Rafter A. T. (1973) Isotopic behaviour of sulphate oxygen in the bacterial reduction of sulphate. *Geochemical Journal* **6**, 183-191.
- Müller I. A., Brunner B., Breuer C., Coleman M. and Bach W. The oxygen isotope equilibrium fractionation between sulfite species and water. *Geochimica et Cosmochimica Acta*, submitted.
- Nelson S. T. (2000) A simple, practical methodology for routine VSMOW/SLAP normalization of water samples analyzed by continuous flow methods. *Rapid Communications in Mass Spectrometry* **14**, 1044-1046.
- Oba Y. and Poulson S. R. (2009a) Oxygen isotope fractionation of dissolved oxygen during abiological reduction by aqueous sulfide. *Chemical Geology* **268**, 226-232.
- Oba Y. and Poulson S. R. (2009b) Oxygen isotope fractionation of dissolved oxygen during reduction by ferrous iron. *Geochimica et Cosmochimica Acta* **73**, 13-24.
- Peck Jr. H. D. (1962) V. Comparative Metabolism of Inorganic Sulfur Compounds in Microorganisms. *Microbiol. Mol. Biol. Rev.* **26(1)**, 67-94.
- Peck Jr. H. D. and Stulberg M. P. (1962) O¹⁸ Studies on the Mechanism of Sulfate Formation and Phosphorylation in Extracts of *Thiobacillus thioparus*. *The Journal of Biological Chemistry* **237**, 1648-1652.
- Pfeffer C., Larsen S., Song J., Dong M., Besenbacher F., Meyer R. L., Kjeldsen K. U., Schreiber L., Gorby Y. A., El-Naggar M. Y., Leung K. M., Schramm A., Risgaard-Petersen N. and Nielsen L.P. (2012) Filamentous bacteria transport electrons over centimetre distances. *Nature* **000**, 1-4.
- Pirlet H., Wehrmann L. M., Brunner B., Frank N., Dewanckele J., Rooij D. V., Foubert A., Swennen R., Naudts L., Boone M., Cnudde V. and Henriët J. P. (2010) Diagenetic formation of gypsum and dolomite in a cold-water coral mound in the Porcupine Seabight, off Ireland. *Sedimentology* **57**, 786-805.
- Pirlet H., Wehrmann L. M., Foubert A., Brunner B., Blamart D., De Mol L., Van Rooij D., Anckele J. D., Cnudde V., Swennen R., Duyck P. and Henriët J-P. (2012)

- Unique authigenic mineral assemblages reveal different diagenetic histories in two neighbouring cold-water coral mounds on Pen Duick Escarpment, Gulf of Cadiz. *Sedimentology* **59**, 578-604.
- Revsbech N. P., Jørgensen B. B., Blackburn T. H. and Cohen Y. (1983) Microelectrode studies of the photosynthesis and O₂, H₂S, and pH profiles of a microbial mat. *Limnol. Oceanogr.* **28**, 1062-1074.
- Revsbech N. P. (1989) An oxygen microsensor with a guard cathode. *Limnol. Oceanogr.* **34**, 474-478.
- Rimstidt J. D. and Vaughan D. J. (2003) Pyrite oxidation: A state-of-the-art assessment of the reaction mechanism. *Geochimica et Cosmochimica Acta* **67**, 873-880.
- Sada E., Kumazawa H., Hashizume I., Shimono M. and Sakaki T. (1987) Oxidation of Aqueous Sodium Sulfide Solutions with Activated Carbon. *Ind. Eng. Chem. Res.* **26**, 1782-1787.
- Schippers A., Jozsa P.-G. and Sand W. (1996) Sulfur Chemistry in Bacterial Leaching of Pyrite. *Applied and Environmental Microbiology* **62**, 3424-3431.
- Schippers A. and Jørgensen B. B. (2001) Oxidation of pyrite and iron sulfide by manganese dioxide in marine sediments. *Geochimica et Cosmochimica Acta* **65**, 915-922.
- Schwedt A., Kreutzmann A-C., Polerecky L. and Schulz-Vogt H. N. (2012) Sulfur respiration in a marine chemolithoautotrophic *Beggiatoa* strain. *Frontiers in Microbiology* **2**, 1-8.
- Singer P. C. and Stumm W. (1970) Acidic Mine Drainage: The Rate-Determining Step. *Science* **167**, 1121-1123.
- Smith J. R., Luthy R. G. and Middleton A. C. (1988) Microbial Ferrous Iron Oxidation in Acidic Solution. *Journal Water Pollution Control Federation* **60**, 518-530.
- Stumm W. and Lee F. G. (1961) Oxygenation of Ferrous Iron. *Industrial and Engineering Chemistry* **53**, 143-146.
- Sugio T., Hirose T., Li-Zhen Y. and Tano T. (1992) Purification and Some Properties of Sulfite:Ferric Ion Oxidoreductase from *Thiobacillus ferrooxidans*. *Journal of Bacteriology* **174** (12), 4189-4192.
- Sugio T., Uemura S., Makino I., Iwahori K., Tano T. and Blake II R. C. (1994) Sensitivity of Iron-Oxidizing Bacteria, *Thiobacillus ferrooxidans* and *Leptospirillum ferrooxidans*, to Bisulfite Ion. *Applied and Environmental Microbiology* **60**(2), 722-725.
- Taylor B. E., Wheeler M. C. and Nordstrom D. K. (1984a) Isotope composition of sulphate in acid mine drainage as measure of bacterial oxidation. *Nature* **308**, 538-541.
- Taylor B. E., Wheeler M. C. and Nordstrom D. K. (1984b) Stable isotope geochemistry of acid mine drainage: Experimental oxidation of pyrite. *Geochimica et Cosmochimica Acta* **48**, 2669-2678.
- Thamdrup B., Fossing H. and Jørgensen B. B. (1994) Manganese, iron, and sulfur cycling in a coastal marine sediment, Aarhus Bay, Denmark. *Geochimica et Cosmochimica Acta* **58**, 5115-5129.
- Tichomirowa M. and Junghans M. (2009) Oxygen isotope evidence for sorption of molecular oxygen to pyrite surface sites and incorporation into sulfate in oxidation experiments. *Applied Geochemistry* **24**, 2072-2092.

- Van Everdingen R. O. and Krouse H. R. (1985) Isotope composition of sulphates generated by bacterial and abiological oxidation. *Nature* **315**, 395-396.
- Van Stempvoort D. R. and Krouse H. R. (1994) Controls of $\delta^{18}\text{O}$ in Sulfate. Review of Experimental Data and Application to Specific Environments. *American Chemical Society*, 446-480.
- Xu Y. and Schoonen M. A. A. (1995) The stability of thiosulfate in the presence of pyrite in low-temperature aqueous solutions. *Geochimica et Cosmochimica Acta* **59**, 4605-4622.
- Zhang J.-Z. and Millero F. J. (1991) The rate of sulfite oxidation in seawater. *Geochimica et Cosmochimica Acta* **55**, 677-685.
- Ziegenbalg S. B., Brunner B., Rouchy J. M., Birgel D., Pierre C., Böttcher M. E., Caruso A., Immenhauser A. and Peckmann J. (2010) Formation of secondary carbonates and native sulphur in sulphate-rich Messinian strata, Sicily. *Sedimentary Geology* **227**, 37-50.

3.8. Appendix

Table 1: Overview of isotope effects	
δO_2	Oxygen isotope composition of O_2 in the headspace (measured value).
$\delta O_2(aq)$	Oxygen isotope composition of $O_2(aq)$.
$\delta O_2(aq)_{steady\ state}$	Oxygen isotope composition of $O_2(aq)$ which is in equilibrium with O_2 in the headspace at steady state.
$\delta O_2(air)$	Oxygen isotope composition of air.
δH_2O	Oxygen isotope composition of water (measured).
δH_2O_{exp}	Oxygen isotope composition of an experimental solution.
δH_2O_{stock}	Oxygen isotope composition of the sulfite stock solution.
$\delta^{18}O_{HCl}$	Oxygen isotope composition of the 6 M hydrochloric acid.
δSO_3^{2-}	Oxygen isotope composition of sulfite.
$\delta SO_3^{2-}(EQ)$	Oxygen isotope composition of sulfite in equilibrium with the surrounding water.
δSO_4^{2-}	Oxygen isotope composition of sulfate (measured).
$\delta SO_4^{2-}(noFe)$	Oxygen isotope composition of sulfate from experiments in absence of dissolved iron species (measured).
$\delta SO_4^{2-}(air)$	Oxygen isotope composition of sulfate adjusted to $\delta O_2(air)$.
$f_{O_2 \rightarrow O_2(aq)}$	Flux of O_2 from the headspace into solution.
$f_{O_2(aq) \rightarrow O_2}$	Flux of $O_2(aq)$ into headspace.
$f_{O_2(aq) \setminus SO_3^{2-} \rightarrow SO_4^{2-}}$	Flux of $O_2(aq)$ that is consumed during sulfite oxidation.
$f_{O_2(aq) \setminus Fe^{2+} \rightarrow Fe^{3+}}$	Flux of $O_2(aq)$ that is consumed during oxidation of Fe^{2+} to Fe^{3+} .
$f_{SO_3^{2-} \leftrightarrow H_2O}$	Oxygen exchange between sulfite and water.
$f_{SO_3^{2-} \setminus O_2(aq) \rightarrow SO_4^{2-}}$	Flux of sulfite that is oxidized by $O_2(aq)$ to sulfate.
$f_{SO_3^{2-} \setminus Fe^{3+} \setminus H_2O \rightarrow SO_4^{2-}}$	Flux of sulfite molecules that are oxidized by Fe^{3+} .
$f_{H_2O \setminus Fe^{3+} \setminus SO_3^{2-} \rightarrow SO_4^{2-}}$	Flux of water oxygen that is consumed during sulfite oxidation by Fe^{3+} .
$f_{Fe^{3+} \setminus SO_3^{2-} \setminus H_2O \rightarrow SO_4^{2-}}$	Flux of Fe^{3+} that is consumed during oxidation of SO_3^{2-} .
$\epsilon_{O_2 \rightarrow O_2(aq)}$	Isotope effects during flux of O_2 from the headspace into solution.
$\epsilon_{O_2(aq) \rightarrow O_2}$	Isotope effects during flux of $O_2(aq)$ into headspace.
$\epsilon_{O_2(aq) \setminus SO_3^{2-} \rightarrow SO_4^{2-}}$	Isotope effects during consumption of $O_2(aq)$ for the oxidation of sulfite.
$\epsilon_{O_2(aq) \setminus Fe^{2+} \rightarrow Fe^{3+}}$	Isotope effects during consumption of $O_2(aq)$ for the oxidation of Fe^{2+} to Fe^{3+} .
$\epsilon^{EQ}_{SO_3^{2-} \leftrightarrow H_2O}$	Oxygen isotope equilibrium fractionation between sulfite and water (from Müller et al., subm.).
$\epsilon^{EQ}_{SO_2 \leftrightarrow H_2O}$	Oxygen isotope equilibrium fractionation between dissolved SO_2 and water (from Müller et al., subm.).

$\epsilon_{\text{SO}_3^{2-}\text{-O}_2(\text{aq})\rightarrow\text{SO}_4^{2-}}$	Isotope fractionation for consumption of sulfite during oxidation by O_2 .
$\epsilon_{\text{SO}_3^{2-}\text{-Fe}^{3+}\text{-H}_2\text{O}\rightarrow\text{SO}_4^{2-}}$	Isotope fractionation for consumption of sulfite during oxidation by Fe^{3+} .
$\epsilon_{\text{H}_2\text{O}\text{-Fe}^{3+}\text{-SO}_3^{2-}\rightarrow\text{SO}_4^{2-}}$	Isotope fractionation for the consumption of water oxygen during sulfite oxidation by Fe^{3+} .
$\epsilon_{\text{O}_2\text{consumption}}$	Isotope effects for consumption of O_2 during oxidation of sulfite by Fe^{3+} and O_2 (determinable by Rayleigh distillation approach).
$\epsilon_{\text{O}_2\text{consumption}(\text{noFe})}$	Isotope fractionation for the consumption of O_2 during oxidation of sulfite without dissolved iron species (determined with Rayleigh distillation approach).
$\Delta^{18}\text{O}_{\text{SO}_4\text{-H}_2\text{O}}$	Isotope offset between sulfate and water.
$\epsilon^{18}\text{O}_{\text{SO}_4\text{-H}_2\text{O}}$	Isotope fractionation between sulfate and water.
$\epsilon^{18}\text{O}_{\text{SO}_4\text{-O}_2}$	Isotope fractionation between sulfate and O_2 .
Y	Fraction of sulfite oxidized by Fe^{3+} .
$(1-Y)$	Fraction of sulfite oxidized by O_2 .
X	Fraction of oxygen in sulfate derived from water.
$(1-X)$	Fraction of oxygen in sulfate derived from O_2 .
k	Sulfite oxidation rate ($\text{M}^{-1} \text{min}^{-1}$).

4. The isotope signature of magmatic SO₂ disproportionation: A comparison between laboratory experiments and a hydrothermally active site in the Manus Basin, Papua New Guinea

Inigo A. Müller^{a,b,*}, Benjamin Brunner^a, Thomas Max^{a,d}, Christian Breuer^{b,c}, Eoghan P. Reeves^{b,c}, Janis Thal^c, Stefano M. Bernasconi^e and Wolfgang Bach^{b,c}

^aBiogeochemistry Department, Max Planck Institute for Marine Microbiology, Celsiusstrasse 1, 28359 Bremen, Germany

^bMARUM-Center for Marine Environmental Sciences, University of Bremen, Leobener Strasse, 28359 Bremen, Germany

^cDepartment of Geosciences, University of Bremen, Klagenfurter Strasse, 28359 Bremen, Germany

^dNIWA-National Institute of Water and Atmospheric Research Ltd, Evans Bay Parade 301, Hataitai, 6021 Wellington, New Zealand

^eGeological Institute, ETH Zurich, Sonneggstrasse 5, 8092 Zurich, Switzerland

*Corresponding author: imueller@mpi-bremen.de; Tel.: 0049 4212028 638

4.1. Abstract

Large amounts of gaseous sulfur dioxide (SO₂) are released from a sulfur-rich magma body and disproportionate to sulfate (HSO₄²⁻) and elemental sulfur (S⁰) during the rise of hydrothermal fluids at North Su in the eastern Manus Basin, Papua New Guinea. This chemical process leads to a drastic drop in the pH of the hydrothermal fluid and to massive outflow of liquid S⁰ at the seafloor. The high concentrations of SO₂(aq) in the hydrothermal fluid allowed for the first time the measurement of the δ³⁴S_{SO₂} of 12.0‰ in a marine hydrothermal system. The SO₂ is enriched in ³⁴S compared to the sulfur of the bulk mantle and shows evidence for the contribution of an isotopically enriched source from the subducted plate. The difference between the sulfur isotope composition HSO₄⁻ and S⁰ revealed equilibrium sulfur exchange at a fluid temperature of approximately 280°C which corresponds probably to the temperatures where most of the SO₂ disproportionated in the hydrothermal fluid at North Su. The observed isotope composition of the discharged HSO₄⁻ (δ³⁴S of 19.3‰ – 19.6‰ and δ¹⁸O of 7.6‰ – 7.9‰) is in the range of the isotope composition of seawater sulfate, thus raising the questions 1) if the oxygen isotope signature of magmatic SO₂ disproportionation is compatible with the oxygen isotope signature observed in seawater sulfate and 2) if the contribution of HSO₄⁻ from magmatic SO₂

disproportionation is large enough to imprint its oxygen isotope signature into the seawater sulfate.

To date there are no quantitative estimates on the SO₂ flux of hydrothermal systems into the ocean but the comparison to terrestrial volcanoes shows that this could be as well a significant source at the seafloor. To analyze the oxygen isotope signature of magmatic SO₂ disproportionation we performed laboratory SO₂ disproportionation experiments at temperatures ranging from 150°C to 320°C. The oxygen isotope composition of the produced HSO₄⁻ revealed indeed an initial kinetic oxygen isotope fractionation (IKF) of 6‰ to 10‰ relative to the oxygen isotope composition of the water which is in the range of today's oxygen isotope offset between seawater sulfate and the seawater of ~8.6‰ (Holser et al., 1979; Claypool et al., 1980). These results open the perspective that the disproportionation of magmatic SO₂ may exert a major control on the oxygen isotope composition of seawater sulfate.

4.2. Introduction

4.2.1. Geochemistry of hydrothermal systems

Marine hydrothermal systems are driven by cold seawater percolating through open cracks in newly formed crust that becomes heated while approaching the magma body and rises rapidly to the crust-seawater interface due to its reduced buoyancy (Alt, 1995; Kelley et al., 2002). The majority of hydrothermal sites have been observed along mid ocean ridges or in back-arc basins (Lalou, 1991; Kelley et al., 2002; Tarasov et al., 2005), where tectonic plates diverge from each other or one is subducted under another tectonic plate, respectively. The two tectonic settings, spreading zones and back-arc basins are volcanically active with the magma source being close to the crust-water interface. With increasing temperatures the seawater undergoes low temperature water-rock reactions where first O₂ is removed from the seawater by the reaction with minerals containing reduced iron, whereas at higher temperatures above 150°C anhydrite (CaSO₄) precipitates due to its decreasing solubility and other elements such as Mg²⁺ and B are fixed in the surrounding rocks (Bischoff and Seyfried, 1978; Lalou, 1991; Hannington et al., 2001; Craddock and Bach, 2010; Reeves et al., 2011). When the altered seawater reaches the proximity of the magma body the temperature further increases allowing for high temperature reactions with the surrounding rocks such as the mobilization of alkaline elements, of Fe²⁺ and of Mn²⁺ (Alt, 1995) and eventually resulting in small modifications of the stable isotope composition of water (δD_{H_2O} , $\delta^{18}O_{H_2O}$; Schmidt et al., 2011). After the reactions with the rocks from the crust, the seawater will be depleted in SO₄²⁻ and Mg²⁺ (Bischoff and Seyfried, 1978), and enriched in alkaline elements as well as reduced metals such as Fe²⁺ and Mn²⁺ (Lalou, 1991). Dissolved Na⁺ and K⁺ in the entrained seawater can react at these high temperatures with surrounding silicate minerals and release high amounts of Ca²⁺, a process termed albitization (Nakamura et al., 2007). The increase in temperature lowers the buoyancy of the entrained altered seawater and leads to its fast ascent to the surface of the crust associated with phase separation which is leading to a vapor phase depleted in ions and a high salinity liquid phase enriched in ions

(e.g. SO₄²⁻, Na⁺, Cl⁻) at a specific pressure dependent temperature (see Cowan and Cann, 1988; Foustoukos and Seyfried Jr., 2007).

The hydrothermal fluid can reach the crust surface sometimes even with boiling temperatures between 300°C to 400°C depending on the water depth and the corresponding surrounding pressure (Spycher and Reed, 1988; Hannington et al., 2001; Reeves et al., 2011). Beside the water rock reactions the hydrothermal fluid can undergo mixing with magmatic fluids discharged from the magma body. Depending on the type of magma source the magmatic fluids can contain high amounts of volatile compounds (e.g. H₂O, H₂, CO₂, SO₂, H₂S, Cl⁻, F) that can reduce the pH of the hydrothermal fluid additionally and lead to further reactions with the surrounding rocks during the ascent of the fluid (Sakai, 1957; Holland, 1965; Alt, 1995; Tivey, 1995; Elderfield and Schultz, 1996; McCollom and Shock, 1997; Rye, 2005; Sun et al., 2007; Lupton et al., 2008; Craddock et al., 2010; Butterfield et al., 2011). The ascending water is expelled into the seawater at focused spots, the orifices of the vent sites and via diffusive venting in the surrounding area. During the discharge of the hydrothermal fluid into the seawater sulfide minerals (FeS₂, CuFeS₂, PbS, FeS and ZnS), metal oxyhydroxides (FeOOH, MnO₂), barite (BaSO₄) and CaSO₄ can precipitate due to the mixing with the cold bottom seawater and form chimney like structures around the orifices (Binns and Scott, 1993; Tivey, 1995; Hrischeva et al., 2007; Marques et al., 2007). Chemoautolithotrophic microbes can dwell near the vent site and live from the expelled reduced chemical compounds (e.g. Fe²⁺, Mn²⁺, H₂S, H₂ and CH₄) which they use as energy source and form the base of unique species-rich vent ecosystems (Desbruyères et al., 1994; McCollom and Shock, 1997; Sarrazin and Juniper, 1999; Alain et al., 2002; Kelley et al., 2002; Tarasov et al., 2005; Desbruyères et al., 2006; Ludwig et al., 2006; Petersen et al., 2011; Zielinski et al., 2011). The lifetime of an active hydrothermal vent site depends strongly on the plate tectonics and the occurring volcanism; it is highly variable and can last for decades up to hundreds of thousand years (Lalou, 1991; Lalou et al., 1995; Kelley et al., 2002; Ludwig et al., 2011).

4.2.2. SO₂ disproportionation at the hydrothermal vent site North Su in the eastern Manus Basin

This study compares the isotope signature of SO₂ disproportionation from laboratory experiments with the signature from the hydrothermally active seamount North Su in the Manus Basin where volatile compounds from a sulfur-rich magma source are mixed with the hydrothermal fluids. The sulfur-rich magma source causes vigorous venting of extremely acidic hydrothermal fluids which render the area an uninhabitable place for macro-organisms. The low pH of the fluid is caused most probably by the disproportionation of magmatic SO₂ (Craddock et al., 2010; Craddock and Bach, 2010), where the SO₂ reacts with water and forms sulfur compounds with higher and lower oxidation state corresponding to Eq. 4.1-4.2 (after Holland, 1965):



In Eq. 4.1, the SO₂ with S in an oxidation state of +IV reacts with water to two HSO₄⁻ (+VI) and one zero valent elemental sulfur (S⁰) and in Eq. 4.2 SO₂ reacts with water to three HSO₄⁻ and one hydrogen sulfide (H₂S, -II). Both disproportionation reactions have

in common that they produce protons and thus drastically lower the pH. Equation 4.1 was observed at high redox potentials, low temperatures and high total sulfur concentrations, whereas Eq. 4.2 was observed at low redox potentials, high temperatures and low total sulfur concentrations (Kusakabe et al., 2000). Kusakabe et al. performed a detailed study on the sulfur isotope signature during the abiotic disproportionation of SO₂ and obtained results similar to findings from studies on the sulfur isotope equilibrium fractionation during the hydrolysis of S⁰ (Robinson, 1973) and studies on the bacterial disproportionation of SO₃²⁻ (Habicht, 1998). During the disproportionation of SO₂, bisulfite (HSO₃⁻) might act as intermediate (Iwasaki and Ozawa, 1960; Kusakabe et al., 2000) or remain as the product of the hydrolysis of SO₂ that occurs at lower temperatures (Eigen et al., 1961; Betts and Voss, 1970; Horner and Connick, 2003; Butterfield et al., 2011):



The process of magmatic SO₂ disproportionation has often been reported for acid hot springs near volcanically active terrestrial environments (Iwasaki and Ozawa, 1960; Williams et al., 1990; Kusakabe et al., 2000 and references therein), but for the marine environment only few studies describe this process (e.g. Gamo et al., 1997; Roberts et al., 2003; Ueno et al., 2008; Craddock and Bach, 2010; Butterfield et al., 2011; Peters et al., 2011). Gamo and colleagues attribute the low pH in hydrothermal fluids emanating at the DESMOS hydrothermal site in the Manus Basin to the disproportionation of magmatic SO₂, and consider this process to be the cause for the observed sulfur isotope composition in HSO₄⁻ which is slightly lighter (depleted in ³⁴S) than the known isotope composition of seawater sulfate of 21.0‰ (Rees et al., 1978). Additional hints for a magmatic SO₂ source at DESMOS and at North Su come from high rare earth element (REE) concentrations from hydrothermal fluids (Craddock et al., 2010). During the SO-216 expedition to the hydrothermally active area of North Su we discovered large amounts of liquid and solid S⁰, which were most probably formed from the disproportionation of magmatic SO₂ which is contributed in large amounts from the underlying felsic magma source. With the remotely operated vehicle (ROV) Quest 4000 m (MARUM, Bremen) we were able to discover an area where yellow greenish liquid S⁰ was flowing out of the seafloor forming candle shaped chimneys of 10 to 20 cm height (“sulfur candle” vent site) and at some places they even formed meter sized knolls of S⁰ (Fig. 4.1 and 4.2). Further down along the flanks of North Su we found former flows of S⁰ with heights from cm up to half meter that percolated in the past through the surrounding volcanic material as can be observed in the altered rims. In the area of the sulfur candle site we found vigorously venting white smokers with extremely low pH similar to the hydrothermal field observed at the NW Rota-1 submarine volcano in the southern Mariana Arc (Butterfield et al., 2011). Butterfield and colleagues discovered also massive amounts of S⁰ in solid and liquid form produced by the disproportionation of magmatic SO₂.

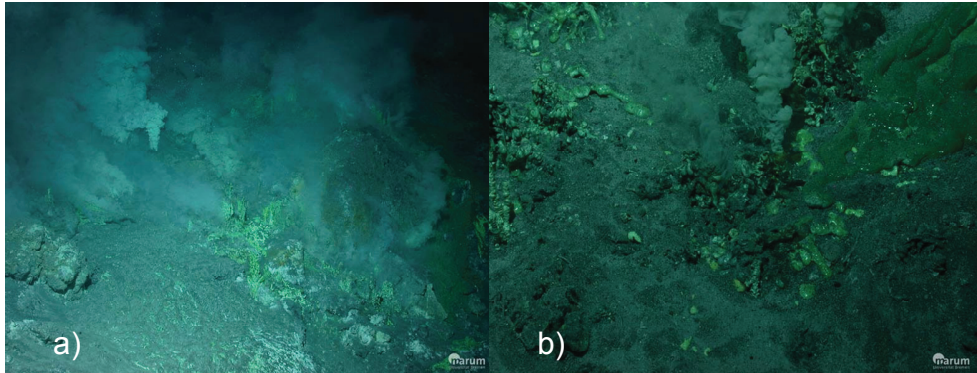


Fig. 4.1: ROV Quest images of the hydrothermal site “sulfur candle” at North Su. The image a) shows the small chimneys of elemental sulfur with white to grey smoke coming out and b) depicts tiny liquid sulfur flows with greenish color. The size of one sulfur chimney is approximately 15 cm in height (Copyright: MARUM University of Bremen).

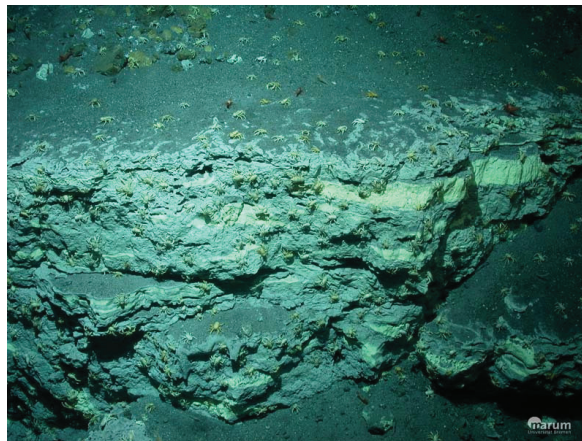


Fig. 4.2: ROV Quest image of old elemental sulfur dykes at the lower southern flank of North Su. The height of the bigger dike on the image is approximately 20 cm. The area is covered with crabs that live probably from S⁰ oxidizing bacteria (Copyright: MARUM University of Bremen).

4.2.3. The oxygen isotope signature of chemical SO₂ disproportionation and consequences for the oxygen isotope composition of seawater sulfate

The sulfur isotope signature of the disproportionation of SO₂ was thoroughly studied by Kusakabe et al. (2000) and already applied for the comparison with sulfur isotope patterns reported in natural environments such as acid hot springs. Meanwhile the oxygen isotope signature of the SO₂ disproportionation was barely touched by the authors and a detailed description on the oxygen isotope signature is still lacking.

In this study we describe the oxygen isotope fractionation during the disproportionation of SO₂, compare the findings to the study site in the Manus Basin and discuss the consequences for the oxygen isotope composition of seawater sulfate. We answer the questions:

- If the oxygen isotope signature of SO₂ disproportionation is compatible with the known oxygen isotope composition of seawater sulfate.
- If the contribution of magmatic SO₂ disproportionation is high enough to be the major factor in controlling the oxygen isotope composition of seawater sulfate.
- If it matters for the oxygen isotope composition of sulfate if it attained equilibrium exchange with the hydrothermal fluid (see Chiba and Sakai, 1985) or if sulfate retains the disproportionation related isotope fractionation.
- If variations of the hydrothermal activity can occur over the Earth's history and how these changes would affect the oxygen isotope composition of the seawater sulfate.

4.3. Study site in the Manus Basin

The Manus Basin is a newly (3.5 – 4 Myr; Taylor, 1979; Falvey et al., 1985) formed back-arc basin in the eastern part of the Bismarck Sea east of the main island of Papua New Guinea. The rapidly opening back-arc basin (~10 cm yr⁻¹; Beaudoin et al., 2007) originates from the complex tectonics surrounding the Manus Basin. It is bordered by the Manus Trench in the northeast, a former subduction zone of the Pacific Plate under the Bismarck Plate (Eocene to Oligocene) and the active New Britain Trench in the south (since ~15 Myr) where the Solomon Plate and the Indo-Australian Plate subduct under the Bismarck Plate (Martinez and Taylor, 1996; Auzende et al., 2000; Hrischeva et al., 2007). Thereby the subducting tectonic plate produces a slab pull on the Bismarck Plate towards the New Britain Trench causing extension of the Bismarck Plate due to enhanced magmatism over the subducting slab (Binns et al., 1993; Martinez and Taylor, 1996; Tregoning et al., 1999; Martinez and Taylor, 2003; Sinton et al., 2003). The eastern Manus Basin is pervaded by a tectonically active zone which is comprised by the three bigger transform faults with northwest direction of which the Willaumez Transform and the Djaul Transform in the central part of the Manus Basin are separated from each other by the active extensional transform zone (ETZ) linked to the Manus Spreading Center (MSC; Taylor et al., 1994; Martinez and Taylor, 1996). In the most easterly part of the Manus Basin the Djaul Transform and the Weitin Transform are displaced by the Eastern Manus Volcanic Zone (EMVZ) and by Graben structures (Auzende et al., 2000; Reeves et al., 2011). Hrischeva et al. (2007) reported more mafic to felsic magmas near the New Britain Trench, which is probably influenced by the distance to the active subduction zone where volatile species (e.g. H₂O, CO₂, H₂, HF, HCl and SO₂) from the subducted slab could be entrained into the overlying crust (Lupton et al., 2008). Due to this transition of the magma sources from mafic magma at the MSC to felsic magma towards the active subduction zone in the south (Auzende et al., 2000; Sinton et al., 2003), the chemistry of the hydrothermal fluids deviates as well depending on the magma source.

Our study area North Su at the SuSu Knolls is located within the EMVZ between the Djaul Transform and the Weitin Transform (Binns and Scott, 1993; Binns et al., 1993; Martinez et al., 1996). The SuSu Knolls are three volcanoes namely from north to south Suzette (1460 m), North Su (1160 m) and South Su (1320 m) with rock compositions consisting of porphyritic dacite on top of the domes and andesite below surrounded by probably Pliocene sediments at the base in 1700 m depth (Binns et al., 1997; Hrischeva et al., 2007). Our study focuses on a hydrothermal field at the southern slope of the North

Su seamount where extremely acidic hydrothermal fluids discharge out of the flanks providing the seawater with high amounts of dissolved and particular sulfur compounds. The finding of large solidified flows of S⁰ and the outflow of S⁰ at some parts indicate the possibility that liquid S⁰ is hidden under the surface of the southern flank of North Su.

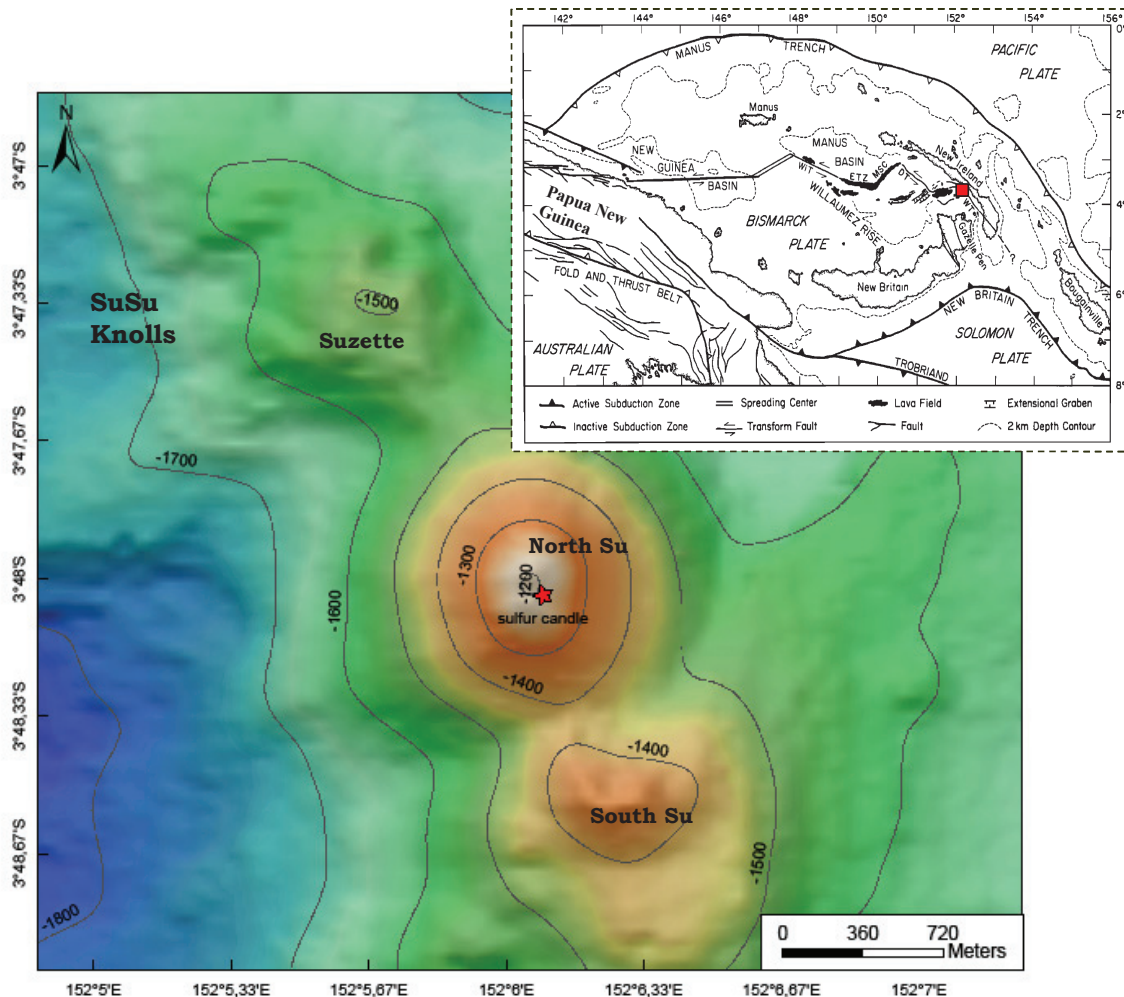


Fig. 4.3: Tectonic settings in the Bismarck Sea, Papua New Guinea. The Manus Basin with its three major transform faults (Willaumez, WiT; Djaul, DT; Weitin, WT), the Manus spreading center (MSC) and the extensional transform zone (ETZ) is surrounded by the island arcs of New Ireland in the east, of New Britain in the south and the Willaumez Rise in the west (modified from Taylor et al., 1994). The study area at SuSu Knolls is marked with a red square on the overview map and magnified on the detailed map. The SuSu Knolls hydrothermal field consists of the three seamounts Suzette, North Su (study site marked with the red star) and South Su.

4.4. Methods

4.4.1. Sampling of hydrothermal fluids in the Manus Basin

Collection of hydrothermal fluids:

During our scientific expedition SO-216 onboard of the RV Sonne we were collecting fluids of the hydrothermal vent sites with a remotely operated vehicle (ROV QUEST 4000 m from the MARUM, University of Bremen) in depths between 1100 to 1700 meters. The ROV collected solid samples of S^0 with a bucket and the hydrothermal fluids with an isobaric gas-tight fluid sampler (IGT; Seewald et al., 2001). In our study we only discuss measurements from the SO-216 sampling campaign that concern the process of SO_2 disproportionation. The IGT fluid sampler is constructed of chemically inert titanium, it can collect fluids with temperatures up to 400°C and maintains fluids with highly volatile compounds (e.g. CO_2 , CH_4 , HS^- , SO_2) at seafloor pressure till the fluid is withdrawn onboard of the ship. The inlet snorkel of the sampler can be held inside the orifice of the vent, which allows direct sampling of the discharging hydrothermal fluid and the seawater entrainment can be minimized by monitoring the in-situ temperature monitoring with a sensor attached to the snorkel (uncertainty $\pm 2^\circ C$). A gas-tight glass syringe (10 ml volume, FORTUNA[®] OPTIMA[®]) with a push-button valve can be attached directly at the IGT sampler to withdraw aliquots of the fluid for further processing in the laboratory.

Sampling procedure of hydrothermal fluids:

Fluid aliquots for concentration measurements of H_2S and HSO_4^- were taken directly from the IGT-fluid sampler after sample retrieval and the pH was measured potentiometrically onboard using a Ag/AgCl combination reference electrode with analytical uncertainty ± 0.02 units at 25°C (2σ). Small aliquots of the vent fluid were flame-sealed in glass ampoules for the oxygen isotope measurements of the H_2O onshore. The fixation of instable sulfur compounds and precipitation of HSO_4^- for stable isotope analysis was done with the fluid that we transferred directly from the fluid sampler into gas-tight glass syringes. The sulfoxy intermediates (e.g. SO_3^{2-} , $S_2O_3^{2-}$, $S_4O_6^{2-}$) are highly sensitive to air contamination, therefore we took first a small aliquot of sample to fix the prevailing SO_3^{2-} and $S_2O_3^{2-}$ compounds with the bimane derivatization method (see Fahey and Newton, 1987; Vetter et al., 1989; Zopfi et al., 2004) and froze them immediately for storage. To minimize the amount of air contamination we attached a precut plastic syringe at the push-button valve of the glass syringe containing the fluid. This setup allowed us the release of small amounts of the fluid that we could pipette out of the precut plastic syringe for the fixation. For the measurements of tetrathionate ($S_4O_6^{2-}$) we took of each fluid aliquot 2 ml in an exetainer (5 ml volume, from LABCO) that we froze immediately for storage. The rest of the sample was transferred in an exetainer (12 ml volume, from LABCO) preloaded with 0.5 ml HCl and purged with Argon gas to strip out the volatile sulfur compounds (SO_2 and H_2S). After 30 minutes the sample solution was considered to contain only HSO_4^- which we precipitated as $BaSO_4$ by adding a barium chloride solution. The precipitates were filtered and washed with de-ionized water and stored at $-20^\circ C$. Onshore the precipitates of each sample were freeze dried on the filters for subsequent isotope measurements.

For the concentration of dissolved H₂S the gas-tight sample was acidified, the H₂S purged into a 5 wt% AgNO₃ solution and precipitated as Ag₂S onboard. The samples were stored as Ag₂S and later the concentration was measured gravimetrically onshore. Aliquots for HSO₄⁻ concentration measurements were purged with N₂ prior to storage in acid-cleaned high-density polyethylene (HDPE) Nalgene™ bottles and analyzed onshore.

Separation of magmatic SO₂ from other sulfur compounds:

Hydrothermal fluids suspected to contain high amounts of SO₂ were treated in a way that allows the separation of the magmatic SO₂ from the other sulfur compounds. Fluid aliquots of 10 ml were withdrawn from the IGT sampler into gas-tight glass syringes and placed in a glove bag filled with Argon gas to prevent the contamination with air. The samples had to be handled carefully to avoid degassing and loss of volatile sulfur compounds. Inside the glove box we transferred the fluid through a rubber sealing into a 12 ml exetainer preloaded with 0.5 ml HCl (10 M). The exetainer was connected via Teflon tubing to a glass bottle (50 ml volume, Duran) filled with 35 ml de-ionized water and 5 ml ZnAc solution (5% w/w) which acted as a trap for the volatile sulfur compounds. The trap was sealed with a rubber stopper. After connecting the fluid exetainer with the trap bottle we started to purge the whole system with Argon gas. The Argon flow stripped the volatile SO₂ and H₂S into the ZnAc trap where the H₂S precipitated as ZnS₂ and the SO₂ reacts to HSO₃⁻ with the water (see Eigen et al., 1961; Betts and Voss, 1970; Horner and Connick, 2003) and rapidly oxidizes to SO₄²⁻ at neutral pH (Zhang and Millero, 1991). The Argon gas could escape the trap through a needle that was poked through the rubber stopper. After we purged the system for one hour we stopped the Argon flow and filtered the ZnS₂ from the trap solution. The filtrate should only contain sulfur derived from SO₂ and possibly from minor amounts of S₂O₃²⁻ which is expected to form SO₂ and S⁰ during acidification. However, as long as the concentrations of S₂O₃²⁻ are minor compared to the SO₂ it can be neglected because only half of the S₂O₃²⁻ sulfur will be trapped. The filtrate was kept in a glass bottle and sporadically shaken for 3 days to make sure that all the HSO₃⁻ was oxidized to SO₄²⁻ (see Zhang and Millero, 1991). Afterwards we precipitated the SO₄²⁻ as BaSO₄ by adding a BaCl₂ solution. The precipitate was filtered and rinsed several times with de-ionized water and finally stored at -20°C. The samples were shipped frozen to our laboratories in Bremen where we freeze dried the BaSO₄ precipitates on the filter for subsequent sulfur isotope measurements.

Retrieval of solid samples:

Solid samples such as elemental sulfur (samples retrieved from a depth of 1220 m at S 03°48.04202', E 152°06.09469) and sulfide chimneys were retrieved by the robotic arm of the ROV or by employing the TV-grab (Greifer A, Preussag Meerestechnik). Pieces of S⁰ from the sampling area "sulfur candles" were cleaned with de-ionized water and measured for their stable sulfur isotope composition.

4.4.2. Laboratory SO₂ disproportionation experiments

Emplacement of liquid SO₂ in inner glass vial:

Sulfur dioxide (SO₂ N38, AIR LIQUIDE with $\delta^{18}\text{O}_{\text{SO}_2} = -6.16 \pm 0.08\text{‰}$ and $\delta^{34}\text{S}_{\text{SO}_2} = 3.06 \pm 0.4\text{‰}$) was filled from the gas cylinder into Teflon tubing, which was partly covered by dry ice to condensate the SO₂ gas inside the tubing. The liquid SO₂ was transferred from the tubing into Glass Pasteur pipettes (BRAND) that were sealed at one end which was standing in pellets of dry ice. By keeping the glass pipettes in dry ice we could seal the upper ends with a Bunsen burner without loss of SO₂. The amount of the trapped SO₂ was determined by weighing the glass pipette before and after we filled it with SO₂ from the weight difference. We call the sealed glass pipettes containing the SO₂ the inner glass vials in our experiments, whose task it was to keep the SO₂ separated from the de-ionized water of the outer vial till the experiment temperature is reached.

Low temperature experiments (150°C to 200°C):

The experiments at lower temperatures were performed in glass test tubes (PYREX[®]) covered by a stainless steel casing (Fig. 4.4; similar to experiments in Kusakabe et al., 2000). The inner glass vials were placed inside the test tubes, de-ionized water was added (between 4.6 to 6.3 g) and the test tubes placed in ice water covered with NaCl₂ to lower the temperature before sealing the upper end of the glass test tube. The glass test tube was sealed with a welding burner fueled with butane and O₂ gas. The amount of water in each experiment was determined gravimetrically with a high precision balance by weighing the empty glass test tube, the inner glass vial and the sealed glass test tube filled with water together with the inner glass vial. The outer experiment vial was placed in a stainless steel casing, filled with de-ionized water and embedded in steel wool in order that the outer glass did not brake during vigorous shaking of the steel casing. A set of experiment containers was heated rapidly in an oven to the designated temperature and allowed to adapt to the temperature for an hour. To start the experiments we took the steel casing quickly out of the oven, shook it vigorously and put it immediately back to keep the temperature at a constant level. At each temperature we had several experiment containers that we analyzed at different time points during the course of the experiment. To stop the experiment we took the steel casing out of the oven and quenched the ongoing process by plunging the casing in a bucket filled with cold water.

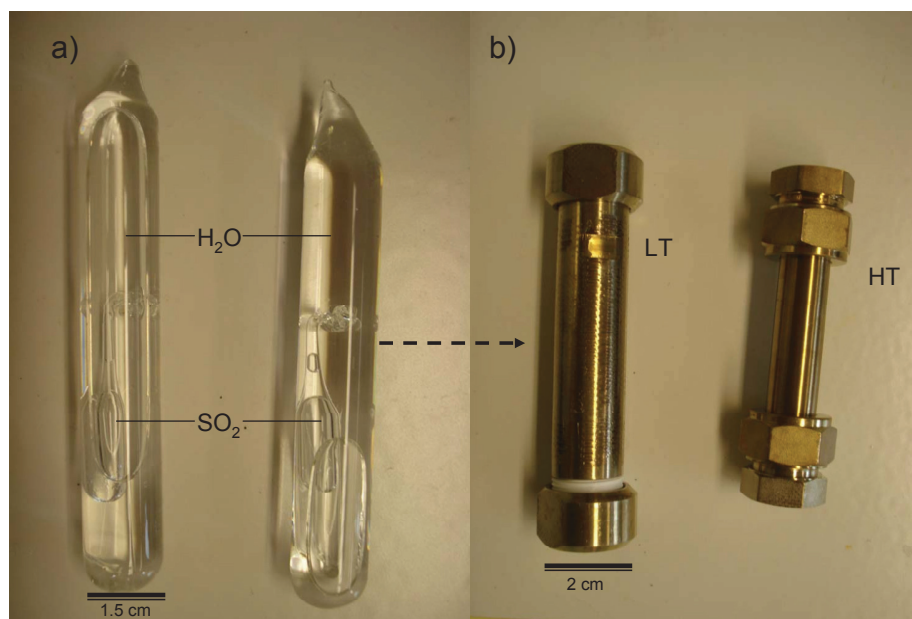


Fig. 4.4: Images of the experiment containers. In a) are two glass containers filled with H₂O and the inner SO₂ vial and b) shows the stainless steel container for the low temperature experiments (LT) and the high temperature experiments (HT).

High temperature experiments (240°C to 320°C):

For the experiments at temperatures above 200°C we used stainless steel containers as outer vials because of the instability of Pyrex glass at these high temperatures. The steel container consisted of a stainless steel tube (10 cm length and 1.4 cm inner diameter) and stainless steel screw caps from Swagelok (see Fig. 4.4b). The steel container was rinsed first with de-ionized water before we filled it with de-ionized water and added carefully the inner glass vial containing the SO₂. The amount of water was determined gravimetrically with a balance from the difference of the filled and empty steel container. After closing the sample containers we heated them rapidly in the oven to the designated temperature, let them adapt to the temperature for half an hour and then took them out of the oven for vigorous shaking to start the experiment. To stop the experiments for subsequent sampling, we quenched the ongoing reaction by plunging the sample container in a bucket with cold water.

Sampling procedure:

We opened the experiment containers for subsequent sampling after they were rapidly cooled to room temperature. In case of the low temperature experiments we had to break the glass vial at one end and in case of the high temperature experiments we opened one of the Swagelok screw caps. First we took small aliquots for concentration analysis of sulfoxo intermediates (SO₃²⁻, S₂O₃²⁻) that were fixed with the bismane derivatization method (see Fahey and Newton, 1987; Vetter et al., 1989; Zopfi et al., 2004) and then we took an aliquot for H₂S concentration analysis with a UV spectrophotometer. The rest of the experiment solution was vacuum filtered to collect the S⁰ on glass microfiber filters (GF/F, Whatman[®]), which were rinsed with de-ionized water and oven dried for two days at 50°C. From the filtrate we took 1 ml for oxygen isotope analyses of the water and measured the pH with pH indicator strips (MACHEREY-NAGEL). The rest of the

sample solution was acidified with 6 M HCl and purged for 30 minutes with N₂ to strip out gaseous SO₂ and H₂S. After the volatile sulfur compounds were stripped out of the solution we took aliquots to determine the HSO₄⁻ concentration and other aliquots were mixed with a barium chloride solution to precipitate HSO₄⁻ as BaSO₄ for subsequent measurements of the stable isotope composition. The precipitation solutions were centrifuged with 2300 rpm for 5 minutes, the supernatant decanted and the precipitate rinsed with de-ionized water. We repeated this cleaning procedure three times before we dried the samples in an oven for two days at 50°C.

4.4.3. Analytical methods

Detection of sulfoxy intermediates:

The concentration of the sulfur intermediates thiosulfate (S₂O₃²⁻) and sulfite (SO₃²⁻) was determined with the bimane derivatization method after Zopfi et al. (2004). We collected 500 µl of sample in 1.5 ml amber vials, added 50 µl HEPES/EDTA buffer (pH 8, 500 mM, 50 mM) and 50 µl monobromobimane (C₁₀H₁₁BrN₂O₂, 45 mM in acetonitrile) stored the samples in the dark for 30 minutes and afterwards stopped the derivatization process by adding 50 µl of 324 mM methane sulfonic acid (after Fahey and Newton, 1987; Vetter et al., 1989 and Zopfi et al., 2004). The samples were frozen at -20°C for storage till analysis by high-performance liquid chromatography (HPLC). The measurements were performed with a Smartline Manager 5000 connected to a Smartline pump 1000 (both from KNAUER) and a S5200 sample injector (SYKAM), which injects 100 µl of sample into the eluent flow (gradient with 0.25% (v/v) acetic acid with pH 3.5 and HPLC Gradient Grade methanol, MeOH) separated by a LiChrosphere 60RP select B column (125 x 4 mm, 5 µm; Merck) and analyzed with a Waters 470 Scanning Fluorescence Detector (excitation at 380 nm; detection at 480 nm). Analyses are based on calibration curves of standards of Na₂SO₃ and Na₂S₂O₃ dissolved in de-ionized water with a detection limit of approximately 0.05 µM and a standard deviation smaller than ±3% based on repeated standard measurements.

Samples for tetrathionate (S₄O₆²⁻) were collected in 1.5 ml glass vials, immediately frozen and stored at -20°C till analysis. The measurements have been performed by liquid chromatography (LC) with UV detection at 220 nm using HPLC Gradient Grade Methanol (MeOH) as mobile liquid phase and a 150 mm x 4.6 mm Develosil C30-UG-5 column from Nomura Chemical to separate the sulfur species (Rong et al., 2005; Kamyshny Jr. et al., 2009). A pump (S1021, SYKAM) generated a flow speed of 1 ml min⁻¹ of the mobile phase, 30 µl per sample were injected in the flow system by the autosampler (from Basic MARATHON), then flow through the separation column and are analyzed by an UV-detector (LINEAR UVIS 200). We dissolved Na₂S₄O₆ in de-ionized water for standard measurements and could detect clear peaks at concentrations down to 0.5 µM standards, what makes us confident that there is no significant amount of S₄O₆²⁻ in our samples, when we do not see any peak at the corresponding retention time.

Analyses of HSO₄⁻ concentrations:

The aliquots for HSO₄⁻ measurements were diluted with de-ionized water for subsequent analyzes of their conductivity with an ion chromatograph (IC, from Metrohm). As eluent

we used a carbonate buffer solution (3.2 mM Na₂CO₃ and 1 mM NaHCO₃). During the analyses the samples were injected in a constant eluent flow, which transports the sample to the conductivity cell.

Analyses of H₂S concentrations:

The H₂S concentrations of the experiments were measured with the diamine complexation method (Cline, 1969). An aliquot of the sample solution (0.1 ml) was injected into a volumetric flask, preloaded with 4.9 ml de-ionized water and 0.4 ml diamine solution and kept in dark for at least 30 minutes. Afterwards the absorbance of the solution placed in an appropriate cuvette was measured with a UV spectrophotometer at 670 mμ (UV-160A, SHIMADZU).

4.4.4. Stable isotope measurements

Sulfur isotope analyses of S⁰ and BaSO₄ were determined with a Carlo Erba Elemental Analyzer (EA) (NCS 2500, CE Instruments) connected via continuous flow to a GV Instruments OPTIMA mass spectrometer. The samples were weighed into tin cups (S⁰ between 0.04 – 0.10 mg and BaSO₄ between 0.25 – 0.35 mg) and vanadium pentoxide (V₂O₅) was added to enhance the conversion of sample-sulfur to SO₂. The samples were combusted in the EA and transported by a continuous helium stream into the isotope ratio mass spectrometer (IRMS). Sulfur isotope values are reported in the standard δ -notation where the isotope ratio ($R = {}^{34}\text{S}/{}^{32}\text{S}$) of the sample is compared to the ratio of the Vienna-Canyon Diablo Troilite (V-CDT), i.e. $\delta^{34}\text{S} = (R_{\text{sample}}/R_{\text{V-CDT}} - 1) \times 10^3\text{‰}$. The system was calibrated using the international standards IAEA-S1 ($\delta^{34}\text{S} = -0.3\text{‰}$), IAEA-S2 ($\delta^{34}\text{S} = 22.7\text{‰}$), NBS123 ($\delta^{34}\text{S} = 0.5\text{‰}$) for sulfide precipitates and for elemental sulfur whereas the measurements of elemental sulfur were controlled with the standard IAEA-S-4 (Soufre de Lacq; $\delta^{34}\text{S} = 16.9\text{‰}$), IAEA-SO5 ($\delta^{34}\text{S} = 0.5\text{‰}$), IAEA-SO6 ($\delta^{34}\text{S} = -34.1\text{‰}$) and NBS127 ($\delta^{34}\text{S} = 21.1\text{‰}$) were used for sulfate precipitates. Analytical reproducibility of replicate measurements of standards is $\pm 0.3\text{‰}$ ($n = 319$).

The oxygen isotope compositions of the precipitated BaSO₄ were measured by isotope ratio mass spectrometry (IRMS) with a Finnigan DELTA^{plus} mass spectrometer coupled to a Finnigan TC/EA. In brief, the precipitates were weighed (BaSO₄ between 0.25 – 0.35 mg) into silver cups which were loaded into an auto sampler coupled to a thermochemical reduction device (TC/EA Finnigan). In the TC/EA the samples were reduced at 1450°C in the presence of carbon. The evolved CO gas was carried through a gas chromatography column and analyzed by continuous flow isotope mass spectrometry. The isotope results are reported in the standard δ -notation where the isotope ratio ($R = {}^{18}\text{O}/{}^{16}\text{O}$) of the sample is compared to the ratio of the Vienna Standard Mean Ocean Water (VSMOW), i.e. $\delta^{18}\text{O} = (R_{\text{sample}}/R_{\text{VSMOW}} - 1) \times 10^3\text{‰}$. Measurements were calibrated using standards NBS 127 ($\delta^{18}\text{O} = 8.7\text{‰}$), SO-5 ($\delta^{18}\text{O} = 12\text{‰}$) and SO-6 ($\delta^{18}\text{O} = -11.3\text{‰}$). The reproducibility based on repeated measurements of the standards is less than 0.5‰ (1 σ).

The oxygen isotope composition of water samples was determined with a Cavity Ringdown Mass spectrometer (Los Gatos Research LGR DLT-100). For the measurements with the DLT-100, a small amount of liquid sample was injected into a heated septum port of the liquid auto sampler where it is quickly vaporized and

transported into a 25 cm laser cell. Here, the relative molecular abundances of $^2\text{H}^1\text{H}^{16}\text{O}$, $^1\text{H}^1\text{H}^{18}\text{O}$, and $^1\text{H}^1\text{H}^{16}\text{O}$ are determined at a wavelength of 1390 nm and converted into atomic ratios of $^2\text{H}/^1\text{H}$ and $^{18}\text{O}/^{16}\text{O}$. The obtained ratios are then converted by post-processing to the δ -scale with respect to VSMOW. Each sample was measured 10 times, the first four measurements were discarded because of potential memory effects and the average of the last six measurements yields the value for the isotope composition of the sample. The reproducibility for the DLT-100 measurements is typically less than 0.3% (1σ). The reported standard deviations are isotope values determined by using linear regression calculated for 95% confidence limits.

We report the isotope offsets of the samples of North Su and the isotopic fractionation factors between HSO_4^- and S^0 and between HSO_4^- and H_2O from the laboratory experiments as $\Delta^{34}\text{S}_{\text{HSO}_4^--\text{S}^0}$ and $\Delta^{18}\text{O}_{\text{HSO}_4^--\text{H}_2\text{O}}$, respectively. In the case of natural samples with normal isotope abundances we can assume that Δ is equal to the difference between the δ -values of the corresponding compounds (see Coplen, 2011).

4.5. Results and discussion

4.5.1. Disproportionation of magmatic SO_2 in a hydrothermal fluid at North Su

Fluid chemistry at one vigorous hydrothermal site of North Su:

At the southern flank of North Su in water depths of 1220 meters we discovered a vigorous venting hydrothermal field with white smokers (fluid samples retrieved from orifice at S $03^\circ48.04240'$ E $152^\circ06.08975'$) that emitted fluids with extremely low pH (pH 1.2 to 1.4, see Table 4.1). The ROV team sampled the fluid directly from the orifice of the white smoker with two IGT samplers. During the sampling the temperature sensor at the tip of the IGT snorkel sensed temperatures between 95°C to 103°C and revealed a maximum temperature of 119°C . The sulfur chemistry of the vent fluid showed extremely high concentrations of sulfate (HSO_4^-) up to $71.8 \text{ mmol kg}^{-1}$ exceeding the normal seawater sulfate concentrations more than twice and the bisulfite (HSO_3^-) concentration was determined to be higher than 4 mmol kg^{-1} . There was no H_2S detected in the hydrothermal fluid but we were able to measure in this highly acidic fluid approximately $300 \text{ } \mu\text{mol kg}^{-1}$ thiosulfate ($\text{S}_2\text{O}_3^{2-}$; Table 4.1). The high HSO_4^- concentrations is probably produced by the disproportionation of magmatic SO_2 during the ascent of the hydrothermal fluid, a hypothesis that is supported by the extremely low pH and the presence of large deposits of elemental sulfur (S^0) in this area. Also, S^0 as the other product of the disproportionation of SO_2 (Eq. 4.1) was flowing out of the ground next to the white smokers forming candle shaped chimney structures (10 to 20 cm in height, see Fig. 4.1).

Table 4.1: Chemical and isotopic analyses of the hydrothermal fluid from North Su (SO-216 expedition)

Sample ID	Sample description	Temperature (°C)	pH	HSO ₄ ⁻ (mmol kg ⁻¹)	HSO ₃ ⁻ (mmol kg ⁻¹)	S ₂ O ₃ ²⁻ (mmol kg ⁻¹)	δ ³⁴ S _{HSO₄⁻ (‰)}	δ ³⁴ S _{HSO₃⁻ (‰)}	δ ³⁴ S _{S₂O₃²⁻ (‰)}	δ ¹⁸ O _{HSO₄⁻ (‰)}	δ ¹⁸ O _{H₂O} (‰)	Δ ¹⁸ O _{HSO₄⁻-H₂O} (‰)
023-ROV-01	Fluid	95	1.4	60.8	4.309	0.376	19.6	12.0		7.9	0.0	7.9
023-ROV-02	Fluid	103	1.2	71.8	3.508	0.328	19.3			7.6	0.0	7.6
021-ROV-12.1	Sulfur chimney									-4.6		
021-ROV-12.2	Sulfur chimney									-5.1		
021-ROV-12.3	Sulfur chimney									-4.1		
021-ROV-12.4	Sulfur chimney									-4.9		
021-ROV-12.5	Sulfur chimney									-3.8		

The $S_2O_3^{2-}$ was most probably produced over the comproportionation reaction of the abundant S^0 and HSO_3^- in the hydrothermal fluid after Eq. 4.4 (after Kusakabe et al., 2000; Kaasalainen and Stefánsson, 2011):



The large amount of HSO_3^- was likely produced beforehand by the hydrolysis of the magmatic SO_2 after Eq. 4.3. Bisulfite is usually very rare in natural environments and detected in the low μM range (see Zopfi et al., 2004), but a previous study by Butterfield et al. (2011) observed in a hydrothermal zone on the Mariana volcanic arc concentrations up to 163 mM originating from the high discharge of magmatic SO_2 . The study of Butterfield and colleagues and our findings indicate that in volcanically active back-arc systems the process of magmatic SO_2 disproportionation might play a more significant role in terms of global sulfur fluxes over geological times and might be an important source of seawater sulfate. The hydrothermal fluid was analyzed as well for tetrathionate ($S_4O_6^{2-}$) but it was not detected although it is thought to be stable under low pH conditions as in the emitted fluid (Xu and Schoonen, 1995; Druschel et al., 2003). We did not detect any H_2S in the hydrothermal fluid, but during the acidification procedure to separate the magmatic SO_2 from the other sulfur species, a white phase was precipitating in the ZnAc trap which is most probably $ZnSO_3$ due to the oversaturation by $SO_2(\text{aq})$ of the solution. However, this seems to be an experimental artifact and does not appear in-situ at North Su.

Possible sources of HSO_4^- in the fluids of “sulfur candle” at North Su:

The amount of HSO_4^- in the hydrothermal fluid that we analyzed at North Su is approximately double as high as normal seawater concentrations. Potential sources for this high concentration can be 1.) disproportionation of magmatic SO_2 , 2.) re-dissolution of anhydrite ($CaSO_4$) or celestite ($SrSO_4$) in the upper crust and 3.) increasing concentration of HSO_4^- due to phase separation. Although we discovered large quantities of liquid and solidified S^0 at the hydrothermal site sulfur candle at North Su that would speak for HSO_4^- contribution from the disproportionation of magmatic SO_2 we cannot fully exclude the other two processes as possible contributors.

If we consider re-dissolution of anhydrite in the shallow crust at North Su, it would have the following consequences for the fluid chemistry. Entrained seawater with temperatures above 120°C re-dissolves previously precipitated anhydrite and mixes with the hydrothermal fluid and leads to enriched concentrations of Ca^{2+} , HSO_4^- and Sr^{2+} with respect to the normal seawater (Monnin et al., 2003). In our system this process can be ruled out, otherwise the pH would be much higher due to entrained seawater. In the hydrothermal fluid at North Su we measured a pH of 1.2 which is best explained by high contributions of SO_2 disproportionation via Eq. 4.1. The third process is the phase separation; in this case the hydrothermal fluid would form two phases during its rise at a specific pressure dependent temperature, thereby forming a vapor phase depleted in ions and a high salinity liquid phase enriched in ions (e.g. HSO_4^- , Na^+ , Cl^- , Fe ; see Cowan and Cann, 1988; Foustoukos and Seyfried Jr., 2007). The high-salinity liquid is thereby thought to discharge at a focused hydrothermal orifice and the former vapor phase emanates more diffusively in the surrounding area (Fox, 1990). The high salinity phase correlates often with increased concentrations of metals (Foustoukos and Seyfried Jr., 2007), which was not the case in our system as we did not observe any metal precipitates

in the surrounding area of the white smoker. Additionally, phase separation is less probably at the depth of our sampling site (1220 m), after Bischoff and Rosenbauer (1984) it would require a seawater temperature above 320°C, which is much higher than the temperatures we measured (103°C). Therefore, we think the process of phase separation is not responsible for the high HSO₄⁻ concentrations, but as previous studies in the area of eastern Manus Basin give strong hints that the disproportionation of magmatic SO₂ takes place in this area, we expect this process to be responsible for the high HSO₄⁻ concentrations (Gamo et al., 1997; Craddock and Bach, 2010). Gamo and colleagues (1997) showed that in hydrothermal sites of DESMOS, which is in close proximity to North Su, the high HSO₄⁻ concentrations come from the disproportionation of magmatic SO₂. Compared to their study, we observed approximately the double of their HSO₄⁻ concentration. High SO₂ concentrations (inferred from the observed high amounts of S⁰, HSO₄⁻ and HSO₃⁻) at North Su are most probably responsible that the disproportionation process goes via Eq. 4.1 and produces HSO₄⁻ and S⁰ instead of H₂S (Eq. 4.2) as observed in hydrothermal fluids at DESMOS.

Isotope patterns at a hydrothermal site of North Su:

The sulfur isotope composition of HSO₄⁻ in the hydrothermal fluid of the white smokers at North Su is between 19.3‰ and 19.6‰ which is slightly lighter than the sulfur isotope composition of seawater sulfate (21.0‰; Rees et al., 1978). The oxygen isotope composition of the sulfate ranged between 7.6‰ and 7.9‰ which is as well lighter than the seawater value of 8.6‰ (Holser et al., 1979, Claypool et al., 1980). The offsets of the oxygen isotope composition between the HSO₄⁻ and the fluid ($\Delta^{18}\text{O}_{\text{HSO}_4^- \leftrightarrow \text{H}_2\text{O}}$) revealed values of approximately +8±‰ (see Table 4.1).

The high amount of magmatic SO₂ in the hydrothermal fluid allowed us to separate the SO₂ by acidification with 32% HCl and simultaneous purging of the fluid with Ar gas (described more in detail in method section). Thus we were able to measure for the first time the sulfur isotope composition of the magmatic SO₂ in a hydrothermal system at the seafloor and obtained a value of 12.0‰. This value mainly reflects the isotope composition of the SO₂ and to a minor part the isotope composition of the S₂O₃²⁻ which was present in the sample and reacted during the acidification procedure to S⁰ and SO₂ (via Eq. 4.5, Xu et al., 2000).



Eq. 4.5

Bisulfite is much more abundant in the hydrothermal fluid than the S₂O₃²⁻ (Table 4.1) which was produced most probably from comproportionation of SO₂ and S⁰ (Eq. 4.4) and only the half of the S₂O₃²⁻ sulfur reaches the ZnAc trap, therefore it is justified to consider the measured sulfur isotope composition as the original value of the magmatic SO₂.

The $\delta^{34}\text{S}_{\text{SO}_2}$ of 12‰ is much heavier than the known $\delta^{34}\text{S}$ of the bulk earth which is estimated to be 0‰ based on values from meteorites (Kaplan and Hulston, 1966; Seal II, 2006) and which is similar to the $\delta^{34}\text{S}$ from basaltic rocks (+0.3‰, Sakai et al., 1984). Due to the fact that this is the first report of the $\delta^{34}\text{S}$ of magmatic SO₂ from a hydrothermal system at the seafloor we cannot compare it directly to SO₂ from other systems. Therefore we compare our value to the values for the bulk earth, basaltic rocks and to the sulfur isotope composition of gaseous SO₂ expelled from terrestrial volcanoes. Most of the measured $\delta^{34}\text{S}$ of SO₂ emitted from volcanoes are only slightly above the $\delta^{34}\text{S}$ of the bulk earth, but there are also exceptions with values as heavy as +10.8‰ in

the Nevado Del Ruiz volcano, Colombia (Williams et al., 1990) or ranging from +5.9‰ to +11.9‰ in Momotombo volcano, Nicaragua (Menyailov et al., 1986). Menyailov and colleagues attribute the observed heavy $\delta^{34}\text{S}_{\text{SO}_2}$ to sulfur isotope fractionations during exchange reactions between gaseous SO_2 and H_2S , which would lead to the heavier sulfur isotope composition of SO_2 . In our case this scenario is rather unlikely because we did not detect any H_2S in our vent fluids. Thus we consider other processes that may be responsible for the heavy sulfur isotope composition in the SO_2 . Sulfur isotope measurements of the sulfur compounds of El Chichón volcano in Mexico revealed a $\delta^{34}\text{S}$ for the bulk magma of 5.8‰ which the authors attributed to either assimilation of isotopically enriched evaporites or prior loss of isotopically depleted H_2S (Rye et al., 1984). Sulfur isotope patterns in volcanic systems over subduction zones are very complex because of mixing of a sulfur source from the mantle with a sulfate mineral source from the subducted slab, which needs to be considered in the case of North Su (e.g. Rye et al., 1984). The sulfate minerals of the subducted oceanic plate (older material from the Pacific plate or younger from the Solomon plate) will undergo heating during the subduction of the corresponding plate inducing the reduction of sulfate to volatile SO_2 (Coleman and Moore, 1978; Ueda and Krouse, 1986). The volatile SO_2 rises from the subducted plate with other volatile compounds released from the subducted plate as H_2O and CO_2 into the overlying mantle wedge. In consequence these volatile compounds, especially the water, will induce partial melting of the magma in the mantle wedge producing the rise of melt with a sulfur source enriched in ^{34}S . With an isotope mass balance approach we can derive the relative contribution of each sulfur source for this scenario.

$$\delta^{34}\text{S}_{\text{measuredSO}_2} = X \cdot \delta^{34}\text{S}_{\text{mantle}} + (1 - X) \cdot \delta^{34}\text{S}_{\text{sulfate mineral}} \quad \text{Eq. 4.6}$$

with X being the relative amount of sulfur compounds derived from the mantle and $(1-X)$ the relative amount of sulfur compounds derived from the slab. Depending if the sulfate mineral source originates from the old Pacific plate or the younger Solomon plate the $\delta^{34}\text{S}$ of the sulfate mineral will vary strongly. The age of the sulfate mineral from the Pacific plate could be up to 180 Myr where the $\delta^{34}\text{S}$ of sulfate precipitates was much lighter with approximately 15‰ and more recent sulfate precipitates from the Solomon Plate probably have a $\delta^{34}\text{S}$ of 21‰ (see Claypool et al., 1980). Depending on the sulfur isotope composition of the sulfate source (15‰ or 21‰) derived from the slab the mantle derived sulfur contribution X would be equal to 0.2 or 0.43, respectively. Such a low mantle sulfur contribution could be explained by the continuous cycle of partial magma melting and ongoing loss of the more volatile sulfur components in the partial melt over the time the Manus Basin was formed, which would lead to strong depletion of the original mantle sulfur (Alt et al., 1993). If we consider an additional source of pyrite or other sulfide minerals from the subducted slab X would become even smaller, due to the expected lighter sulfur isotope composition of sulfide minerals. However, the source of a sulfate mineral source is more plausible as we detected in the hydrothermal fluid the more oxidized sulfur compound SO_2 . The studies which observed enriched sulfur isotope composition in the volcanically expelled SO_2 or in the magma source were located above subduction zones which support the hypothesis that sulfur compounds from subducted sediments (released as metasomatic fluid) influence the sulfur isotope composition of the SO_2 that is discharged in the hydrothermal fluid (Rye et al., 1984; Alt et al., 1993).

Strong evidence that disproportionation of magmatic SO₂ is the main process in the fluids of the white smokers at North Su comes from the observation of massive amounts of liquid and solidified S⁰ and from the isotope composition of the S⁰. The average sulfur isotope composition of the S⁰ chimney is -4.5‰, which is approximately 24‰ lighter than the δ³⁴S of the HSO₄⁻. If we consider that all the HSO₄⁻ and S⁰ were produced from magmatic SO₂ via Eq. 4.1 we can calculate the isotope composition of the original SO₂ according to (δ³⁴S_{HSO₄⁻} = 19.5‰ and δ³⁴S_{S⁰} = -4.5‰):}}

$$3 \cdot \delta^{34}\text{S}_{\text{SO}_2} = 2 \cdot \delta^{34}\text{S}_{\text{HSO}_4^-} + \delta^{34}\text{S}_{\text{S}^0}$$

→

$$\delta^{34}\text{S}_{\text{SO}_2} = \frac{2}{3} \cdot (19.5\text{‰}) + \frac{1}{3} \cdot (-4.5\text{‰}) = 11.5\text{‰}$$

Eq. 4.7

With the mass balance above a δ³⁴S value of 11.5‰ would be obtained for the magmatic SO₂ which fits well to our measured value of 12‰. The isotope mass balance would support that the disproportionation of magmatic SO₂ is the most important source of the discharged sulfur compounds (with elevated HSO₄⁻ concentrations) in the hydrothermal fluid at North Su.

Additionally, the high sulfur isotope composition of the SO₂ can also be explained by another scenario, where the rising SO₂ equilibrates its sulfur isotope with a sulfate mineral source with sulfur isotope composition of the actual seawater sulfate. Subduction zones are highly dynamic areas and the processes that occur at the interface between the subducted plate and the overlying plate are not well known. It is known that metasomatic fluid is released from the subducted sediments and pore fluids into the overlying mantle wedge (see Alt et al., 1993), but heated pore fluids might rise as well along the plate intersection towards the seafloor. If these fluids rise to shallower depths of the subduction zone they will interact with entrained seawater and promote the precipitation of anhydrite (CaSO₄) in the sediments. This anhydrite precipitation would increase the amount of sulfate minerals in the sediment of the plate which will be subducted and could contribute additional sulfate into the subduction factory. The SO₂ probably originates from deeper layers of the subducted plate with higher temperatures that enabled the reduction of sulfate minerals to SO₂ (Coleman and Moore, 1978; Ueda and Krouse, 1986). Due to the volatile properties the SO₂ will start to rise through the overlying crust and sediments with the anhydrite source, or the SO₂ encounters the sulfate in dissolved form in rising metasomatic fluids (Alt et al., 1993), as the anhydrite is prone to dissolve at the prominent conditions in subducted sediments (high T, high P and high salinity, see Newton and Manning, 2005). This scenario is highly speculative as it proclaims that HSO₄⁻ of the subducted sulfate minerals will reach the hydrothermal system at North Su as HSO₄⁻ and the other part as SO₂. However, partial contribution of HSO₄⁻ to the SO₂ in the hydrothermal fluids at North Su can not be excluded alone from the stable isotope analyses.

Estimated temperature range for the SO₂ disproportionation at North Su:

Robinson (1973) investigated the sulfur isotope equilibrium offset between SO₄²⁻ and H₂S during the hydrolysis of S⁰ at temperatures ranging from 200 to 320°C and by comparing the $\Delta^{34}\text{S}_{\text{HSO}_4^- \leftrightarrow \text{S}^0}$ of 24‰ obtained at North Su to their study it would correspond to the value for equilibrium fractionation at approximately 280°C (see Fig. 4.5). A similar sulfur isotope offset was determined in experiments on magmatic SO₂ disproportionation by Kusakabe et al. (2000) where they extrapolated similar values for the equilibrium fractionation from their longest experiments and an older study by Sakai (1968) revealed similar temperatures for sulfur isotope equilibrium fractionation between SO₄²⁻ and S⁰ of 24‰. Kusakabe et al. (2000) determined as well an initial kinetic sulfur isotope fractionation that is produced by the SO₂ disproportionation which is at temperatures between 150°C to 320°C smaller than the observed offset of 24‰. In their experiments the sulfur isotopes in ongoing experiments rapidly approach the sulfur isotope equilibrium fractionation. Sulfur isotope exchange at the high temperatures of 280°C and extreme acidic conditions as at North Su (pH 1.2) must be extremely fast (Ohmoto and Lasaga, 1982) and we expect that this 24‰ difference between the sulfur isotope composition of HSO₄⁻ and S⁰ is equal to the equilibrium isotope fractionation. If this is the case the 280°C must be the lower temperature limit, where most of the magmatic SO₂ disproportionated to the two products HSO₄⁻ and S⁰. In our sampling campaign at North Su we measured as well the oxygen isotope composition of the expelled HSO₄⁻ and the hydrothermal fluid to gain further insights on the disproportionation mechanism. By doing so we obtained a value for the $\Delta^{18}\text{O}_{\text{HSO}_4^- \leftrightarrow \text{H}_2\text{O}}$ of 8‰ which is surprisingly similar to the known offset of the oxygen isotope composition of the seawater sulfate and the seawater (8.6‰, Holser et al., 1979). When we compare this value with existing studies on the oxygen isotope equilibrium fractionation between HSO₄⁻ and water at hydrothermal temperatures (Lloyd et al., 1967; Mizutani and Rafter, 1969; Zeebe, 2010) the obtained $\Delta^{18}\text{O}_{\text{HSO}_4^- \leftrightarrow \text{H}_2\text{O}}$ of 8‰ would be equal to oxygen isotope equilibrium exchange between 210°C to 230°C (see Fig. 4.6). The oxygen isotope equilibrium fractionation between HSO₄⁻ and water at 280°C would be approximately 2‰ (~6‰ in Lloyd et al., 1967; ~5.3‰ in Mizutani and Rafter, 1969). The HSO₄⁻ seems to retain the sulfur isotope equilibrium fractionation from a fluid temperature of approximately 280°C and the oxygen isotope equilibrium fractionation from fluid temperature of approximately 220°C. The difference between the sulfur isotope and oxygen isotope signature might be explained by the molecular structure of the HSO₄⁻ molecule, where the four oxygen atoms are bond to the sulfur atom. The oxygen atoms are in direct contact with the surrounding water molecules which makes oxygen isotope exchange much feasible than sulfur isotope exchange between HSO₄⁻ and other sulfur compounds which requires a reconfiguration of the entire sulfate molecule. Thus, at identical conditions (i.e. pH and temperature), sulfur isotope exchange between sulfate and other sulfur species is expected to be slower than oxygen isotope exchange between sulfate and water. Consequently, although both sulfur and oxygen isotope exchange rates are rapid at high temperatures and low pH (Ohmoto and Lasaga, 1982; Chiba and Sakai, 1985) we expect the oxygen exchange to proceed slightly faster. As consequence, during the fast ascent of hydrothermal fluids the sulfur isotope composition will retain the equilibrium fractionation of a certain temperature whereas oxygen isotope exchange between HSO₄⁻ and water is still proceed until the fluid reached lower temperatures where also the

oxygen isotope signatures will be retained because the oxygen isotope exchange rates drop below a certain threshold. These differences in the isotope exchange properties should be investigated more in detail. Additional information such as the thermal gradient for a specific hydrothermal vent system could then be used as tool to measure the speed of the hydrothermal fluid during its ascent. During fast ascent of the hydrothermal fluid the temperatures of the obtained sulfur isotope equilibrium fractionation and the oxygen isotope equilibrium fractionation will be in a more narrow range whereas during a slower ascent of the hydrothermal fluid, the temperature range will be broader. However, the application of combined measurement of the $\delta^{34}\text{S}_{\text{HSO}_4^-}$ and the $\delta^{18}\text{O}_{\text{HSO}_4^-}$ in hydrothermal fluids with magmatic SO₂ disproportionation as a relative “speedometer” would need further studies to validate this hypothesis.

The observation that the $\delta^{34}\text{S}_{\text{HSO}_4^-}$ and the $\delta^{18}\text{O}_{\text{HSO}_4^-}$ are very similar to the known seawater sulfate values (21.0‰, Rees et al., 1978; 8.6‰, Holser et al., 1979) raises the question if the disproportionation of magmatic SO₂ might be an important process in shaping the isotope composition of the seawater sulfate. The sulfur isotope signature of SO₂ disproportionation is well studied and showed rapid approach of the temperature dependent isotope fractionation. The in-situ temperature in hydrothermal systems where the SO₂ disproportionates could be highly variable and as consequence SO₂ disproportionation in hydrothermal systems would produce HSO₄⁻ with a highly variable sulfur isotope composition. To find out more about the role of SO₂ disproportionation in shaping the oxygen isotope composition of sulfate we performed laboratory experiments that simulated the process at temperatures in the range of hydrothermal fluids.

4.5.2. Laboratory insights on the abiotic disproportionation of SO₂

Laboratory SO₂ disproportionation at temperatures between 150 to 320°C:

During the abiotic experiments the gaseous SO₂ reacted rapidly with the de-ionized water at the designated temperature and formed the products of Eq. 4.1 or Eq. 4.2 depending on the temperature and total concentration of the SO₂ (see Table 4.2; Kusakabe et al., 2000). Corresponding to Kusakabe et al. (2000) the SO₂ will disproportionate to HSO₄⁻ and S⁰ in a ratio of 2:1 if first the concentration of the starting SO₂ is high, second preferentially at lower temperatures and third at high redox potential. In contrast the disproportionation will produce HSO₄⁻ and H₂S in a ratio of 3:1 if first the SO₂ concentration is low, second the temperature is high and third the redox potential is low. It is exactly this order that decides via which reaction pathway the disproportionation run in our experiments (see Table 4.2). In all the experiments the high HSO₄⁻ production caused a massive drop in the pH of the experiment solution to approximately 1.

In the duration time experiments at higher temperatures the sulfur compounds in the acidic solution started to undergo redox reactions with the iron from the metal cover, thereby S⁰ was probably reduced to sulfide and the iron (Fe⁰) was oxidized to ferrous iron (Fe²⁺). Subsequently the sulfide precipitated as iron monosulfide at the surface of the steel container:



As consequence we did not consider the results from long duration experiments for the isotope analyses of the high temperature experiments (R-7, R-8).

The HSO_4^- to H_2S ratio in our measurements was much higher than expected, that could be due first to loss of gaseous H_2S during the opening of the experiment containers, second to precipitation of sulfide-iron precipitates and third due to the extremely high concentrations of HSO_4^- which caused errors in the concentration measurements due to strong dilutions. In Table 4.2 we did not report a value for the HSO_4^- concentration for experiments R-2 to R-5, because an error occurred during the dilution that resulted in erroneously high concentrations, exceeding the supplied amount of SO_2 . We indicated this with a star in Table 4.2. All runs at different temperatures had in common that HSO_3^- was detected only in the first time points decreasing rapidly with time and the $\text{S}_2\text{O}_3^{2-}$ was detected only in minor concentrations. The measurements of the HSO_3^- indicate how extremely fast the disproportionation reaction proceeds, although we started with high SO_2 concentrations, within 30 minutes or one hour most of the reaction already occurred. The pH was in all experiments approximately 1, but by measuring the pH with pH strips it is related to a wider error range of approximately ± 0.5 pH units. However, the pH is accurate enough to mirror the production of sulfuric acid during the disproportionation reaction. For the experiments of R-3 we unfortunately did not weigh the SO_2 in the beginning and therefore we did not display any concentration in Table 4.2, but we were able to precipitate high quantities of BaSO_4 for the isotope measurements.

Table 4.2

Hydrochemistry of the laboratory SO_2 disproportionation experiments at temperatures from 150°C to 320°C:

Run number	Temperature (°C)	$10^6/T^2$ (T in °K)	Duration (Minutes)	pH	Initial SO_2 (ppm S)	HSO_3^- (ppm S)	HSO_4^- (ppm S)	$\text{S}_2\text{O}_3^{2-}$ (ppm S)	H_2S (ppm S)	Precipitate
R-2-1	150	5.59	225	1	7120	6402.2	*	134.3	0.0	S^0
R-2-2	150	5.59	1165	0.5	5654	465.9	*	6.9	0.5	S^0
R-2-3	150	5.59	1567	0.5	14307	0.0	*	35.6	0.0	S^0
R-3-1	150	5.59	190				*			
R-3-2	150	5.59	450	1			*			
R-3-3	150	5.59	4133	1			*			
R-4-1	200	4.47	100	1	2911	458.2	*	11.5	0.0	S^0
R-4-2	200	4.47	1035		2589	0.0	*	0.0	4.8	S^0
R-4-3	200	4.47	1313		2957	0.2	*	1.3	21.7	-
R-5-1	200	4.47	1103	0.5	6113	0.0	*	0.2	9.6	S^0
R-6-1	240	3.80	60	1	1954	0.0	1351.2	1.4	37.1	-
R-6-2	240	3.80	120	1	4529	649.0	3212.5	17.4	1.1	S^0
R-6-3	240	3.80	363	2	1873	0.0	1176.8	1.8	13.4	S^0
R-6-4	240	3.80	393	1.5	4844	5.0	1911.5	6.1	7.8	S^0
R-7-1	280	3.27	32	0.5	5381	69.3	2465.4	24.2	2.5	FeS
R-7-2	280	3.27	62	1.5	6155	0.0	3119.2	12.2	46.5	FeS
R-7-3	280	3.27	92		6113	0.0	3006.0	4.6	44.4	FeS
R-8-1	320	2.84	32	0.5	9840	2789.0	3812.8	201.6	1.0	S^0
R-8-2	320	2.84	70	1	7946	0.0	3056.7	10.5	33.6	FeS

* HSO_4^- was precipitated from these samples, but due to strong dilution it was not possible to quantify accurately the HSO_4^- concentration.

- no sulfur mineral in solution.

The concentration of sulfur compounds is displayed in ppm of the weight of sulfur atoms of the respective sulfur compound compared to the weight of the total H_2O molecules used in the corresponding experiment.

Isotopic signature of the laboratory SO₂ disproportionation:

The sulfur isotope composition from the SO₂ disproportionation experiments showed rapid equilibration at highest experiment temperatures of 320°C, there the isotope fractionation reached already in 32 minutes (R-8-1) the equilibrium isotope fractionation between HSO₄⁻ and S⁰ ($\Delta^{34}\text{S}_{\text{HSO}_4^- \leftrightarrow \text{S}^0}$) which was determined in the study by Kusakabe et al. (2000). The experiments at lower temperatures are still far from being in equilibrium and lie somewhere in between the initial kinetic isotope fractionation (IKF, drawn after Kusakabe et al., 2000) and the equilibrium fractionation line (Fig.4.5). Although there is not a clear time dependent trend to recognize in our data, they reproduce nicely the experimental data from the study of Kusakabe and colleagues. The only exception with a sulfur isotope fractionation below the IKF is found in the first time point of R-7. The lower values can be explained with the disproportionation reaction running via Eq. 4.2 due to smaller total sulfur concentrations in R-7 and that the IKF between HSO₄⁻ and H₂S is smaller than the IKF between HSO₄⁻ and S⁰, which is in agreement with findings in Kusakabe et al. (2000). Additionally, the sulfur isotope composition of the H₂S was measured in FeS, which was produced during the experiment and might have caused some minor isotope fractionations during its production. The isotope fractionations in the experiments at other temperatures will vary slightly depending on the product of the disproportionation reaction, which explains as well that no clear trend was observed in the sulfur isotope data. The difference of the sulfur isotope composition of the products compared to the starting value of the SO₂ ($\delta^{34}\text{S}_{\text{SO}_2} = 3.06\text{‰}$) revealed that the $\delta^{34}\text{S}$ of the HSO₄⁻ is approximately 6‰ heavier in experiments with temperatures up to 240°C and at higher temperatures the $\delta^{34}\text{S}$ of the HSO₄⁻ is 9‰ heavier (all experimental isotope data are listed in Table 3). The isotope fractionation between the sulfur isotope composition of the added SO₂ and the isotope composition of S⁰ or H₂S respectively is up to -16.9‰ which is in the range of the observed sulfur isotope fractionation at North Su.

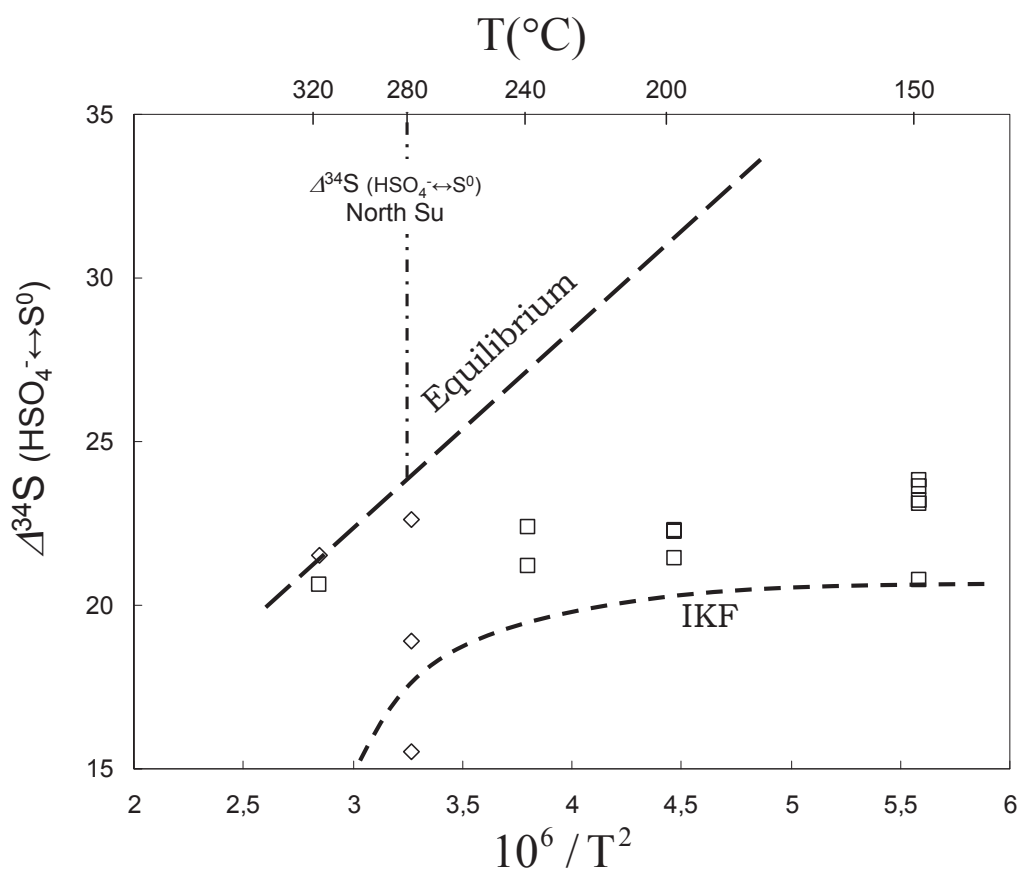


Fig. 4.5: Sulfur isotope fractionation between HSO_4^- and S^0 (squares) and between HSO_4^- and FeS (hollow diamonds). Values of the sulfur isotope equilibrium fractionation and line of the initial kinetic isotope fractionation (IKF) are from Kusakabe et al. (2000). The isotope fractionation values of our experiments lie between the IKF and the equilibrium isotope fractionation with the exception of one time point at 240°C which expresses slightly smaller fractionation than the estimated IKF. The sulfur isotope fractionation measured at North Su would correspond to the equilibrium isotope fractionation at 280°C.

The oxygen isotope composition of the produced HSO_4^- exhibits a fractionation with respect to the oxygen isotope composition of the experimental solution ($\Delta^{18}\text{O}_{\text{HSO}_4^- \leftrightarrow \text{H}_2\text{O}}$) ranging between 3.5‰ and 11.5‰ (see Table 4.3). The oxygen isotope fractionation of most experiments is similar to the oxygen isotope equilibrium fractionation determined by Mizutani and Rafter (1969). The oxygen isotope fractionation of the first time points of our experiments lie in a narrow range between 6‰ to 11‰ (see Fig. 4.6) which is astonishingly close to the known oxygen isotope offset between seawater sulfate and seawater (8.6‰, Holser et al., 1979). The first time points of the high temperature experiments (R-7, R-8) which are the shortest experiments (~30 minutes, see Table 4.2), are slightly heavier than the oxygen isotope equilibrium fractionation line between HSO_4^- and water (Lloyd, 1967; Lloyd, 1968; Mizutani and Rafter, 1969; Zeebe, 2010). This is an indication of an initial kinetic isotope fractionation (IKF) during the disproportionation process. If we consider an IKF independent of the temperature we would obtain an IKF of approximately 10.5‰ (horizontal line labeled with IKF? in Fig. 4.6) at the initial disproportionation and subsequent rapid approach of the oxygen isotope equilibrium

fractionation at the corresponding temperature. This is exactly what we see in our experiments, the oxygen isotope composition of the HSO₄⁻ is getting heavier with time in experiment R-2 and R-3 and lighter in experiments R-7 and R-8 at higher temperatures. In the other experiments at temperatures of 200°C and 240°C the IKF was too close to the equilibrium value that we could not observe any movement in the oxygen isotope composition of the HSO₄⁻. In addition we can say that the oxygen isotope composition of the HSO₄⁻ seems to attain the isotopic equilibrium much faster than the sulfur isotope composition of the HSO₄⁻, probably, due to its molecular structure that allows more rapid exchange of the oxygen atoms (Ohmoto and Lasaga, 1982; Chiba and Sakai, 1985). This observation is in agreement with the finding of distinct isotope equilibrium temperatures derived from the sulfur and oxygen isotope composition of the HSO₄⁻ in the hydrothermal fluid at North Su.

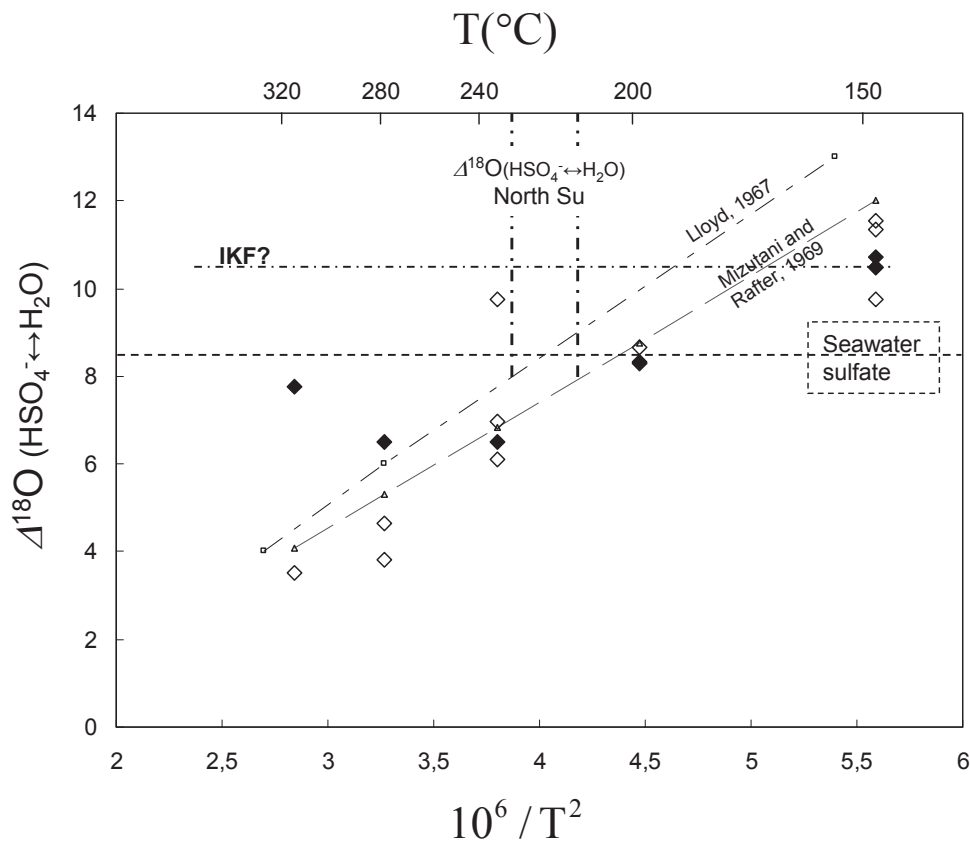


Fig. 4.6: Oxygen isotope fractionation between HSO₄⁻ and H₂O during the SO₂ disproportionation at temperatures between 150 to 320°C. The thin lines indicate the oxygen equilibrium fractionation for the corresponding water temperatures (Lloyd, 1967; Mizutani and Rafter, 1969). Filled diamonds are the measurements from the first time points of each run and the empty diamonds are the measurements of the following time points. The initial kinetic isotope fractionation (IKF) could be at all temperatures approximately 10‰ (horizontal line) rapidly approaching the equilibrium fractionation. The oxygen isotope fractionation measured at North Su corresponds to the equilibrium isotope fractionation at approximately 230°C and the horizontal dashed line displays the modern oxygen isotope offset between seawater sulfate and the seawater (Holser et al., 1979). The oxygen isotope fractionation between the HSO₄⁻ and the hydrothermal fluid at North Su correspond to the equilibrium isotope fractionation at temperatures between 210°C to 230°C.

Table 4.3

Isotope data of the laboratory disproportionation of SO₂ at temperatures from 150°C to 320°C

Run	Temperature (°C)	10 ⁶ /T ² (T in °K)	Duration (minutes)	δ ¹⁸ O _{H₂SO₄} (‰)	δ ¹⁸ O _{H₂O} (‰)	10 ³ lnα _{H₂SO₄↔H₂O} (‰)	δ ³⁴ S _{H₂SO₄} (‰)	δ ³⁴ S _{H₂S} (‰)	δ ³⁴ S _{S⁰} (‰)	10 ³ lnα _{H₂SO₄↔H₂S} (‰)	10 ³ lnα _{H₂SO₄↔S⁰} (‰)
R-2-1	150	5.59	225	3.1	-7.3	10.5	9.6		-13.4		23.1
R-2-2	150	5.59	1165	2.8	-7.6	10.5	9.8		-13.4		23.2
R-2-3	150	5.59	1567	3.7	-7.9	11.5	10.3		-13.3		23.6
R-3-1	150	5.59	190	4.0	-6.7	10.7					
R-3-2	150	5.59	450	3.1	-6.7	9.8	9.9		-10.9		20.8
R-3-3	150	5.59	4133	3.7	-7.6	11.3	9.9		-13.9		23.8
R-4-1	200	4.47	100	1.0	-7.4	8.3	9.0		-12.5		21.4
R-4-2	200	4.47	1035	0.9			9.0		-13.3		22.3
R-4-3	200	4.47	1313	0.9	-7.3	8.3	9.8				
R-5-1	200	4.47	1103	0.8	-7.9	8.7	9.3		-13.0		22.3
R-6-1	240	3.80	60	-1.0	-7.6	6.5	8.8				
R-6-2	240	3.80	120	2.2	-7.5	9.7	10.3		-12.1		22.4
R-6-3	240	3.80	363	-1.5	-7.7	6.1	8.4		-12.1		20.5
R-6-4	240	3.80	393	-0.8	-7.7	7.0	9.3		-11.9		21.2
R-7-1	280	3.27	32	-0.7	-7.2	6.5	10.2	-5.3		15.5	
R-7-2	280	3.27	62	-2.9	-7.5	4.6	12.4	-10.2		22.6	
R-7-3	280	3.27	92	-3.0	-6.8	3.8	12.5	-6.4		18.9	
R-8-1	320	2.84	32	0.2	-7.5	7.7	10.5		-10.1		20.6
R-8-2	320	2.84	70	-3.9	-7.5	3.5	13.2	-8.3		21.5	

4.5.3. Consequences of magmatic SO₂ disproportionation for the oxygen isotope composition of seawater sulfate

Our experiments revealed that the disproportionation of SO₂ produces indeed sulfate with an oxygen isotope composition in the range of the modern seawater sulfate (8.6‰, Holser et al., 1979) and that this range is independent of HSO₄⁻ being in equilibrium with the hydrothermal fluid or not. The disproportionation of SO₂ contributes continuously HSO₄⁻ into the seawater within a relatively narrow range of oxygen isotope values (i.e. narrow range of offsets with respect to the hydrothermal fluid). The contribution of HSO₄⁻ from the magmatic SO₂ disproportionation into the oceans is hard to quantify as there are only few studies which described this process marine environment (Gamo et al., 1997; Craddock and Bach, 2010; Butterfield et al., 2011). It is probably that this process plays an important role as Butterfield et al. (2011) recorded SO₂(aq) concentrations up to 163 mmol kg⁻¹ in hydrothermal fluids at a submarine volcano in the southern Mariana Arc, where the active disproportionation of SO₂ produced high amounts of HSO₄⁻. Butterfield and colleagues stated that these SO₂ rich fluids might have a significant impact on the global hydrothermal flux of sulfur into the oceans if such vigorous venting hydrothermal systems are representative for submarine arc eruptions and the comparison to terrestrial volcanoes supports this statement. Many studies measured high emissions of SO₂ at terrestrial volcanoes located at subduction zones (Menyailov et al., 1986; Williams et al., 1990; Bernard et al., 1991; Khokhar et al., 2005) or at mantle hotspot related volcanoes as on the Hawaiian islands (Gerlach and Graeber, 1985; Sutton et al., 2001; Hager et al., 2008) where they even mentioned that SO₂ disproportionation might occur in the hydrothermal system (see Gerlach and Graeber, 1985) and global estimates on the emissions of SO₂ (1.5-50 Tg yr⁻¹) exceed the estimates for H₂S (1-2.8 Tg yr⁻¹, see Von Glasow et al., 2009 and references therein). It is not possible to extrapolate these estimates into the marine environment, however, they demonstrate that large amounts of SO₂ are contributed by a volcanic source from a similar tectonic environment into the atmosphere and the flux should be similar in the oceans. To date it is not known if the disproportionation of magmatic SO₂ also occurred in the early Earth, but a study by Ueno et al. (2008) shows evidence of abiotic SO₂ disproportionation from a multiple sulfur isotope analysis in 3.5 Gyr old sulfur minerals from the Dresser Formation of Western Australia. This indicates that the specific oxygen isotope signature of the SO₂ disproportionation could have been imprinted in the oxygen isotope composition of seawater sulfate since the early Archean.

Although we cannot quantify the contribution of HSO₄⁻ from the SO₂ disproportionation into the oceans, we propose that the SO₂ disproportionation with its specific oxygen isotope signature keeps the oxygen isotope composition of the seawater sulfate like an anchor in a narrow range and damp the isotopic effects of other sulfate sources and processes that induce fluctuations in the oxygen isotope signature of sulfate. This would explain as well why the variations in the oxygen isotope record of the seawater sulfate over geological times are much smaller compared to the high variations of the sulfur isotope composition (see Claypool et al., 1980; Turchyn et al., 2004; Turchyn and Schrag, 2006). Factors controlling the minor variations in the oxygen isotope record of the seawater sulfate could be increased weathering of evaporites (sulfate input with heavier δ¹⁸O) and re-oxidation of reduced sulfur compounds such as pyrite

(sulfate input with lighter $\delta^{18}\text{O}$), the contribution of both factors might undergo high variations during geological time scales (Turchyn et al., 2004; Turchyn and Schrag, 2006).

In contrast to these factors, the disproportionation of magmatic SO_2 might be a more continuous source of HSO_4^- , since plate tectonics with the recycling of oceanic lithosphere and mantle hotspot volcanism is expected to act as a convective cooling mechanism of the mantle since the early history of the Earth, although the exact mechanism of tectonics in the Archean are still debated (van Hunen and van den Berg, 2008; Sizova et al., 2010; Condie and Kröner, 2013).

4.6. Conclusions

We analyzed the sulfur chemistry and the isotope patterns during the disproportionation of SO_2 in a hydrothermal system at North Su, Papua New Guinea and in laboratory experiments. The disproportionation of magmatic SO_2 is expected to be a major contributor of HSO_4^- into the seawater and its process specific oxygen isotope signature is thought to significantly shape the oxygen isotope composition of seawater sulfate of 8.6‰ (Holser et al., 1979). The major outcomes of this SO_2 disproportionation study are the following points:

- We present for the first time a thorough study on the oxygen isotope signature of SO_2 disproportionation at temperatures between 150–320°C.
- The disproportionation of SO_2 at hydrothermal temperatures produces HSO_4^- with an oxygen isotope composition in the range of 6 to 10‰. The produced HSO_4^- will obtain an oxygen isotope composition in the range of the seawater sulfate independent if it retains the initial oxygen isotope fractionation of the SO_2 disproportionation (~10.5‰) or if HSO_4^- equilibrates its oxygen isotopes with the hydrothermal fluid.
- We report for the first time the sulfur isotope composition of the SO_2 source in a marine hydrothermal system of 12.0‰.
- The $\Delta^{34}\text{S}_{\text{HSO}_4^- \leftrightarrow \text{S}^0}$ and the $\Delta^{18}\text{O}_{\text{HSO}_4^- \leftrightarrow \text{H}_2\text{O}}$ in the hydrothermal fluid at North Su revealed two different equilibrium exchange temperatures due to differences in the exchange velocity between the sulfur and oxygen isotopes. This difference can be used as a tool to measure the relative speed of the fluid ascent, whereas smaller equilibrium temperature difference is an indication for fast fluid ascent and *vice versa*.

It is not possible so far to quantify the volcanic SO_2 discharge into the seawater, but the comparison to terrestrial volcanoes shows that emissions of SO_2 outweigh the emissions of H_2S . Thus, we assume similar conditions in the marine environment, where SO_2 was abundantly contributed over the geological past into hydrothermal systems. Therefore the disproportionation of magmatic SO_2 with its specific oxygen isotope signature must act like an anchor for the oxygen isotope composition of seawater sulfate. As a result, the disproportionation of SO_2 is most probably responsible for the smaller variations observed in the oxygen isotope record of seawater sulfate compared to the large variations observed in the sulfur isotope record (see Claypool et al., 1980).

4.7. Acknowledgments

The authors would like to thank Captain Lutz Mallon and the crew of the RV Sonne, the operation team of the ROV Quest 4000 from the MARUM for providing us with samples under these difficult conditions and the other scientist on board, which made the BAMBUS cruise an unforgettable journey. We thank Jeffrey S. Seewald for borrowing us the IGT water samplers, which enabled the direct sampling of hydrothermal fluids. We would like to acknowledge Timothy G. Ferdelman and Marcel M.M. Kuypers from the Max Planck Institute for Marine Microbiology for their support. This study was funded by the German Research Foundation (DFG) and the Max Planck Society (MPG).

4.8. References

- Alain K., Ollagnon M., Desbruyères D., Pagé A., Barbier G., Juniper S. K., Quérellou J. and Cambon-Bonavita M.-A. (2002) Phylogenetic characterization of the bacterial assemblage associated with mucous secretions of the hydrothermal vent polychaete *Paralvinella palmiformis*. *FEMS Microbiology Ecology* **42**, 463-476.
- Alt J. C., Shanks III W. C. and Jackson M. C. (1993) Cycling of sulfur in subduction zones: The geochemistry of sulfur in the Mariana Island Arc and back-arc trough. *Earth and Planetary Science Letters* **119**, 477-494.
- Alt J. C. (1995) Subseafloor processes in mid-ocean ridge hydrothermal systems, in *Seafloor Hydrothermal Systems: Physical, Chemical, Biological, and Geological Interactions, Geophys. Monogr. Ser.*, vol. **91**, edited by S. E. Humphris et al., pp. 85-114, AGU, Washington, D. C., doi:10.1029/GM091p0085.
- Auzende J.-M., Ishibashi J., Beaudoin Y., Charlou J.-L., Delteil J., Donval J.-P., Fouguet Y., Gouillou J.-P., Ildefonse B., Kimura H., Nishio Y., Radford-Knoery J. and Ruellan É. (2000) Les extrémités orientale et occidentale du bassin de Manus, Papouasie-Nouvelle-Guinée, explorées par submersible: la campagne Manaute. *Earth and Planetary Sciences* **331**, 119-126.
- Beaudoin Y., Scott S. D., Gorton M. P., Zajacz Z. and Halter W. (2007) Effects of hydrothermal alteration on Pb in the active PACMANUS hydrothermal field, ODP Leg 193, Manus Basin, Papua New Guinea: A LA-ICP-MS study. *Geochimica et Cosmochimica Acta* **71**, 4256-4278.
- Bernard A., Demaiffe D., Mattielli N. and Punongbayan R. S. (1991) Anhydrite-bearing pumices from Mount Pinatubo: further evidence for the existence of sulphur-rich silicic magmas. *Nature* **354**, 139-140.
- Betts, R. H. and Voss, R. H. (1970) The kinetics of oxygen exchange between the sulfite ion and water. *Canadian Journal of Chemistry* **48**, 2035-2041.
- Binns R. A. and Scott S. D. (1993) Actively forming polymetallic sulfide deposits associated with felsic volcanic rocks in the eastern Manus Back-Arc Basin, Papua New Guinea. *Economic Geology* **88**, 2226-2236.
- Binns R. A., Scott S. D., Bogdanov Y. A., Lisitsin A. P., Gordeev V. V., Gurvich E. G., Finlayson E. J., Boyd T., Dotter L. E., Wheller G. E. and Muravyev K. G. (1993) Hydrothermal oxide and gold-rich sulfate deposits of Franklin Seamount, Western woodlark Basin, Papua New Guinea. *Econ. Geol.* **88** (8), 2122-2135.

- Binns R. A., Scott S. D., Gemmell J. B., Crook K. and Shipboard Scientific Party (1997) The SuSu Knolls Hydrothermal Field, Eastern Manus Basin, Papua New Guinea. *Eos Trans. AGU* 78 (722), Fall Meet. Suppl. Abstract V22E-02.
- Bischoff J. L. and Seyfried W. E. (1978) Hydrothermal chemistry of seawater from 25° to 350°C. *American Journal of Science* **278**, 838-860.
- Bischoff J. L. and Rosenbauer R. J. (1984) The critical point and two-phase boundary of seawater, 200-500°C. *Earth and Planetary Science Letters* **68**, 172-180.
- Butterfield D. A., Nakamura K., Takano B., Lilley M. D., Lupton J. E., Resing J. A. and Roe K. K. (2011) High SO₂ flux, sulfur accumulation, and gas fractionation at an erupting submarine volcano. *Geology* **39** (9), 803-806.
- Chiba, H. and Sakai, H. (1985) Oxygen isotope exchange rate between dissolved sulfate and water at hydrothermal temperatures. *Geochimica et Cosmochimica Acta* **49**, 993-1000.
- Claypool G. E., Holser W. T., Kaplan I. R., Sakai H. and Zak I. (1980) The age curves of sulfur and oxygen isotopes in marine sulfate and their mutual interpretation. *Chemical Geology* **28**, 199-260.
- Cline J. D. (1969) Spectrophotometric determination of hydrogen sulfide in natural waters. *Limnology and Oceanography* **14**, 454-458.
- Coleman M. L. and Moore M. P. (1978) Direct Reduction of Sulfates to Sulfur Dioxide for Isotopic Analysis. *Analytical Chemistry* **50**, 1594-1595.
- Condie K. C. and Kröner A. (2013) The building blocks of continental crust: Evidence for a major change in the tectonic setting of continental growth at the end of the Archean. *Gondwana Research* **23**, 394-402.
- Coplen T. B. (2011) Guidelines and recommended terms for expression of stable-isotope-ratio and gas-ratio measurement results. *Rapid Commun. Mass Spectrom.* **25**, 2538-2560.
- Cowan J. and Cann J. (1988) Supercritical two-phase separation of hydrothermal fluids in the Troodos ophiolite. *Nature* **333**, 259-261.
- Craddock P. R., Bach W., Seewald J. S., Rouxel O. J., Reeves E. and Tivey M. K. (2010) Rare earth element abundances in hydrothermal fluids from the Manus Basin, Papua New Guinea: Indicators of sub-seafloor hydrothermal processes in back-arc basins. *Geochimica et Cosmochimica Acta* **74**, 5494-5513.
- Craddock P. R. and Bach W. (2010) Insights to magmatic-hydrothermal processes in the Manus back-arc basin as recorded by anhydrite. *Geochimica et Cosmochimica Acta* **74**, 5514-5536.
- Desbruyères D., Alayse-Danet A.-M., Ohta S. And the Scientific Parties of BIOLAU and STARMER Cruises (1994) Deep-sea hydrothermal communities in Southwestern Pacific back-arc basins (the North Fiji and Lau Basins): Composition, microdistribution and food web. *Marine Geology* **116**, 227-242.
- Desbruyères D., Hashimoto J. and Fabri M.-C. (2006) Composition and biogeography of hydrothermal vent communities in Western Pacific Back-Arc Basins. *Geophysical Monograph Series* **166**, 215-234.
- Druschel G. K., Schoonen M. A. A., Nordstrom D. K., Ball J. W., Xu Y. and Cohn C. A. (2003) Sulfur geochemistry of hydrothermal waters in Yellowstone National Park, Wyoming, USA. III. An anion-exchange resin technique for sampling and preservation of sulfoxyanions in natural waters. *Geochem. Trans.* **4**(3), 12-19.

- Eigen, M., Kustin, K., and Maass, G. (1961) Die Geschwindigkeit der Hydratation von SO₂ in wässriger Lösung. *Zeitschrift für Physikalische Chemie Neue Folge* **30**, 130-136.
- Elderfield H. and Schultz A. (1996) Mid-ocean ridge hydrothermal fluxes and the chemical composition of the ocean. *Annual Review of Earth and Planetary Sciences* **24**, 191-224.
- Fahey R. C. and Newton G. L. (1987) Determination of low-weight thiols using monobromobimane fluorescent labeling and high-performance liquid chromatography. *Methods in Enzymology* **143**, 85-96.
- Falvey D. A. and Pritchard T. (1985) Preliminary paleomagnetic results from northern Papua New Guinea: evidence for large microplate rotations. Transactions of the 3rd Circum-Pacific Council for Energy and Mineral Resources Conference, Honolulu, 593-599.
- Foustoukos D. I. and Seyfried Jr. W. E. (2007) Fluid Phase Separation Processes in Submarine Hydrothermal Systems. *Reviews in Mineralogy & Geochemistry* **65**, 213-239.
- Fox C. G. (1990) Consequences of Phase Separation on the Distribution of Hydrothermal Fluids at ASHES Vent Field, Axial Volcano, Juan de Fuca Ridge. *Journal of Geophysical Research* **95**, 12923-12926.
- Fritz, P., Basharmal, G. M., Drimmie, R. J., Ibsen, J., and Qureshi, R. M. (1989) Oxygen isotope exchange between sulphate and water during bacterial reduction of sulphate. *Chemical Geology (Isotope Geoscience Section)*, **79**, 99-105.
- Gamo T., Okamura K., Charlou J.-L., Urabe T., Auzende J.-M., Ishibashi J., Shitashima K., Chiba H. and Shipboard Scientific Party of the ManusFlux Cruise* (1997) Acidic and sulfate-rich hydrothermal fluids from the Manus back-arc basin, Papua New Guinea. *Geology* **25** (2), 139-142.
- Gerlach T. M. and Graeber E. J. (1985) Volatile budget of Kilauea volcano. *Nature* **313**, 273-277.
- Habicht K. S., Canfield D. E. and Rethmeier J. (1998) Sulfur isotope fractionation during bacterial reduction and disproportionation of thiosulfate and sulfite. *Geochimica et Cosmochimica Acta* **62**, 2585-2595.
- Hager S. A., Gerlach T. M. and Wallace P. J. (2008) Summit CO₂ emission rates by the CO₂/SO₂ ratio method at Kilauea Volcano, Hawai'i, during a period of sustained inflation. *Journal of Volcanology and Geothermal Research* **177**, 875-882.
- Hannington M., Herzig P., Stoffers P., Scholten J., Botz R., Garbe-Schönberg D., Jonasson I. R., Roest W. and Shipboard Scientific Party (2001) First observations of high-temperature submarine hydrothermal vents and massive anhydrite deposits off the north coast of Iceland. *Marine Geology* **177**, 199-220.
- Holland H. D. (1965) Some applications of thermochemical data to problems of ore deposits II. Mineral assemblages and the composition of ore-forming fluids. *Economic Geology* **60**, 1101-1166.
- Holser W. T., Kaplan I. R., Sakai H. and Zak I. (1979) Isotope geochemistry of oxygen in the sedimentary sulfate cycle. *Chemical Geology* **25**, 1-17.
- Holt, B. D., Cunningham, P. T., Engelkemeir, A. G., Graczyk, D. G., and Kumar, R. (1983) Oxygen-18 study of nonaqueous-phase oxidation of sulfur dioxide. *Atmospheric Environment* **17**, 625-632.

- Holt, B. D., Kumar, R., and Cunningham, P. T. (1981) Oxygen-18 study of the aqueous-phase oxidation of sulfur dioxide. *Atmospheric Environment* **15**, 557-566.
- Horner, D. A. and Connick, R. E. (2003) Kinetics of Oxygen Exchange between the Two Isomers of Bisulfite Ion, Disulfite Ion ($S_2O_5^{2-}$), and Water As Studied by Oxygen-17 Nuclear Magnetic Resonance Spectroscopy. *Inorg. Chem.* **42**, 1884-1894.
- Hrischeva E., Scott S. D. and Weston R. (2007) Metalliferous Sediments Associated with Presently Forming Volcanogenic Massive Sulfides: The SuSu Knolls Hydrothermal Field, Eastern Manus Basin, Papua New Guinea. *Economic Geology* **102**, 55-73.
- Iwasaki I. and Ozawa T. (1960) Genesis of sulfate in acid hot spring. *Bull. Chem. Soc. Jpn.* **33** (7), 1018-1019.
- Kaasalainen H. and Stefánsson A. (2011) Sulfur speciation in natural hydrothermal waters, Iceland. *Geochimica et Cosmochimica Acta* **75**, 2777-2791.
- Kamyshny Jr. A., Borkenstein C. G. and Ferdelman T. G. (2009) Protocol for Quantitative Detection of Elemental Sulfur and Polysulfide Zero-Valent Sulfur Distribution in Natural Aquatic Samples. *Geostandards and Geoanalytical Research* **33**, 415-435.
- Kaplan I. R. and Hulton J. R. (1966) The isotopic abundance and content of sulfur in meteorites. *Geochimica et Cosmochimica Acta* **30**, 479-496.
- Kelley D. S., Baross J. A. and Delaney J. R. (2002) Volcanoes, fluids, and life at mid-ocean ridge spreading centers. *Annual Reviews in Earth and Planetary Science* **30**, 385-491.
- Khokhar M. F., Frankenberg C., Van Roozendaal M., Beirle S., Kühl S., Richter A., Platt U. and Wagner T. (2005) Satellite observations of atmospheric SO_2 from volcanic eruptions during the time-period of 1996-2002. *Advances in Space Research* **36**, 879-887.
- Kusakabe M. and Komoda Y. (1992) Sulfur Isotopic Effects in the Disproportionation Reaction of Sulfur Dioxide at Hydrothermal Temperatures. *Rept. Geol. Surv. Japan* **279**, 93-96.
- Kusakabe, M., Komoda, Y., Takano, B. and Abiko, T. (2000) Sulfur isotopic effects in the disproportionation reaction of sulfur dioxide in hydrothermal fluids: implications for the $\delta^{34}S$ variations of dissolved bisulfate and elemental sulfur from active crater lakes. *Journal of Volcanology and Geothermal Research* **97**, 287-307.
- Lalou C. (1991) Deep-sea hydrothermal venting: A recently discovered marine system. *Journal of Marine Systems* **1**, 403-440.
- Lalou C., Reyss J.-L., Brichet E., Rona P. A. and Thompson G. (1995) Hydrothermal activity on a 10^5 -year scale at a slow-spreading ridge, TAG hydrothermal field, Mid-Atlantic Ridge 26°N. *Journal of Geophysical Research* **100**, 17855-17862.
- Lloyd, R. M. (1967) Oxygen-18 Composition of Oceanic Sulfate. *Science* **156**, 1228-1231.
- Lloyd, R. M. (1968) Oxygen Isotope Behavior in the Sulfate-Water System. *Journal of Geophysical Research* **73**, 6099-6110.
- Ludwig K. A., Kelley D. S., Butterfield D. A., Nelson B. K. and Früh-Green G. (2006) Formation and evolution of carbonate chimneys at the Lost City Hydrothermal Field. *Geochimica et Cosmochimica Acta* **70**, 3625-3645.

- Ludwig K. A., Shen C.-C., Kelley D. S., Cheng H. and Edwards R. L. (2011) U-Th systematics and ²³⁰Th ages of carbonate chimneys at the Lost City Hydrothermal Field. *Geochimica et Cosmochimica Acta* **75**, 1869-1888.
- Lupton J., Lilley M., Butterfield D., Evans L., Embley R., Massoth G., Christenson B., Nakamura K. and Schmidt M. (2008) Venting of a separate CO₂-rich gas phase from submarine arc volcanoes: Examples from the Mariana and Tonga-Kermadec arcs. *Journal of Geophysical Research* **113**, 1-21.
- Makishima A., Mackenzie J. D. and Hammel J. J. (1979) The leaching of phase-separated sodium borosilicate glasses. *Journal of Non-Crystalline Solids* **31**, 377-383.
- Marques A. F. A., Barriga F. J. A. S. and Scott S. D. (2007) Sulfide mineralization in an ultramafic-rock hosted seafloor hydrothermal system: From serpentinization to the formation of Cu-Zn-(Co)-rich massive sulfides. *Marine Geology* **245**, 20-39.
- Martinez F. and Taylor B. (1996) Backarc Spreading, Rifting, and Microplate Rotation, Between Transform Faults in the Manus Basin. *Marine Geophysical Researches* **18**, 203-224.
- Marinez F. and Taylor B. (2003) Controls on back-arc crustal accretion: insights from the Lau, Manus and Mariana basins. *Geological Society, London, Special Publications* **219**, 19-54.
- McCollom T. M. and Shock E. L. (1997) Geochemical constraints on chemolithoautotrophic metabolism by microorganisms in seafloor hydrothermal systems. *Geochimica et Cosmochimica Acta* **61**, 4375-4391.
- Menyailov I. A., Nikitina L. P., Shapar V. N. and Pilipenko V. P. (1986) Temperature increase and chemical change of fumarolic gases at Momotombo Volcano, Nicaragua in 1982-1985: Are these indicators of a possible eruption? *Journal of Geophysical Research* **91**, 12199-12214.
- Mizutani Y. and Rafter T. A. (1969) Oxygen isotopic composition of sulphates—Part 3. Oxygen isotopic fractionation in the bisulphate ion-water system. *N.Z. J. Sci.* **12**, 54-59.
- Mizutani, Y. and Rafter, T. A. (1973) Isotopic behaviour of sulphate oxygen in the bacterial reduction of sulphate. *Geochemical Journal* **6**, 183-191.
- Monnin C., Balleur S. and Goffe B. (2003) A thermodynamic investigation of barium and calcium sulfate stability in sediments at an oceanic ridge axis (Juan de Fuca, ODP legs 139 and 169). *Geochimica et Cosmochimica Acta* **67**, 2965-2976.
- Nakamura K., Kato Y., Tamaki K. and Ishii T. (2007) Geochemistry of hydrothermally altered basaltic rocks from the Southwest Indian Ridge near the Rodriguez Triple Junction. *Marine Geology* **239**, 125-141.
- Newton R. C. and Manning C. E. (2005) Solubility of Anhydrite, CaSO₄, in NaCl-H₂O Solutions at High Pressures and Temperatures: Applications to Fluid-Rock Interaction. *Journal of Petrology* **46**, 701-716.
- Ohmoto H. and Lasaga A. C. (1982) Kinetics of reactions between aqueous sulfates and sulfides in hydrothermal systems. *Geochimica et Cosmochimica Acta* **46**, 1727-1745.
- Petersen J. M., Zielinski F. U., Pape T., Seifert R., Moraru C., Amann R., Hourdez S., Girguis P. R., Wankel S. D., Barbe V., Pelletier E., Fink D., Borowski C., Bach W. and Dubilier N. (2011) Hydrogen is an energy source for hydrothermal vent symbioses. *Nature* **476**, 176-180.

- Rees C. E., Jenkins W. J. and Monster J. (1978) The sulphur isotopic composition of ocean water sulphate*. *Geochimica et Cosmochimica Acta* **42**, 377-381.
- Reeves E. P., Seewald J. S., Saccoccia P., Bach W., Craddock P. R., Shanks W. C., Sylva S. P., Walsh E., Pichler T., Rosner M. (2011) Geochemistry of hydrothermal fluids from the PACMANUS, Northeast Pual and Vienna Woods hydrothermal fields, Manus Basin, Papua New Guinea. *Geochimica et Cosmochimica Acta* **75**, 1088-1123.
- Riedinger, N., Brunner, B., Formolo, M. J., Solomon, E., Kasten, S., Strasser, M. and Ferdelman, T. G. (2010) Oxidative sulfur cycling in the deep biosphere of the Nankai Trough, Japan. *Geology* **38**, 851-854.
- Roberts S., Bach W., Binns R. A., Vanko D. A., Yeats C. J., Teagle D. A. H., Blacklock K., Blusztajn J. S., Boyce A. J., Cooper M. J., Holland N. and McDonald B. (2003) Contrasting evolution of hydrothermal fluids in the PACMANUS system, Manus Basin; the Sr and S isotope evidence. *Geology* **31**, 805-808.
- Robinson B. W. (1973) Sulphur isotope equilibrium during sulphur hydrolysis at high temperatures. *Earth and Planetary Science Letters* **18**, 443-450.
- Rong L., Lim L. W. and Takeuchi T. (2005) Determination of Iodide and Thiocyanate in Seawater by Liquid Chromatography with Poly(ethylene glycol) Stationary Phase. *Chromatographia* **61**, 371-374.
- Rye R. O., Luhr J. F. and Wasserman M. D. (1984) Sulfur and oxygen isotopic systematics of the 1982 eruptions of El Chichón volcano, Chiapas, Mexico. *Journal of Volcanology and Geothermal Research* **23**, 109-123.
- Rye R. O. (2005) A review of the stable-isotope geochemistry of sulfate minerals in selected igneous environments and related hydrothermal systems. *Chemical Geology* **215**, 5-36.
- Sakai H. (1957) Fractionation of sulphur isotope composition in nature. *Geochimica et Cosmochimica Acta* **12**, 150-169.
- Sakai H. (1968) Isotopic properties of sulfur compounds in hydrothermal processes. *Geochemical Journal* **2**, 29-49.
- Sakai H., Des Marais D. J., Ueda A. and Moore J. G. (1984) Concentrations and isotope ratios of carbon, nitrogen and sulfur in ocean-floor basalts. *Geochimica et Cosmochimica Acta* **48**, 2433-2441.
- Sarrazin J. and Juniper K. (1999) Biological characteristics of a hydrothermal edifice mosaic community. *Marine Ecology Progress Series* **185**, 1-19.
- Schmidt K., Garbe-Schönberg D., Koschinsky A., Strauss H., Jost C. L., Klevenz V. and Königer P. (2011) Fluid elemental and stable isotope composition of the Nibelungen hydrothermal field (8°18'S, Mid-Atlantic Ridge): Constraints on fluid-rock interaction in heterogeneous lithosphere. *Chemical Geology* **280**, 1-18.
- Seal II R. R. (2006) Sulfur Isotope Geochemistry of Sulfide Minerals. *Reviews in Mineralogy & Geochemistry* **61**, 633-677.
- Seewald J. S., Doherty K. W., Hammar T. R. and Liberatore S. P. (2001) A new gas-tight isobaric sampler for hydrothermal fluids. *Deep-Sea Research I* **49**, 189-196.
- Sinton J. M., Ford L. L., Chappell B. and McCulloch M. T. (2003) Magma Genesis and Mantle Heterogeneity in the Manus Back-Arc Basin, Papua New Guinea. *Journal of Petrology* **44**, 159-195.

- Sizova E., Gerya T., Brown M. and Perchuk L. L. (2010) Subduction styles in the Precambrian: Insight from numerical experiments. *Lithos* **116**, 209-229.
- Spycher N. F. and Reed M. H. (1988) Fugacity coefficients of H₂, CO₂, CH₄, H₂O and of H₂O-CO₂-CH₄ mixtures: A virial equation treatment for moderate pressures and temperatures applicable to calculations of hydrothermal boiling. *Geochimica et Cosmochimica Acta* **52**, 739-749.
- Sun W. D., Binns R. A., Fan A. C., Kamenetsky V. S., Wysoczanski R., Wei G. J., Hu Y. H. and Arculus R. J. (2007) Chlorine in submarine volcanic glasses from the eastern Manus basin. *Geochimica et Cosmochimica Acta* **71**, 1542-1552.
- Sutton A. J., Elias T., Gerlach T. M. and Stokes J. B. (2001) Implications for eruptive processes as indicated by sulfur dioxide emissions from Kilauea Volcano, Hawai'i, 1979-1997. *Journal of Volcanology and Geothermal Research* **108**, 283-302.
- Tarasov V. G., Gebruk A. V., Mironov A. N. and Moskalev L. I. (2005) Deep-sea and shallow-water hydrothermal vent communities: Two different phenomena? *Chemical Geology* **224**, 5-39.
- Taylor B. (1979) Bismarck Sea: Evolution of a back-arc basin. *Geology* **7**, 171-174.
- Taylor B., Crook K. A. W. and Sinton J. M. (1994) Extensional transform zones and oblique spreading centers. *Journal of Geophysical Research* **99**, 19707-19718.
- Tivey M. K. (1995) The influence of hydrothermal fluid composition and advection rates on black smoker chimney mineralogy: Insights from modeling transport and reaction. *Geochimica et Cosmochimica Acta* **59**, 1933-1949.
- Tregoning P., Jackson R. J., McQueen H., Lambeck K., Stevens C., Little R. P., Curley R. and Rosa R. (1999) Motion of the South Bismarck Plate, Papua New Guinea. *Geophysical Research Letters* **26**(23), 3517-3520.
- Turchyn, A. V. and Schrag, D. P. (2004) Oxygen Isotope Constraints on the Sulfur Cycle over the Past 10 Million Years. *Science* **303**, 2004-2007.
- Turchyn A. V. and Schrag D. P. (2006) Cenozoic evolution of the sulfur cycle: Insight from oxygen isotopes in marine sulfate. *Earth and Planetary Science Letters* **241**, 763-779.
- Ueda A. and Krouse H. R. (1986) Conversion of sulphide and sulphate minerals to SO₂ for isotope analyses. *Geochemical Journal* **20**, 209-212.
- Ueno Y., Ono S., Rumble D. and Maruyama S. (2008) Quadruple sulfur isotope analysis of ca. 3.5 Ga Dresser Formation: New evidence for microbial sulfate reduction in the early Archean. *Geochimica et Cosmochimica Acta* **72**, 5675-5691.
- van Hunen J. and van den Berg A. P. (2008) Plate tectonics on the early Earth: Limitations imposed by strength and buoyancy of subducted lithosphere. *Lithos* **103**, 217-235.
- Vetter R. D., Matrai P. A., Javor B. and O'Brian J. (1989) Reduced sulfur compounds in the marine environment, in Saltzman, E. S., and Cooper, W. J., eds., Biogenic sulfur in the environment: Washington, D.C., American Chemical Society, 243-261.
- Von Glasow R., Bobrowski N. and Kern C. (2009) The effects of volcanic eruptions on atmospheric chemistry. *Chemical Geology* **263**, 131-142.
- Walton, G. and George H. Walden, J. (1946a) The Contamination of Precipitated Barium Sulfate by Univalent Cations. *Journal of the American Chemical Society* **68**, 1742-1750.

- Walton, G. and George H. Walden, J. (1946b) The Nature of the Variable Hydration of Precipitated Barium Sulfate. *Journal of the American Chemical Society* **68**, 1750-1753.
- Webber A. P., Roberts S., Burgess R. and Boyce A. J. (2011) Fluid mixing and thermal regimes beneath the PACMANUS hydrothermal field, Papua New Guinea: Helium and oxygen isotope data. *Earth and Planetary Science Letters* **304**, 93-102.
- Williams S. N., Sturchio N. C., Calvache M. L. V., Mendez R. F., Londoño A. C. and García N. P. (1990) Sulfur dioxide from Nevado del Ruiz volcano, Colombia: total flux and isotopic constraints on its origin. *Journal of Volcanology and Geothermal Research* **42**, 53-68.
- Xu Y. and Schoonen M. A. A. (1995) The stability of thiosulfate in the presence of pyrite in low-temperature aqueous solutions. *Geochimica et Cosmochimica Acta* **59**, 4605-4622.
- Xu Y., Schoonen M. A. A., Nordstrom D. K., Cunningham K. M. and Ball J. W. (2000) Sulfur geochemistry of hydrothermal waters in Yellowstone National Park, Wyoming, USA. II. Formation and decomposition of thiosulfate and polythionate in Cinder Pool. *Journal of Volcanology and Geothermal Research* **97**, 407-423.
- Zeebe, R. E. (2010) A new value for the stable oxygen isotope fractionation between dissolved sulfate ion and water. *Geochimica et Cosmochimica Acta* **74**, 818-828.
- Zeng Z., Ouyang H., Yin X., Chen S., Wang X. and Wu L. (2012) Formation of Fe-Si-Mn oxyhydroxides at the PACMANUS hydrothermal field, Eastern Manus Basin: Mineralogical and geochemical evidence. *Journal of Asian Earth Sciences* **60**, 130-146.
- Zhang, J.-Z. and Millero, F. J. (1991) The rate of sulfite oxidation in seawater. *Geochimica et Cosmochimica Acta* **55**, 677-685.
- Zielinski F. U., Gennerich H.-H., Borowski C., Wenzhöfer F. and Dubilier N. (2011) In situ measurements of hydrogen sulfide, oxygen, and temperature in diffuse fluids of an ultramafic-hosted hydrothermal vent field (Logatchev, 14°45'N, Mid-Atlantic Ridge): Implications for chemosymbiotic bathymodiolin mussels. *Geochemistry Geophysics Geosystems* **12**, 1-21.
- Zopfi J., Ferdelman T. G. and Fossing H. (2004) Distribution and fate of sulfur intermediates – sulfite, tetrathionate, thiosulfate, and elemental sulfur – in marine sediments. *Geological Society of America Special Paper* 379, 97-116.

5. Synthesis and outlook

5.1. Synthesis

The work of this dissertation revealed the significant role of SO_3^{2-} in shaping the oxygen isotope composition of the SO_4^{2-} during the oxidative part of the sulfur cycle and in form of SO_2 sulfite seems to be even an important compound for the oxygen isotope composition of seawater sulfate. In this work I could show the elaborate way to determine the oxygen isotope equilibrium fractionation between sulfite species and water, which is a fundamental value for the further oxidation experiments in which I could show strong evidence that SO_3^{2-} is the final sulfoxy intermediate and therefore has to be included in the interpretation of the oxygen isotope composition of SO_4^{2-} from the oxidation of reduced sulfur compounds. In the final project I could demonstrate with our SO_2 disproportionation experiments that its specific oxygen isotope signature might be highly relevant for the interpretation of the oxygen isotope composition of seawater sulfate. In the following I will repeat the three studies, try to express the link between them and indicate the importance of them in the broader context of sulfur cycling.

As mentioned before the oxygen isotope composition of SO_4^{2-} is highly important to identify in the natural environment the processes of sulfur cycling. Sulfate does not exchange its oxygen isotopes with water with the exception of extreme pH-, temperature-conditions (Lloyd, 1968; Chiba and Sakai, 1985) what makes its oxygen isotope composition the ideal archive of oxidative processes of the sulfur cycle. Sulfite was often mentioned to be the final intermediate during the oxidation of reduced sulfur compounds (Druschel and Borda, 2006) and in contrast to the inert SO_4^{2-} , SO_3^{2-} rapidly exchange its oxygen with the water (Horner and Connick, 2003), but to date thorough research on the effect of SO_3^{2-} on the oxygen isotope composition of SO_4^{2-} is lacking. There are only some studies on the isotopic patterns of SO_2 as it is a major anthropogenic pollutant and thereof, one study analyzed the value of the oxygen isotope equilibrium fractionation between gaseous SO_2 and water vapor ($\sim 24\%$, Holt, 1983). Without knowing the actual isotopic properties of sulfite it was still often mentioned in studies to explain certain oxygen isotope signatures which were not understood properly. Therefore it was a fundamental task to investigate the oxygen isotope patterns of SO_3^{2-} with respect to water and with respect to its role as important sulfoxy intermediate.

With the anoxic oxygen exchange experiments with sodium sulfite in isotopically distinct solution and the adequate SO_3^{2-} precipitation techniques for subsequent oxygen isotope measurements, it was possible to pinpoint the oxygen isotope equilibrium fractionation between SO_3^{2-} and water ($\epsilon^{18}\text{O}_{\text{SO}_3^{2-} \leftrightarrow \text{H}_2\text{O}} = 15.2\%$) and to give a rough estimate for the oxygen isotope equilibrium fractionation between $\text{SO}_2(\text{aq})$ and water ($\epsilon^{18}\text{O}_{\text{SO}_2(\text{aq}) \leftrightarrow \text{H}_2\text{O}} = 37.0\%$).

The determined equilibrium value helps to narrow the responsible isotope effects for the apparent oxygen isotope equilibrium between the residual SO_4^{2-} during dissimilatory sulfate reduction (DSR) and water. The oxygen isotope composition of the residual SO_4^{2-} during DSR is approaching a plateau value that is dependent on the oxygen isotope

composition of the water (Mizutani and Rafter, 1973), which was explained by the indirect oxygen isotope exchange via sulfoxy intermediates during the DSR. Sulfite and adenosine-5'-phosphosulfate (APS) were thought to be responsible for the DSR mediated oxygen exchange. In case of the SO_3^{2-} the oxygen exchange could run on one side via the oxygen that is supplied from adenosine monophosphate (AMP) during the re-oxidation and on the other side the direct oxygen exchange with the cell-internal water (Wortmann et al., 2007). The study by Brunner et al. (2012) and Kohl et al. (2012) revealed that APS does not exchange its oxygen with water and from the determined value for the oxygen isotope equilibrium exchange fractionation between SO_3^{2-} and water (15.2‰) we can also exclude the direct oxygen exchange between SO_3^{2-} and water from being responsible for the high DSR mediated oxygen equilibrium fractionation between HSO_4^- and water (~29‰, Fritz et al., 1989). Therefore, it seems that the relevant oxygen exchange mechanism is related to the AMP. The AMP eventually exchanges its oxygen directly with the cell-internal water and the oxygen atom that is used to re-oxidize the SO_3^{2-} might undergo as well a certain isotope fractionation during the reversible enzymatic step.

Changing our focus on the oxidative part of sulfur cycling we could use the value for the oxygen isotope equilibrium fractionation between SO_3^{2-} and water to identify the role of SO_3^{2-} as final sulfoxy intermediate during the oxidation of reduced sulfur compounds. We performed SO_3^{2-} oxidation experiments described in chapter 3 to investigate the influence of different oxidizing conditions such as the pH of the solution or the presence or absence of O_2 and Fe^{3+} as oxidants.

Our experiments revealed that SO_3^{2-} only fully exchanged its oxygen with the water before being oxidized at pH 1 and in the absence of Fe^{3+} , but in the other experiments at higher pH or in the presence of Fe^{3+} the oxidation rate is faster than the oxygen exchange rate between sulfite and water. From this finding we can say that under most natural conditions SO_3^{2-} retains the oxygen isotope signature of its production process before being oxidized. This enables to make further statements on how the SO_3^{2-} was produced from the oxygen isotope composition of SO_4^{2-} . As consequence of the chemical conditions during the oxidation of reduced sulfur compounds the SO_3^{2-} will exchange more or less of its oxygen with the water and plays therefore a major role on how much oxygen of water or O_2 will be incorporated in the final product SO_4^{2-} . This explains the observation of varying relative contributions of oxygen sources from water or O_2 into the sulfate in pyrite oxidation studies (see Balci et al., 2007 and references therein) and explains as well the differences in the oxygen isotope composition of SO_4^{2-} . The obtained offset between the oxygen isotope composition of the SO_4^{2-} and the water in our experiments range between 5.9‰ (experiment at pH 1 and Fe^{3+} as sole oxidant) and 17.9‰ (experiment at pH 1 and O_2 as sole oxidant) and cover the observed range of oxygen isotope offsets between SO_4^{2-} and water in natural environments ($\Delta^{18}\text{O}_{\text{SO}_4\text{-H}_2\text{O}}$ values from 3.9‰ to 13.6‰, by Hubbard et al., 2009). In addition our experiments revealed similar oxygen isotope fractionation factors as obtained in oxidation studies on reduced sulfur compounds (Balci et al., 2007). Our oxidation experiments reveal a smooth explanation for the apparently inverse oxygen isotope effect between SO_4^{2-} and water observed in studies on the oxidation of reduced sulfur compounds with the combination of oxygen isotope exchange between SO_3^{2-} and water (^{18}O goes preferentially into SO_3^{2-}) and normal isotope fractionation during the oxidation of SO_3^{2-} .

to SO_4^{2-} . The findings of the SO_3^{2-} oxidation experiments give strong evidence that SO_3^{2-} is the final sulfoxy intermediate during the oxidation of reduced sulfur compounds.

The biggest reservoir of SO_4^{2-} on our planet is the water in our oceans with concentrations of approximately 28 mM. The seawater sulfate drives the metabolism of sulfate reducers in the anoxic sediments so that they can oxidize the organic matter in the absence of O_2 . Geological records of the stable isotope composition of the seawater sulfate revealed strong fluctuations in the sulfur isotope record and smaller fluctuations in the oxygen isotope record, whereas the factors causing the fluctuations of the $\delta^{18}\text{O}_{\text{SO}_4^{2-}}$ seem not to be identical as for the $\delta^{34}\text{S}_{\text{SO}_4^{2-}}$ (Claypool et al., 1980). The reason for the decoupled isotopic behavior of the two elements is not known to date.

During the SO-216 expedition to the eastern Manus Basin, Papua New Guinea, we had the chance to analyze the sulfur chemistry and analyze the isotope compositions of the sulfur compounds in a hydrothermal fluid that was driven by the disproportionation of magmatic SO_2 . The pH of the hydrothermal fluid was extremely low (pH 1.2) and we could not see any sign of life in the near proximity. Instead we discovered massive amounts of liquid and solidified S^0 and high discharge of HSO_4^- . The stable isotope analyses of the HSO_4^- revealed an oxygen isotope composition of approximately 7.8‰ and a sulfur isotope composition of approximately 19.5‰ which is in the range of the isotope composition of the modern seawater sulfate ($\delta^{18}\text{O} = 8.6\text{‰}$, Holser et al., 1979; $\delta^{34}\text{S} = 21.0\text{‰}$, Rees et al., 1978). From the literature it is known that the sulfur isotope signature of SO_2 disproportionation is strongly temperature dependent (e.g. Kusakabe et al., 2000), but studies on the oxygen isotope signature during this process are lacking. To find out more about the oxygen isotope signature of SO_2 disproportionation we performed laboratory experiments at temperatures in the range of hydrothermal fluids.

The results of the SO_2 disproportionation experiments produced HSO_4^- with an oxygen isotope composition ranging from 6‰ to 10‰ which is close to the known oxygen isotope composition of the seawater sulfate proving that our observations in North Su were not just coincidence. The oxygen isotope signature is retaining the initial oxygen isotope fractionation of the disproportionation or approaches the oxygen isotope equilibrium fractionation with respect to the water, but interestingly at these high temperatures the values of the oxygen isotope composition of HSO_4^- will always fall in the same range. To make further statements on the consequences of this observation for the seawater sulfate we need to know the magmatic SO_2 flux in hydrothermal systems at the seafloor. There are many studies that measured significant SO_2 emissions at terrestrial volcanoes, whereas there are only few studies in the marine realm. Anyhow, there is a study by Butterfield et al. (2011) that reported massive discharge of HSO_4^- and SO_2 from the disproportionation of magmatic SO_2 in hydrothermal fluids of a submarine volcano at the Mariana Arc and speculated that this process could contribute significantly to the global sulfur budget in the oceans. Therefore the disproportionation of magmatic SO_2 with its specific oxygen isotope signature could be an anchor for the oxygen isotope composition of the seawater sulfate and would explain the smaller fluctuations in the oxygen isotope record of the seawater sulfate over geological time scales.

In conclusion this dissertation reveals the pivotal role of SO_3^{2-} as final sulfoxy intermediate in shaping the oxygen isotope composition of SO_4^{2-} during the oxidation of reduced sulfur compounds and shows that SO_3^{2-} has to be always considered in the interpretation of the oxygen isotope composition of SO_4^{2-} produced during oxidative

sulfur cycling. This work demonstrates the power of isotope mass balance approaches in explaining the mechanisms of nebulous biogeochemical processes and the new finding on the significant role of SO_2 disproportionation for the oxygen isotope composition of seawater sulfate is essential for the interpretation of the geological record of the oxygen isotope composition of seawater sulfate.

5.2. Outlook

In this section I want to sum up some points that were mentioned in my work but were only marginally discussed and needs to be investigated more in detail in future research.

This work is the first in its kind which investigated thoroughly the role of SO_3^{2-} for the oxygen isotope composition of SO_4^{2-} and could give some new insights that are important for the interpretation of the oxygen isotope composition of SO_4^{2-} in natural environments. However, there are more experiments to perform to understand properly the oxygen isotope signature in SO_4^{2-} and this work was a small contribution and a starting point from a SO_3^{2-} perspective. The work of my dissertation revealed that differences in the concentrations of $\text{O}_2(\text{aq})$, of SO_3^{2-} and of Fe^{3+} influence as well the oxygen isotope effects during the oxidation of SO_3^{2-} to SO_4^{2-} to some extent, an observation which is important for most isotope studies. It is important to assess these concentration patterns and to investigate if they are more related to the experimental conditions with its high concentrations (much higher than in most natural environments) or could play as well a role in natural environments. By measuring the oxygen isotope fractionation of the O_2 in the gas-phase, we obtained inverse isotope fractionations, where ^{18}O was preferentially consumed during the oxidation of SO_3^{2-} , whereas Oba and Poulson (2009) obtained a normal isotope effect with ^{16}O being preferentially consumed during the oxidation of SO_3^{2-} . We explained this difference in chapter 3 with the lower concentration in the experiments of Oba and Poulson, however, these concentration dependent differences in the oxygen isotope effects needs to be investigated more in detail.

Another attempt is to investigate more the role of dissolved Fe^{3+} as oxidant of reduced sulfur compounds. Chapter 3 demonstrated that the availability of Fe^{3+} has a strong impact on the oxygen isotope composition of SO_4^{2-} which must be visible in natural environments. As mentioned in chapter 3, the availability of ferric iron could explain the observed differences between the oxygen isotope compositions of the SO_4^{2-} produced in the initial phase and in the main phase of microbial pyrite oxidation (Brunner et al., 2008). During the initial phase of pyrite leaching O_2 is the dominant oxidant producing SO_4^{2-} with a heavy oxygen isotope composition, but in the main oxidation phase Fe^{3+} accumulated to a higher extent and the oxidation of reduced sulfur compounds will run via the anoxic oxidation by Fe^{3+} .

The oxygen isotope signature of SO_2 disproportionation in hydrothermal sites at the seafloor might be the anchor for the oxygen isotope composition of seawater sulfate, but how stable the contribution of magmatic SO_2 into the seawater is over geological time scales is not clear. Eventually it is possible to find out by comparison with other approximations for the tectonic activity as the subduction of tectonic plate is closely related to the production of new oceanic lithosphere at mid ocean ridges. Comparison of the oxygen isotope record of seawater sulfate (Claypool et al., 1980) with the strontium

isotope record (Veizer et al., 1999) demonstrate already the problems of such a comparison, on one side the resolution of the oxygen isotope record is not so precise and minor fluctuations might be overseen. On the other side, the ratio of the strontium isotopes ($^{87}\text{Sr}/^{86}\text{Sr}$) does not only depend on the hydrothermal flux of the mantle but also on the flux of strontium from the weathering of the continents, and during times with active mountain building (e.g. Himalayan Orogeny) the high input from the weathering will make it impossible to recognize the hydrothermal signal anymore (Veizer et al., 1999). Thus we have to search for other geochemical tracers that indicate more clearly the input from the mantle or the tectonic activity and improve the oxygen isotope record of the seawater sulfate. Baker et al. (2002) compared the input of hydrothermal vent sites along different plate segments of the East Pacific Rise where new oceanic lithosphere is formed at different spreading rates. Similar studies at hydrothermal sites related to subduction zones would be highly interesting and necessary to see if differences in the speed of the subducting plate correlate with the hydrothermal activity and its discharge of chemical compounds.

The observed differences in the equilibrium exchange temperatures between the sulfur isotope fractionation between HSO_4^- and S^0 and the oxygen isotope fractionation between the HSO_4^- and the hydrothermal fluid at North Su reveal the possibility to use the different isotope properties of the two elements as a tool to measure the relative speed of the hydrothermal fluid ascent to the seafloor. From approximations of the thermal gradient the depth of the respective equilibrium temperature could be estimated, further experiments on SO_2 disproportionation need to be performed to determine the exact time that the oxygen isotope system needs to approach the isotope equilibrium and mathematic models might help to develop the relative ascent speed estimate into a more accurate speedometer.

5.3. References

- Baker E. T., Hey R. N., Lupton J. E., Resing J. A., Feely R. A., Gharib J. J., Massoth G. J., Sansone F. J., Kleinrock M., Martinez F., Naar D. F., Rodrigo C., Bohnenstiehl D. and Pardee D. (2002) Hydrothermal venting along Earth's fastest spreading center: East Pacific Rise, 27.5°-32.3°S. *Journal of Geophysical Research* **107**, 1-14.
- Balci N., Shanks III W. C., Mayer B. and Mandernack K. W. (2007) Oxygen and sulfur isotope systematics of sulfate produced by bacterial and abiotic oxidation of pyrite. *Geochimica et Cosmochimica Acta* **71**, 3796-3811.
- Brunner B., Yu J.-Y., Mielke R. E., MacAskill J. A., Madzunkov S., McGenity T. J. and Coleman M. (2008) Different isotope and chemical patterns of pyrite oxidation related to lag and exponential growth phases of *Acidithiobacillus ferrooxidans* reveal a microbial growth strategy. *Earth and Planetary Science Letters* **270**, 63-72.
- Brunner B., Einsiedl F., Arnold G. L., Müller I., Templer S. and Bernasconi S. M. (2012) The reversibility of dissimilatory sulphate reduction and the cell-internal multi-step reduction of sulphite to sulphide: insights from the oxygen isotope composition of sulphate. *Isotopes in Environmental and Health Studies* **48**, 33-54.

- Butterfield D. A., Nakamura K., Takano B., Lilley M. D., Lupton J. E., Resing J. A. and Roe K. K. (2011) High SO₂ flux, sulfur accumulation, and gas fractionation at an erupting submarine volcano. *Geology* **39** (9), 803-806.
- Chiba, H. and Sakai, H. (1985) Oxygen isotope exchange rate between dissolved sulfate and water at hydrothermal temperatures. *Geochimica et Cosmochimica Acta* **49**, 993-1000.
- Claypool G. E., Holser W. T., Kaplan I. R., Sakai H. and Zak I. (1980) The age curves of sulfur and oxygen isotopes in marine sulfate and their mutual interpretation. *Chemical Geology* **28**, 199-260.
- Druschel G. and Borda M. (2006) Comment on "Pyrite dissolution in acidic media" by M. Descostes, P. Vitorge, and C. Beaucaire. *Geochimica et Cosmochimica Acta* **70**, 5246-5250.
- Fritz P., Basharmal G. M., Drimmie R. J., Ibsen J. and Qureshi R. M. (1989) Oxygen isotope exchange between sulphate and water during bacterial reduction of sulphate. *Chemical Geology (Isotope Geoscience Section)*, **79**, 99-105.
- Holser W. T., Kaplan I. R., Sakai H. and Zak I. (1979) Isotope geochemistry of oxygen in the sedimentary sulfate cycle. *Chemical Geology* **25**, 1-17.
- Holt B. D., Cunningham P. T., Engelkemeir A. G., Graczyk D. G. and Kumar R. (1983) Oxygen-18 study of nonaqueous-phase oxidation of sulfur dioxide. *Atmospheric Environment* **17**, 625-632.
- Horner D. A. and Connick R. E. (2003) Kinetics of Oxygen Exchange between the Two Isomers of Bisulfite Ion, Disulfite Ion (S₂O₅²⁻), and Water As Studied by Oxygen-17 Nuclear Magnetic Resonance Spectroscopy. *Inorganic Chemistry* **42**, 1884-1894.
- Hubbard C. G., Black S. and Coleman M. L. (2009) Aqueous geochemistry and oxygen isotope compositions of acid mine drainage from the Río Tinto, SW Spain, highlight inconsistencies in current models. *Chemical Geology* **265**, 321-334.
- Kohl I. E., Asatryan R. and Bao H. (2012) No oxygen isotope exchange between water and APS-sulfate at surface temperature: Evidence from quantum chemical modeling and triple-oxygen isotope experiments. *Geochimica et Cosmochimica Acta* **95**, 106-118.
- Kusakabe, M., Komoda, Y., Takano, B. and Abiko, T. (2000) Sulfur isotopic effects in the disproportionation reaction of sulfur dioxide in hydrothermal fluids: implications for the δ³⁴S variations of dissolved bisulfate and elemental sulfur from active crater lakes. *Journal of Volcanology and Geothermal Research* **97**, 287-307.
- Lloyd R. M. (1968) Oxygen Isotope Behavior in the Sulfate-Water System. *Journal of Geophysical Research* **73**, 6099-6110.
- Mizutani Y. and Rafter A. T. (1973) Isotopic behaviour of sulphate oxygen in the bacterial reduction of sulphate. *Geochemical Journal* **6**, 183-191.
- Oba Y. and Poulson S. R. (2009) Oxygen isotope fractionation of dissolved oxygen during abiological reduction by aqueous sulfide. *Chemical Geology* **268**, 226-232.
- Rees C. E., Jenkins W. J. and Monster J. (1978) The sulphur isotopic composition of ocean water sulphate*. *Geochimica et Cosmochimica Acta* **42**, 377-381.
- Veizer J. Ala D., Azmy K., Bruckschen P., Buhl D., Bruhn F., Carden G. A. F., Diener A., Ebner S., Godderis Y., Jasper T., Korte C., Pawellek F., Podlaha O. G. and

- Strauss H. (1999) $^{87}\text{Sr}/^{86}\text{Sr}$, $\delta^{13}\text{C}$ and $\delta^{18}\text{O}$ evolution of Phanerozoic seawater. *Chemical Geology* **161**, 59-88.
- Wortmann U. G., Chernyavsky B., Bernasconi S. M., Brunner B., Böttcher M. E. and Swart P. K. (2007) Oxygen isotope biogeochemistry of pore water sulfate in the deep biosphere: Dominance of isotope exchange reactions with ambient water during microbial sulfate reduction (ODP Site 1130). *Geochimica et Cosmochimica Acta* **71**, 4221-4232.

Appendix

Isotopes in Environmental and Health Studies 48 (2012), 33-54;
doi:10.1080/10256016.2011.608128

6. The reversibility of dissimilatory sulphate reduction and the cell-internal multi-step reduction of sulphite to sulphide: insights from the oxygen isotope composition of sulphate

Benjamin Brunner^{a*}, Florian Einsiedl^b, Gail L. Arnold^a, Inigo Müller^{a,c}, Stefanie Templer^d and Stefano M. Bernasconi^e

^aMax Planck Institute for Marine Microbiology, Bremen, Germany

^bDepartment of Environmental Engineering, Technical University of Denmark (DTU), Lyngby, Denmark

^cMARUM Center for Marine Environmental Sciences and Department of Geosciences, University of Bremen, Germany

^dDepartment of Earth, Atmospheric, and Planetary Sciences, Massachusetts Institute of Technology, Cambridge, USA

^eGeological Institute, ETH Zürich, Switzerland

*Corresponding author. Email: bbrunner@mpi-bremen.de

6.1. Abstract

Dissimilatory sulphate reduction (DSR) leads to an overprint of the oxygen isotope composition of sulphate by the oxygen isotope composition of water. This overprint is assumed to occur via cell-internally formed sulphuroxy intermediates in the sulphate reduction pathway. Unlike sulphate, the sulphuroxy intermediates can readily exchange oxygen isotopes with water. Subsequent to the oxygen isotope exchange, these intermediates, e.g. sulphite, are re-oxidised by reversible enzymatic reactions to sulphate, thereby incorporating the oxygen used for the re-oxidation of the sulphur intermediates. Consequently, the rate and expression of DSR-mediated oxygen isotope exchange between sulphate and water depend not only on the oxygen isotope exchange between sulphuroxy intermediates and water, but also on cell-internal forward and backward reactions. The latter are the very same processes that control the extent of sulphur isotope fractionation expressed by DSR. Recently, the measurement of multiple sulphur isotope fractionation has successfully been applied to obtain information on the reversibility of individual enzymatically catalysed steps in DSR. Similarly, the oxygen isotope signature of sulphate has the potential to reveal complementary information on the reversibility of DSR. The aim of this work is to assess this potential.

We derived a mathematical model that links sulphur and oxygen isotope effects by DSR, assuming that oxygen isotope effects observed in the oxygen isotopic

composition of ambient sulphate are controlled by the oxygen isotope exchange between sulphite and water and the successive cell-internal oxidation of sulphite back to sulphate. Our model predicts rapid DSR-mediated oxygen isotope equilibrium values are observed, depending on the importance of oxygen isotope exchange between sulphite and water relative to the re-oxidation of sulphite. Comparison of model results to experimental data further leads to the conclusion that sulphur isotope fractionation in the reduction of sulphite to sulphide is not a single-step process.

Keywords: isotope fractionation; isotope exchange; oxygen-18; sulphate reduction; sulphur-34

The complete article is available online:

<http://dx.doi.org/10.1080/10256016.2011.608128>

Acknowledgments

First at all I want to thank Beno for being my supervisor in this three years, it has been a great time to work with you and learn from you. I am glad that you always took your time if I needed your help and our discussions were very motivating to me. When we struggled with the challenges of the equilibrium experiment it was your optimism and enthusiasm that kept me going on with my work. After this time I know what mathematics is good for and what power it has to explain problems that we cannot comprise with our blank eyes. It was funny to be so far away from home and still discuss things in Swiss German and stay like that in touch with the homeland. Hopefully we will have the possibility to do some more projects together in future. We did it!

Wolfgang I am thankful for giving me the chance to work on this project within the MARUM GB3 frame, for you open ears, the modeling help and discussions concerning my work. It was a great experience to be member of the BAMBUS cruise, to see this liquid elemental sulfur in this extreme environment. Thank you for your support through these years.

Tim thank you for giving me the chance to work on this project, being part of the old Biogeochemistry Group, for the comments on my work, for the support and the chance to go on the cruise to Japan, although it was bit stormy, it was an unforgettable adventure going there. The conference experiences helped me a lot to develop myself and I am thankful that you allowed me the visits to the AGU and EGU conferences and Workshops in Tübingen and Göttingen.

I would like to thank Marcel Kuypers for giving me the possibility to work in his labs and being part of the Biogeochemistry Group and for the financial support in the final stage of my PhD.

Mike I enjoyed the time with you on the Natsushima and I am thankful that I could learn the bimane method from you and for being so patient with me.

I want to acknowledge as well the crews of the RV Sonne and RV Natsushima and the scientific party on both cruises; it was always a great adventure for someone more used to the mountain being on the open ocean.

I want to thank the technicians of the Biogeochemistry Group as well as the ones from the Microsensor Group for all their help, support and friendship, I enjoyed much the time with you, joking around or learning something about the instruments. Thomas for all the help with my experiments, the stable isotope measurements and the introduction on how to treat the mass spec. Swantje also for the isotope measurements and for helping me with my incubation preparation, in the end I could not do them but I am still glad you helped me. Kirsten and Gabi for mentoring me with the HPLC and GC techniques, for the help if the instrument did not work again and Andrea for the introduction into the diamine method and freeze drying. Unforgettable the xmas market visits with Kirstens mother, we have to repeat this once in the future. I also want to thank Daniela F., Daniela N. and

Mirja+Nadine for their friendship and help if I had questions. Ulrike for the organization of trips and cruises and for the advices how to survive in Tokyo.

During the time at the MPI I had the chance to meet so many nice people and I want to thank all the friends I made her, mainly from the Biogeochemistry Group and the Microsensor Group, as I was kind of member of both groups. Thank you for having an open ear for me, for spending some free time in the city center and enjoying some beers or cokes with me.

Gail I am glad that you helped me so much with the writing, giving me advices how to improve my presentations taking me to Aarhus with Beno...I expect a second time in the next year to find out more about the mystical sulfur cycle, alternatively another drink in the Marriot Hotel in Frisco would also do it. It was great to have you in the group as you did so much for all of us and organized the Schnitzel Mondays or the Ratskeller Tours, which was always fun and interesting at the same time.

Stefano I guess that I was very lucky to have your support during my PhD, thank you for all the water analyses and in the end also the analyses of the solid samples, without your help we could not have finished our project here in Bremen. At the same time I have to thank Stewart and Maria for the measurements or sample preparation, respectively. Stewart I guess we will meet some day at a marathon in the Alps, I count on you. And Stefano I hope we will have in future some collaborations that I have the possibility to visit you sometimes and enjoy a coffee with you.

I want to thank Patrick and Carolina for going out with me sometimes, being so spontaneous and Patrick a friend throughout this time, it was also very gracious of you to accommodate me and Anna-Lena some years ago, I did not expect at that time to be once a co-worker of you and of Laura. It was funny when it turned out to be like that. I am very glad that I became a friend of Chia-I and we could share so many conversations and time together, for a short period I even had a running Spezi here in Bremen!

As a kind of guinea pig I started in Bremen being member of the Biogeochemistry Group but having my office in the Microsensor wing, due to that I had the chance to meet many nice friends over there. I am thankful to Anja and Raphaela for treating me so well and helping me to get rapidly integrated in the Microsensor Group, it was great to share offices with you and later as well with Arjun and Bettina. I want to thank Olivera for being a good friend from beginning on, helping me wherever needed and being my lunch-fellow for a long time (long time in the sense for so many years and not because I was such a slow eater..), it was a great time and I enjoyed the conversations with you.

With time I became good friends with Duygu and Anna which I am very happy for, thanks for the conversations, watching Tatort or talking trash in the breaks. I am happy to have this distraction and that I could talk as well about other things not related to work. Good to have you here in the MPI and hopefully we stay in contact. This will be our year, we can do it! Olaf and Olli for the IT support and one of you as well for swimming with me in the Kuhgraben.

Joanna, Aude, Sergio, Laura, Thang, Soeren, Kristiina, Bo, Abdul and all the others, thank you for being friends, making me work more focused and sharing some moments with me. I am glad that I came along very well with all the colleagues at the MPI and therefore had some three nice years in Bremen.

I want to thank as well the friends from the University or the MARUM, Niels, Christian, Janis, Chen Liang, Michi it was great to have you around and to talk to you. I enjoyed the cruise with some of you, the AGU conference and the road trip through California, it was splendid. To Janis and Christian I am very thankful for the help related to my work, some spontaneous measurements, for sending me literature that I needed, preparing maps and for being friends.

I am thankful to Peter for introducing me into the microsensor world, for helping me with the measurements and being always in a good mood, as well I want to thank Judith for the help when the Daqpad did not work and the Microsensor technicians for preparing the microsensors for me and Dirk for giving his blessing to it.

Sasha and Nurgül thank you for your motivating discussions and your interest in my work. I was glad to have you in my thesis committee Sasha, thanks for all the support.

All and all I had some nice years and enjoyed the time in Bremen a lot and could learn a lot. But I have to thank as well my family for support and just for being their and giving me some new energy when I needed it.

Curriculum vitae

Personal data

Name Inigo Andreas Müller

Address Geisbergstrasse 18
28211 Bremen

E-mail imueller@mpi-bremen.de

Birth date 19th of June 1983

Born in Lausen (Switzerland)

Nationality German

Education

Since October 2009 -

Doctoral candidate at the Max Planck Institute for marine Microbiology (Department of Biogeochemistry) within the GB 3 project of the MARUM, Bremen.

Supervisors: Prof. Dr. Wolfgang Bach (University of Bremen) and Dr. Benjamin Brunner (Max Planck Institute for Marine Microbiology, Bremen)

HIGH TEMPERATURE RELATED SULFUR CYCLING AND OXYGEN ISOTOPE SIGNATURE OF SULFATE

2007-2009

Master of Earth Sciences (Major in Geology & Geochemistry), ETH Zurich, Switzerland

Master Thesis under supervision of Stefano M. Bernasconi:

RECONSTRUCTION OF THE CLIMATE VARIATIONS OF THE LAST 760 YEARS WITH A MARINE HIGH-RESOLUTION RECORD ON FORAMINIFERA FROM THE GULF OF TARANTO

2004 – 2007

Bachelor of Earth Sciences, ETH Zurich, Switzerland

Bachelor Thesis under supervision of Flavio S. Anselmetti:

DER ÄGERISEE UND SEINE SEDIMENTE ALS PALÄOSEISMISCHES ARCHIV (The lake Ägeri and its sediments as a palaeo-seismic archive)

1999 – 2002

Matura Type E (economics)

Gymnasium Liestal, Switzerland

Publications

In the pipeline:

-Müller Inigo A., Brunner Benjamin and Coleman Max.

Isotopic evidence of the pivotal role of sulfite oxidation in shaping the oxygen isotope signature of sulfate.

Submitted in *Chemical Geology*.

-Müller Inigo A., Brunner Benjamin, Breuer Christian, Coleman Max and Bach Wolfgang.

The oxygen isotope equilibrium fractionation between sulfite species and water.

Submitted in *Geochimica et Cosmochimica Acta*.

Peer reviewed:

-Brunner B., Einsiedl F., Arnold G. L., Müller I., Templer S. and Bernasconi S. M.

(2012) The reversibility of dissimilatory sulphate reduction and the cell-internal multi-step reduction of sulphite to sulphide: insights from the oxygen isotope composition of sulphate. *Isotopes in Environmental and Health Studies* **48 (1)**, 33-54.

Poster and oral presentations

Müller I. A., Brunner B. (2012) The influence of oxygen exchange between sulfite and water on the oxygen isotope composition of sulfate. Poster presented at 2012 Fall Meeting, AGU, San Francisco, CA, 3-7 December.

Müller I. A., Brunner B., Ferdelman T. G. (2011) The oxygen isotope signature of sulfate derived from abiotic sulfite oxidation under different pH conditions. Oral presentation (Abstract PP51E-08) at the 2011 Fall Meeting, AGU, San Francisco, CA, 5-9 December.

Müller I., Brunner B., Ferdelman T. G. (2010) The influence of pH on the oxygen isotope equilibrium fractionation between sulfite and water. Oral presentation at the General Assembly 2010, EGU, Vienna, Austria, 2-7 May.

Müller I., Brunner B., Ferdelman T. G. (2009) Determining the Oxygen Isotope Equilibrium Fractionation Between Sulfite and Water. Poster presented (Abstract B13D-0551) at 2009 Fall Meeting, AGU, San Francisco, CA, 14-18 December.

Müller I., Bernasconi S. M., Grauel A., Zonneveld K., Versteegh G. and De Lange G. (2009) Reconstruction of the Climate Variations of the last 760 Years with a marine High-Resolution Record on Foraminifera from the Gulf of Taranto. Oral presentation at the SECOND EUROMARC CONFERENCE, ESF, 2009, Presqu'île de Giens, France, 13-16 September.

Erklärung

Erklärung gemäß § 6 Abs. 5 der Promotionsordnung der Universität Bremen für die mathematischen, nature- und ingenieurwissenschaftlichen Fachbereiche.

Name: Inigo Andreas Müller
Anschrift: Geisbergstrasse 18
28211 Bremen

Hiermit versichere ich, dass ich

1. die Arbeit ohne unerlaubte fremde Hilfe angefertigt habe,
2. keine anderen als die von mir angegebenen Quellen und Hilfsmittel benutzt habe
und
3. die den benutzten Werken wörtlich oder inhaltlich entnommenen Stellen als solche kenntlich gemacht habe.

Bremen, den 20. Januar 2013

Inigo Müller